WELDING Journal

March 2006

•Friction Stir Welding: Past, Present, and Future

•Resistance Welding Analyzed

•Looking for PWHT Code Exemptions

PUBLISHED BY THE AMERICAN WELDING SOCIETY TO ADVANCE THE SCIENCE, TECHNOLOGY AND APPLICATION OF WELDING AND ALLIED PROCESSES, INCLUDING JOINING, BRAZING, SOLDERING, CUTTING, AND THERMAL SPRAYING

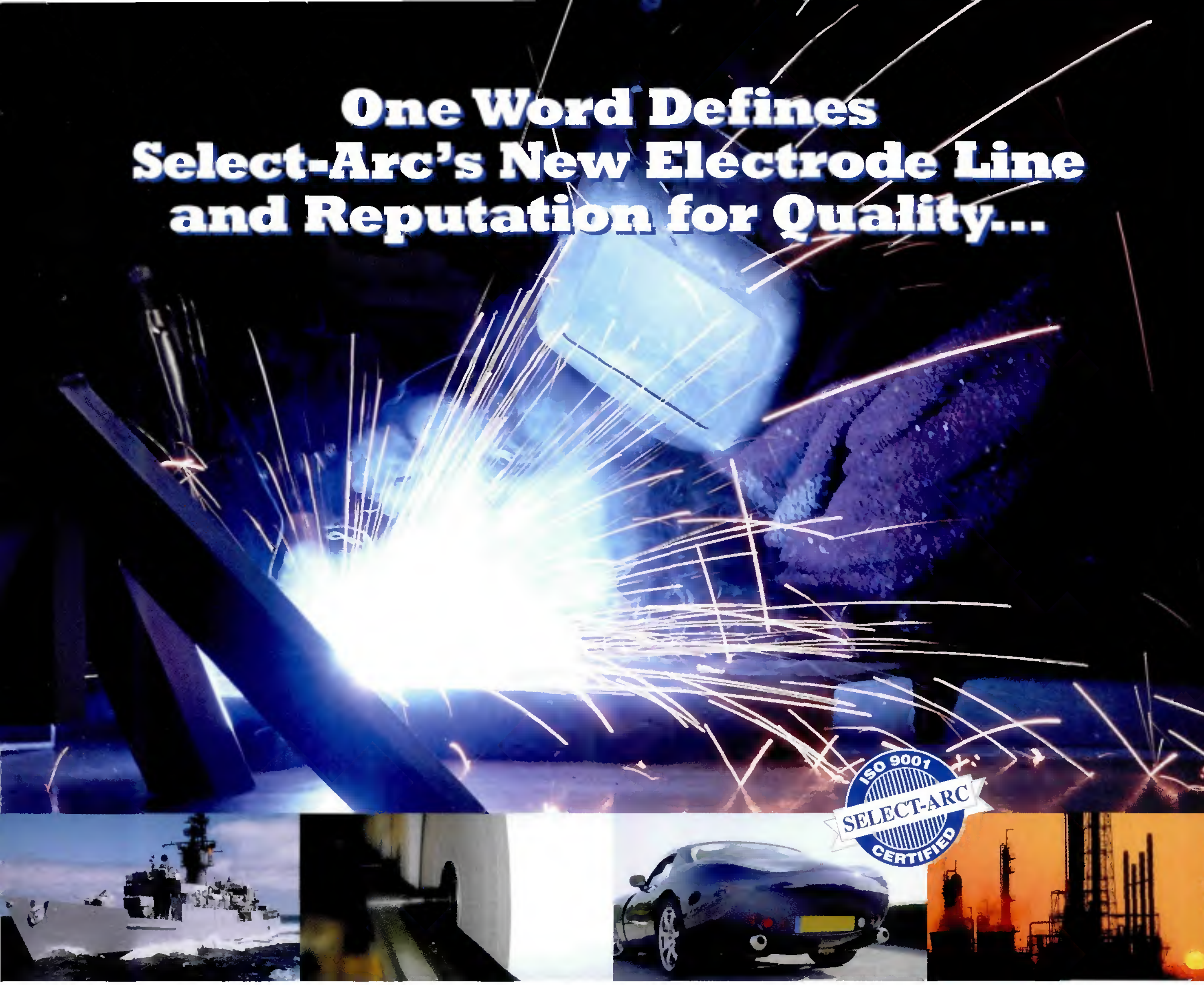

Stainless.

Select-Arc, Inc. has earned an outstanding reputation in the industry as a manufacturer of premium quality tubular welding electrodes for carbon and low alloy steel welding.

Now Select-Arc has expanded its range of exceptional products with the introduction of a complete line of austenitic, martensitic and ferritic stainless steel electrodes. Both the new SelectAlloy and Select stainless steel wires deliver the superior feedability, superb welding characteristics, consistent deposit chemistry and excellent overall performance you have come to expect from Select-Arc.

The chart below shows that SelectAlloy flux cored electrodes' higher deposition rates improve productivity and reduce welding costs.

Typical Deposition Rates for Various Stainless Steel Consumables

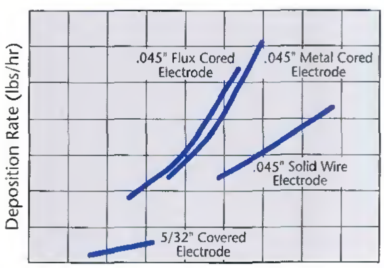

SelectAlloy's smooth bead contour, easy peeling slag, minimal spatter, closely controlled weld deposit compositions and metal soundness deliver additional savings.

The Select 400-Series metal cored electrodes offer the same advantages as SelectAlloy and are ideally suited for difficult-to-weld applications, such as auto exhaust systems.

Discover for yourself the many benefits of specifying Select-Arc's new premium stainless steel electrodes. Call us today at **1-800-341-5215** or you can visit our website at **www.select-arc.com** for more information.

SELECT ARC INC.®

600 Enterprise Drive
P.O. Box 259
Fort Loramic, OH 45845-0259
Phone: (937) 295-5215
Fax: (888) 511-5217
www.select-arc.com

Circle No. 48 on Reader Info-Card


FACTORY DIRECT REBATE
April 1 - June 30, 2006
40% LARGER VIEWING AREA
THAN ANY OTHER AUTO-DARKENING PRODUCT
XTREME FIXED
$20.00
REBATE
Fixed Shade 10.5.
XTREME VARIABLE
$30.00
REBATE
Variable Shade 9-12.
INDUSTRIAL XTREME
$40.00
REBATE
Variable Shade 7-14 and 3 LCDs for unsurpassed optical quality.
Circle No. 6 on Reader Info-Card
CALL 800-223-4685 FOR A PARTICIPATING ARCONE® DISTRIBUTOR NEAR YOU.
Visit our website at arc1weldsafe.com for more information.
Rebate limited to end users only.
ARCONE® is a division of A.C.E. International
Ph: 800-223-4685
85 Independence Dr.
Fax: 508-884-9666
Taunton, MA 02780
www.arc1weldsafe.com
ARCONE

CONTENTS

March 2006 • Volume 85 • Number 3

AWS Web site *http://www.aws.org*

Features

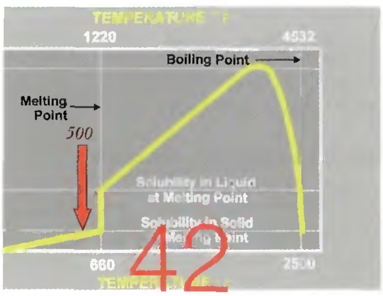

Welding Research Supplement

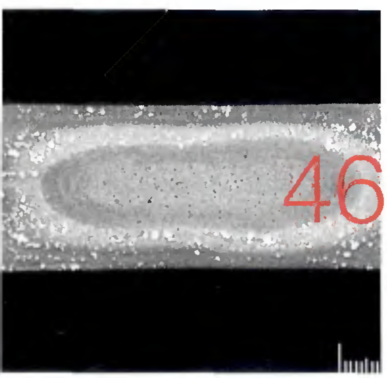

Cover Photo. A self-reacting friction stir weld being conducted using the horizontal weld tool. It was part of the Next Generation Launch Technology program demonstrating full-scale circumferential welding. (Courtesy of NASA, Marshall Space Flight Center.)

Departments

Welding Journal (ISSN 0043-2296) is published monthly by the American Welding Society for $120.00 per year in the United States and possessions, $160 per year in foreign countries: $7.50 per single issue for AWS members and $10.00 per single issue for nonmembers. American Welding Society is located at 550 NW LeJeune Rd., Miami, FL 33126-5671; telephone (305) 443-9353. Periodicals postage paid in Miami, Fla., and additional mailing offices. **POSTMASTER:** Send address changes to Welding Journal, 550 NW LeJeune Rd., Miami, FL 33126-5671.

Tenaris Completes Acquisition of Acindar Welded Pipe Plant

Tenaris S.A., Luxembourg, recently announced through its Argentine welded pipe subsidiary, Siat S.A., it has completed the acquisition of the welded pipe assets and facilities of Acindar Industria Argentina de Aceros S.A. (Acindar) located in Villa Constitucion, Santa Fe, for $28 million.

The facilities acquired have an annual capacity of 80,000 tons of welded pipes whose small diameter range complements the range of welded pipes that the company currently produces in Argentina.

General Dynamics NASSCO Receives Navy Contract to Build Ninth T-AKE Dry Cargo/Ammunition Ship

General Dynamics NASSCO, a wholly owned subsidiary of General Dynamics, has received a contract option from the U.S. Navy to build an additional ship under the T-AKE program, a new class of combat logistics force ships.

The $317 million contract brings the total number of T-AKE ships awarded to the company to nine, and the total contract value to $2.8 billion. Options for three additional T-AKE ships remain available under the existing contract as well.

The T-AKE is a dry cargo/ammunition ship that will be operated by the Military Sealift Command, providing logistic support from sources of supply either in port or at sea. It will upgrade the Navy's ability to maintain its forward-deployed forces, replacing aging T-AE ammunition ships and T-AFS combat stores ships that are nearing the end of their service lives.

Divers Academy Moves to Atlantic City Area

Divers Academy has moved to a 10,000-sq-ft modern, state-of-the-art facility in the Atlantic City, N.J., area effective March 1. For the last 30 years the company has been located in Camden, N.J., where it specialized in training welders for high-paying careers in underwater welding. The new facility will allow training from a deep water quarry and a new barge complex. It also will enable Divers Academy to expand the range of underwater training classes it offers to welders.

Terra Nostra Resources Commences Production at Casting Mill in Its New Stainless Steel Facility

Terra Nostra Resources Corp., Los Angeles, Calif., has commenced production at the 180,000 ton casting mill in its new state-of-the-art stainless steel production facility, through its majority-owned joint venture company Shandong Quanxin Stainless Steel Co. Ltd., situated in the Zibo City High Tech Zone, Shandong Province, China.

The production output from the casting mill will be utilized in the rolling mill, presently under construction. The rolling mill will initially be comprised of a stainless steel strip line that is expected to be operational in the second quarter of 2006. In addition, the company is planning to phase in new production lines for stainless steel rods and welded pipes. The total design capacity of the rolling mill is 450,000 tons per annum. Currently, Shandong Quanxin employs more than 600 people, and a total of 1000 will be required upon startup of the rolling mill.

Granite Construction Awarded Joint Venture Bridge Replacement Project in Mississippi

Granite Construction, Inc., Watsonville, Calif., recently announced that Granite Construction Co., in joint venture with Archer Western Contractors of Atlanta, Ga., has been awarded a $266.8 million bridge replacement project at St. Louis Bay, near Gulfport, Miss. The company's portion of the contract is approximately $160.1 million. The award was made by the Mississippi Department of Transportation.

The project encompasses the removal and replacement of the U.S. 90 highway bridge over St. Louis Bay, which was destroyed by Hurricane Katrina, and includes the design and construction of the bridge and approaches on each end. The scope of the project includes two lanes in each direction, approximately 1.9 miles long.

Work began in February, and the estimated completion date is November 2007.

WELDING Journal

Publisher *Andrew Cullison*

Editorial
Editor/Editorial Director *Andrew Cullison*
Senior Editor *Mary Ruth Johnsen*
Associate Editor *Howard M. Woodward*
Assistant Editor *Kristin Campbell*
Peer Review Coordinator *Doreen Kubish*

Publisher Emeritus *Jeff Weber*

Graphics and Production
Managing Editor *Zaida Chavez*
Production Assistant *Brenda Flores*

Advertising
National Sales Director *Rob Saltzstein*
Advertising Sales Representative *Lea Garrigan Badwy*
Advertising Production *Frank Wilson*

Subscriptions
Leidy Brigman
leidy@aws.org

American Welding Society
550 NW LeJeune Rd., Miami, FL 33126
(305) 443-9353 or (800) 443-9353

EDITORIAL

Share the Wealth

If you grew up in an era when the circus coming to town was an eagerly anticipated event, you'll remember your wide-eyed wonder about the characters who populated the big top. The costumes, the grease paint, the showmanship, the daring, and the dazzle of the acts brought a brief and welcome relief from the ordinary monotony of everyday life. While each act and character riveted my attention, I always had a partiality to the juggler's skill. Whether the suspended objects were plates, bowling pins, balls, or flaming torches, the seemingly effortless coordination of their rotation fascinated me. Little did I know I would one day practice the juggler's skill — not as a performer under the big top, but in the arena of a more staid occupation — as editor of the *Welding Journal.*

By its nature, the *Welding Journal* is many things to many people. It is first and foremost the face of AWS; it is a source for scientists to publish their latest research; it is a mechanism for transferring technology to welding engineers and supervisors; it is a conveyor of practical information to the welder; it is discussion material for welding educators and their students; it is a report on the activities of the Society; and it is a vehicle that informs members of news, events, and products pertinent to the industry.

In selecting articles for publication, I am always juggling those many interests. Throughout the 1500–1600 pages the *Journal* publishes every year, we strive to find articles that will fit the many needs of our members. Sometimes the juggle is flaming torches, but other times, it's just plain plates. In other words, not every member's interests will always be satisfied to the fullest. We get those who say we are too technical, and then those who say we are not technical enough. It can get downright confusing sometimes, and I must admit, maybe once in a while I drop a ball. But like any good juggler, I pick it up and nonchalantly start juggling again.

What keeps me going is my firm belief that the *Welding Journal* gains its strength from the very diversity that it strives to satisfy. For example, this issue contains articles on friction stir welding, a process only a decade old and still searching for applications. There are articles on resistance welding, a very mature process, but still the predominant choice of the auto industry. I know these processes may not interest everyone, but I want those who are interested to know the *Welding Journal* will be the source to learn the latest on these processes, and to those who are not, to know this is the reference source for it all. No doubt a future issue will have a topic of interest. Upcoming issues will have articles on thermal spraying, hardfacing, stud welding, explosion welding, welding in the auto industry, welding racing cars, fighting corrosion, fume extraction, and pipe welding to name just a few.

My father told me of going to a one-room schoolhouse, grades one through eight together. I, in my infinite wisdom as a youth, placed the "old fashioned" hat on him. He explained to me with a wisdom I would only learn later he possessed in abundance that it was a great way to learn. As the teacher taught lessons to each grade, all the other students were exposed to the lesson. It didn't matter if the six-grade lesson was entirely comprehensible to the third grader, or whether the first grader could grasp what the teacher was saying to the fourth grader, they could not help but absorb some of it. When it came time for students to advance to the next grade, they were already familiar with what would be taught and better able to grasp the next level of learning. Something similar happens with the *Welding Journal.* Everything is not for immediate use, but you can't help but learn from it, and when the time comes, you know where to go to move on to the next level.

The *Welding Journal*'s vitality depends on your willingness to share. You, the experts, supply more than 85% of articles. So the next time you feel the *Welding Journal* has too much of this, or not enough of that — contribute. It is the medium members can use to communicate with each other and to share knowledge within this close-knit group known as the welding community. The *Welding Journal* is a way to leave a record of your expertise, and a means to expand your knowledge. My greatest hope, though, is that every issue is a learning experience. Juggle away.

Andrew Cullison
Publisher/Editor Welding Journal

University of Northwestern Ohio Unveils High-Performance Motorsports Education Complex

In January, the University of Northwestern Ohio revealed its 70,000-sq-ft High-Performance Motorsports Complex. Pictured above is welding student Josh Gabor performing gas tungsten arc welding on 0.100-in.-thick 3003 h-14 aluminum.

The University of Northwestern Ohio, Lima, Ohio, unveiled its new High-Performance Motorsports Complex on January 20. The construction of the complex is the result of escalating enrollments and industry demands for highly trained and qualified graduates.

"The 70,000-sq-ft complex is the future of high-performance motorsports education. We've incorporated the latest technology in chassis and engine dynamometers, suspension and drive line setups and welding classes for exotic materials into the complex," according to University President Jeffrey A. Jarvis. "Plus, just outside of the buildings, students will find a 500-ft launching pad for drag racing classes, an eighth-mile asphalt oval for stock car testing, and an obstacle course/rock crawling hill for testing off-road technology."

According to the college, it established the first High-Performance Motorsports education program in the United States in 1992. Additionally, Limaland Motorsports Park, a quarter-mile dirt track, was purchased in 1998 to provide students the opportunity to work on race cars and learn the intricacies of chassis tuning at this 40-acre classroom.

The University's reputation for excellence in education has earned it the recognition as Official High Performance Technical Training University of ARCA, USAC, and DIRT Motorsports. Many of the college's students work with race teams from these sanctioning bodies each week, giving them the opportunity to apply what they learn in the classroom.

TWI Purchases Friction Stir Link's RoboStir System

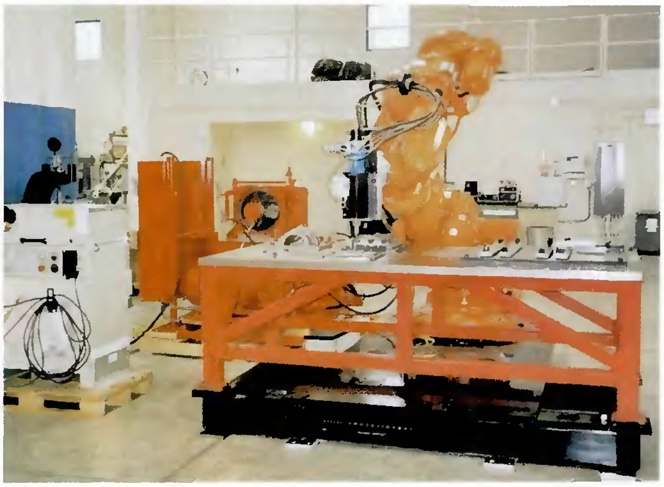

The RoboStir System by Friction Stir Link combines friction stir welding technology with the flexibility of a robot to provide 3D welding techniques. The Welding Institute bought the system for its new facility at the Advanced Manufacturing Park in South Yorkshire, UK.

The Welding Institute (TWI) recently purchased the RoboStir System from Friction Stir Link, Waukesha, Wis., that combines friction stir welding (FSW) technology with the flexibility of a robot. The advanced welding system will provide the opportunity for TWI to develop further 3D welding techniques and applications.

It will be installed in the company's new facility at the Advanced Manufacturing Park in South Yorkshire, UK. Delivery of the equipment is expected in spring 2006.

The addition of this machine will create a suite of FSW equipment at the facility, as it already runs a research and development FSW machine, and a second machine is used for the development of procedures for welding materials not previously processed by this technique.

NASA Extends Funding to Develop Delphi Welding Technology

Delphi Corp., Troy, Mich., after a year of successful collaboration between the company, the National Aeronautics and Space Administration (NASA), and Michigan Research Institute (MRI) in the field of advanced welding, will receive $870,000 to help fund the continuing development of deformation resistance welding (DRW) through June. This is the second grant for DRW from NASA; the first was a year-long grant for $1.3 million.

The DRW process, developed by Delphi, joins metal tubes to solids, sheet metal, and other tubes. The development work among engineers at the company, NASA, and MRI involves perfecting existing techniques and creating new innovative ways to use this welding process on suspension subframes and other unique manufacturing techniques.

"Our plans involve developing specific shipping containers, advancing our study of joining dissimilar material joints, and creating more automotive applications all with the unique DRW technology," said Tim Forbes, director, new markets, commercialization and licensing for Delphi Corp.

Air Liquide Presents Acme Cryogenics with Supplier Excellence Award

Last year, Acme Cryogenics received the Award for Supplier Excellence from Air Liquide. Pictured (left to right) are David Mudd, Air Liquide; Brad Christians, Air Liquide; Michael Fink, CEO Acme Cryogenics; Dave Edge, sales manager, Acme Cryogenics; Clair Wheeler, Air Liquide; and Sharon Gammell, Air Liquide.

Air Liquide presented Acme Cryogenics, Lehigh Valley, Pa., a manufacturer and service provider of gas and cryogenic liquid handling solutions, with the Award for Supplier Excellence at a supplier recognition ceremony in Houston, Tex., on November 30.

Acme was one of 10 suppliers chosen by Air Liquide's business groups to be recognized for its performance as a supplier in 2005. The company was recognized for continually working to meet Air Liquide's objectives for supplier innovation, product quality, customer service, and reduction in total supply chain costs.

Northwest Pipe to Supply Welded Steel Pipe for Water Treatment Plant

Northwest Pipe Co., Portland, Ore., has received a letter of intent from Kenny/Shea/Traylor, a joint venture of Wheeling, Ill., to supply approximately $10 million of welded steel pipe for a water treatment plant.

The company will supply approximately 56,000 ft of large-diameter steel pipe that will be used in a tunnel that is part of the Brightwater treatment plant in King County, Wash. The tunnel will be 14,000 ft long and approximately 18 ft in diameter at depths to 260 ft. The pipe will be installed inside the tunnel in four separate lines ranging from 27 to 84 in. in diameter.

The pipe is expected to be manufactured in the company's

Portland, Ore., division beginning in 2007 with final delivery in 2008. The contract for the tunnel and related pipe is the first phase of this $1.4 billion wastewater treatment plant.

Transbotics to Distribute KUKA Robots

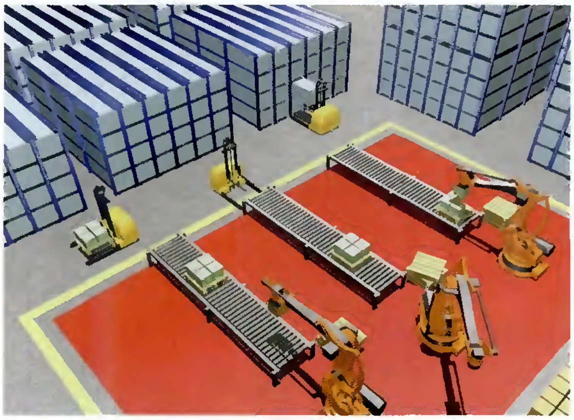

Transbotics Corp., Charlotte, N.C., recently entered into a systems partner agreement with KUKA Robotics Corp. The agreement authorizes the company to offer KUKA's entire line of industrial robots to its customers for integrated, Tailor Made™, automatic material handling systems.

Industry Notes

- Airgas, Inc., Radnor, Pa., has acquired Oxygen Service Co., Inc., Macon, Ga., and its four other locations in central and southern Georgia. Also, in a separate transaction, the company has acquired Alabama Cylinder Gas with one location in Enterprise, Ala. The six locations, which had more than $7 million in annual sales during the past year, have been integrated into Airgas South, one of the 13 regional companies within Airgas.

- The Nuclear Management Co. (NMC) recently contacted COB Industries, Inc., about its Argweld® water soluble purge film, due to the recent rise in concern in the nuclear industry about the high sodium content in many purge dam materials. The NMC decided to conduct its own chemical analysis in conjunction with another nuclear facility, and the test results showed that the purge film contains 9 parts per million sodium content. This was within the acceptable levels outlined by the nuclear facility, and the product was approved for use in purge dam applications.

- Harris Steel Group, Inc., Toronto, recently announced Harris Steel, Inc., through its newly established subsidiary, Harris Rebar Fresno, Inc., has signed an agreement to purchase the Fresno, California-based assets and business of Franklin Reinforcing Steel Co., Inc. Harris will acquire the business, fixed assets, working capital items, and employees of Franklin's Fresno operation.

- Noble International, Ltd., Warren, Mich., began production of laser-welded blanks (LWBs) for the Dodge Durango at its new facility in Stow, Ohio.

- Norcross Safety Products L.L.C., Oak Brook, Ill., has signed a definitive agreement to acquire all of the outstanding capital stock of Fibre-Metal Products Co., Concordville, Pa., a privately held designer and manufacturer of head protection equipment including protective caps, face shields, and welding helmets. Fibre-Metal has additional locations in Aston, Pa., and Mississauga, Ont., Canada.

• Macsteel Service Centers USA, Inc., Newport Beach, Calif., recently aquired Alpha Steel, a large distributor of hot rolled and structural steel products in the Midwest, which will now operate under the name Macsteel Service Centers USA. The newly named Hammond, Ind., plant processes and distributes a broad inventory of structural steel beams, shapes, plate, sheet, tubing, and pipe products.

• Bonal Technologies, Inc., Royal Oak, Mich., a provider of sub-harmonic stress relief technology for metal improvement solutions and a subsidiary of Bonal International, Inc., recently announced two new sales agents — KENFO AB and Gearing Moss Supplies (Pty) Ltd. KENFO will represent the company in Sweden, with sales offices in Sater and Norrkoping. Gearing Moss, with offices in Johannesburg, Durban, and Cape Town, will represent the company in South Africa and surrounding countries.

• The American National Standards Institute recently announced the addition of more than 13,000 Chinese national standards to the inventory of products available on its eStandards Store at *webstore.ansi.org*. The standards are delivered in electronic (PDF) format. The addition of the new collection of Chinese national standards will facilitate access to the procedures, guidelines, and requirements necessary for companies who intend to do business in the People's Republic of China.

Reader Comments on Thermite Weld Article

The letter below was sent by a reader in reference to Fui Tong Lee's article Managing Thermite Weld Quality for Railroads *published in* Welding Journal, *January 2006. The author's response follows.*

Dr. Lee has written a most thorough (for a six-page length) and readable article on the above topic. The bulk of his thesis is, in my opinion, correct.

I do wish to express one potential difference in interpretation as to the cause of the single defect shown on page 25, Fig. 2C. This defect is labeled by Dr. Lee as an "engine burn."

Figure 2C displays three distinct aggregations of linear surface defects along the top center of the rail. Only one of the defect aggregations (far right) has generated a compression depression across the head surface. I believe this depressed area is what Dr. Lee considers to be the "engine burn" defect.

I have examined numerous cases of compression overload spalling on the top of rail surfaces. Their appearances have been quite similar (or possibly identical to the linear spalling shown in Fig. 2C). If these linear spalls are not removed by grinding, and are left in track to continue to be run over by wheels, they can and do generate deep internal shear cracks that will essentially "collapse" the rail head. In other words, the defect geometry shown in Fig. 2C can be developed by simple overload contact rolling without sliding.

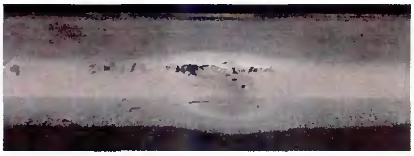

Fig. 2 — Typical examples of surface rail defects initiated and aggravated by high wheel-rail contact stresses. C — Wheel burn cracks caused by the slipping of a wheel axle.

This matter can be resolved by section examination of the rail head. If the indicated "engine burn" damage was the result of a wheel spinning in the depressed portion of the head, it would show evidence of severe shear deformation beneath that depressed surface and possibly evidence of local heating of the surface layer material (and possibly the formation of martensite in the surface).

James R. Hornaday Jr.
Alpha Gamma Transform, Inc.
Consultant
Member, AWS 15C
Subcommittee on Track Welding
Springfield, Mo.

The main issue of this paper should be focused on managing the thermite welds. As far as the various types of defects are concerned, indeed I would agree with Mr. Hornaday that the issue can only be resolved positively by cross sectioning the relevant area of the railhead.

Indeed I would like to thank Mr. Hornaday for his constructive thoughts and comments on this matter.

Fui Tong Lee

AWS Member Reacts to Building a 'Lean' Team

After reading How to Build a 'Lean' Team (*Welding Journal*, January 2006), I was compelled to write on behalf of the workers who actually do the work, produce a product, and are on the shop floor.

The copyrighted People-Powered Lean slogan is nothing new. It's just a rehash of every human resource department blunder of the past. How do you think all these seminar-producing salesmen stay in business? They produce a new slogan (corporate culture, adding value, TQM, CQI, synergy, cross training, etc.) and try to market it as something new, and then to keep the human resource and management do-nothings busy, they're sent to these expensive seminars so they can come back to the shop floor and try to screw up the production process, which would probably work better if they just left it alone.

The real new ideas such as would increase production, streamline manufacturing, design new products, will never come from another waste of time and money seminar. It will always come from the people who are actually doing the work. But these very people are seldom asked, and if they are, and contribute, are seldom rewarded for it. Plus, they are rarely adequately compensated to begin with, to compel them to contribute.

The older I get, the less common sense I see in management, which is one of the reasons I see for the decline in manufacturing in this country. The other reason is blatant greed by shipping jobs to other countries.

So I had to laugh at the latest snake oil seminars and slogans peddled on the human resource and management types. They eat that right up, thinking that they're accomplishing something.

Meanwhile, while they're wasting all that time and money, you know what's happening? The workers on the shop floor or out on the job are actually working, using their brains and hands to actually produce a product, doing the work!

Jim Cuccia
AWS Member

BY DAMIAN J. KOTECKI

Q: We need to weld some cast iron fittings to the outside of 304L stainless steel tanks. We tried 309L filler metal, as we would for mild steel fittings, but with the cast iron fittings, the welds cracked. Would 312 filler metal work ?

A: Type 312 filler metal is quite risky for this application. Even though 312 is a very high ferrite filler metal, dilution from the high carbon in the cast iron (typically 2.5 to more than 4% C) will result in a root pass without any ferrite. Such a root pass of stainless steel weld metal is often prone to centerline cracking, especially when there is significant restraint.

I have made small fillet welds with little restraint using 312 filler metal, without cracking, but the weld metal tends also to be rather brittle. Furthermore, the stainless weld metal has a high coefficient of thermal expansion, which leads to high heat-affected zone (HAZ) stresses and can result in HAZ cracking in the cast iron.

The problem with weld brittleness stems from the carbon in the cast iron combining with the chromium in the 312 to produce networks of eutectic chromium carbides in austenite. Because the eutectic forms networks, there are plenty of available brittle paths for cracking. You may encounter transverse cracking as the weld cools. These cracks are similar to those encountered in welding the hardfacing filler metals that are described as primary austenite with austenite-carbide eutectic. In fact, the weld metal microstructure of the 312 root pass looks very much like that hardfacing microstructure.

Figure 1 shows the root pass microstructure of a fillet weld between 304L stainless and gray cast iron using 312 stainless filler metal. The microstructure, as expected, contains no ferrite. The structure is mainly cellular austenite, with the austenite-carbide eutectic in the intercellular spaces. The eutectic exists as nearly continuous networks.

The EDAX capability of the scanning electron microscope was used to positively identify the fine eutectic constituent, visible in the SEM image of Fig. 1, as chromium carbides with partial substitution of iron for chromium.

Figure 2 shows HAZ cracking in a gray iron casting fillet welded to 304L with a 312 electrode. The HAZ has little ductility because it is a mixture of white iron, martensite, and retained austenite.

A better choice for this joint is electrodes of the AWS A5.15 classification ENi-CI. Table 1 compares the composition requirements of the 312 covered electrodes of AWS A5.4 with that of the ENi-CI covered electrodes. It is noteworthy that the ENi-CI contains no chromium, so the only chromium available in the weld metal must come from the 304L base metal. This small amount of chromium picked up in the weld metal by dilution is not enough to produce significant chromium carbides in the microstructure of that weld, as will be seen later.

The high-nickel ENi-CI filler metal produces a root pass between cast iron and 304L that consists of nickel-alloy solid solution and spheroidal graphite, as shown in Fig. 3. With the ENi-CI electrodes, not all of the carbon in the root pass comes from the cast iron dilution — typically ENi-CI weld metal contains more than 1% carbon to promote spheroidal graphite formation in the nickel-base alloy that contains no strong carbide formers. The spheroidal graphite does not provide networks of brittle microstructure for easy crack propaga-

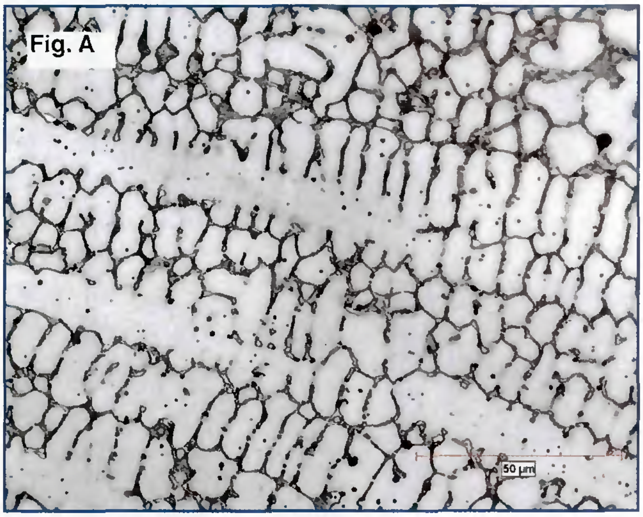

Fig. 1 — Root pass microstrucure of gray cast iron welded to 304L with 312 covered electrode. A — Optical photomicrograph; B — scanning electron microscope image.

Table 1 — Composition Requirements for E312-XX and ENi-CI Covered Electrodes

All-Weld Metal Chemical Composition, % (single values are maxima unless otherwise stated; N.S. = Not Specified)

	C	Mn	P	S	Si	Cr	Ni	Mo	Fe	Cu	Al
E312-XX	0.15	0.2 to 2.5	0.04	0.03	0.90	28.0 to 32.0	8.0 to 10.5	0.75	bal.	0.75	N.S.
ENi-CI	2.0	2.5	N.S.	0.03	4.0	N.S.	85 min.	N.S.	8.0	2.5	1.0

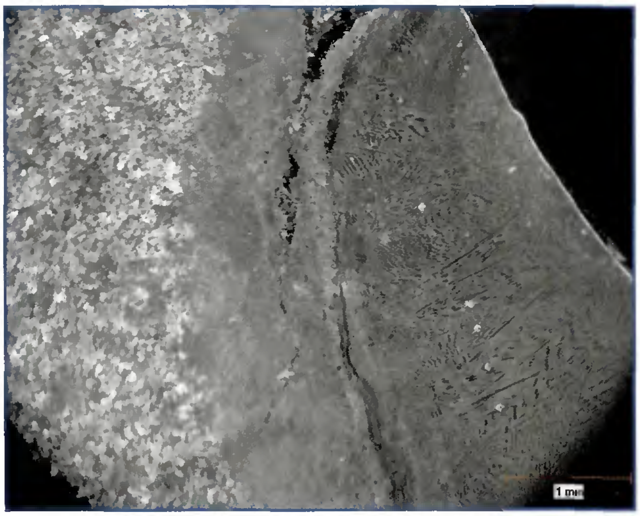

Fig. 2 — *Heat-affected zone crack in gray cast iron welded to 304L with 312 filler metal.*

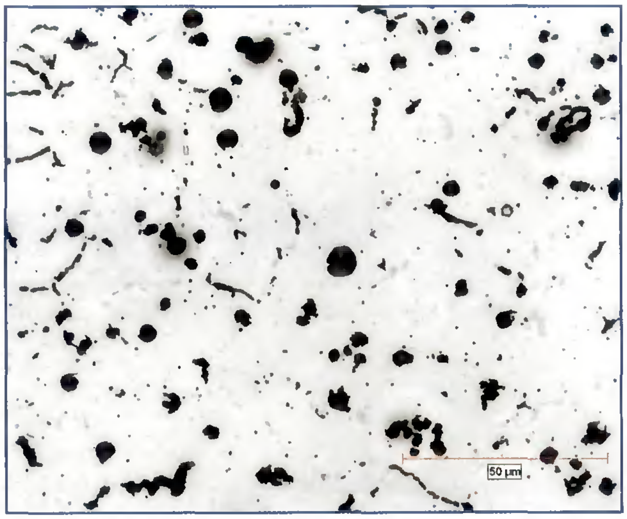

Fig. 3 — *Spheroidal graphite in ENi-CI root pass between gray cast iron and 304L.*

Table 2 — Vickers Hardness of Root Pass Weld Metal (Gray Cast Iron to 304L Joints)

Filler Metal	500 g Vickers Hardness
E312-17	336 to 374
ENi-CI	175 to 201

tle microstructure for easy crack propagation. The nickel-alloy filler metal also has a much lower coefficient of thermal expansion so it strains the cast iron HAZ much less than does the 312 filler metal due to shrinkage during cooling. No cracking was found in the samples welded for this column.

Furthermore, the weld metal from ENi-CI is much softer than that from 312 filler metal when used to make the gray cast iron to 304L joint. The range of hardness measurements made on the root pass of fillet welds, shown in Table 2, illustrate this point quite well. The softer nickel filler metal yields more easily during cooling than does the harder stainless filler metal, lessening the strain on the HAZ.

In view of the above evidence, I suggest that you use the ENi-CI type filler metal for your joints of cast iron to 304L stainless steel.

However, be aware that the HAZ of the cast iron is still a zone of potential cracking or fracture because it consists of a thin layer of white iron (cementite) at the fusion boundary with high-carbon martensite and retained austenite beyond the white iron. It is much less likely to crack when the ENi-CI filler metal is used than when 312 filler metal is used. But shock loading can still produce fracture later — that is always the risk in welding cast iron.♦

DAMIAN J. KOTECKI is Technical Director for Stainless and High-Alloy Product Development for The Lincoln Electric Co., Cleveland, Ohio. He is president of the American Welding Society, and a vice president of the International Institute of Welding (IIW). He is a member of the A5D Subcommittee on Stainless Steel Filler Metals; D1 Committee on Structural Welding, D1K Subcommittee on Stainless Steel Welding; and a member and past chair of the Welding Research Council Subcommittee on Welding Stainless Steels and Nickel-Base Alloys. Questions may be sent to Dr. Damian Kotecki c/o Welding Journal, 550 NW LeJeune Rd., Miami, FL 33126; or send e-mail to Damian_Kotecki@lincolnelectric.com.

Correction

In January 2006, p. 12, Stainless Q&A, column 2, sentence 2, it reads "... in nitrogen (Ni) ...". This should read "... in nickel (Ni) ...".

American Welding Society

Friends and Colleagues:

The American Welding Society established the honor of *Counselor* to recognize individual members for a career of distinguished organizational leadership that has enhanced the image and impact of the welding industry. Election as a Counselor shall be based on an individual's career of outstanding accomplishment.

To be eligible for appointment, an individual shall have demonstrated his or her leadership in the welding industry by one or more of the following:

• Leadership of or within an organization that has made a substantial contribution to the welding industry. The individual's organization shall have shown an ongoing commitment to the industry, as evidenced by support of participation of its employees in industry activities.

• Leadership of or within an organization that has made a substantial contribution to training and vocational education in the welding industry. The individual's organization shall have shown an ongoing commitment to the industry, as evidenced by support of participation of its employees in industry activities.

For specifics on the nomination requirements, please contact Wendy Sue Reeve at AWS headquarters in Miami, or simply follow the instructions on the Counselor nomination form in this issue of the *Welding Journal.* The deadline for submission is July 1, 2006. The committee looks forward to receiving these nominations for 2007 consideration.

Sincerely,

H. E. Cable
Chairman, Counselor Selection Committee

(please type or print in black ink)

CLASS OF 2007

COUNSELOR NOMINATION FORM

DATE_______________NAME OF CANDIDATE______________________________________

AWS MEMBER NO._______________________YEARS OF AWS MEMBERSHIP____________________________

HOME ADDRESS____

CITY_______________________________________STATE______ZIP CODE________PHONE____________________

PRESENT COMPANY/INSTITUTION AFFILIATION____

TITLE/POSITION____

BUSINESS ADDRESS____

CITY_______________________________________STATE______ZIP CODE________PHONE____________________

ACADEMIC BACKGROUND, AS APPLICABLE:

INSTITUTION____

MAJOR & MINOR____

DEGREES OR CERTIFICATES/YEAR____

LICENSED PROFESSIONAL ENGINEER: YES_______NO_______ STATE__________________________________

SIGNIFICANT WORK EXPERIENCE:

COMPANY/CITY/STATE____

POSITION____YEARS__________________

COMPANY/CITY/STATE____

POSITION____YEARS__________________

SUMMARIZE MAJOR CONTRIBUTIONS IN THESE POSITIONS:

____

____

____

IT IS MANDATORY THAT A CITATION (50 TO 100 WORDS, USE SEPARATE SHEET) INDICATING WHY THE NOMINEE SHOULD BE SELECTED AS AN AWS COUNSELOR ACCOMPANY NOMINATION PACKET. IF NOMINEE IS SELECTED, THIS STATEMENT MAY BE INCORPORATED WITHIN THE CITATION CERTIFICATE.

****MOST IMPORTANT****

The Counselor Selection Committee criteria are strongly based on and extracted from the categories identified below. All information and support material provided by the candidate's Counselor Proposer, Nominating Members and peers are considered.

SUBMITTED BY:
PROPOSER_______________________________________Print Name____________________________________
AWS Member No.________________
The proposer will serve as the contact if the Selection Committee requires further information. The proposer is encouraged to include a detailed biography of the candidate and letters of recommendation from individuals describing the specific accomplishments of the candidate. Signatures on this nominating form, or supporting letters from each nominator, are required from four AWS members in addition to the proposer. Signatures may be acquired by photocopying the original and transmitting to each nominating member. Once the signatures are secured, the total package should be submitted.

NOMINATING MEMBER:____________________________Print Name____________________________________
AWS Member No.____________
NOMINATING MEMBER:____________________________Print Name____________________________________
AWS Member No.____________
NOMINATING MEMBER:____________________________Print Name____________________________________
AWS Member No.____________
NOMINATING MEMBER:____________________________Print Name____________________________________
AWS Member No.____________

SUBMISSION DEADLINE JULY 1, 2006

American Welding Society

Nomination of AWS Counselor

I. HISTORY AND BACKGROUND

In 1999, the American Welding Society established the honor of Counselor to recognize individual members for a career of distinguished organizational leadership that has enhanced the image and impact of the welding industry. Election as a Counselor shall be based on an individual's career of outstanding accomplishment.

To be eligible for appointment, an individual shall have demonstrated his or her leadership in the welding industry by one or more of the following:

- Leadership of or within an organization that has made a substantial contribution to the welding industry. (The individual's organization shall have shown an ongoing commitment to the industry, as evidenced by support of participation of its employees in industry activities such as AWS, IIW, WRC, VICA, NEMA, NSRP SP7 or other similar groups.)
- Leadership of or within an organization that has made substantial contribution to training and vocational education in the welding industry. (The individual's organization shall have shown an ongoing commitment to the industry, as evidenced by support of participation of its employees in industry activities such as AWS, IIW, WRC, VICA, NEMA, NSRP SP7 or other similar groups.)

II. RULES

A. Candidates for Counselor shall have at least 10 years of membership in AWS.
B. Each candidate for Counselor shall be nominated by at least five members of the Society.
C. Nominations shall be submitted on the official form available from AWS headquarters.
D. Nominations must be submitted to AWS headquarters no later than July 1 of the year prior to that in which the award is to be presented.
E. Nominations shall remain valid for three years.
F. All information on nominees will be held in strict confidence.
G. Candidates who have been elected as Fellows of AWS shall not be eligible for election as Counselors. Candidates may not be nominated for both of these awards at the same time.

III. NUMBER OF COUNSELORS TO BE SELECTED

Maximum of 10 Counselors selected each year.

Return completed Counselor nomination package to:

Wendy S. Reeve
American Welding Society
550 N.W. LeJeune Road
Miami, FL 33126

Telephone: 800-443-9353, extension 293

SUBMISSION DEADLINE: July 1, 2006

Online Factory Adds Welding, Plasma Cutting, and Other New Services

eMachineShop (*www.emachineshop.com*) recently expanded its capabilities with the addition of plasma arc cutting, rubber molding, steel rule die blanking, and welding. The site is an online machine shop through which customers can design, price, and order custom parts.

"We added plasma cutting to allow our online customers to order larger and heavier metal shapes at low cost," said Jim Lewis, president. "Rubber molding and die cutting open completely new capabilities to meet the production needs of our customers. Each of the new services helps companies, organizations, and individuals gain the convenience and cost advantages of getting parts via the Internet."

To use the site's services, users download the company's free computer-aided design (CAD) software. During the design phase, eMachineShop's automated machining expert analyzes the shape, material, and finish to keep the user informed of any physical limitations. A 3-D preview spins the object around on the user's screen so the person can view the final part before ordering.

The company currently offers CNC milling, turning, punching, blanking, laser beam cutting, plastic extrusion, thermoforming, tapping, bending, water jet cutting, wire EDM, and injection molding. Finishes include brushing, plating, powder coating, anodizing, polishing, and grinding. Parts can be made of a broad selection of metals, plastics, woods, composites, and other materials.

Videos Show Destructive Testing

Triangle Engineering, Inc. Visitors to this Web site can watch video clips of the company's destructive weld testing equipment in action while a narrator describes how the equipment works. The company supplies equipment and consulting for welder testing, welder training, and procedure qualification. Products include weld test coupons, test stands, procedure qualification materials, and destructive test equipment. Besides details on the company's products and services, the site includes a company history, contact information, and an extensive list of customers.

www.trieng.com

Welding Accessories Highlighted

Atlas Welding Accessories, Inc. According to the detailed history provided on its Web site, this Michigan-based company began in 1939 with the introduction of a welder's hammer. Many modern-day versions of that hammer are showcased on the site. The company manufactures a variety of welding and safety products, which it sells through welding distributors. These products include pipe supports, roller stands, and dollies; weld cleaning tools; welding positioners; cylinder wrenches; and safety enclosures. The site offers plenty of product information as well as answers to frequently asked questions.

www.atlasweld.com

Site Offers Online Help with Industrial Gases

Linde Gas LLC. The company provides industrial and specialty gas services for industries such as manufacturing, food processing, energy, chemicals, metals, environmental conservation, pharmaceutical, biotechnology, health care, and construction. The Web site offers company news, a listing of retail locations, safety information, career opportunities, and ordering information. A Web site finder helps visitors locate Web sites for global Linde subsidiaries and local business partners.

The section titled My Industry — Applications and Equipment includes a 20-page downloadable PDF file describing the company's technology center, which provides research, development, and consulting services. The document includes listings of the facility's equipment and capabilities for gas shielded welding, oxyfuel and other thermal cutting processes, laser beam welding and cutting, thermal spraying, and heat treatment. In addition, the site details various welding processes and offers product information on the gases suitable for those processes.

www.us.lindegas.com

Site Features Resistance Welding Products

Centerline (Windsor) Ltd. Visitors to this site can download video clips of the company's resistance welding machines and other products in action as well as a promotional video about the company itself. Downloads are available whether the visitor is accessing the site through a 56-k modem or DSL/cable. The site also includes several technical articles and a variety of product literature that can be downloaded in PDF, a detailed company history, and forms for requesting a price quote or other information. The company's line of resistance welding products includes configurable fastener welding machines, welding electrodes, welding guns, and weld cylinders; other metalworking equipment includes press packages (ranging from 4–70 tons), piercing cylinders, date stamp units, and self-equalizing piercing units.

www.cntrline.com

Larger Sizes Introduced of Flowmeter and Temperature Transmitter for Resistance Welding

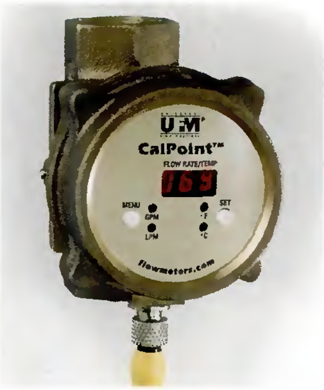

The CalPoint™ flowmeter and temperature transmitter is offered in two new pipe sizes to measure higher flow rates of water used to cool weld electrode tips, cables, and transformers. The sizes are 3 in., which provides a flow rate of 300 gal/min, and 4 in., with a flow rate of 600 gal/min. The meter provides temperature readouts ranging from 32° to 210°F, which can be expressed in Fahrenheit or Celsius on the local LED readout. Repeatability of the meter is ±1% of actual flow and ±0.25% of actual temperature. Accuracy is ±2% of actual flow. In addition, the meter has a scaled pulse output as a standard selectable option. It also measures flow rate and temperature of water-based machine coolant and water-glycol mixtures in addition to water.

Universal Flow Monitors, Inc. **100**
1755 E. Nine Mile Rd., Hazel Park, MI 48030

Machines Designed for Easy Utilization of Friction Stir Welding

The company's LEGIO machines are a standardized, flexible, modular system designed for easy utilization of friction stir welding. All the machines have an ESAB HMI control system developed for friction stir welding. The user has the capability of controlling the welding process (the vertical z-axis) by force or position control. A hydraulic cylinder with a closed loop system controls the z-axis. The machines come in a series of seven sizes, and there are five basic designs — S, ST, U, UT, and double-headed ST. The S and ST models are designed for linear welding (x and z), U and UT models for 2-D (x-y and z), and double-headed versions are for welding hollow profiles. All machines are designed with a rigid framework for high performance during load conditions. The welding head travels on heavy-duty linear bearings and is driven by a rack and pinion drive system.

ESAB Welding & Cutting Products **101**
PO Box 100545, 411 S. Ebenezer Rd., Florence, SC 29501-0545

Measuring Systems Give Accurate Length Setting

The company's measuring systems are manufactured from high-quality stainless steel investment castings. The multi loc and quick loc systems are designed to give the user a quick, easy, and accurate length setting. With the quick loc system, the user moves the stop on the rail to the desired length. The multi loc allows the user to put several stop blocks on one rail for multiple settings. The user moves the material from one stop to the next. This patented design eliminates any tightening of nuts, bolts, or locking devices. The user sets the stop at the desired length, and the stop automatically locks in place for an accurate length setting without any stop movement.

Scotchman Industries, Inc. **102**
PO Box 850, Philip, SD 57567

Abrasive Grind and Blend Kit Removes Heavy Welds

The Rex-Cut® Grind and Blend Kit includes a Sigma Green wheel featuring a zirconia-ceramic grain and proprietary bonding for aggressively grinding-out cracks and removing welds, and a cotton fiber Type 27 blending and finishing wheel that leaves a 32 RMS or better finish on stainless steel. The two 4½-in.-diameter wheels are offered with or without hubs. Also, according to the company, the Sigma Green wheel cuts up to 50% faster than aluminum oxide, and the Type 27 wheel is resilient for smooth operation.

Rex-Cut Products, Inc. 103
960 Airport Rd./PO Box 2109, Fall River, MA 02722

Welding Helmets Feature Internally Adjustable Autodarkening Shade

The XTV Series of lightweight, high-performance autodarkening welding helmets darken in 1/12,000 of a second after arc start and feature an internally adjustable autodarkening shade (#9–12), lens sensitivity, and delay controls. The Blue Flame model features metallic blue flames outlined with a green classic pinstripe. The Avenger model features three-dimensional silver metallic highlights outlined by a red pinstripe on a gloss black background. All the XTV Series designs have a 3.74 × 1.57-in. viewing area with two independent arc sensors that provide continuous arc-sensing capability. The helmets feature a solar-assisted autodarkening lens and two easy-to-replace AAA batteries, with a life of 2000 h on GMAW, no recharging required. In addition, the helmets are lightweight, weighing in at 1 lb, comfortable, and come with five external and two internal protective lens covers. Ratchet-style headgear adjusts for size and features a CoolMax® odor-absorbing sweatband.

Hobart Welders 104
PO Box 100, Lithonia, GA 30058

Downdraft Tables Require No External Exhaust

The Extreme Air downdraft tables are self-contained and do not require external exhaust hoses. Designed for applica-

— *continued on page 25*

— *continued from page 23*

tions such as welding, grinding, and soldering, they draw contaminants away from the worker's vision and breathing zones, and reduce hazards to workers in surrounding areas. The tables feature 99.99% efficient cartridge filters. Additionally, they come with a built-in tool tray, an energy-efficient EPACT motor, and the RotoPulse™ cartridge cleaning system.

Micro Air **105**
2009 S. West St., Wichita, KS 67213

Liner Available in Longer Lengths

The company has introduced the addition of longer lengths to its Tough Gun® Quick Load Liner™ product offering. The liner, which loads from the front of the GMAW gun, can be purchased in lengths of up to 15 ft for robotic applications. It is also available for semiautomatic applications in lengths of up to 25 ft. The two-piece system allows the installation to occur through the gooseneck of the torch, while the torch remains attached to the feeder.

Tregaskiss Ltd. **106**
2570 N. Talbot Rd.
Oldcastle (Windsor), ON, Canada N0R 1L0

Head Welds Stainless Steel, Titanium Tubes

The M45 weld head has been designed to weld thin-walled stainless steel return bends to tubes fitted into heating and cooling equipment. It allows this task to be car-

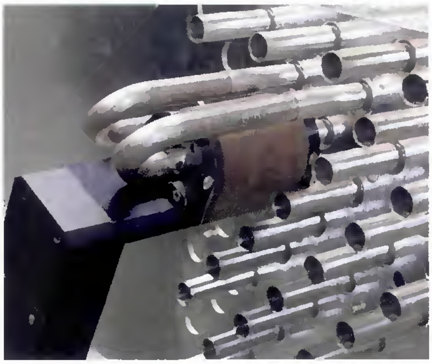

ried out using a precision orbital welding power supply. The heads are controlled with closed-loop servos, and parameters are monitored 500 times per second to provide a precise and accurate control of the weld profile. It can be used for tubes that are flush, recceded, or protruding from the tube plate, and the tungsten can be angled to suit the specific application. Because the welding arc is contained in an enclosed chamber, which is filled with inert gas, the weld head can be used to weld stainless steel, nickel alloys, and titanium tubes.

Orbimatic (UK) Ltd. **107**
7 Manor Grove Centre, Vicarage Farm Rd.,
Peterborough, PE1 5UH, UK

Flexible Heat Gun Offers Multiple Speeds

The H1600 heat gun features a 13-A motor with a double fan for sustained power. The easy-to-clean air filter keeps debris away from the motor and extends tool life. Airflow and temperature are easily adjusted with one hand and nonslip pads allow users to stand the tool on end for stationary use. The heat gun offers airflow rates of 8.8, 12.4, and 17.7 ft^3/min, and air temperatures of 120°, 660°, and 1000°F. It weighs 2 lb and measures 11¼ in.

Metabo Corp. **108**
1231 Wilson Dr., West Chester, PA 19380

— *continued on page 27*

— *continued from page 25*

Stainless Steel Spray Coatings Resist Scratching

STEEL IT® antirust stainless steel spray coatings resist chipping and scratching. They are formulated to withstand chemicals, solvents, salt spray, UV light, detergents, and high-pressure power washing. The coatings feature a 316 stainless steel leafing pigment that carries a metallic barrier. They also exhibit 2H pencil hardness, are USDA approved, and can last up to 10 years, depending on the environment. The coatings frequently eliminate the need for breaking down a production line to repaint and are offered in cans for aplication by brush or roller.

Stainless Steel Coatings, Inc. **109**
835 Sterling Rd./PO Box 1145, S. Lancaster, MA 01561

Cutting Attachment Makes Clean, Bevel Cut

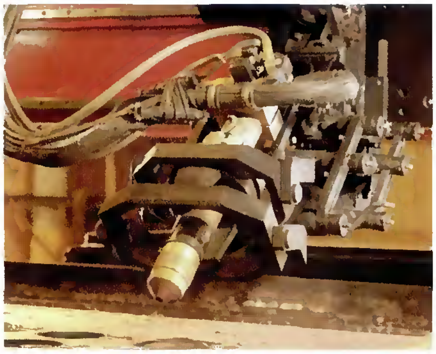

The 3D-Link contour plasma bevel cutting attachment is a new option for the

— *continued on page 103*

Friction Stir Welding After a Decade of Development

It's not just welding anymore

BY WILLIAM J. ARBEGAST

Friction stir welding (FSW) is an innovative solid-state welding process invented in 1991 by The Welding Institute (TWI) (Ref. 1). Friction stir welding represents one of the most significant developments in joining technology over the last half century. The initial development by TWI and its industrial partners under various Group Sponsored Projects focused on single pass, complete joint penetration of arc weldable (5XXX and 6XXX) and unweldable (2XXX and 7XXX) aluminum alloys up to 1 in. thick.

By 1995, FSW had matured to a point where it could be transitioned and implemented into the U.S. aerospace and automotive markets. The many advantages of FSW compared to conventional arc welding have repeatedly been demonstrated with both improved joint properties and performance. Often, production costs are significantly reduced. Other times, FSW enables new product forms to be produced or skilled labor freed to perform other tasks. Research and development efforts over the last decade have resulted in improvements in FSW and the spin-off of a series of related technologies.

Introduction

In the 1920s and 1930s, arc welding replaced rivets as the joining method for pressure vessels. Weld usage expanded through the 1940s with application to buildings, structures, and ships. By 2006, arc welding has evolved into an international industry complete with welder education and certification programs and governed by extensive specifications, design criteria, and standards. A 2002 survey by the American Welding Society (AWS) estimated that U.S. manufacturing industries spend more than $34.4 billion annually on arc welding of metallic materials with an anticipated growth rate averaging 5 to 15% per year. The construction, heavy manufacturing, and light manufacturing industries make up the majority with $25 billion in annual expenditures. Industry-wide repair and maintenance of welded structures are estimated to cost $4.4 billion annually. In doing so, these industries are a major consumer of energy and a producer of airborne emissions and solid waste.

Conventional arc welding of metals creates a structural joint by local melting and subsequent solidification. This normally requires the use of expensive consumables, shielding gas, and filler metal. The melting of materials is energy intensive and solidifying metals are often subject to cracking, porosity, and contamination. Undesirable metallurgical changes can occur in the cast nugget due to alloying with filler metals, segregation, and thermal exposure in the heat-affected zones. These may result in degraded joint strengths, extensive and costly weld repairs, and unanticipated in-service structural failures. Solid-state (nonmelting) joining avoids these undesirable characteristics of arc welding.

Implementation Incentives

Friction stir welding is one such nonmelting joining technology that has produced structural joints superior to conventional arc welds in aluminum, steel, nickel, copper, and titanium alloys. Friction stir welding produces higher strength, increased fatigue life, lower distortion, less residual stress, less sensitivity to corrosion, and essentially defect-free joints compared to arc welding. Since melting is not involved, shielding gases are not used during FSW of aluminum, copper, and NiAl bronze alloys while argon gas may be used during FSW of the higher-temperature ferrous and nickel alloys, mainly to protect the ceramic and refractory pin tools from oxidation. Simple argon environmental chambers and trailing shields are used during FSW of titanium alloys to minimize interstitial pickup and contamination. Expensive consumables and filler metals are not required. An excellent state-of-the-art review of FSW technology is provided by Mishra and Ma (Ref. 2).

Friction stir welding researchers and producers (AJT, Inc.) estimate that if 10% of the U.S. joining market can be replaced by FSW, then 1.28×10^{13} Btu/year energy savings and 500 million lb/year greenhouse gas emission reductions can be realized. Hazardous fume emissions during the FSW of high-temperature and

WILLIAM J. ARBEGAST (William.arbegast@sdsmt.edu) *is director, NSF Center for Friction Stir Processing, South Dakota School of Mines and Technology, Rapid City, S.Dak.* (http://ampcenter.sdsmt.edu).

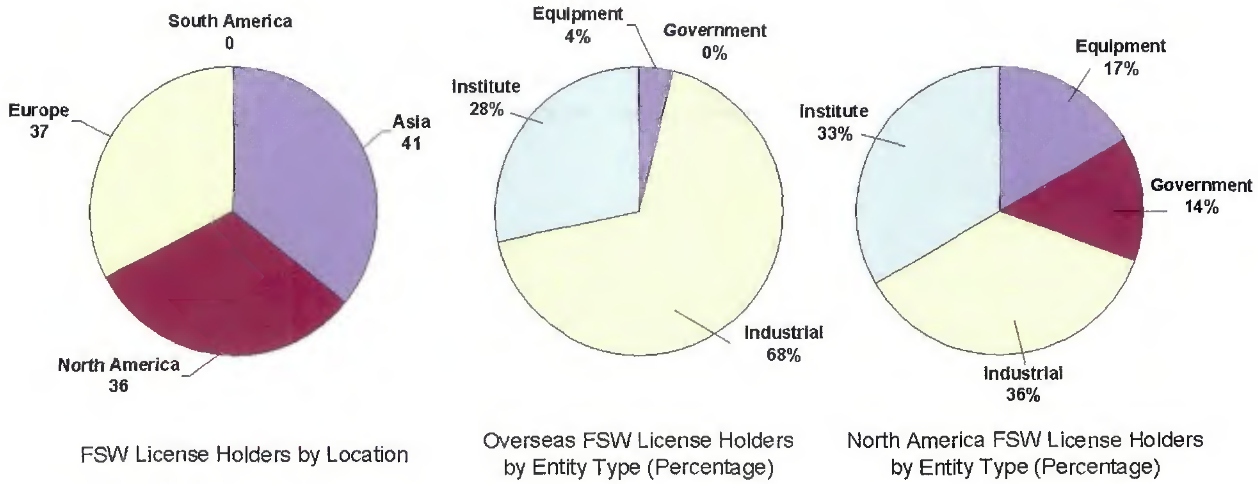

Fig. 1 — Demographics of FSW licensees as of January 2005 (Source: TWI).

chromium-containing alloys are eliminated. Rockwell Scientific reports emission levels of Cr, Cu, Mn, and Cr^{+6} (<0.03, <0.03, <0.02, and <0.01 mg/mm^3, respectively) during FSW of ferrous alloys considerably lower than those measured during GTAW (0.25, 0.11, 1.88, and 0.02 mg/mm^3, respectively). The simplified processing, higher structural strength, increased reliability, and reduced emissions of FSW are estimated to create annual economic benefit to U.S. industry of more than $4.9 billion/year.

Fig. 2 — Edison Welding Institute used a combination of friction stir welding, GMAW, and hybrid laser beam welding to fabricate this demonstration article from thick-section titanium plates. FSW was used to join the 0.50-in.-thick plates in a corner joint configuration (arrows) to establish the basic shape of the article, and GMAW and hybrid laser beam welding were used to complete the assembly. Courtesy of Edison Welding Institute.

Barriers to Implementation

The aeronautic and aerospace industries represent less than 1% ($300 million) of the total U.S. annual welding expenditures since mechanical fastening is the joining method of choice. However, the bulk of FSW development dollars has been spent by these sectors. As a result, the broader industrial market for FSW implementation has been neglected.

As of January 2005, there were 114 FSW licenses granted by TWI — Fig. 1. These were almost equally split between North America (36), Europe (37), and Asia (41) with no reported licensees in South America. Overseas, 68% of the licensees are industrial while only 36% of the North America licensees are industrial and the remaining 64% are held by government laboratories, equipment manufacturers, and academic and research institutes. This suggests that industrial implementation of the FSW process in the United States is lagging behind the overseas industries.

Several overriding issues have been identified as barriers to more extensive FSW implementation in U.S. markets.

- Lack of industry standards and specifications
- Lack of accepted design guidelines and design allowables
- Lack of an informed workforce, and,
- The high cost of capital equipment.

In 1998, the AWS D17J Subcommittee on Friction Stir Welding for Aerospace began development of a specification for friction stir welding to address these issues. Acceptance and release is anticipated in the near term. In the meantime, most FSW users have developed internal specifications for application to their products. In 2002, AJT, Inc., secured American Bureau of Shipping (ABS) approval to use FSW in marine applications.

These barriers to broader market implementation in the United States are also being addressed through national FSW research programs and various successful industrial implementations.

Research Programs

In 2004, the Center for Friction Stir Processing (CFSP), a National Science Foundation Industry/University Cooperative Research Center (NSF I/UCRC), was established to bring the South Dakota School of Mines and Technology (SDSMT), University of South Carolina (USC), Brigham Young University (BYU), and the University of Missouri-Rolla (UMR) together in a collaborative FSW research program. The CFSP currently has 22 government laboratory and

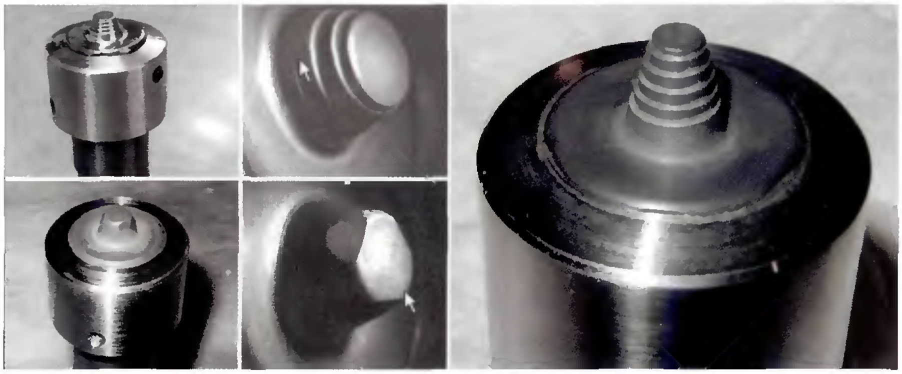

Fig. 3 — 0.25 in. tapered with flats (left, bottom), 0.25-in. stepped spiral (left, top), and 0.500-in. stepped spiral high-temperature PCBN FSW pin tools. Courtesy of MegaStir, Inc.

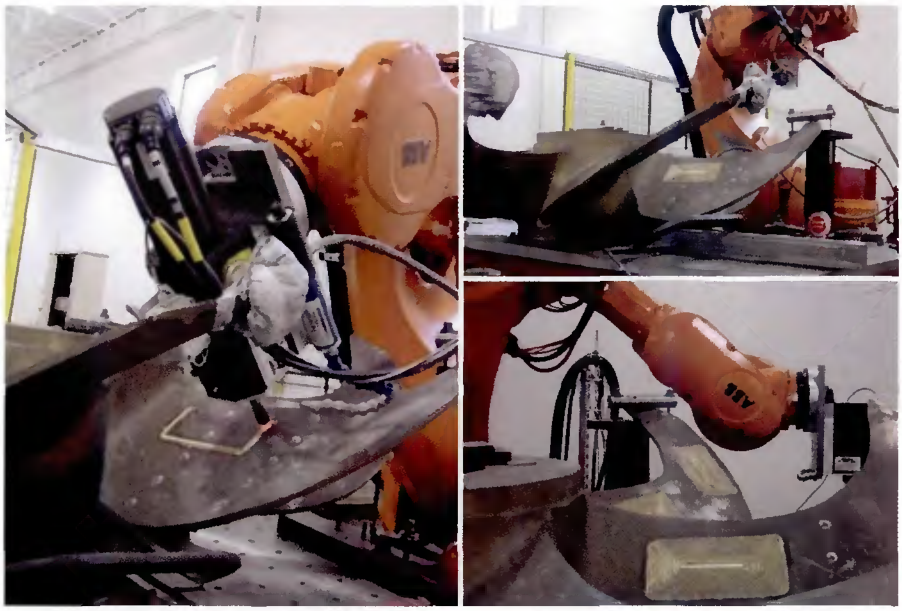

Fig. 4 — Friction Stir Link, Inc., robotic FSW system processing large areas of NiAl bronze propellers to remove near-surface casting defects. Courtesy of Rockwell Scientific.

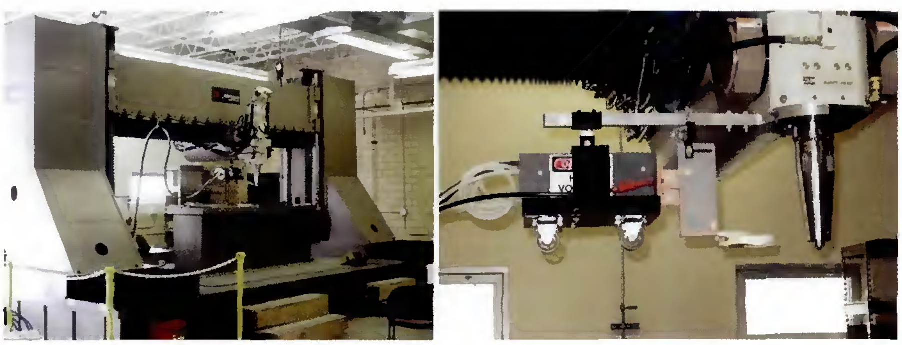

Fig. 5 — MTS ISTIR 10 friction stir weld system (left) with the Ameritherm 20-kW remote heat station and induction preheating coil (right). Courtesy of South Dakota School of Mines.

industrial sponsors. The center mission is to perform advanced and applied research, develop design guidelines and allowables, train scientists and engineers, and transfer the FSW technology into a broader base within the industrial sector. Current research programs at the CFSP include the following:

- Design allowables and analysis methodologies for FSW beam and skin stiffened panel structures
- Intelligent FSW process control algorithms
- Thermal management of titanium and aluminum FSW for property control
- Microstructural modification of aluminum and magnesium castings
- FSW of HSLA and 4340 steels
- FSW of austenitic steels and Inconel® alloys
- Interactive database of FSW properties and processing parameters

The CFSP has also teamed with Iowa State University Center for Nondestructive Evaluations (CNDE) to assess the effects of defects in aluminum alloy FSW. The probability of detection (POD) of various nondestructive examination (NDE) methods are being established for the volumetric and geometric characteristic discontinuities and the relationship between flaw size and reduction in static strength and fatigue life are being determined. Statistical process control (SPC) methods are being developed based on process force and torque responses in frequency space and are being compared to the POD of the NDE methods.

The Edison Welding Institute Navy Joining Center (NJC) has continued to develop and demonstrate FSW technologies in thick-section aluminum and titanium alloys for a variety of DOD applications. One recent technology demonstration program at the NJC used a combination of FSW, GMAW, and hybrid laser beam welding to fabricate a large titanium structure from 0.50-in.-thick Ti-6Al-4V plates — Fig. 2. In this assembly, the initial corner joints were friction stir welded from the outside of the structure to establish the basic shape, with the remaining structure assembled using GMAW and hybrid laser welding.

Under a recently completed DARPA program, Rockwell Scientific and the NAVSEA Carderock Surface Warfare Center, in conjunction with 13 university and industrial partners, performed extensive development of friction stir processing on Al-, Cu-, Mn-, and Fe-based alloys. Within this program, MegaStir developed an advanced grade of polycrystalline cubic boron nitride (PCBN) capable of FSW of ferrous alloys up to 0.500 in. thick — Fig. 3. The fracture toughness of the PCBN is sufficiently high to allow features to be machined on the tool pin, thus accommodating material flow around the tool to fill the cavity in the tool's wake.

Also, this same DARPA program demonstrated the ability to friction stir process large areas on the surface of complex-shaped propellers using large industrial robotic FSW systems provided by Friction Stir Link, Inc. — Fig. 4. Friction stir processing eliminates near-surface casting discontinuities, increases the yield strength (>2X), and increases fatigue life (>40%) compared to as-cast NiAl bronze. In addition, FSW equipment manufacturers (General Tool Corp.) are exploring alternatives to high-cost multifunctional FSW equipment by developing lower-cost, dedicated, single-purpose systems.

A new national FSW task coordinated by Boeing is being launched under the next-generation manufacturing technology initiative (NGMTI). The NGMTI program is designed to accelerate the development and implementation of breakthrough manufacturing technologies to support the transformation of the defense industrial base and to increase the global economic competitiveness of U.S.-based manufacturing. This FSW task will bring together the DOD Tri-Services, JDMTP, DLA, FAA, NASA, and DOE with a large contingent of industrial and university partners to perform enabling and applied research to correct overriding implementation barriers, and, to perform ManTech-type demonstrations to accelerate industrial and government acceptance and implementation of friction stir welding.

A second NGMTI FSW task, coordinated by Friction Stir Link, Inc., in conjunction with the University of Wisconsin, is being developed to provide a low-mass, low-power, and high-mobility robotic FSW system. Friction Stir Link has been developing robotic FSW and friction stir spot welding (described later) for a variety of automotive and commercial applications. Integrating the FSW technology with robotics allows for flexible manufacturing approaches and reductions in production costs.

Concurrent Technologies Corp. (CTC), through the Navy ManTech National Metalworking Center (NMC), has advanced the development of FSW in thick-section 5083, 2195, and 2519 aluminum for ground and amphibious combat vehicles. Several large-scale prototypes have been completed. The work by CTC and NMC has provided a valuable transition of the technology from subscale laboratory work to full-scale prototype construction — the last major step before production implementation.

Process Innovations

Innovations to the FSW process are ongoing. Since 1995, more than 50 U.S. patents in FSW have been issued. Pin tool designs have evolved from those originally developed by TWI to unique designs for thick-section, lap joint, high-temperature, and fast travel speed joining. For example, in 2005, GKSS-GmbH reported that successful FSW at welding speeds in excess of 780 in./min in thin-gauge aluminum butt joints had been achieved.

In 1999, NASA Marshall Space Flight

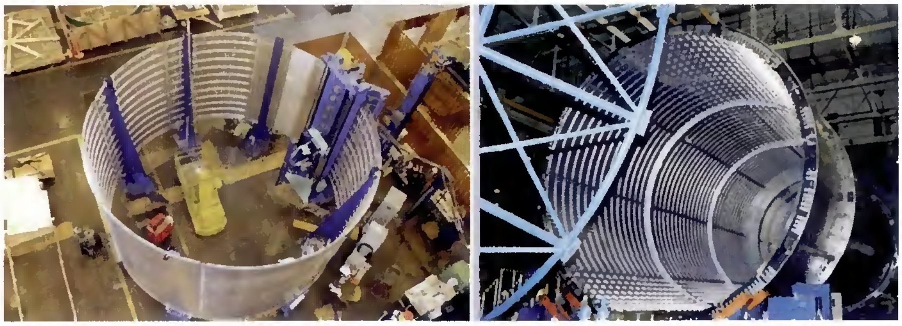

Fig. 6 — FSW process development tool at the Marshall Space Flight Center shown with a 27-ft-diameter LH_2 barrel segment of the 2195 Al-Li Space Shuttle external tank (left). Full-scale LH2 tank (right) at the NASA Michoud Assembly Facility in New Orleans. Courtesy of NASA MSFC.

Fig. 7 — The Eclipse 500 business class jet is currently in final FAA certification trials (left). The internal longitudinal and circumferential aluminum stiffeners (right, top) and window and door doublers (right, bottom) are attached to the aluminum fuselage section with friction stir welded lap joints. Courtesy of Eclipse Aviation.

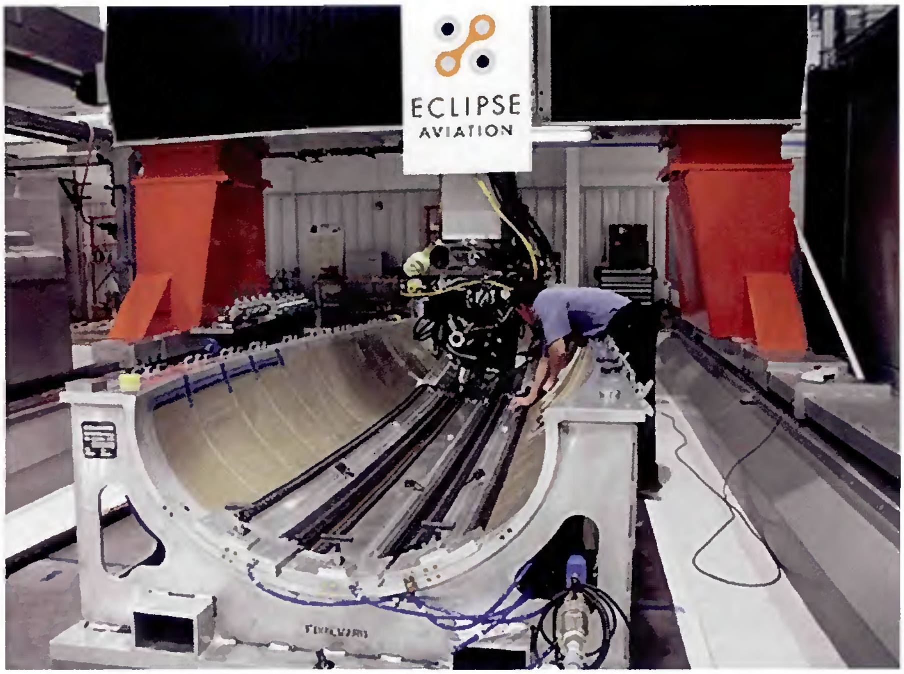

Fig. 8 — The friction stir welding equipment used to attach the stiffeners and doublers to the Eclipse 500 fuselage sections was designed and fabricated by MTS Systems Corp. It is capable of welding a variety of component geometries through the use of interchangeable holding fixtures located beneath the multiaxis FSW head and movable gantry frame. Courtesy of Eclipse Aviation.

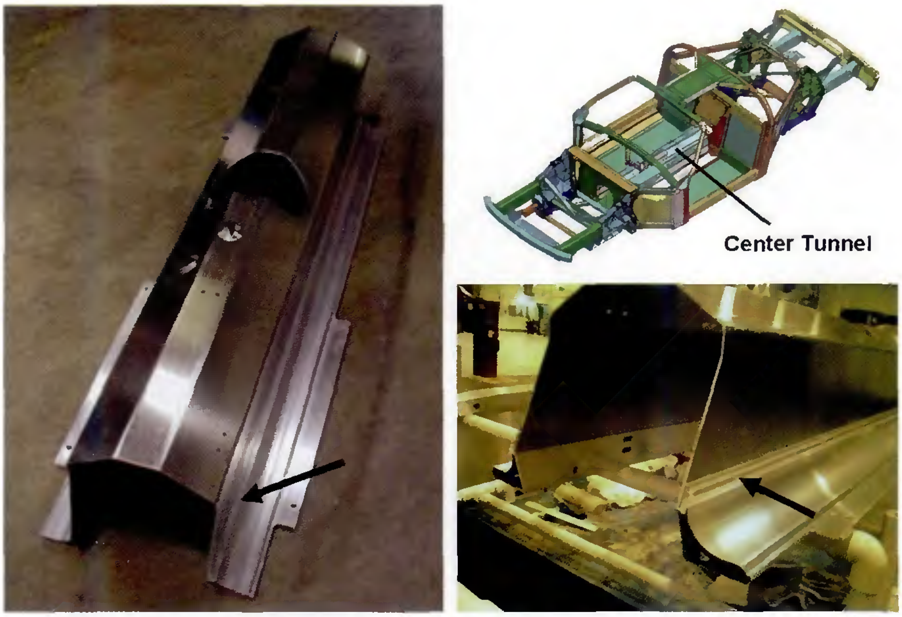

Fig. 9 — The central tunnel assembly of the Ford GT is a FSW assembly made from aluminum stampings and extrusions. Courtesy of Ford Motor Co.

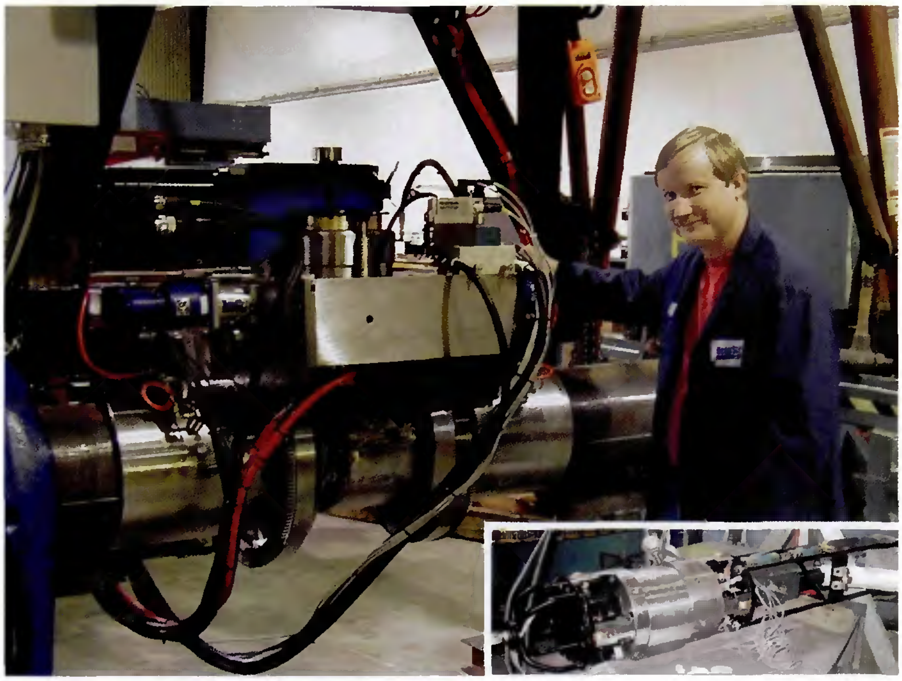

Fig. 10 — Prototype pipe welding system showing external FSW head and internal mandrel (inset). Courtesy of MegaStir, Inc.

Center (MSFC) and the Boeing Co. developed the retractable pin tool (Ref. 3) for FSW of tapered thickness joints. Marshall is currently investigating the use of very high rotation speed (>50,000 rpm) FSW, thermal stir welding (TSW), and the integration of ultrasonic energy during FSW to enable portable hand-held devices. Other researchers are also evaluating modifications to the FSW process. For example, the University of Missouri — Columbia is evaluating electrically enhanced friction stir welding (EEFSW) where additional heat is applied by resistance heating through the pin tool. The University of Wisconsin is developing laser-assisted friction stir welding (LAFSW) of aluminum lap joints where a laser is trained ahead of the pin tool to preheat the material.

Under a collaborative research program between the Army Research Laboratory (ARL) and the SDSMT Advanced Materials Processing and Joining Center (AMP), a variety of FSW technologies are being developed, including complex curvature FSW, friction stir spot welding (FSSW), dissimilar alloy FSW, low-cost fixturing and tooling, and thick-plate titanium and aluminum FSW. Prototypes of advanced fuselage structures (Boeing), helicopter beams (Sikorsky), and naval gun turret weather shields (BAE Systems) have been built. The AMP Center is also developing induction preheated friction stir welding (IPFSW) using an Ameritherm 20-kW remote heat station to preheat thick-plate aluminum, steel, cast iron, and titanium alloys to increase travel speeds, reduce process forces, and reduce pin tool wear — Fig. 5.

In 2001, MTS Systems Corp. patented the self-reacting pin tool technology (Ref. 4). This innovation allows the FSW of tapered joints and eliminates the need for back side anvil support to react the process loads. Lockheed Martin Space Systems and the University of New Orleans National Center for Advanced Manufacturing (NCAM) have demonstrated this self-reacting pin tool on the 27-ft-diameter domes of the Space Shuttle external tank. In this application, multiple gore sections of 0.320-in.-thick 2195 Al-Li were joined along a simple curvature path to create the full-scale dome assembly.

Industrial Implementations

The technology readiness level (TRL) for the FSW of aluminum alloys is high with successful industrial implementation and space flight qualification by Boeing on the 2014 aluminum propellant tanks of the Delta II and Delta IV space launch vehicles. Lockheed Martin and NASA MSFC have developed and implemented FSW on the longitudinal welds of the 2195 Al-Li liquid hydrogen and liquid oxygen barrel segments of the external tank for the Space Shuttle — Fig. 6. Lockheed Martin Missiles and Fire Control and the SDSMT have developed square box beams for mobile rocket launch systems that are fabricated from thick-wall "C" section extrusions joined by FSW to replace the current hollow, square tube extrusions. Airbus has announced the use of FSW in selected locations on the Airbus A350 and two new versions of the A340 (A340-500, A340-600).

In 2000, the Air Force Metals Affordability Initiative (MAI) brought together a consortium of industry and university partners to develop FSW for a variety of DOD applications. Under Task 1, Joining of Traditional Aluminum Assemblies, Lockheed Martin completed a development program that replaced the riveted aluminum floor structure of the C130J air transport with a FSW floor structure. Under Task 2, Joining of Complex Alu-

Fig. 11 — Joining of long lengths of contamination-free Ti-6Al-4V are possible with "out of chamber" friction stir welding using shrouds and trailing shoe shielding gas systems. Courtesy of Lockheed Martin Space Systems.

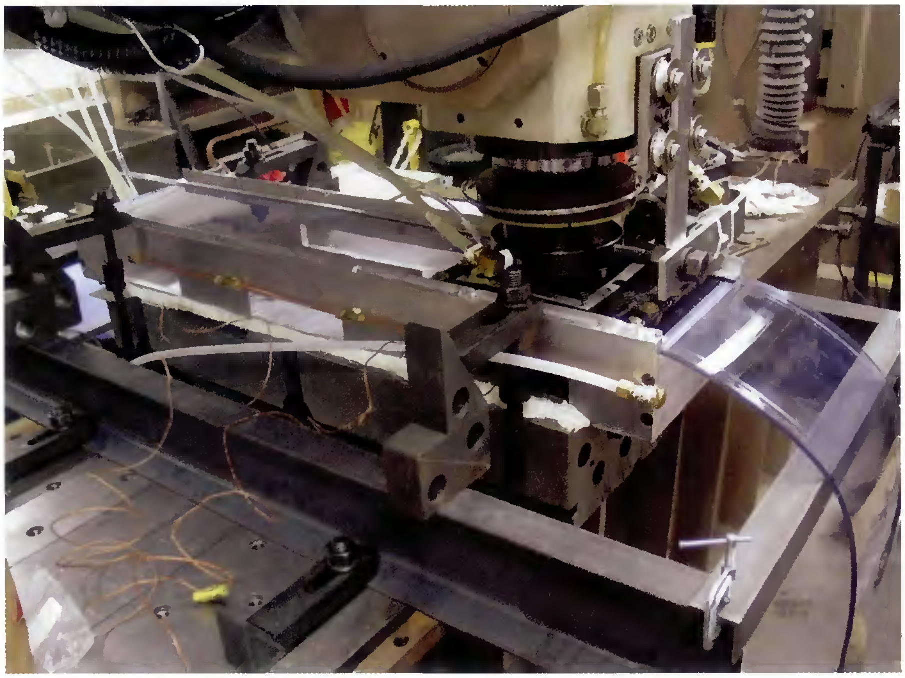

Fig. 12 — Environmental chambers are used to provide an argon atmosphere and to minimize interstitial contamination in titanium FSW. Courtesy of South Dakota School of Mines.

minum Assemblies, Boeing developed a FSW cargo "slipper" pallet and implemented a FSW cargo ramp toenail on the C17 transport. The toenail is the only known friction stir welded part flying on a military aircraft. Under Task 3, Hard Metals Joining Development, the Edison Welding Institute and the General Electric Corp. (Engines Div.) developed high-temperature pin tools for the FSW of steel, titanium, and Inconel® alloys for aircraft engine applications.

Eclipse Aviation is in final FAA certification for the Eclipse 500 business class jet. First customer deliveries are scheduled for 2006. Friction stir welded lap joints are used as a rivet replacement technology to join the longitudinal and circumferential internal stiffeners to the aft fuselage section and to attach doublers at window and door cutout locations — Fig. 7. The use of FSW eliminates the need for thousands of rivets and results in better quality and stronger and lighter joints at reduced assembly costs. MTS Systems Corp. designed and fabricated the custom FSW equipment and production tooling for Eclipse Aviation. This equipment permits welding complex curvatures over many sections of the fuselage, cabin, and wing structures at travel speeds in excess of 20 in./min — Fig. 8. Because the process is faster than more conventional mechanical joining processes, production cycle time is significantly reduced.

Over the last three years, the Ford Motor Co. has produced several thousand Ford GT automobiles with a FSW central tunnel assembly — Fig. 9. This tunnel houses and isolates the fuel tank from the interior compartment and contributes to the space frame rigidity. The top aluminum stamping is joined to two hollow aluminum extrusions along the length of the tunnel using a linear FSW lap joint. The use of FSW results in improved dimensional accuracy and a 30% increase in strength over similar GMA welded assemblies.

The TRL for FSW of ferrous, stainless steel, nickel, copper, and titanium alloys is also high with a variety of full-scale demonstration programs completed. MegaStir, Inc., has developed an improved grade of the polycrystalline cubic boron nitride (PCBN) high-temperature pin tools (HTPT) that has shown an acceptable service life for welding steels, nickel, and copper alloys.

In 2004, MegaStir, Inc., completed a prototype oil field pipeline FSW demonstration program that successfully joined 12-in.-diameter x 0.25-in. wall thickness X-65 steel pipe segments using an automated internal mandrel and external FSW tooling system — Fig. 10.

Chemical compatibility issues arise when welding titanium alloys with the PCBN pin tools. The University of South Carolina has shown the suitability of tungsten-rhenium (W-Re) HTPT for most titanium alloys. However, issues with pin tool wear and excessive metal adhesion still arise when welding Ti-6Al-4V. This is possibly due to reactions between the rhenium in the pin tool and the vanadium alloying elements in the titanium. Other refractory HTPT materials, such as tungsten-iridium (W-Ir), are under development at the Oak Ridge National Laboratory.

In 2005, Lockheed Martin staff performed FSW on 0.20-in.-thick Ti-6Al-4V sheets using dispersion-strengthened tungsten HTPT that alleviated the sticking problem and allowed for many meters of welding — Fig. 11. They report that the joint efficiency ranged from 98 to 100% of base metal strength at testing

Fig. 13 — Use of the plunge friction spot welding (PFSW) method on the Mazda RX-8 rear door structure provides for structural stability against side impact and five-star rollover protection at reduced production costs. Courtesy of Mazda Motor Corp.

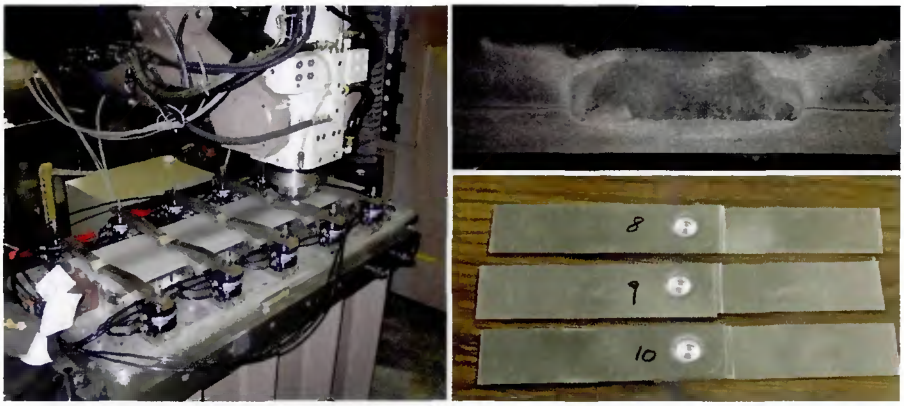

Fig. 14 — Refill friction spot welding (RFSW) using MTS ISTIR 10 system and custom-designed head adapter (left). RFSW lap shear coupons (right, bottom) and metallurgical cross section of RFSW showing complete joint penetration in 0.080-in.-thick 7075-T73 aluminum (right, top). Courtesy of South Dakota School of Mines.

temperatures ranging from –320° to 500°F. Titanium FSW produced at the CFSP using custom-designed environmental chambers and an argon atmosphere (Fig. 12) showed no evidence of surface discoloration or interstitial (O, N, and H) contamination.

Friction Stir Spot Welding

If FSW is considered as a "controlled path extrusion" rather than a "welding" process, several spin-off technologies can be realized. Friction stir spot welding (FSSW) has been in development over the last five years and has seen industrial implementation as a rivet replacement technology. Currently, two variations to FSSW are being used. The "plunge" friction spot welding (PFSW) method was patented by Mazda in 2003 (Ref. 5) and the "refill" friction spot welding (RFSW) method was patented by GKSS-GmbH in 2002 (Ref. 6).

In the Mazda PFSW process, a rotating fixed pin tool similar to that used in linear FSW is plunged and retracted through the upper and lower sheets of the lap joint to locally plasticize the metal and stir the sheets together. Even though this approach leaves a pull-out hole in the center of the spot, the strength and fatigue life is sufficient to allow application at reduced production costs on the Mazda RX-8 aluminum rear door structure — Fig. 13. Since 2003, Mazda has produced more than 100,000 vehicles with this PFSW rear door structure. These PFSW doors provide structural stability against side impact and impart five-star rollover protection.

The GKSS RFSW is being developed at the SDSMT AMP Center under license to RIFTEC-GmbH. This process uses a rotating pin tool with a separate pin and shoulder actuation system that allows the plasticized material initially displaced by the pin to be captured under the shoulder during the first half of the cycle and subsequently reinjected into the joint during the second half of the cycle. This completely refills the joint flush to the surface — Fig. 14. In addition to development as a rivet replacement technology for aerospace structures, RFSW is also being developed as a tacking method to hold and restrain parts during welding by linear FSW.

Friction Stir Joining

Friction stir joining (FSJ) of thermoplastic materials uses the controlled path extrusion characteristics of the process to join 0.25-in.-thick sheets of polypropylene (PP), polycarbonate (PC), and high-density polyethylene (HDPE) materials. Recent work at Brigham Young University has shown joint efficiencies for these materials ranging from 83% for PC to 95% for HDPE and 98% for PP. These joint efficiencies compare favorably with other polymer joining methods such as ultrasonic, solvent, resistance, hot plate, and adhesive bonding. Current work at the SDSMT AMP Center in collaboration with the Air Force Research Laboratory - Kirtland is investigating the use of FSJ to join fiber-, particulate-, and nanoparticle-reinforced thermoplastic materials.

Friction Stir Processing

Friction stir processing (FSP) uses the controlled-path metalworking characteristics of the process to perform metallurgical processing and microstructural modification of local areas on the surface of a part. In 1997, FSP was used by Lockheed Martin to perform microstructural modification of the cast structure of 2195 Al-Li VPPA welds to remove porosity and hot short cracks. This also improved room-temperature and cryogenic strength, fatigue life, and reduced the sensitivity to intersection weld cracking by crossing VPPA welds (Ref. 7).

In 1998, the DOE Pacific Northwest National Laboratory (PNNL) began investigating the processing of SiC powders into the surfaces of 6061 aluminum to increase wear resistance. Initial studies showed that both SiC and Al_2O_3 could be emplaced into the surface of bulk materials to create near-surface-graded MMC structures. The University of Missouri-Rolla (UMR) has shown that a uniform SiC particle distribution can be achieved

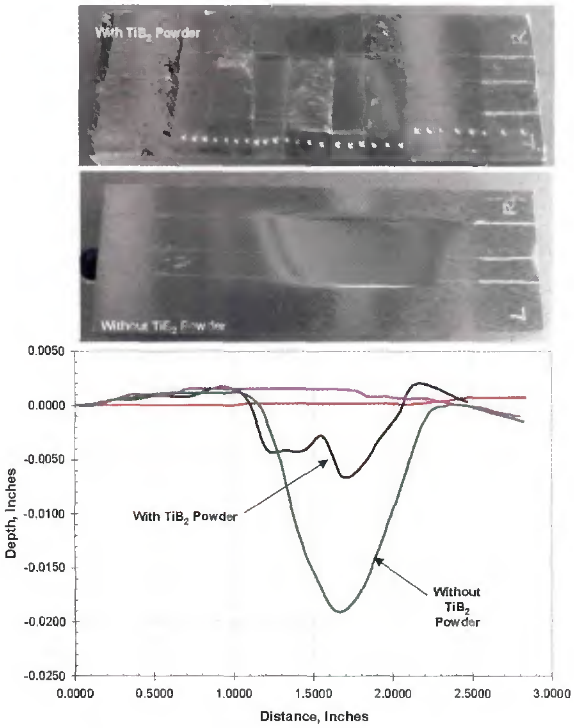

Fig. 15 — Grade 40 gray cast iron ASTM G65 wear test results. Friction stir processing TiB_2 particles into the surface resulted in a fourfold increase in ASTM G65 dry abrasive wear resistance over that seen in samples without TiB_2 particles. Courtesy of South Dakota School of Mines.

with appropriate tool designs and techniques, leading to significant increases in surface hardness.

In 2004, a PNNL/SDSMT AMP Center collaborative research program investigated increasing the wear resistance of heavy vehicle brake rotors by processing TiB_2 particles into the surface of Class 40 gray cast iron. This resulted in a fourfold increase in the dry abrasive wear resistance when tested per ASTM G65 — Fig. 15. PNNL and Tribomaterials, LLC have performed subscale brake rotor/pad wear tests on FSP/TiB_2 cast iron rotors. These subscale brake tests have shown that FSP/TiB_2 processed brake rotors have improved friction characteristics and wear resistance over baseline heavy-vehicle brake friction pairs.

Friction stir reaction processing (FSRP) was also investigated under this PNNL/ SDSMT FSP/TiB_2 program. Friction stir reaction processing uses the high temperatures and strain rates seen during processing to induce thermodynamically favorable in-situ chemical reactions on the surface to a depth defined by the pin tool geometry and metal flow patterns. This provides an opportunity for innovative processing methods to create new alloys on surfaces of materials and locally impart a variety of chemical, magnetic, strength, stiffness, and corrosion properties.

Studies performed at the University of Missouri-Rolla in conjunction with Rockwell Scientific have shown FSP to produce a fine grain size material and create low-temperature, high-strain rate superplasticity in aluminum and titanium alloys. Pacific Northwest National Lab is currently investigating the application of this FSP-induced superplasticity in the fabrication of large integrally stiffened structures.

Summary

Friction stir welding (FSW) has matured since its introduction into the U.S. market in 1995. The technology readiness level for aluminum alloys is high with several industrial implementations. While development efforts and property characterizations have shown that FSW can be used in ferrous, stainless, nickel, copper, and titanium alloys, an industrial champion is needed.

The metalworking nature of the process leads to the plunge (PFSW) and refill (RFSW) friction stir spot welding (FSSW) methods with properties comparable to riveted and resistance spot welded joints. The use of friction stir processing (FSP) to locally modify the microstructure of arc welds and castings has been shown to increase strength, improve fatigue life, and remove defects. Using FSP to stir particulate materials into the surface has shown increased wear resistance and creates particulate-reinforced surface layers. Friction stir reaction processing (FSRP) can be used to create new materials and alloy combinations on part surfaces.

The higher-strength, nonmelting, and environmentally friendly nature of the FSW process has shown cost reductions in a variety of applications and has enabled new product forms to be developed. Only a small percentage of the U.S. welding and joining market has been targeted for implementation. A variety of government, industry, and university collaborations are underway to accelerate the development and implementation of FSW and FSSW into these markets.

During the last decade, the defense and aerospace sectors have taken the lead in implementing FSW. Recent advances in pin tool designs and optimized processing parameters have enabled FSW and FSSW applications in the marine, ground transportation, and automotive industries. Further innovations in low-cost equipment and the development of industry standards, design guidelines, and a trained workforce will enable the introduction of FSW and FSSW into the broader light manufacturing, heavy manufacturing, and construction industries during the next decade. ♦

Acknowledgments

Contributions to this article were received from Gilbert Sylva and Mike Skinner (MTS Systems Corp.), Glenn Grant (PNNL), Brent Christner (Eclipse Aviation), Doug Waldron (AJT, Inc.), Jeff Ding (NASA MSFC), Tim Trapp (EWI), Tracy Nelson and Carl Sorensen (BYU), Tony Reynolds (USC), Zach Loftus (Lockheed Martin), Murray Mahoney (Rockwell Scientific), John Baumann (Boeing), Raj Talwar (Boeing), Dana Medlin (SDSMT), Anil Patnaik (SDSMT), Casey Allen (SDSMT), Rajiv Mishra (UMR), Chuck Anderson (ATI, Inc.), John Hinrichs (Friction Stir Link, Inc.), Kevin Colligan (CTC Corp.), Scott Packer (MegaStir), and Tsung -Yu Pan (Ford Motor Co.).

The research programs at the Center for Friction Stir Processing (CFSP) are conducted by the faculty and students at the SDSMT, BYU, UMR, and USC university sites and are funded under a grant from the National Science Foundation I/UCRC program office and the membership of the industrial and government partners. The research programs at the SDSMT Advanced Materials Processing and Joining Center are funded by the Army Research Laboratory, Air Force Research Laboratory- Kirtland, DOE Pacific Northwest National Laboratory, and the Edison Welding Institute.

References

1. Thomas, W .M. et al., Friction Stir Butt Welding, U.S. Patent No. 5,460,317.

2. Mishra, R.S., and Ma, Z.Y. 2005. Friction stir welding and processing. *Materials Science and Engineering* R50, pp. 1–78.

3. Ding, J., and Oelgoetz, P. 1999. Auto-Adjustable Pin Tool for Friction Stir Welding, U.S. Patent No. 5,893,507.

4. Campbell, Fullen, and Skinner. 2001. Welding Head, U.S. Patent No. 6,199,745.

5. Iwashita, T. et al., 2003. Method and Apparatus for Joining, U.S. Patent No. 6,601,751 B2.

6. Schilling, C., and dos Santos, J. Method and Device for Joining at Least Two Adjoining Work Pieces by Friction Welding, U.S. Patent Application 2002/0179 682.

7. Arbegast, W. J., and Hartley, P. J. 2001. Method of Using Friction Stir Welding to Repair Weld Defects and to Help Avoid Weld Defects in Intersecting Welds, U.S. Patent No. 6,230,957.

An Analysis of Resistance Spot Welding

A finite element model was used to obtain the thermal history of the process and temperature distributions, and to predict weld nugget size and HAZ width

BY ZHIGANG HOU, YUANXUN WANG, CHUNZHI LI, AND CHUANYAO CHEN

The resistance spot welding (RSW) process has been widely employed in sheet metal fabrication because of its high speed and suitability for automation. In this process, two metal sheets are compressed between a pair of water-cooled copper-alloy electrodes by an external applied force, then an electric current is passed through the sheets via the two electrodes to generate concentrated Joule heating at the contact surface. This results in a molten nugget forming at the intersection of the two sheets. After the current flow ceases, the electrode force is maintained for a short duration to allow the workpiece to rapidly cool and solidify.

Resistance spot welding is a complex process in which coupled interactions exist between electrical, thermal, mechanical, and metallurgical phenomena, and even surface behaviors. Because of this complexity, it is difficult to obtain insightful information on the welding process through experiments alone. On the other hand, the finite element method (FEM), which can deal with nonlinear behaviors and complex boundary conditions, provides a powerful tool for studying these interactions and has become the most important method for analysis of RSW.

Nied (Ref. 1) developed the first finite element (FE) model for RSW, and investigated the effect of electrode geometry on workpiece deformation and stresses. However, the model was restricted to elastic deformation and did not calculate the contact areas at the electrode-workpiece interface and faying surface. Afterward, many researchers developed more sophisticated FE models that considered temperature-dependent material properties, contact status, phase changing, and coupled field effects (Refs. 2–5). Recently, the iterative method was employed to simulate the interaction between coupled electrical, thermal, and structural fields (Refs. 6–8). Initially, the stress field and contact status were obtained from the thermomechanical analysis, and then the temperature field was obtained from the fully coupled thermoelectrical analysis based on the contact area at the electrode-workpiece interface and the faying surface. The calculated temperature field was then passed back to the thermostructural analysis to update the stress field and contact status.

Even if the iterative method provides the stress field, electric potential field, current density distribution, and the transient temperature history in one calculation, the modeling of the transient process with such a methodology would probably require a tremendous computing time. Therefore, a relatively simple method should be considered for analyzing a large, complex structure such as an automobile body component with thousands of welding spots.

The objective of this research is to develop a simplified method for predicting thermal behavior of the RSW process, and to prepare for further stress and strain analysis of the RSW proces for large complex structures. Transient thermal analysis of RSW was performed using the commercial FEM program *ANSYS*, and only the energy equation was consid-

ZHIGANG HOU (ythzg@163.com), *YUANXUN WANG, and CHUANYAO CHEN are with Huazhong University of Science and Technology, Wuhan, China. ZHIGANG HOU is also with Yantai University, Yantai, China, as is CHUNZHI LI.*

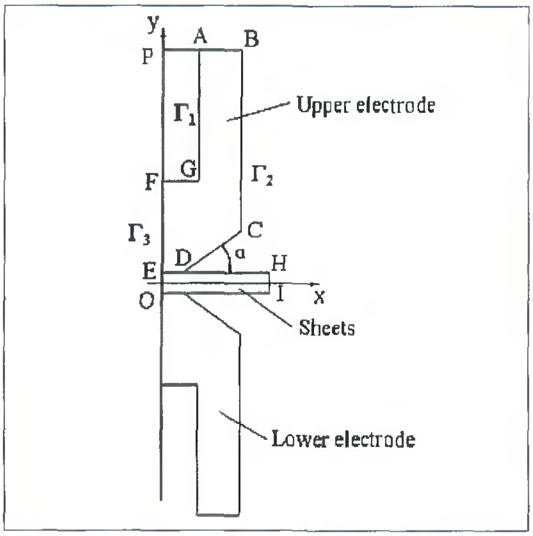

Fig. 1 — Schematic diagram of the RSW model.

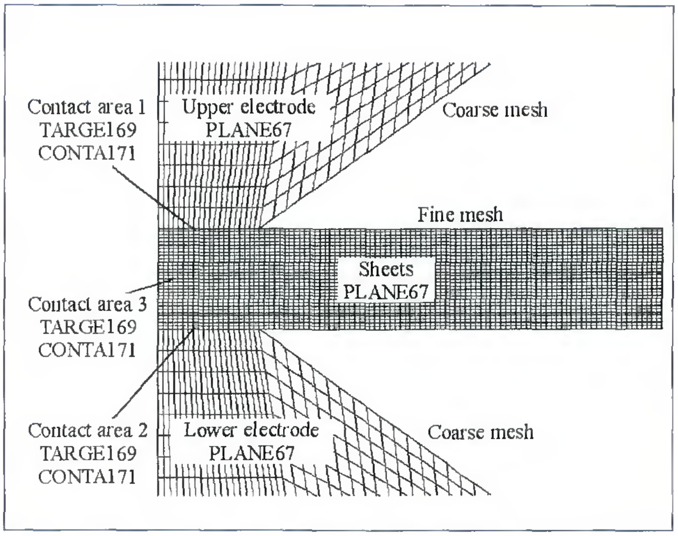

Fig. 2 — Mesh generation of the developed model.

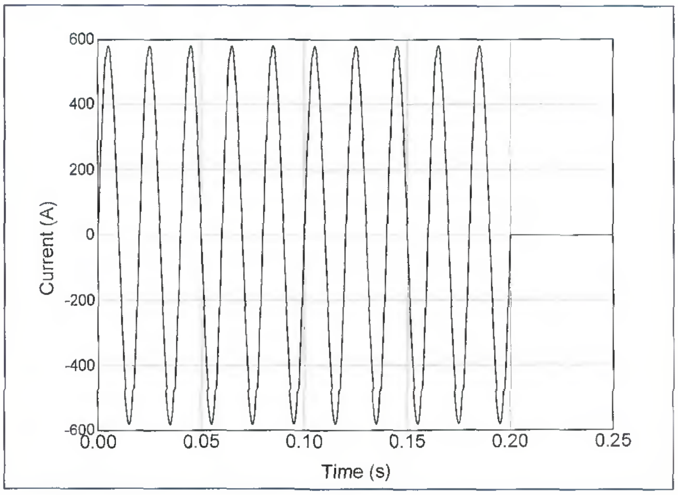

Fig. 3 — Pattern of input electric current.

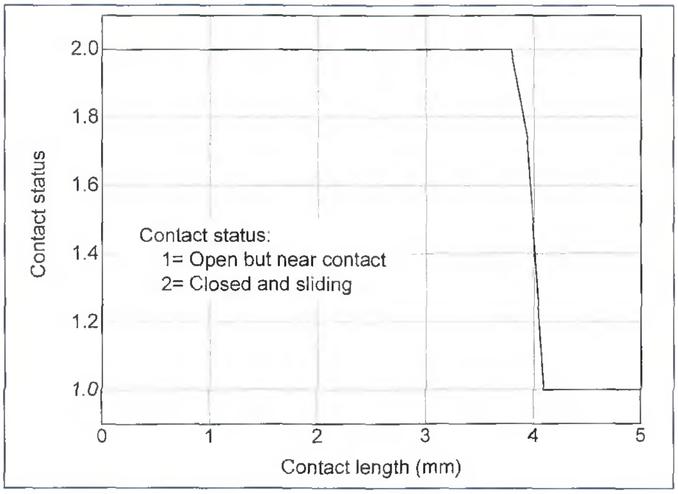

Fig. 4 — Contact status of the faying surface.

ered due to the limitation of thermal analysis. To keep the calculation accurate, temperature-dependent material properties, phase change, and coupled thermo-electrical field were taken into account. To reduce the computing time, the relation between temperature field and contact status was moderately simplified.

Computational Model

The transient thermal analysis of the RSW process in this research was modeled as an axisymmetric problem, as shown in Fig. 1. Figure 2 shows its mesh generation. The solid element was employed to simulate the thermoelectrical interaction, while the contact pair elements were employed to simulate the contact behaviors. There were three contact areas in the model. Contact areas 1 and 2 represented the electrode-workpiece interface; contact area 3 represented the faying surface. In order to obtain reliable results, fine meshes were generated near these contact areas, while other areas were relatively coarse.

Governing Equation and Boundary Conditions

The governing equation for axisymmetric transient thermal analysis is given by

$$\rho c\frac{\partial T}{\partial t}=\frac{\partial}{\partial r}\left(k\frac{\partial T}{\partial r}\right)+\frac{k}{r}\frac{\partial T}{\partial r}+\frac{\partial T}{\partial z}\left(k\frac{\partial T}{\partial z}\right)+q_v \quad (1)$$

Where ρ is the density of the material, C is the specific heat capacity, T is the temperature, t is the time, k is the thermal conductivity, and q_v is the rate of internal heat generation.

The following boundary conditions were specified on the model (since the model is also mirror symmetric about the faying surface, only values of the upper half are listed, see Fig. 1):

$$(AGF): -k\frac{\partial T}{\partial n}=h_w\left(T-T_w\right)$$

where h_w is the convection heat transfer coefficient of cooling water, T_w is the temperature of water.

$$(BCDHI): -k\frac{\partial T}{\partial n}=h_a\left(T-T_a\right)$$

where h_a is the convection heat transfer coefficient of ambient air, T_a is the temperature of air.

$$(OEF): -k\frac{\partial T}{\partial n}=0$$

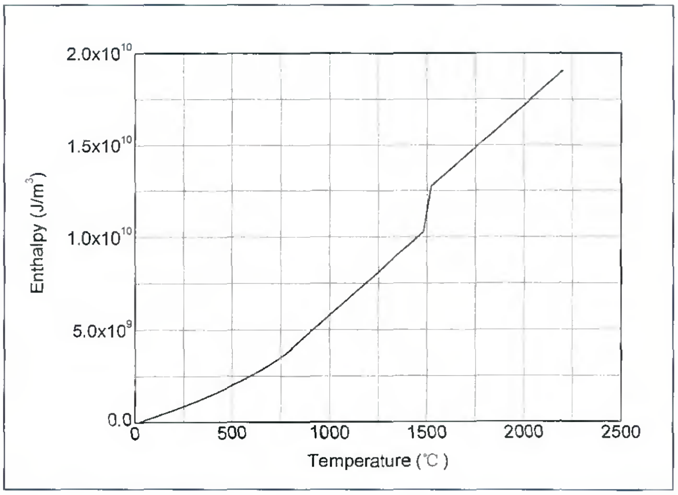

Fig. 5 — Enthalpy of mild steel.

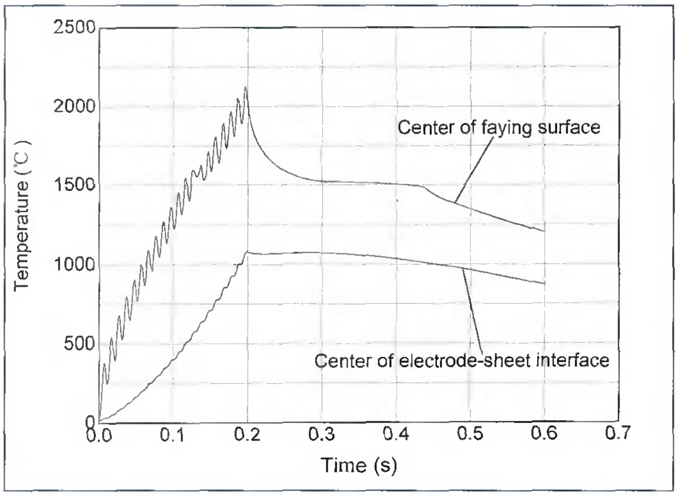

Fig. 6 — Temperature histories of two points.

Table 1 — Material Properties for the Simulation

Temp. °C	21	93	204	316	427	538	649	760	871	982	1093	1204	
Thermal conductivity	64.75	63.25	55.33	49.94	44.86	39.77	34.91	30.50	28.41	27.66	28.56		Mild steel
W/m-°C	390.3	380.6	370.1	355.1	345.4	334.9	320	315.5	310.3	305	300.1		Copper electrode
Resistivity	14.2	18.6	26.7	37.6	49.5	64.8	81.8	101.1	111.5	115.8	117.9	120.9	Mild steel
Ω m × 10^{-8}	2.64	3	4	5.05	6.19	6.99	8	8.98	9.48	9.98			Copper electrode
Temp. °C	21	93	204	316	427	538	649	732	760	774	799	1204	
Specific heat	443.8	452.2	510.8	561.0	611.3	661.5	762.0	1004	2386	1004	1189	1189	Mild steel
J/(kg-°C)	397.8	401.9	418.7	431.2	439.6	452.2	464.7		477.3			502.4	Copper electrode

Mild steel: Solidus, 1482°C; Liquidus, 1521°C; Latent heat, 2.72° × 10^5 J/kg; Density, 7800 kg/m^3
Copper electrode: Density, 8900 kg/m^3

Table 2 — Electric Contact Conductance of Faying Surface

Temp (°C)	ECC (1/(Ω m^2) × 10^8)
21	4.57
93	4.69
204	4.83
316	5.11
427	5.63
538	6.06
649	8.31
760	19.14
871	22.06
982	26.03
1093	31.69

Material Properties

All the thermal and electric properties of both the electrode and the workpiece, such as thermal conductivity, electric resistivity, specific heat, density, latent heat, and solidus and liquidus temperatures, are given in Table 1 (Refs. 9–11). Because the materials were subjected to a wide range of temperatures, these properties, except latent heat and density, were considered as temperature dependent.

Input Current

The input current in this simulation was 50-Hz sine wave AC of 12.2 kA, applied for 0.2 s (10 cycles). In order to simulate the cooling process of the welding, the input current was set to zero after 0.2 s, up to 0.6 s. The current was imposed as a nodal load on the top surface of the upper electrode (line AB in Fig. 1). Figure 3 shows the pattern of the input current.

Contact Resistance

Generally speaking, the contact resistance of the faying surface is a dependent function of load, temperature, and average yield strength of two contact materials. To simplify the problem, many researchers take the contact resistance as a function of temperature (Refs. 2, 6, 9). This simplification is reasonable since the load is constant in a specified RSW process; secondly, the yield strength of the materials, which determines the contact status in the contact area, is essentially influenced by temperature. Therefore, in this research, the temperature-dependent contact resistance was imposed at the faying surface contact area (contact line in a 2-D axisymmetric model). In the *ANSYS* program, the contact resistance is required to be input as electric contact conductance (ECC). Using the value of contact resistance obtained from the experiments (Ref. 9), the ECC of the faying surface was calculated and shown in Table 2.

During the RSW process, the contact length did not change very much, even if the contact status continuously changed because the yield strength of the materials changed with temperature. Therefore, a constant contact length was adopted in this research. Figure 4 shows typical contact status of the faying surface, where the contact status value 1 means the two surfaces were open but near contact, while value 2 means closed and sliding. According to the position that the contact status changed abruptly, the average contact length could be calculated.

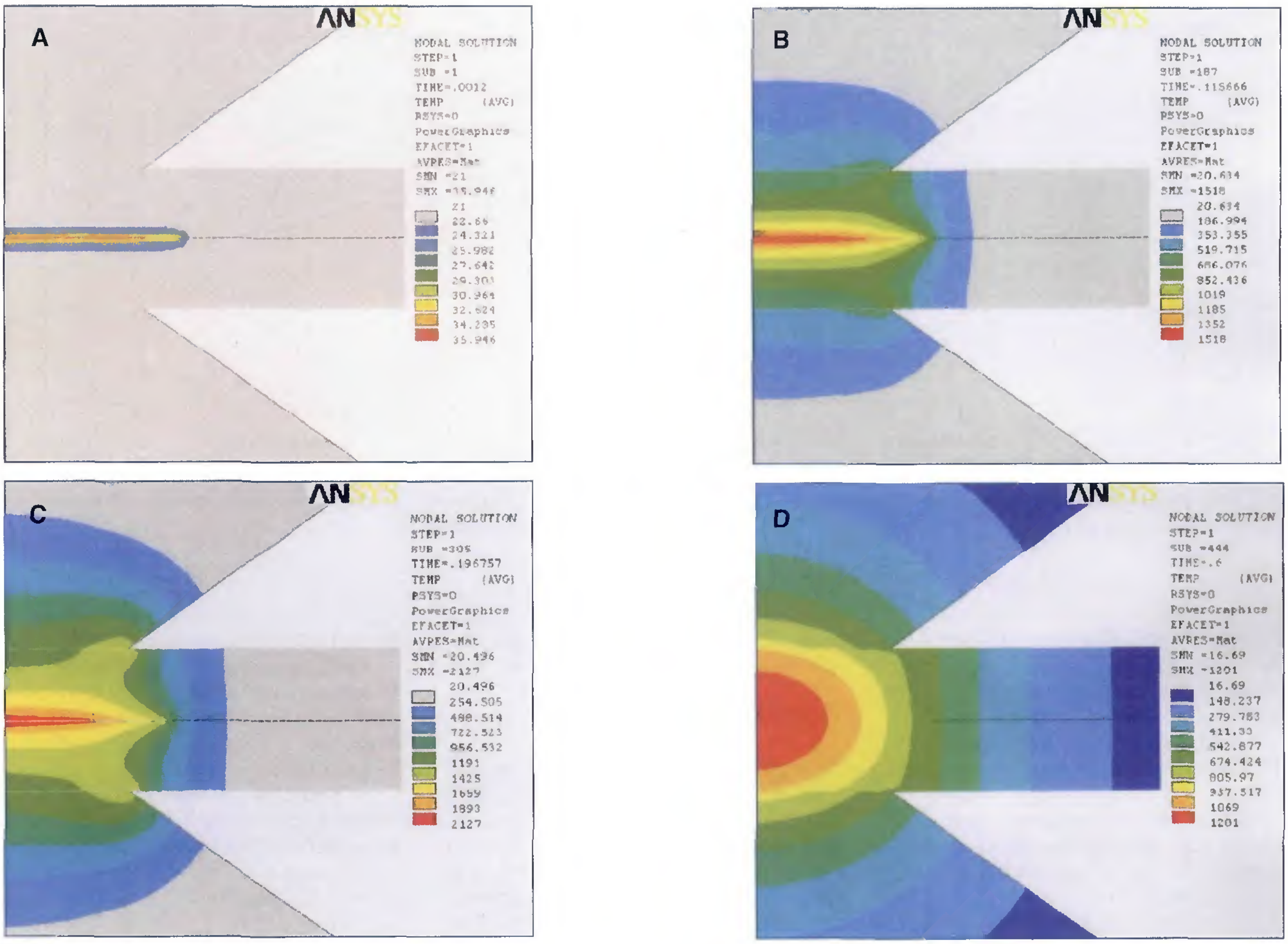

Fig. 7 — Temperature distributions at four different times during RSW. A — Temperature distribution of the first calculated substep; B — temperature distribution at the time of the nugget starting to form; C — temperature distribution at the time of maximum temperature; D — temperature distribution at the end of the welding process.

Phase Change

In the *ANSYS* program, phase change is taken into account by defining the enthalpy of the material as a function of temperature, as formulated below:

$$H = \int \rho C(T) dT \qquad (2)$$

where ρ is the density of the material and *C(T)* is the specific heat of the material as a function of temperature.

Using the material properties provided in Table 1, the enthalpy of mild steel was calculated and graphed in Fig. 5.

Results and Discussion

The temperature fields and their changing of the whole weldment were obtained through the simulation. Figure 6 shows the temperature changing histories at the center of the weld nugget and the center of the electrode-workpiece interface from which we can see the changing of temperature during the welding process.

At the start of the welding process, the temperature at the center of the faying surface increased quickly. At the first half of the first cycle, the temperature exceeded 350°C, whereas the temperature of the electrode-workpiece interface rose slowly. Figure 7A shows the temperature distribution of the first calculated substep. It can be seen that the Joule heat generated along the contact line of the faying surface due to the contact resistance, while the temperature of the electrode- workpiece interface was still the initial value.

The highest temperature was kept at the center of the faying surface through out the whole welding process. Melting would first occur at the faying surface, and then expanded to the material near the faying surface. At the sixth cycle, the highest temperature

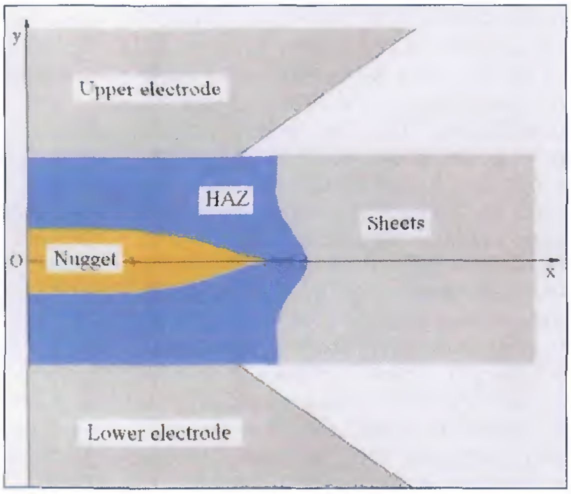

Fig. 8 — Illustration of nugget and heat-affected zone.

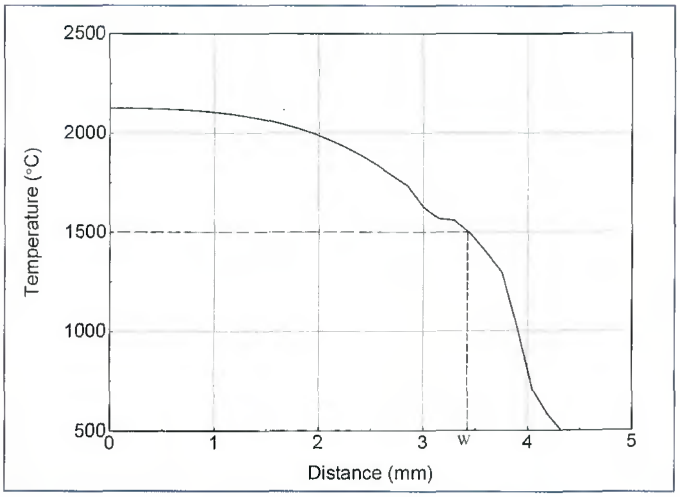

Fig. 9 — Temperature distributions along the faying surface used to measure the nugget width.

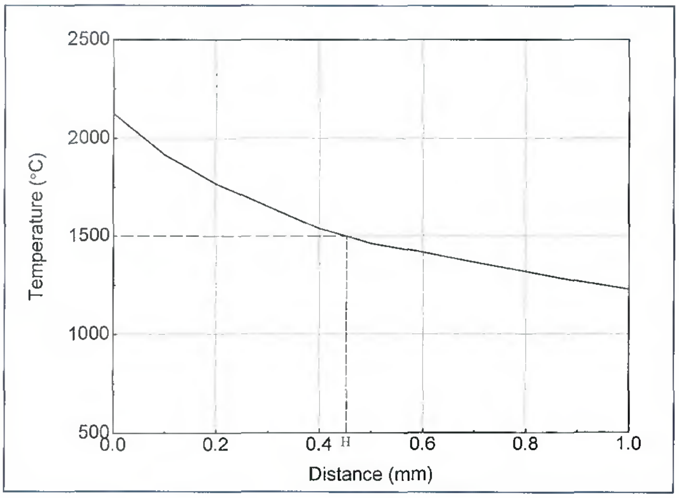

Fig. 10 — Temperature distributions along the centerline used to measure the nugget height.

reached 1500°C. We take this temperature as the molten point of mild steel, which means the nugget started to form at this temperature. The temperature distribution at that time is shown in Fig. 7B. The shape of the nugget is a very flat ellipse.

When the temperature rose, the nugget kept growing. The maximum temperature of the nugget center, 2127°C, occurred at the first half of the last AC cycle, as shown in Fig. 7C. The nugget geometry had completely formed at that time. Figure 8 illustrates the geometry of the nugget and the HAZ.

Figure 9 shows the temperature distribution along the faying surface (x-axis in Fig. 8), where the horizontal axis represents the distance from the center of the faying surface (i.e., the nugget center). Since 1500°C is the molten temperature of the mild steel, we first found the point of 1500°C on the curve of temperature distribution, then the corresponding point could be determined on the horizontal axis. Its horizontal axis value indicated the width of the nugget. Using the same method, the height of the nugget could be measured from Fig. 10, which shows the temperature distribution along the axisymmetric centerline (y-axis in Fig. 8). The results show that the nugget was 6.8 mm wide and 0.9 mm high.

As the electric current ceased at 0.2 s, the weldment started to cool down. In a very short time, the temperature of the nugget center decreased to 1500°C. It then kept this temperature for a while due to the latent heat of phase change being released. At the end of the simulation, as shown in Fig. 7D, the temperature of the nugget center was 1021°C. The temperature at the center of the electrode-workpiece interface decreased more slowly but continuously, and was 871°C at the end of the simulation.

Conclusions

A thermoelectrical 2-D FE model has been developed to analyze the transient thermal behavior of the RSW process. The developed model took into account the following considerations: electric and thermal conduction in the solid, convection of cooling water and ambient air, latent heat of fusion due to solid-liquid phase change, and material properties as functions of temperature.

The contact problem was moderately simplified to decouple the interaction between the thermoelectrical and structural fields. The contact resistance was considered as a temperature-dependent function, and the contact length was assumed to be constant.

The *ANSYS* finite element program was employed to construct the RSW process model. The temperature distributions in the weldment and thermal histories of the whole process were obtained through the analysis. The model can also predict weld nugget size and width of the heat-affected zone.♦

References

1. Nied, H. A. 1984. The finite element modeling of the resistance spot welding process. *Welding Journal* 63(4): 123-s to 132-s.

2. Cho, H. S., and Cho, Y. J. 1989. A study of the thermal behavior in resistance spot welds. *Welding Journal* 68(6): 236-s to 244-s.

3. Han, Z., Orozco, J., Indacochea, J. E., and Chen, C. H. 1989. Resistance spot welding: A heat transfer study. *Welding Journal* 68(9): 363-s to 371-s.

4. Browne, D. J., Chandler, H. W., Evans, J. T., and Wen, J. 1995. Computer simulation of resistance spot welding in aluminum: Part I. *Welding Journal* 74(10): 339-s to 344-s.

5. Yeung, K. S., and Thornton, P. H. Transient thermal analysis of spot welding electrodes. *Welding Journal* 78(1): 1-s to 6-s.

6. Khan, J. A., Xu, L., Chao, Y., and Broach, K. 2000. Numerical simulation of resistance spot welding process. *Numerical Heat Transfer, Part A*, 37: 425–446.

7. Chang, B. H., and Zhou, Y. Numerical study on the effect of electrode force in small-scale resistance spot welding. *Journal of Materials Processing Technology*, in press, corrected proof available online May 21, 2003.

8. Richard, D., Fafard, M., Lacroix, R., Clery, P., and Maltais, Y. 2003. Carbon to cast iron electrical contact resistance constitutive model for finite element analysis. *Journal of Materials Processing Technology* 132: 119–131.

9. Tsai, C. L., Dai, W. L., Dickinson, D. W., and Papritan, J. C. 1991. Analysis and development of a real-time control methodology in resistance spot welding. *Welding Journal* 70(12): 339-s to 351-s.

10. Zhu, Y. 1999. Application handbook of welding technology. *Science and Technology Press of Jiangsu Province*, Nanjing, P.R. China.

11. Yang, S., and Tao, W. 1998. Theory of heat transfer. *Higher Education Press*, Beijing, P.R. China.

Friction Stir Welding VS. Fusion Welding

When it comes to welding aluminum, FSW has some advantages over other welding processes

BY JEFF DEFALCO

Friction stir welding (FSW) is a proven nonferrous metal joining process in which base metal melting, filler metal, and shielding gases are absent. Because it is a solid-state joining process, friction stir welding eliminates most of the ill effects associated with resolidification inherent to conventional fusion welding. The process also can be applied in all welding positions.

Evaluating the Pros and Cons

Three important features outline friction stir welding's advantages over conventional fusion welding processes: high production output, low production costs, and the ability to effectively join aluminum alloys that are difficult or impossible to weld by conventional fusion methods.

Of course, each of these claims must be evaluated in order to best determine friction stir welding's potential advantage or disadvantage. For example, if a company needs to factor in associative equipment costs to establish the cost of producing parts, friction stir welding's advantage only shines in high-production applications due to its relatively high initial capital costs. Job assemblies having long continuous weld lengths or require welding 2xxx or 7xxx series aluminum are particularly good candidates for this process. Aluminum alloy types and thickness ranges also may play a major role in determining the best solution.

Establishing Advantages of FWS

Friction stir welding is a speedy process complemented by low distortion, lack of porosity, no hot cracking, and its ability to weld thick aluminum sections in a single pass. These all contribute to higher output and lower production costs.

Table 1 shows data comparing FSW with GMAW for welding a 2-in. hollow profile. Although the FSW capital cost is higher, the cost per length is less due to fast welding speeds and low preparation costs.

Table 1 — Example of Welding with FSW

Category	FSW	GMAW
Arc time	2:25	7:22
Lifting and clamping	8:05	3:11
Welding head cold runs	2:25	5:13
Oxide removal	0:00	6:14
Welders' protection	0:00	2:00
Total Prep Time	12:55	24:00
Welding Speed (mm/min.)	2000	750
Investment Costs $	400,00	200,00
Weld Length	2000	2000
Fixed hourly costs $		
Location rent	13	13
Amorization- 4 Yrs	52	26
Variable hourly costs $		
Labor costs	30	30
Energy	1	3
Welding costs		
consumables		2
gases		2
Total Cost/h	96	76
Weld Length/h	11.40	5.47
Cost/Length	8.38	13.81

For welding thick aluminum sections, friction stir welding does not require multipass schedules to limit the amount of heat input since it does not melt the aluminum. It applies enough heat to plasticize it, much like what is experienced with extruding.

Dual welding head setups are also available enabling users to simultaneously weld opposite sides of thick sections or sandwich panels simultaneously, thereby reducing the heat input further. Also, the aggregate weld speed is essentually doubled since each weld head "sees" half the material thickness.

One drawback of using friction stir welding, especially in more complicated welding applications, might be the fixture(s) capital costs. Sufficient sideways and downward clamping pressures must be applied to each piece to sufficiently hold them in place. The solution may require hydraulics. The requisite pressure may be appreciable but not unreasonable.

JEFF DEFALCO (jdefalco@esab.com) *is welding automation business manager for engineering systems, ESAB Welding and Cutting, Florence, S.C.*

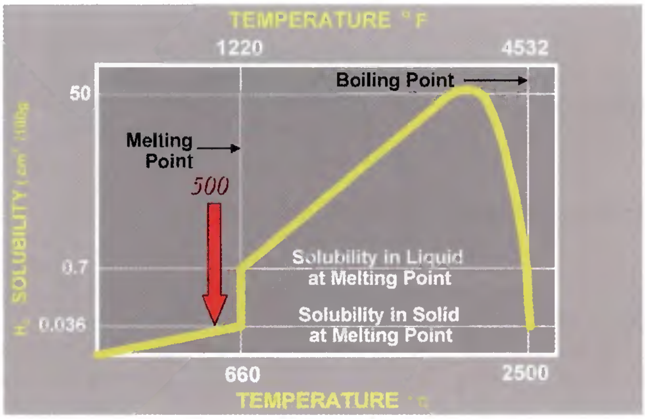

Fig. 1 — Graph showing FSW joining temperature relative to melting temperature of aluminum.

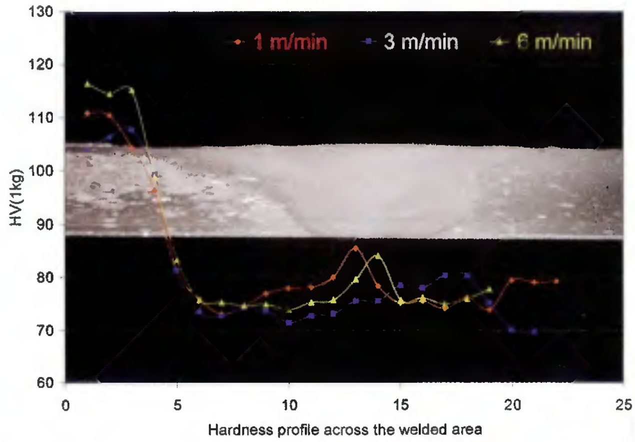

Fig. 2 — Hardness profile at different welding speeds.

Table 2 — Strength Characteristics when Friction Stir Welding 1, 3, and 6 m/min

Welding Speed	$Rp_{0.2}$ (MPa)	dev.	Rm (MPa)	dev.	Bend test	Elongation%	dev.
1 m/min	155.9	0.56	256.2	0.04	180 deg	10.76	2.72
3 m/min	171.1	1.71	268.5	0.24	180 deg	11.46	0.75
6 m/min	173.8	1.66	268.7	1.29	180 deg	9.20	0.46

Reducing Production Costs

Production costs using friction stir welding are appreciably lower because porosity and hot cracking are all but eliminated due to the process's 500°C maximum joining temperature. This is shy of aluminum's 660°C melting temperature (Fig. 1) and is particularly advantageous in situations where fatigue life is critical.

Related to this is friction stir welding's ability to eliminate fusion or weld penetration concerns due to its reliance on a rotating stylus. Only fairly large changes in the the tool's length, in excess of 15%, would adversely affect the weld integrity as manifested in a bend test. Tool wear is minimal and tools are expected to last for many miles of weld while retaining the same quality.

Weld gases and consumables[1] are not needed for friction stir welding. Production cost savings are therefore high. Process variabilities in gas metal arc welding such as wire diameter tolerances and wire feeding issues are not a concern with friction stir welding.

Reduced Preparation Time

Weld preparation for friction stir welding is relatively simple, which further contributes to the cost savings. Grease or other lubricating solutions that would prevent the tool's shoulder from creating a sufficient friction boundry should be removed. Otherwise, surface oxidation and corrosion do not seem to adversely affect friction stir welding. In fact, the process has effectively repaired welds made with the GTAW or GMAW processes. This is especially important in cases requiring zero defects such as in aerospace.

Postweld Finishing

Due to friction stir welding's autogenous nature, the finished weld profile is aesthetically pleasing, which greatly reduces postweld processes such as slag and spatter removal. Smut removal and excessive grinding are not necessary with friction stir welding. This attribute is a major consideration as grinding normally takes a lot of time, especially for long weldments.

Low Heat Input Advantage

Due to friction stir welding's low joining temperature and its ability to weld without prepared joints, postweld deformations are minor or nonexistant in the fabricated assemblies, particularly evident in large panel assemblies where deformations become quite problematic. Various case studies have shown production cost savings of up to 20% just from the elimination of subsequent straightening processes.

The Environment Factor

Harmful fumes and arc flash produced by fusion welds are absent with friction stir welding. Also, the process does not require the same protective equipment as needed with arc welding processes; therefore, the time to find, outfit, and remove this equipment is saved.

Weld Properties

In many cases fabrication designs can be simplified and costs reduced as a result of friction stir welding's as-welded fatigue, tensile, and yield strengths. After attaining a T6 temper by postweld heat treatment, friction stir butt joint welds in 6xxx series aluminum can typically achieve 90–100% of the unwelded base metal strength.

In the as-welded condition, friction stir welded metals possess yield and ultimate tensile strengths noticeably higher than fusion-welded counterparts. An interesting attribute of FSW is its ability to keep these properties when the welding speed is increased. Table 2 shows the effect on properties as the speed is increased

Also, it has been shown that friction stir welding produces a similar hardness profile regardless of its welding speed — Fig. 2. This seems to be due to the lower heat input in the weld zone.

Friction stir welding also displays less variability in tensile strength in the as-welded condition. Table 3 shows a 10–22% advantage in ultimate tensile strength and a lower degree of variability compared to the variable polarity plasma arc (VPPA) process.

1. *At a cost of $1500 and a service life for 2000 m of weld, the FSW tool is not normally considered a consumable.*

Table 3 — Tensile Property Results in 2195-T8 Weld

Thickness	Form	Ultimate Tensile Strength (ksi) VPPA Average	VPPA Minimum	FSW Average	FSW Minimum
0.2	Plate	51.9	45	56.9	54.8
0.32–0.385	Extrusion	46.9	29	57.2	53.5

(Source: Lockheed Martin)

What about Fillet Welds?

Welding fillets with friction stir welding is a challenge, since the tool's shoulder must always be in contact with the target material to produce the required heat.

Therefore, friction stir welding cannot weld fillets directly at the joint. It is common practice to weld through the flange into the web, which produces a very strong T weld. This approach eliminates the need to perform a multipass weld, or having to invest in a dual-head fillet welding system.

Corrosion Concerns

Friction stir welds show resistance to stress corrosion cracking (SCC). This is due to the low heat input of the process and its ability to dissolve hardening precipitates. In particular, the process evades most of the postcorrosion effects found with fusion welding of 2xxx (Cu) and 7xxx (Zn) series aluminum alloys.

Fusion welding of 7075 and 2014 aluminum produces grain boundry precipitation in the HAZ, which in turn increases their respective electrical potential differences. This promotes electrostatic corrosion, which further accelerates mechanical stress effects.

Thermal cycling during friction stir welding is sufficient to dissolve hardening precipitates. It was found welds made in 2014A had greater resistance to exfoliation corrosion than the base metal, although the HAZ was slightly more susceptible. On the other hand, exfoliation resistance in 7075 was worse than the base metal, although it did not show signs of intergranular corrosion. The same has been found with the 5xxx and 6xxx series aluminum.

Moving Forward

The aerospace industry has found friction stir welding to be less expensive than riveting, VPPA, or GMA welding.

Friction stir welding's abilty to avoid the high temperatures inherent to fusion welding makes it capable of joining Al to dissimilar Al alloys or other metal alloys including copper, lead, zinc, and magnesium. Its process characteristics eliminate the ill effects produced by brittle intermetallic compounds.

As with any advanced welding process, friction stir welding's acceptance on the U.S. factory floor will depend on those who are willing to step forward to improve their production environment and open their doors to new technology. For many applications, friction stir welding is the clear-cut answer to replace older and less-effective technology.◆

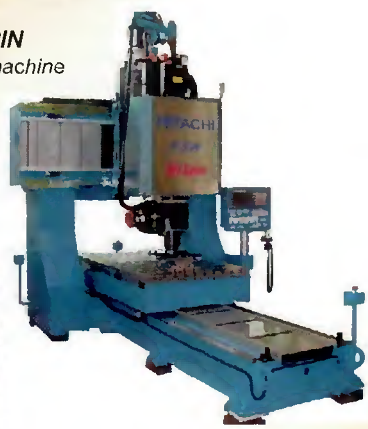

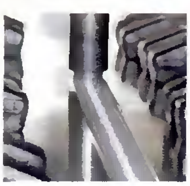

Investigating Resistance and Friction Stir Welding Processes for Joining Magnesium

BY J. E. GOULD AND W. CHUKO

High-productivity welding methods are compared for the most efficient way of joining Mg alloys

International interest in developing lighter, more fuel-efficient automobiles has resulted in the introduction of a new round of alternative construction materials. Of recent interest has been the exploitation of magnesium (Mg) alloys. Magnesium, with a density of 1.74 g/cm^3, has roughly that of Al, and one-fourth that of steel. With proper alloying, the strength-to-weight ratio of Mg-based products is similar to many Al alloys, as well as many common grades of automotive sheet steels. Magnesium is particularly of interest for automotive applications given its natural corrosion resistance and ease of casting. Magnesium has seen limited use in automotive applications since the 1920s. Most applications are cast components such as crankcases, oil pans, gearbox housings, and wheels. However, as the industry has advanced, Mg has found its way into other applications, including body pillars, hoods, deck lids, and inner doorframes.

As the application of this class of materials increases, so does the need for joining. Previous work has shown that Mg alloys are joinable by a wide array of processes (Ref. 1). This work, however, focuses on joining some of the more popular cast alloys (AZ91 and AM60) with a range of high-productivity joining processes. These processes include resistance spot welding (RSW), conductive heat resistance seam welding (CHRSEW), and friction stir welding (FSW). Processing conditions are presented, as well as some representative mechanical properties and metallographic results.

The Experiments

Materials for study include the popular alloys used for automotive applications. These include a 5-mm cast AZ91, a 2-mm vacuum cast AZ91, a 1.5-mm Thixomolded AZ91 D, and a 1.5-mm AM60. Nominal chemical compositions and base metal mechanical of the respective Mg alloys studied are presented in Tables 1 and 2.

Spot Welding

Resistance spot welding was done on a Newcor 200-kVA, 1ϕ, AC pedestal-type spot welding machine fitted with a low-inertia head and Medar Legend controller. Welding was done with 7.87-mm Class II Cu truncated-cone electrodes. Studies were done on similar joints of 2-mm vacuum cast AZ91, as well as thixotropoic molded 1.5-mm cast AZ91 and 1.5-mm AM60 materials. All materials were wire brushed before welding to reduce the surface oxides. The weld trials were performed in an iterative fashion, based on previous published work (Refs. 2, 3). Initial weld quality was assessed according to presence/absence of expulsion, surface indent, and resulting button size after chisel testing. Chisel testing was performed by hand, and continued until either failure of the weld or base metal was observed. Based on these results, additional welds were made for metallurgical evaluation and mechanical testing.

Seam Welding

Conductive heat resistance seam welding (CHRSEW) is a new technology developed at Edison Welding Institute. The details of the process are provided in other publications. The process here utilized a Sciaky seam-welding frame equipped with a medium-frequency Myiachi DC Tech IS-460A controller. The seam welding machine was equipped with 241-mm-diameter Class II Cu welding wheels that were 8.4 mm thick with a 25.4-mm face radius. Mild steel cover plates 1.1 mm thick were used for all thicknesses of material welded.

J. E. GOULD and W. CHUKO are with Edison Welding Institute, Columbus, Ohio.

Paper based on a presentation at Sheet Metal Welding Conference XI, 2004, Sterling Heights, Mich.

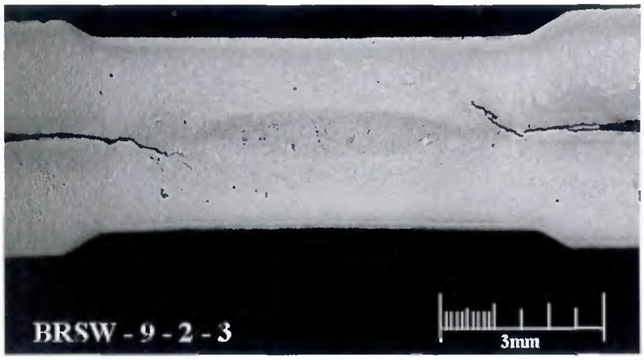

Fig. 1 — Cross section of a 2-mm AZ91 spot weld (F = 5.11 kN, weld time = 6 cycles, I = 20.4 kA, downslope time = 4 cycles, downslope current = 20.4–13.5 kA).

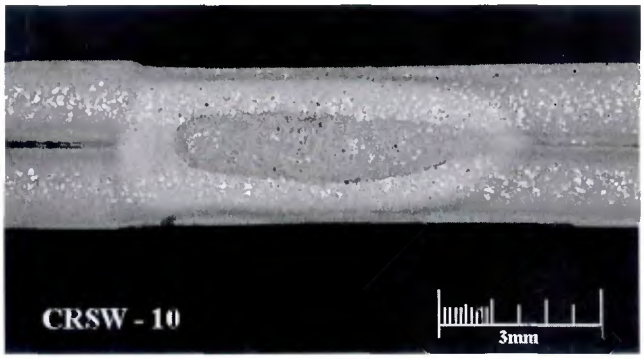

Fig. 2 — Cross section of a 1.5-mm Thixomolded AZ91 spot weld (F = 2.7 kN, weld time = 10 cycles, I = 20.5 kA).

Table 1 — BM Processing, Gauges, and Compositions

Alloy	Casting Process	Thickness (mm)	% Al	% Mn	%Zn (max)
AZ91	Conventional cast	5	8.3–9.7	0.13–0.5	0.35–1.0
AZ91	Vacuum cast	2	8.3–9.8	0.13–0.6	0.35–1.0
AZ91D	Thixotropic molded	1.5	8.5–9.5	0.17–0.4	0.45–0.9
AM60	Thixotropic molded	1.5	5.6–6.4	022–0.48	0.2

Table 2 — BM Properties of the Materials of Interest

BM	Width (mm)	Thickness (mm)	Ultimate Strength (MPa)	Yield Strength (MPa)	Elongation (%)	Reduction of Area (%)
AZ91 Conventional cast	18.97	5	161	120	3.8	3.5
AZ91 vacuum cast	18.92	2	216	152	1.8	1.6
AZ91 Thixotropic molded	18.92	22.8	228	165	3.9	6.6
AM60 Thixotropic molded	18.92	1.5	213	138	10.8	5.4

Material combinations included similar material welds with 5-mm cast AZ91, 2-mm vacuum cast AZ91, 1.5-mm Thixomolded AZ91, and 1.5-mm Thixomolded AM60. Iterative trials were again performed with each material combination.

For all welding trials, 101- x 152-mm samples were welded longitudinally using a butt joint configuration. In the initial trials, weld quality was based upon visual inspection and manual bend testing of the weld interface. Upon destruction of the weld, the fusion area was examined for depth of penetration and tearing of the base metal. Acceptable welds were defined by fracture in the base metal away from the weld interface. After acceptable welding parameters were found, additional weld samples were made for metallurgical examination and mechanical testing.

Friction Stir Welding

Friction stir welding (FSW) was performed on a modified 50-hp Kearney & Trecker milling machine. Material combinations investigated included similar thickness 5-mm cast AZ91, 2-mm vacuum cast AZ91, 1.5-mm Thixomolded AZ91, and 1.5-mm Thixomolded AM60. Iterative trials were performed on each material combination. Welding parameters used were based nominally on past experience with FSW of Al.

Examining the Welds

Welds were inspected visually for uniform surface appearance. Welds were then bend tested along the weld interface. Evidence of base metal tearing compared with a fracture down the weld interface indicated a feasibility of strength of the weld. When a visually acceptable weld was made that showed evidence of base metal tearing, additional samples were made for metallurgical examination and mechanical testing. The samples were sectioned and mounted using standard procedures. Etching was done in a 2% Nital solution.

The observed weld zones were then examined for depth of penetration and apparent quality. Hardness traverses were also performed on each weld. Vickers microhardness testing was done with a diamond indenter and a 0.5-kg load. A minimum of 10 hardness measurements were recorded through each traverse. All mechanical testing was done on a Southwark Emery tensile test machine, with a crosshead speed of 10 mm/min. Coupons for RSW lap-shear testing measured 50 x 100 mm, with a 50-mm overlap. Offset tabs of equal thickness were placed in the grip area of the coupon to ensure vertical alignment of the sample. Transverse tensile tests were performed on representative CHRSEW and FSW sections from multiple locations along the weld length.

Results

Welds Made with RSW

The best spot welding schedules for each material studied, based on the visual inspection and chisel testing, are presented in Table 3. Chisel testing resulted in full button morphologies with no evidence of surface expulsion. However, ex-

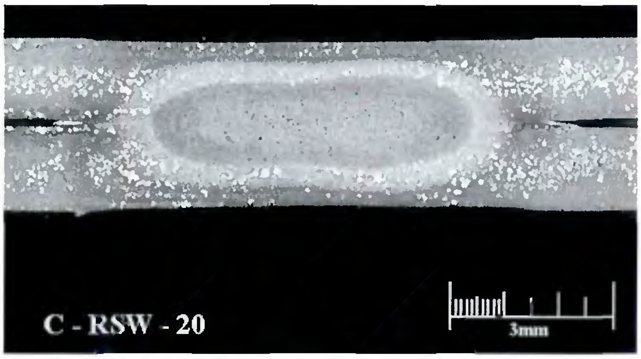

Fig. 3 — Cross section of a 1.5-mm AZ91 spot weld (F = 4.0 kN, weld time = 6 cycles, I = 19.7 kA, downslope time = 4 cycles, downslope current = 19.7–14.7 kA).

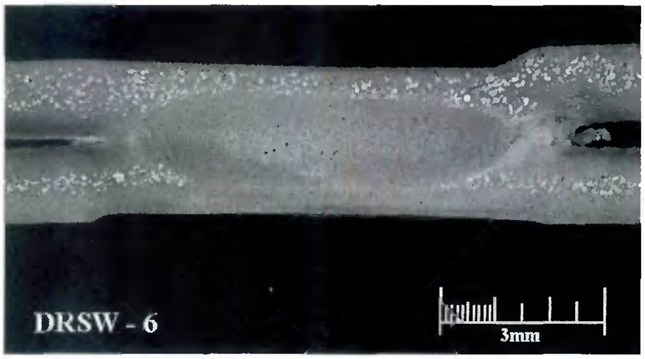

Fig. 4 — Cross section of 1.5-mm Thixomolded AM60 spot weld (F = 4.0 kN, weldtime = 6 cycles, weld current = 23 kA, downslope time = 4 cycles, downslope current = 23–16.5 kA).

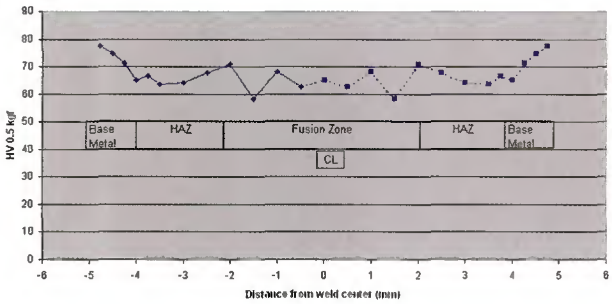

Fig. 5 — Hardness traverse through a 1.5-mm Thixomolded AZ91 spot weld (C-RSW-10) (F = 2.7 kN, weld time = 10 cycles, I = 20.5 kA).

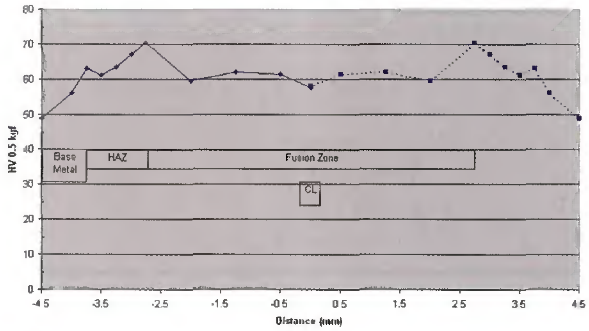

Fig. 6 — Hardness traverse through a 1.5-mm Thixomolded AM60 resistance spot weld (F = 4.0 kN, weld time = 6 cycles, I = 21.3 kA, downslope time = 4 cycles, downslope current = 23–16.5 kA). Hardness data taken from center of nugget to base metal. Dotted line represents full traverse.

Table 3 — RSW Conditions for the Materials of Interest

Materials	Weld Force (kN)	Weld Time (cycles)	Weld Current (kA)	Downslope Time (cycles)	Downslope I (kA)
2- to 2-mm AZ91 vacuum cast	5.1	6	20.4	4	20.4–13.5
1.5 to 1.5-mm AZ91D Thixotropic molded	2.7	10	20.5	N/A	N/A
1.5 to 1.5-mm AZ91D Thixotropic molded	4	6	19.7	4	19.7–14.7
1.5- to 1.5-mm AM60 Thixotropic molded	4	6	21.3	4	23–16.5

pulsion at the faying surface was observed in every case. Generally, a 6-cycle weld time followed by a 4-cycle downslope produced a weld with good fusion and minimal expulsion or electrode indentation. For the 1.5-mm Thixomolded AZ91, a straight 10-cycle weld time with no downslope also resulted in a good weld nugget with somewhat less porosity.

What the Cross Sections Reveal

Metallurgical examinations revealed that the 2-mm AZ91 vacuum cast material was somewhat underwelded. This is shown in Fig. 1. Using higher weld currents (to increase weld size) resulted in surface expulsion. The micrograph also shows evidence of cracking in the HAZ at the faying surface of the weld, faying surface expulsion, and electrode indentation. Porosity, however, appears to be less than that of the base metal.

Figures 2 and 3 present cross sections of the 1.5-mm Thixomolded AZ91 welds. The weld shown in Fig. 2 was made using the 10-cycle at 20.7-kA weld time. The weld in Fig. 3 was made using a 6-cycle weld time at 19.7-kA followed by a 4-cycle downslope. The weld made using downslope also employed a higher weld force. This weld exhibited deeper penetration, lower surface indentation, less expulsion, and a smaller HAZ compared with the weld made using a single impulse weld schedule.

The cross section of a spot weld made in the AM60 alloy (Fig. 4) exhibits good nugget penetration and minimal porosity in the fusion zone. Vickers hardness traverses through the Thixomolded AZ91 and Thixomolded AM60 weld nuggets (Fig. 5 and 6) revealed that hardness remained relatively constant from the fusion zone through the HAZ. Lap-shear test results

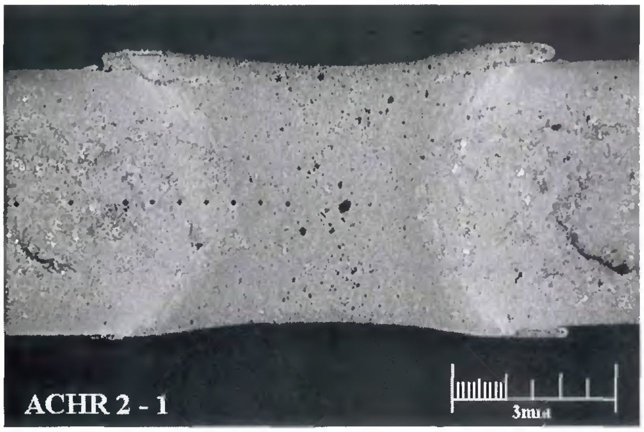

Fig. 7 — Cross section of a conductive heat seam weld made on 5-mm cast AZ91.

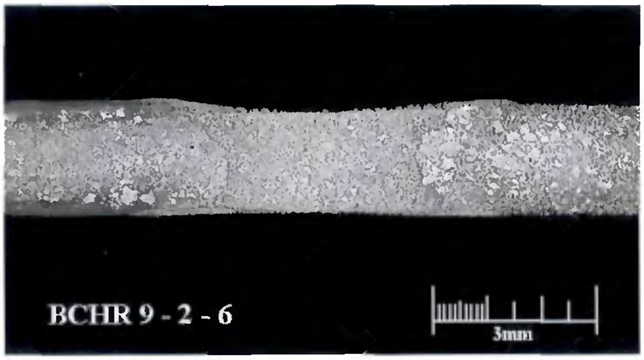

Fig. 8 — Cross section of a conductive heat seam weld made on 2-mm vacuum cast AZ91.

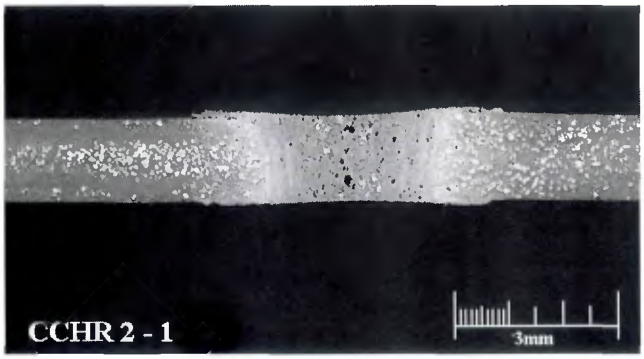

Fig. 9 — Cross section of a conductive heat seam weld made on 1.5-mm Thixomolded AZ91.

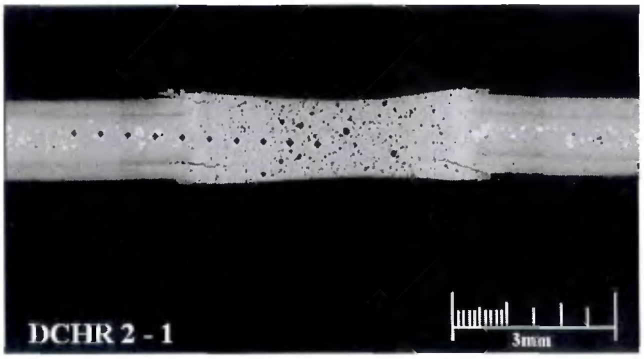

Fig. 10 — Cross section of a conductive heat seam weld made on 1.5-mm Thixomolded AM60.

for replicate sets of welds made with each of the materials and weld schedules are presented in Table 4. The most consistent results were found with the Thixomolded AZ91 when using downslope. Here, the samples failed in the HAZ and there were no occurrences of interfacial failure. Expulsion at the faying surface of the welds was minimal and deviation in strength across the sample set was low.

Table 4 — Tensile Shear Strength Results for Resistance Spot Welds on the Materials of Interest

Material	Replicate	RSW (kN)	RSW(a) (kN)
2-mm AZ91 Vacuum cast	1	3.1	--
	2	5	--
	3	5.7	--
	4	2.7	--
	5	4.1	--
1.5-mm AZ91D Thixotropic molded	1	2.7	3.1
	2	2.9	3.3
	3	2.4	4
	4	2.9	3
	5	2.7	2.3
1.5-mm Am60 Thixotropic molded	1	4.2	--
	2	1.3	--
	3	2.4	--
	4	2.8	--
	5	2.8	--

Welds Made with CHRSEW

The developed schedules for successful CHRSEW joints on the four materials of interest are presented in Table 5. Travel speeds obtained for the samples ranged from 1.33 to 2.44 m/min. In all cases, no loss of nugget constraint (in the form of surface expulsion) was observed. There also was no secondary joining of the steel cover sheets to the fusion area. All samples broke away from the weld interface upon bend testing. Surfaces of the welds were smooth and slightly concave. A cross section from a 5-mm AZ91 weld (Fig. 7) revealed that the fusion zone took on a typical CHRSEW hourglass geometry. Extensive weld metal porosity (similar to the base metal) is readily observed. The weld is also slightly unsymmetrical, wider at the top than the bottom. This deviation from a symmetrical geometry is evidence of uneven heating in the weld.

The cross section of a 2-mm AZ91 vacuum cast weld is shown in Fig. 8. This weld also shows evidence of uneven heating as described above. The fusion zone here is relatively wide compared to that of Fig. 7, suggesting higher specific heat inputs compared with the 5-mm sample. This is probably related to the slower speeds used here. These slower welding speeds may also account for the lack of porosity observed in the fusion zone. Cross sections for the two Thixocast materials (AZ91 and AM60) are shown in Figs. 9 and 10, respectively. It is of interest that even though the Thixocast base materials show reduced porosity, the welds show levels consistent with the 5-mm AZ91 die cast material described previously. This porosity in the AZ91 is primarily concentrated along the centerline of the weld, while

Table 5 — CHRSEW Conditions for the Materials of Interest

Material	Cover Sheet	Force (kN)	On Time (ms)	Off Time (ms)	Current (kA)	Travel Speed (mm/min)
5-mm AZ91 Conventional cast	1.1-mm mild steel	2.7	20	6	12	2300
2-mm AZ91 Vacuum cast	1.1-mm mild steel	3.3	25	2	6.1	1330
1.5-mm Thixotropic molded AZ91	1.1-mm mild steel	2.7	24	5	9	2440
1.5-mm Thixotropic molded AM60	1.1-mm mild steel	2.7	24	5	12.5	2440

Table 6 — Mechanical Properties Results for the Conductive Heat Resistance Seam and Friction Stir Welds Made in this Study

		CHRSEW		FSW	
Material	Replicate	UTS (MPa)	Joint Eff. (%)	UTS (MPa)	Joint Eff. (%)
5-mm AZ91	1	—	—	174.45	108
Conventional cast	2	—	—	151.97	94
	3	—	—	143.03	89
2-mm AZ91	1	165.76	76	180.88	83
Vacuum cast	2	156.8	72	217.99	101
	3	142.68	66	223.41	103
	4	188.55	87	—	—
1.5-mm AZ91D	1	173.13	76	216.06	95
Thixotropic molded	2	182.34	80	211.52	93
	3	172.62	76	219.2	96
1.5-mm Am60	1	144.01	68	188.19	88
Thixotropic molded	2	160.69	75	211.51	99
	3	147.93	69	199.14	93

Table 7 — FSW Conditions for the Materials of Interest

Material	Travel Speed (mm/min)	Rotations Speed (rpm)
5-mm AZ91 Conventional cast	279	1250
2-mm AZ91 Vacuum cast	235	1250
1.5-mm AZ91D Thixotropic molded	279	1250
1.5-mm Am60 Thixotropic molded	235	1250

porosity in the AM60 is fairly uniform throughout. The AM60 weld also shows evidence of cracking in the fusion zone, apparently related to heterogeneities in the original cast base metal structure. Corresponding hardness profiles for these welds are presented in Figs. 11–14.

For the most part, the hardness data were relatively uniform from the base metal through the fusion zone. Any significant deviations away from the average hardness were attributed to areas of porosity that affected the measurements. Transverse tensile results are given in Table 6. These welds showed resultant joint efficiencies from 71 to 77%. These efficiencies are typical of Mg welds where extensive gas porosity is present (Refs. 6, 7). Based on previous work with Al sheet, it is believed that thinner cover sheets and higher weld forces would suppress this porosity.

Welds Made with Friction Stir Process

Friction stir welding conditions yielding acceptable welds for each material of interest are provided in Table 7. These schedules were verified through manual bend testing, and then used to produce additional welds for metallurgical examination and mechanical testing. Sections from the 5-mm AZ91, 2-mm AZ91 VC, 1.5-mm Thixocast AZ91, and Thixocast AM60 are shown in Figs. 15–18, respectively. The macrostructures of the welds are similar, showing distinct delineation of the stir zone (SZ), thermomechanically affected zone (TMAZ), heat-affected zone (HAZ), and base metal. As with typical friction stir welds, the microstructure shows a distinct taper, widest where the shoulder of the tool is in contact with the workpiece. The relatively featureless weld is indicative of the fine structure associated with the heavily worked SZ. Corresponding microhardness plots for these welds are presented in Figs. 19–22. Similar to the results for the CHRSEW process presented above, the hardness remains relatively uniform across the weld zone. Tensile test results, transverse the weld direction, are presented for each material

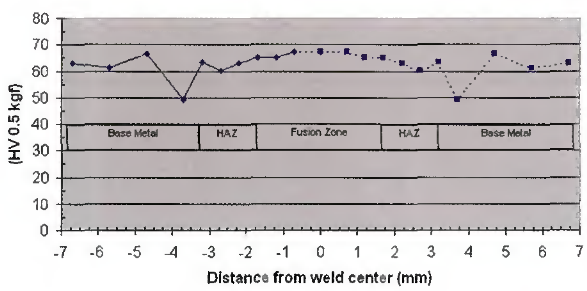

Fig. 11 — Cross section hardness traverse from a conductive heat seam weld on 5-mm cast AZ91.

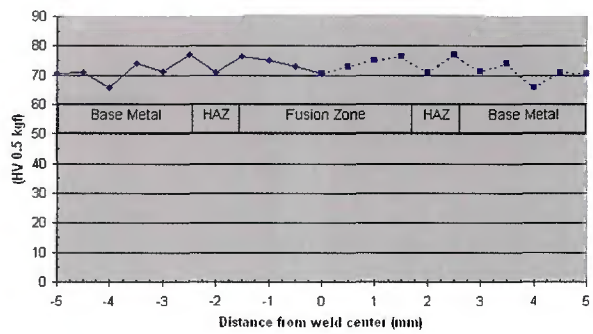

Fig. 12 — Cross section hardness traverse from a conductive heat seam weld on 2-mm vacuum cast AZ91.

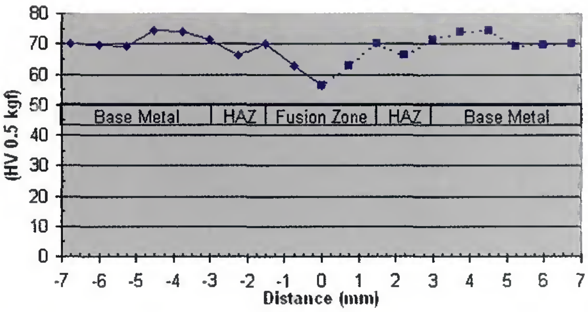

Fig. 13 — Cross section hardness traverse from a conductive heat seam weld on 1.5-mm Thixomolded AZ91.

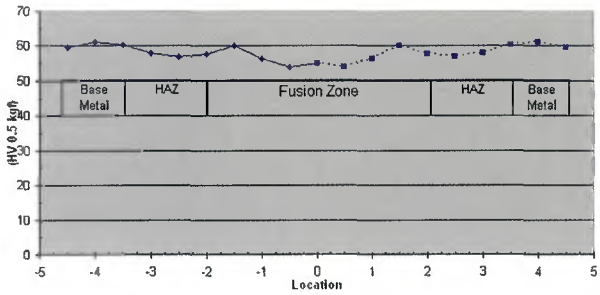

Fig. 14 — Cross section hardness traverse from a conductive heat seam weld on 1.5-mm Thixomolded AM60.

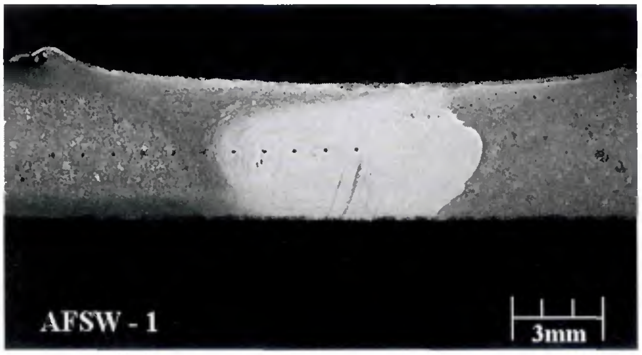

Fig. 15 — Cross section of a friction stir weld made on 5-mm cast AZ91 (right side is advancing side).

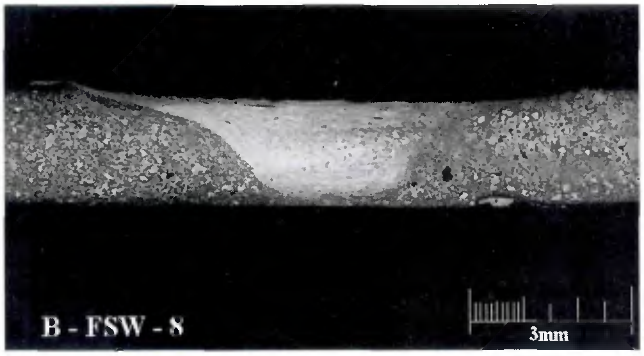

Fig. 16 — Cross section of a friction stir weld made on 2-mm vacuum cast AZ91 (left side is advancing side).

Fig. 17 — Cross section of a friction stir weld made on 1.5-mm Thixomolded AZ91 (right side is advancing side).

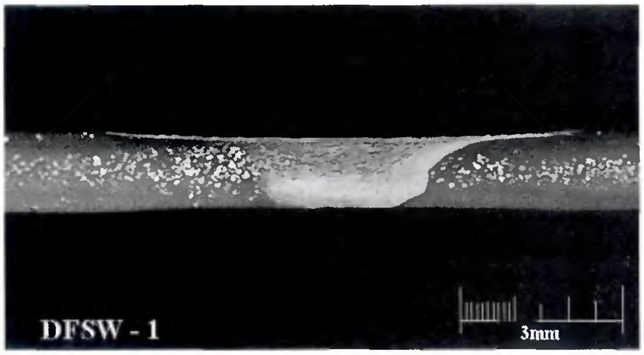

Fig. 18 — Cross section of a friction stir weld made on 1.5-mm Thixomolded AM60 (right side is advancing side).

in Table 6. Joint efficiencies here ranged from 94 to 97%. These joint efficiencies are typical for welds without porosity (Refs. 8–10).

Discussion

Magnesium alloys, much like Al alloys, are characterized by high thermal and electrical conductivities (typically 60% that of Al) and high stability of surface oxides. Not surprisingly, joining of Mg alloys is most commonly compared with that of Al. The resistance spot weldability of the Mg alloys studied here can be viewed in that light.

Details of RSW

Essentially, resistance welding exhibited largely defined surface expulsion and small ultimate nugget sizes (60–80% of the electrode diameter). Surface expulsion appeared to be an artifact of the high initial contact resistances. The reaction of this resistance to the high currents required for forming adequate weld nuggets inevitably led to expulsion, most commonly between the contact sheets and to a lesser degree at the electrode sheet interfaces. Reducing the current to minimize such surface expulsion, of course, limited the size of the weld formed. This is reflected in the micrographs shown. Clearly, achieving larger weld sizes without excessive expulsion will require process enhancements (e.g., upslopes to minimize contact resistance effects) or material precleaning. This latter approach has been used extensively to improve the stability of Al spot welds (Ref. 10).

Another interesting observation in

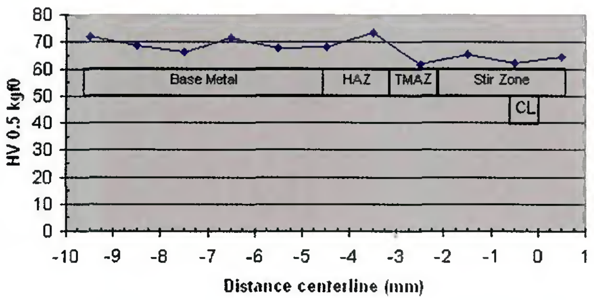

Fig. 19 — Cross section hardness traverse from a friction stir weld on 5-mm cast AZ91.

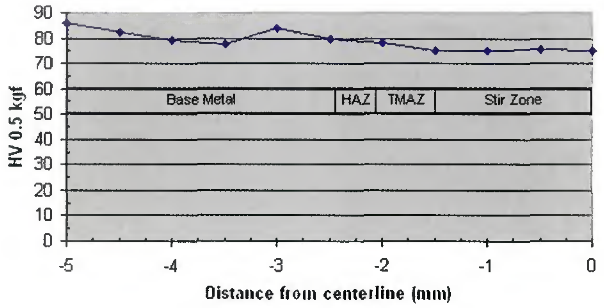

Fig. 20 — Cross section hardness traverse from a friction stir weld on 2-mm vacuum cast AZ91.

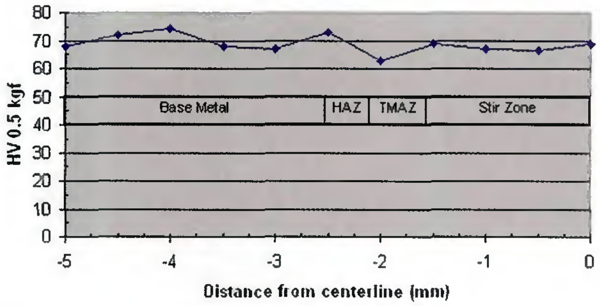

Fig. 21 — Cross section hardness traverse from a friction stir weld on 1.5-mm Thixomolded AZ91.

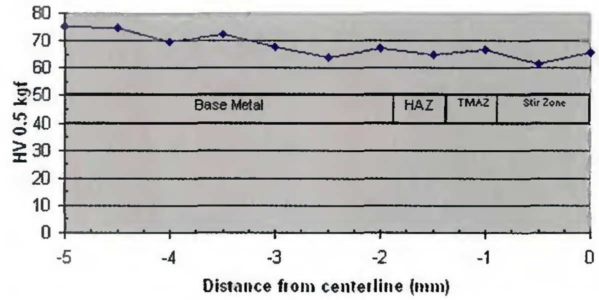

Fig. 22 — Cross section hardness traverse from a friction stir weld on 1.5-mm Thixomolded AM60.

these studies was the advantages in downsloping the welding current. Downsloping generally is used to control the cooling characteristics of the part. Cooling characteristics include solidification and cooling rates in the solid state. The former can be used to vary the scale of the solidification structure as well as the degree of segregation and porosity in the weld nugget. The latter can be used to affect solid-state phase transformations in the weld.

It is believed in this case that downsloping has beneficial effects on the solidification behavior of Mg spot welds. The major concern is gas-related porosity evolution during spot welding. As has been documented for Al alloys (Ref. 11), gas evolution during solidification of spot weld nuggets can lead to a distribution of porosity that facilitates interfacial failure. It appears that downsloping during RSW of Mg alloys reduces solidification rates and redistributes the evolved porosity away from the nugget periphery, thus promoting button-type failures on peel testing.

What Was Learned from CHRSEW Process

Conductive heat resistance seam welding also appeared quite applicable to the Mg alloys studied here. In general, the CHRSEW processes should be readily adaptable to this class of materials. Magnesium alloys, as mentioned above, have thermal conductivities comparable with Al alloys, and even lower (~430°C for initial melting) melting points. In addition, the surface oxides described above also aid in preventing wetting of the liquid Mg to the steel cover sheets. Generally, the metallographic results supported these observations. The only concern is the level of porosity present in the fusion zones of many of these conductive heat resistance seam welds. This to some degree is probably related to the residual porosity present in the base materials. However, previous work on Al has suggested that the pressures present in the fusion zones of conductive heat resistance seam welds is sufficient to suppress the occurrence of such porosity. This suggests the weld forces or thickness of the cover sheets may be inadequate for the types of Mg alloys joined. This retained porosity, combined with the gauge reductions and as-cast properties of the CHRSEW fusion zone, probably combine to produce the relatively poor joint efficiencies seen with these welds (65–90%).

Friction Stir Welding

Friction stir welding was also quite adaptable to the Mg alloys studied here. Again, the high thermal conductivity and low melting point of these Mg alloys allowed FSW to be adapted in a fashion similar to Al alloys. Of particular note on these welds was the fine structure of the SZ itself. This structure is the result of heavy working (Ref. 12) in the SZ, with subsequent mechanical refining of the microstructure. This working had the effect of collapsing any residual porosity from the base metal, resulting potentially in higher integrity material than the base metal itself. Not surprisingly, the friction stir welds showed excellent mechanical properties, with joint efficiencies from 90% to more than 100%.

Conclusions

Work was conducted to examine, in a preliminary way, the applicability of a range of high-productivity joining processes to a range of cast Mg alloys. Magnesium alloys considered included AZ91 and AM60, ranging from 1.5 to 5 mm thick. The welding processes evaluated included RSW, CHRSEW, and FSW. In general, the joining of these materials could be done, reliably, by any of these methods.

Resistance spot welds were noted to require downslopes to achieve quality welds without surface expulsion. Welds were also relatively small compared to the thicknesses of the attached materials.

The conductive heat resistance seam welds could be made at speeds approaching 2.5 m/min. Resulting joints showed a degree of porosity, with a subsequent drop in joint efficiency. It is believed such porosity could be suppressed with thinner cover sheets and higher welding forces.

Friction stir welds showed the best overall performance, with joint efficiencies near 100%.◆

References

1. Chuko, W. L., and Gould, J. E. 2001. Magnesium joining for automotive applications. EWI Research Report, Edison Welding Institute, Columbus, Ohio.

2. Ryazantsev, V. I., and Pugachev, A. I. 1974. Resistance spot welding of deformable magnesium alloys. *Welding Production* 21(2).

3. Busk, R. S. 1987. Magnesium products design. International Magnesium Association.

4. Gould, J. E., and Lehman, L. R. 1999. Metallurgical characteristics of conductive heat resistance seam welds on aluminum sheet. *Automotive Alloys III*, The Metals Society, Warrendale, Pa.

5. Gould, J. E., Workman, D., and Lehman, L. R. 1999. Application of conductive heat resistance seam welding to some representative joint assemblies. *Euromat 99*, Paper No. 129.

6. Murthy, M. S., Ghosh, B. R., Mittal, M. C., and Nagarajan, K. V. 1985. TIG welding DTD5101 magnesium alloy. *Metal Construction*, 17(6): 367–369, The Welding Institute Journal.

7. Matsumoto, J., Kobayashi, M., and Hotta, M. 1990. Arc welding of magnesium casting alloy AM60. *Welding International* 4(1): 23–28.

8. Nakata, K. 1995. Welding of magnesium alloys using carbon dioxide gas laser. *New Technology Japan* 22(11).

9. Ivanov, V. Y., and Zhullin, A. I. The electron-beam welding of magnesium alloy MA2-1. *Welding Production* 23(1).

10. Patrick, E. P., Auhl, J. R., and Sun, T. S. 1984. Understanding the process mechanisms is key to reliable resistance spot welding aluminum auto body components. SAE Technical Paper 840292. SAE, Warrendale, Pa.

11. Chuko, W., and Gould, J. E. 2002. Metallurgical interpretation of electrode life behavior in resistance spot welding 6111 aluminum sheet. *Sheet Metal Welding Conference X*, AWS Detroit Section, Detroit, Mich.

12. Lienert, T. J., Grylls, R. J., Gould, J. E., and Fraser, H. L. 1998. Deformation microstructures in friction stir welds on 6061-t651. *Hot Deformation of Aluminum Alloys II*, AIME, Warrendale, Pa.

Friction Stir Welding Flies High at NASA

From a small initial investment, FSW R&D at Marshall Space Flight Center has flourished and brought NASA cost savings, higher-quality hardware, and prestige

BY JEFF DING, ROBERT CARTER, KIRBY LAWLESS, ARTHUR NUNES, CAROLYN RUSSELL, MICHAEL SUITS, AND JUDY SCHNEIDER

Welding at NASA's Marshall Space Flight Center (MSFC), Huntsville, Ala., has taken a new direction during the past 12 years. In 1994, fusion welding processes, namely variable polarity plasma arc (VPPA) and gas tungsten arc (GTA), were the cornerstone of welding development in the Space Flight Center's welding laboratories, located in the part of MSFC known as National Center for Advanced Manufacturing (NCAM). Developed specifically to support the Space Shuttle's external tank and later the International Space Station's manufacturing programs, VPPA was viewed as the paragon of welding processes for joining aluminum alloys.

A major change began in 1994 when NASA's Jeff Ding brought the friction stir welding (FSW) process to NASA. At that time, FSW was little more than a lab curiosity. The first welds were made in fall 1995. NASA's small initial investment in FSW has paid off in cost savings, hardware quality, and prestige.

Friction stir welding is now part of Shuttle external tank production and is the preferred weld process for manufacturing components for the new Crew Launch Vehicle and Cargo Lift Vehicle that will take U.S. astronauts back to the moon. It is being considered for in-orbit space welding and repair. It is also of considerable interest for Department of Defense (DOD) manufacturing programs. Marshall's involvement in these and other programs makes NASA a driving force in this country's development of FSW and other solid-state welding technologies. At present, almost the entire ongoing welding R&D at MSFC focuses on FSW and other more advanced solid-state welding processes.

Fig. 1 — Vertical weld tool for friction stir welding.

MSFC Begins FSW Development

Friction stir welding development studies at MSFC were first carried out on a Kearney and Trecker 200 5-axis CNC horizontal boring mill. This 14-ton, 25-hp machining center was totally dedicated to FSW process development. Traditional FSW, as originally conceived at The Welding Institute (TWI), Cambridge, U.K., is performed using a pin tool comprised of a shoulder and smaller pin. In short, the process works as follows: The rotating pin, slightly shorter than the weld depth, plunges into a weld joint until the tool shoulder contacts the surface. The shoulder frictionally heats the weld metal and confines it so that welding and not plowing takes place. The rotating pin within the joint "stirs" the metal together. As the rotating pin tool is moved along the joint, the leading face of the pin engulfs and rotates weld metal to the back of the pin while the pressure under the confining

JEFF DING (Robert.J.Ding@nasa.gov), ROBERT CARTER, KIRBY LAWLESS, ARTHUR NUNES, CAROLYN RUSSELL, and MICHAEL SUITS are with Marshall Space Flight Center, National Center for Advanced Manufacturing, Huntsville, Ala. JUDY SCHNEIDER is with Mississippi State University, Starkville, Miss.

Fig. 2 — Circumferential weld tool for FSW with recently welded transition rings and dome.

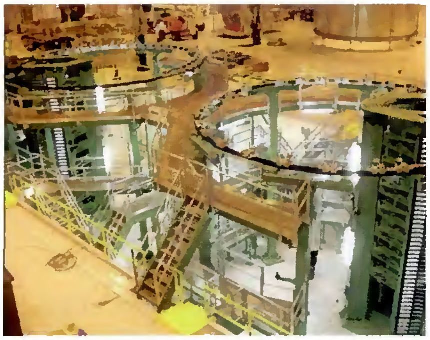

Fig. 3 — Friction stir welding production tools at the Michoud Assembly Facility.

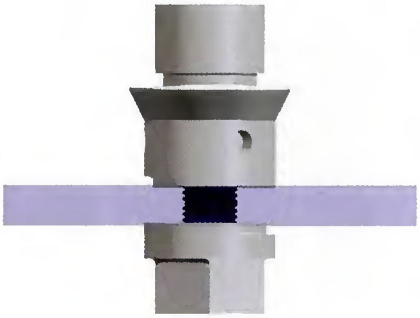

Fig. 4 — Self-reacting pin tool.

Fig. 5 — Horizontal weld tool for FSW.

shoulder maintains weld metal integrity and prevents the opening up of voids. In general, this process produces a higher-strength, higher-quality weld than fusion weld processes. The FSW process leaves behind a fine, dynamically recrystallized grain structure instead of the large dendritic grain structure left in the wake of fusion welds.

Welding metals in the solid state (also referred to as the solid phase or plastic state) is a significant advancement for man-rated hardware manufacturing. At NASA, there are two quality-level requirements. The first is for unmanned hardware; the second, even more stringent, is for equipment designed to support human life (man-rated).

Welding metals without melting avoids weld defects found in fusion welds such as liquation cracking, solidification cracking, and oxide formation. It further minimizes the potential of other undesirable weld anomalies such as thermal distortion and high residual stresses. The FSW process is very forgiving. Keeping materials in the solid phase during FSW results in greater retention of metallurgical properties of the base metal; in many cases, mechanical and fatigue properties are near those of the base metal.

In addition to the superior mechanical properties realized from FSW, the overall cost of using the process is significantly lower than for fusion welding. No consumables are required. Careful removal of oxides from the joint area immediately prior to welding is often unnecessary. The FSW machine is ideally suited to automation and integration with other machine tool operations and equipment maintenance is minimal. Extensive operator training is not necessary.

Early friction stir welding trials at MSFC were conducted on various aluminum alloys (2219, 2195, 7075, 5XXX and 6XXX series). Development was subsequently expanded to include metal matrix composites and high-melting-temperature alloys including steel, Narloy-Z, GRCop-84, and titanium alloys. Copious data collected during the early development phase of FSW demonstrated a high degree of process repeatability. Friction stir welding requires control of only three process variables: shoulder plunge depth, tool rotational speed, and welding travel speed. Once the variables are optimized, the resultant weld properties are highly repeatable. The same weld quality results time and time again. Friction stir welding allows removal of the human element (the welder) from the process. This minimizes risk of weld defects.

Superior mechanical properties, process reliability, plus expected cost savings influenced NASA's decision to begin studying the feasibility of implementing FSW into Shuttle external tank production.

Implementing FSW into the Space Shuttle External Tank

Friction stir welding studies targeting the external tank (ET) manufacturing program began in 1998. The FSW process was first demonstrated on simulated ET hydrogen barrel welds. The demonstration was completed jointly between NASA and the prime contractor, Lockheed-Martin. Engineers fabricated a 27.5-ft-diameter simulated hydrogen tank barrel section comprised of eight barrel panels measuring 15 ft tall.

Marshall's vertical weld tool (VWT) (Fig. 1) was used for the welding. The weld joints included 15 ft of constant thickness as well as thickness tapers from 0.32 to 0.65 in. The FSW retractable pin tool was demonstrated for the first time in making the taper welds. The retractable pin tool, currently licensed from NASA by MTS, Eden Prairie, Minn., and Nova Tech Engineering, Seattle, Wash., is capable of automatically adjusting the length of the pin extension into the weld joint. This automatic adjustment is critical when welding material tapering between two thicknesses. Further characterization of FSW for ET welding was carried out through two subsequent studies between 1999 and 2001. NASA's circumferential weld tool (CWT) (Fig. 2) was modified to demonstrate circumferential welding and fixturing techniques.

The processs was implemented into production in 2001. Figure 3 shows the two FSW production tools located at the Michoud Assembly Facility, New Orleans, La., where the Shuttle external tank is manufactured. Eight longitudinal weld joints on the liquid hydrogen barrel and four longitudinal welds on the liquid oxygen barrel are welded using FSW. There is approximately one-half mile of weldments on each ET. Approximately 700 ft is now done using FSW with VPPA welding still used for the remainder of the weldments.

Fabrication of man-rated hardware for NASA's manned space programs requires manufacturing processes with a high degree of reliability and repeatability. Once optimal weld parameters are established, a large population of weld test samples is generated. These samples are subjected to mechanical testing. The test data are used to evaluate weld strength and quality, and assist in defining critical flaw size and margins of safety. Qualifying a welding process for manufacturing requires precise statistical evaluation of weld mechanical property data generated using optimal welding parameters for a given material, joint design, and thickness. Statistically speaking, the fracture and structural analysis of the weld mechanical test data results require a 99% confidence level that 90% of the weld strength values fall within structural design criteria.

This statistical evaluation process establishes margins of safety required to safely support and protect human life in space. This statistical approach defining hardware quality was implemented soon after the ET manufacturing program began. At that time, VPPA was used as the primary weld process, and the margins of safety for the ET were partly determined using the standard deviation of VPPA weld test data. Today, the ET has a greater margin of safety using the FSW process because of increased weld strength and the standard deviation of test data is smaller.

Current FSW Development Activity

The self-reacting friction stir welding process is a current major object of development in FSW technology — Fig. 4. The self-reacting pin tool has two shoulders: one positioned on the top surface of the weld piece and the other on the bottom side. A threaded pin, captured by each shoulder, protrudes through the material thickness. During a weld, the two shoulders are tightened against the crown and root surfaces of the weld joint, thus, "pinching" it to apply the required forging loads. The dual shouldered/pin assembly rotates as a single unit while traversing the weld joint. The primary advantage of using the self-reacting pin tool (instead of the traditional single-piece pin tool) is that it removes the requirement for expensive tooling that is needed to react the mechanical forging forces generated during the FSW process.

The self-reacting tool could not be employed, however, without new NASA design features incorporated into the shoulders. They enable the self-reacting pin tool to operate perpendicular to the surface instead of at a slight angle as required of the single-piece pin tool.

NASA is focusing on the development of this self-reacting tool for circumferential welds in the external tank and Crew Launch Vehicle upper stage hardware. The self-reacting friction stir welding pin tool has been used successfully to weld 27.5-ft-diameter ring test sections located between barrel sections in the Shuttle ET. The horizontal weld tool (Fig. 5) was used for the demonstration.

Another FSW advancement being investigated at Marshall is the welding of very thick materials. The approach is to use a modified, retractable pin tool designed by Ding of NASA and Peter Oelgoetz of Pratt and Whitney, Rocketdyne, Inc. The new retractable pin tool is de-

Fig. 6 — An artist's rendering of the Cargo Lift Vehicle (left) and the Crew Launch Vehicle (right).

signed to weld and close out the keyhole in materials 2.0 in. and greater in thickness. Another area of interest is friction stir welding of lines and ducts for space vehicles. This would be done using a NASA-patented orbital weld head. The device is capable of welding smaller diameters typical of those found on the Crew Launch Vehicle and Heavy Lift Launch Vehicle, as well as larger-diameter piping systems found in the oil industry.

Nondestructive Examination Techniques for FSW

Nondestructive examination (NDE) requirements for external tank friction stir welds are currently the same as for fusion welds. These inspections include dye penetrant, film radiography, ultrasonic, and visual techniques. However, new NDE advancements, such as phased array ultrasonics, eddy current arrays, and digital X ray, are emerging, and NASA engineers are investigating these techniques for implementation into the Shuttle external tank and Crew Launch Vehicle manufacturing programs.

Phased array ultrasound uses multi-element piezoelectric and composite transducer technology with sophisticated software timing routines to generate and analyze tightly controlled elastic waves in materials being tested. Phased array ultrasonic inspection produces much higher resolution and provides much more detection sensitivity with lower noise than conventional ultrasonic inspection. For the Space Shuttle's external tank, an RD Tech Tomoview with 128-element transducers is used to detect embedded and near-surface flaws such as lack of adequate forging (similar to incomplete fu-

Fig. 7 — Schematic of the new robotic FSW system.

Fig. 8 — High-speed friction stir weld system.

sion in conventional welds), incomplete penetration (considered embedded when root side is in compression, a condition detectable by penetrant methods), wormholes, surface galling, tears, and residual oxides.

Advanced flexible circuit boards and microstrips have enabled the use of multielement eddy current sensors, which have also improved the resolution, detection, and coverage of near-surface defects in metallic materials, and allow for more accurate measurements of electrical characteristics. Multielement eddy current will someday replace fluorescent dye penetrant in many FSW applications for the detection of surface galling, incomplete penetration, and tears.

For FSW technology, many of the flaws are planar and do not have much volume, but film radiography is still utilized for wormholes and larger, through-thickness, lack-of-forging flaws. NASA has begun to incorporate the use of digital X rays using fiber-optic-coupled scintillation detectors and flexible phosphor plates with conventional X-ray tubes. Continuing resolution and detectability improvments in the future will make this technique a more effective complementary technique to ultrasonics.

Modeling the FSW Process

In parallel with process development, NASA has also employed mathematical

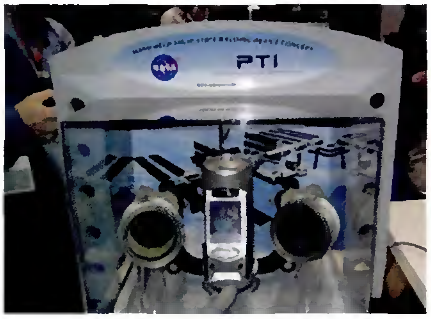

Fig. 9 — Conceptual prototype of a hand-held, solid-state welding device for in-space applications.

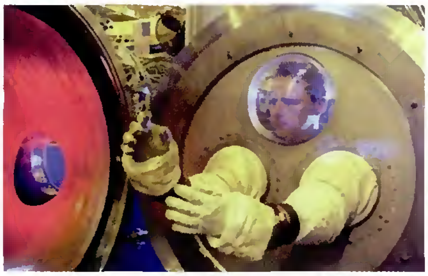

Fig. 11 — Marshall's vacuum chamber facility includes a space suit viewing port and gloves.

modeling to better understand the physics of the metal flow in the FSW process. The rotating surfaces of pin and shoulder in contact with the weld metal force a rotational flow within the weld metal. This deformation as well as frictional slippage at the contact surface generates heat, which softens the metal and makes it all the easier to deform. The flow conditions are critical to the quality of the weld. For example, extrusion of metal from under the shoulder of an excessively hot weld may relax local pressure and result in hole defects. The trace of the weld joint in the wake of the weld may vary geometrically depending upon the flow streamlines around the tool with some geometries more vulnerable to loss of strength from joint contamination than others.

The material flow path around the tool cannot be seen in real time during the weld. By using analytical "tools" based upon the principles of mathematics and physics, investigators can create a weld model able to compute features that can be observed. By comparing the computed observables with actual data, the weld model can be validated or adjusted to get better agreement. Given a completed model, weld metal property data, pin tool geometry, travel rate data, etc., can be entered into the model and weld structures and properties generated by computer. Once this stage is reached, the weld modeling process can save significant development costs by reducing costly trial-and-

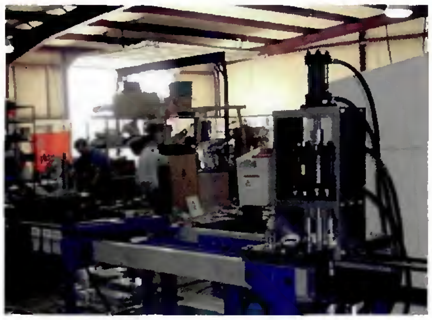

Fig. 10 — Thermal stir welding prototype system.

error approaches to obtaining quality welds.

Over the past decade, the MSFC weld modeling effort has generated a number of concepts useful to engineers for innovating, and especially for diagnosing problems, in FSW. Examples would be temperature requirements on pin tool materials or the relation of joint trace configurations to tool geometry. A good semiquantitative understanding of the FSW flow field enabling the qualitative interpretation of complex-appearing weld structures has been attained.

Going to the Moon

On January 4, 2004, the Vision for Space Exploration was released giving the directive to NASA to pursue human exploration to the moon and beyond. The current schedule calls for a 2010 launch of a test vehicle. This short preparation time presents a tremendous challenge to the Marshall Space Flight Center engineers as they are responsible for the overall design and manufacture of the new lunar space vehicles. Although the design is not yet complete, the approach is to launch two vehicles called the Crew Launch Vehicle (CLV) and the Cargo Lift Vehicle (CaLV) — Fig. 6. The Crew Exploration Vehicle (CEV) sits on top of the CLV. During the actual mission, the CLV will be launched and will place the CEV into earth orbit. A subsequent launch of the CaLV will place it in earth orbit. The CEV will then mate with the second stage of the CaLV to form the Earth Departure Stage (EDS). The EDS will then proceed to the moon.

Marshall welding engineers are already planning for their role in the fabrication of the CLV upper stage components where FSW is the baseline weld process. Recognizing that the manufacturability of the final design must be conducive to welding, welding engineers are working as part of an Integrated Product Team from a welding viewpoint. Welding representation on the Integrated Product Team ensures the design concepts are compatible with the baselined FSW process. The final design of the CEV and CaLV will follow. Engineers at MSFC are preparing to fabricate full-scale hardware test articles and possibly flight hardware articles. There is already a new robotic friction stir welding system being planned — Fig. 7. This will be among the largest FSW systems in the country. It will be capable of welding full-scale man-rated space vehicle hardware comprised of complex geometries such as domes and ogive sections.

In-Space Welding and Weld Repair

Welding technologies must be developed to support the many roles required for long-duration space travel. Human existence during long-range space travel will rely, to a large extent, on the ability to react to unexpected scenarios, such as micrometeoroid impact and mechanical failure. There will be the routine maintenance and repair activities. There must be capabilities to generate original space flight hardware, spare parts, and consumables.

Welding in space is not new to NASA. Important lessons were learned from the International Space Welding Experiment designed at MSFC in the late 1980s and 1990s but never flown. The experiment was intended to address the high risk and unknowns associated with welding operations in the vacuum and microgravity of space. Welding was to be carried out by an electron beam fusion process. Much of the effort for this experiment was devoted to assessing the potential dangers of high-voltage electron beams, molten metal, and sparks. Welds carried out in vacuum sometimes exhibited severe porosity if outgassing contaminants are present and in microgravity porosity tends to remain in the weld as it is not expelled by buoyancy forces. Solid-state FSW eliminates both safety concerns and porosity concerns.

Several new solid-state welding concepts have been initiated over the past several years for the purpose of welding and weld repair in space. Both a small, manual hand-held unit for thin materials and a larger, portable unit for thicker materials are envisioned.

High-speed FSW (HS-FSW) is under investigation as a potential basis for hand-held manual welding. The concept behind HS-FSW is based on the premise that high spindle speeds (tens or hundreds of thousands of revolutions per minute) in FSW reduce the forces necessary to produce sound welds to a level permitting manual hand-held devices. Engineers have already begun studying the effects of high rpm pin tools using the high-speed machine tool for FSW (Fig. 8) located at MSFC. The machine is capable of 30,000 rpm, with a travel speed up to 200 in./min. It has been used to weld 0.060-in. GRCop-84, a copper alloy being investigated for thrust chambers. Further research is planned to investigate high-speed phenomena relative to forces, feed rates, pin-tool designs, and robotic applications.

A parallel development effort is also in place between MSFC and the University of Wisconsin to study the feasibility of robotic operation of a manual hand-held solid-state apparatus. Robotic operation may be required to effectively operate a solid-state welding device in space. Dr. Weija Zhow, director of the Wisconsin Center for Space Automation and Robotics, Madison, is currently working on the design and fabrication of the first robotically assisted hand-held high-speed FSW prototype. Delivery is expected late this year.

"The challenge for space welding technology," Zhow said, "is the constraints placed upon mass, power, and volume. Therefore, a low mass, portable device is critical to NASA's in-space, in situ fabrication and repair."

A process called ultrasonic stir welding (USW) (patent pending) is also being investigated at MSFC for hand-held welding applications. In USW, ultrasonic energy heats the material into the plastic state. Unlike FSW, there are no rotating shoulders producing frictional heat. This concept may be more practical than HS-FSW as an in-orbit welding and repair process because high rotational speed stability issues will be avoided. Solidica, Inc., Ann Arbor, Mich., has completed initial assessment of integrating ultrasonic technology with a hand-held solid-state weld apparatus. "The feasibility of integrating ultrasonic heating into a weld tool looks promising," said Dawn White, president of Solidica, Inc. Solidica is a recognized leader in the application of ultrasonics for solid-state bonding systems. "This technology should leverage into a hand-held manual device for both space-based and land-based applications," she continued. Figure 9 shows a conceptual prototype of a hand-held solid-state welding device for in-space applications.

Thermal stir welding (TSW) (patent pending) is yet another weld process under study at MSFC as a candidate for in-space welding of thicker members — Fig. 10. Thermal stir welding is different from FSW in that the heating, stirring, and forging process elements found in FSW are controlled independently. There is little frictional heating and no high-speed rotating shoulders. As is the case for USW, TSW also avoids stability issues associated with high-speed rotational parts.

Marshall Space Flight Center has facilities to test prototype welding hardware for space applications. Figure 11 shows part of Marshall's vacuum chamber facilities, which includes viewing ports and space suit gloves. The 4- x 4-ft chamber can be pumped down to 10^{-6} torr to simulate the vacuum of space.

> Marshall has perhaps the most concentrated capabilities and expertise in the nation for FSW.

The Space Act Agreement and Military and Private Sector Applications

"NASA's Marshall Space Flight Center has perhaps the most concentrated capabilities and expertise in the nation for FSW and other solid-state welding development," said John Vickers, manager of the National Center for Advanced Manufacturing at Marshall. "Welding engineering is a core competency for us that includes technology development and engineering for large complex aerospace structures. Continued technological innovation is critical for NASA in this area because it improves performance and reliability, and increases productivity and cost-effectiveness. We have established broad collaborative partnerships with industry, government, and academia that are an essential element of successful research and development. Through the Space Act Agreement (SAA), companies, large and small, can gain access to our facilities and engineering expertise to pursue welding R&D."

The SAA process has been used by numerous companies pursuing FSW capabilities at MSFC including Hayes Wheels, Williams International, and more recently, the U.S. Army, Lockheed-Martin, and Keystone Synergistic Enterprises, Inc.

In order to qualify for a SAA, the proposed R&D must benefit NASA programs and interests. "There are several types of SAAs available to industry," explained Sammy Nabors of the Technology Transfer Office. "The type of SAA depends on the proposed statement of work and the relevance to the overall NASA mission. The important thing about the SAA is that all data generated from the effort are proprietary to the company that is doing the work."

Work done at MSFC through the Space Agreement Act program provides engineers the opportunity to expand NASA technology applications beyond the applications of specific NASA projects and "return" the taxpayer's technology development investment to the commercial sector. "We call this technology spin-off," said Nabors. "The spin-off process is an important part of the civil service worker. We, the government, are obligated to take the technology developed with the taxpayer dollars, and return it back into the private sector. This is done through the licensing of NASA-owned technology. The SAA process allows NASA to work closely with U.S. companies willing to invest in technology and develop the technology for specific industry segments."

An example of such an effort is ongoing with a Florida company, Keystone Synergistic Enterprises, Inc. Keystone's intent is to develop and commercialize technologies for both defense and commercial applications and offer other companies licenses for the use of thermal stir joining. Keystone works closely with DOD primary contractors to develop technologies closely aligned with the needs of defense systems while looking for near-term commercial spin-offs to establish a commercialization foundation. While the Navy is interested in effective titanium alloy joining technologies for shipbuilding, application of TSW for fabrication of high-performance personal yachts from titanium is a potential spin-off catering to an emerging high-performance yacht market.◆

A Look at Rocker Arm Spot Welding Machines

Some of the features and concerns of rocker arm machines are discussed

BY JIM DALLY

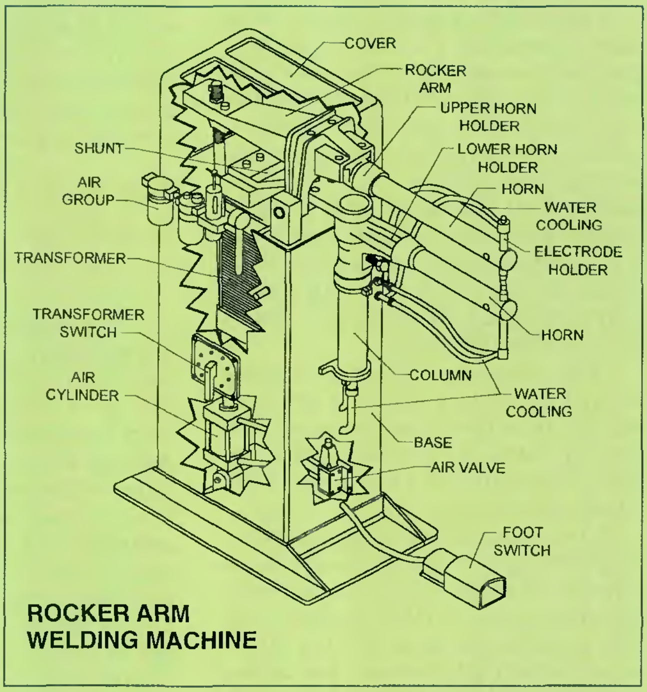

Fig. 1 — A diagram of a typical rocker arm spot welding machine.

Rocker arm spot welding machines (Fig. 1) are commonly used to assemble sheet metal parts, wire displays, make repairs to electrical motors and starters, weld nuts to sheet metal parts, and join numerous other assemblies. The name 'rocker arm' comes from the pivoting arm used to apply the force to the electrodes during welding.

Basic Force

The welding force is applied to the electrodes when the rocker arm is lifted. Commonly, the lifting is applied by either a spring compressed by means of a foot treadle (foot kicker), or a double-acting air cylinder. The air cylinder is controlled by a four-way solenoid air valve with an air regulator.

Electrode Force

The amount of clamping force exerted by the electrodes on the parts is an important factor for making good resistance spot welds.

This force can be accurately measured with a force gauge, or it can be approximated mathematically from the formula: Electrode Force = cylinder area ($\neq r^2$) x cylinder pressure x the ratio of the length of the pivot-to-cylinder connection to the length of the pivot to electrode.

As an example, use this formula to calculate the electrode force for a machine with the following features — Fig. 2.

The length of the pivot-to-cylinder connection measures 14 in.,

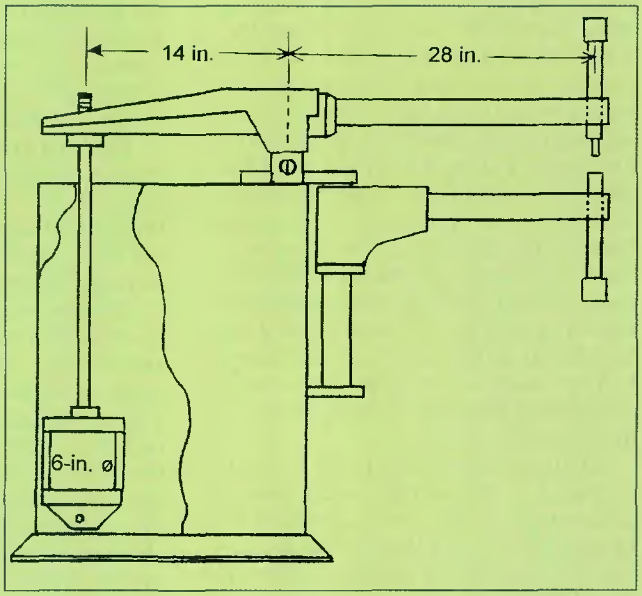

Fig. 2 — Sketch of a rocker arm spot welding machine with a 6-in.-diameter cylinder, 14-in. arm from cylinder connection point to the pivot, and 28-in. arm from the pivot to the electrode centerline.

JIM DALLY is president of Standard Resistance Welder Co., Winston, Ga.

and the pivot-to-electrode arm is 28 in. (ratio is 1 : 2). The machine has a 6-in.-diameter air cylinder pressurized at 50 lb/in.^{2}. Then, the electrode force = (3.14 x 3^2 in.^{2}) x 50 lb/in.^{2} × ½ = 706½ lb force.

Effect of Horn Alignment

Maintaining parallel alignment of the horns (the electrode-supporting arms) during the weld is of prime importance. Failure to keep the horns parallel and aligned can cause off-center contact on the parts being assembled, resulting in a dent, inconsistent welds resulting from welding on a side of the electrode point, cosmetic problems, and/or part skidding out of position during the weld.

Maintaining parallel alignment is especially important when welding file cabinets, computer cases, store shelves, automotive show panels, displays, etc.

Controls

All RWMA NEMA-type controls are suitable for rocker arm spot welding machines from the basic 1A weld timer to constant current, multifunction combination controls.

Welding Machine Sizes

Typical foot treadle welding machine designations include the following:

- Size 1 — 10 kVA, 15 kVA.
- Size 2 — 20 kVA, 30 kVA.
- Size 3 — 50 kVA.

The following are typical air-operated rocker arm spot welding machines:

- Size 1 — 10, 15, and 20 kVA. Typical 3¼-in.-diameter air cylinder
- Size 2 — 20 and 30 kVA. Typical 4-in. bore air cylinder
- Size 3 — 50, 75, and 100 kVA. Typical 5-in. bore cylinder, optional 6-in. bore
- Size 4 — 100, 150, 200, and 300 kVA. Six and 8 in. cylinder
- Size 5 — 300, 400, and 500 kVA. Typical 8-, 10-, and 12-in. cylinder.

Larger welding machines are supplied with larger air cylinders to provide greater force. However, as the throat depth increases and the pivot point-to-cylinder length remains constant, the electrode force is decreased.

It is common to use a Size 4 rocker arm spot welding machine to weld two pieces of 10-gauge HRS at a 36-in. throat and meet all required electrode forces as published in RWMA/AWS weld schedules.

Optional Features

Numerous optional features are available including the following.

Retractable stroke (quick lift) to allow easy access on deep flanges and boxes.

Extended lower column for welding parts as deep as 27 in.

Forge system for Sizes 3, 4, and 5 to use in welding aluminum and high-strength low-alloy steels.

Two-stage foot switch to allow operator to clamp and/or reposition parts before initiating the weld sequence.

Low press electrode cleaning

Lower horn brace

Dual weld or triple weld using two or three foot switches to permit welding different thicknesses, such as 10 gauge to 10 gauge, 10 gauge to 16 gauge, or 16 gauge to 22 gauge. Can also offer two or more electrode forces with corect control.

Inverter control and transformer.

Specialized options include forklit rails, casters, water recirculator, water chiller mounted to a frame, quick-disconnects for power, water, and air, electrode force sense control, water-flow switches, and pressure switches. ♦

A Review of Postweld Heat Treatment Code Exemptions

Similarities and differences of exemptions from PWHT for C-Mn and low-alloy steels in several current codes are reviewed, and some rationalizations are considered

BY D. J. ABSON, Y. TKACH, I. HADLEY, V. S. WRIGHT, AND F. M. BURDEKIN

This article compares and contrasts the current rules and guidelines present in various fabrication standards (mainly U.S. and UK) regarding the postweld heat treatment (PWHT) requirements of welds and the limits for as-welded construction made in pipes, pressure vessels, and structures, including bridges, buildings, and offshore structures, as discussed below. It is recognized that some codes now include provision for repair without PWHT (Refs. 1–3), and that there have also been investigations aimed at providing recommendations for acceptable thickness limits for the as-welded condition for general structural conditions (Refs. 4, 5). It is noted that steel making technology has changed over the last thirty years or so (although steels are also produced in parts of the world where steel making technology lags behind best practice). However, the fabrication codes were generally devised for older, normalized steels with higher carbon contents (Refs. 6, 7), and often with no toughness requirement.

In addition, a number of methods available for gaining exemption from PWHT are examined, including specially designed weld repair procedures and a case-specific fracture mechanics approach (in Part 2). The general method adopted is that of Ref. 8, for which fracture mechanics testing, e.g., as in Ref. 9, is normally required. This investigation relates only to C-, C-Mn, and low-alloy steels. Some of the similarities and differences are considered, and testing required to move toward elimination of the apparent anomalies is considered. In compiling this article, the views of representatives of fabricators and end users have been sought.

The objectives of the study were to identify the types of materials where industry considers that there are grounds for seeking wider exemption from PWHT; to compare and contrast the limiting thickness requirements above which PWHT is required and the associated Charpy test requirements for the as-welded condition in standards relevant to the fabrication industry; to investigate the methods available for gaining exemption from PWHT, namely the use of specially designed repair procedures and the specification of a minimum Charpy energy, calculated by a fracture mechanics approach; and to identify whether a future program of toughness testing and residual stress measurements on specific steels is needed to demonstrate a case for exemption from PWHT.

D. J. ABSON and I. HADLEY are with TWI, Granta Park, Great Abington, Cambridge, U.K. Y. TKACH, formerly with TWI, is now with Corus Swinden Technical Center, Moorgate, Rotherham, UK. V.S. WRIGHT is a consultant, recently retired; formerly general manager IRD, Rolls-Royce. F. M. BURDEKIN was formerly professor at University of Manchester Institute of Technology.

Table 1 — Limiting Thickness for which Postweld Heat Treatment Is Not Required for C-Mn Steels According to Various Standards

Code	ASME P1 Group 1/C-Mn, and BS EN Group 1	ASME P3 Groups 1 and 2, and BS EN Group 1.4	ASME P4 Groups 1 and 2, and BS EN Group 5.1	ASME P5 Group 1, and BS EN Group 5.2	Comments	
ASME VIII (14)	32 mm increase to 38 mm with 93°C preheat	16 mm, 93°C preheat, C≤0.25%	16 mm, 121°C preheat, C≤0.15%	16 mm, 149°C preheat, C≤0.15%	≥ 27J at 20°C for 32 mm and R_e ≤448MPa (≥ 20J at 20°C for ≥ 34 mm and R_e ≤345MPa)	Toughness requirement increases as strength increases; allowable thickness increases as toughness increases and as strength decreases.
ASME B31.1 (15)	19 mm	16 mm, 95°C preheat, C≤0.25%	13 mm, 120°C preheat, C≤0.15%	13 mm, 150°C preheat, C≤0.15%	No explicit Charpy test requirement in the standard.	
ASME B31.3 (16)	19 mm	19 mm	13 mm, 149°C preheat	13 mm, 177°C preheat, C≤0.15%	R_e≤448MPa, C_V≥ 18J R_e≤517MPa, C_V≥ 20J R_e<656MPa, C_V≥ 27J	Room temperature Charpy toughness requirement for carbon- and low alloy steels:
ASME B31.8 (17)	32 mm				No explicit Charpy test requirement in the standard.	
API 650 (18)	32 mm increase to 38 mm with 90°C preheat				Gp I-III & IIIA (defined in the standard) C_v ≥ 20J. Gp IV-VI C_v ≥ 41J; Gp VIA, C_v≥ 48J if Q & T or TMCP	
API 620 (19)	32 mm, increase to 38 mm with 93°C preheat				PWHT required for nozzles and attachments when wall thickness exceeded.	
					C_v≥ 34J (≥ 40J for Q&T grades)	Test temperature ≤ (design metal temperature –17°C).
					C_v ≥ 34J	For design metal temperature > –40°C, if tested at or below this temperature
					C_v ≥ 40J	Acceptable for design metal temperatures ≤–40°C.
					C_v ≥ 27J (≥ 34J in longitudinal direction)	Test temperature of –196°C for liquefied hydrocarbon gasses.
AWS D1/1 (29)					Limits set by contract drawings or specifications.	
JIS B.8243 (20)	32 mm, increase to 38 mm with 95°C preheat	16 mm, C≤0.25% 95°C preheat preheat;	Tubing 16 mm, C ≤0.15, 120° 120°C preheat; PWHT all thicknesses of vesel	Tubing 16 mm, C ≤0.15, Cr ≤3.0, 120°C preheat; PWHT all thicknesses of vessel	R_m <490MPa, C_V≥ 20J R_m ≥ 490MPa, C_V≥ 27J	At T ≤ minimum operating temperature.
Stoomwezen(21)	32 mm, C≤0.23%, may increase to 40 mm				Fine-grained steel: C ≤0.23 and CE ≤0.55 and R_e ≤370 MPa and KV (perpendicular) ≥ 31J at 0°C and also KV (parallel) ≥ 27J at –50°C and 32 mm <t≤40 mm and weld metal KV (perpendicular) ≥ 31J at 0°C, and as long as there is no accumulation of weldments or extensive local stiffening, and a hydrotest is carried out. Fine-grained steel; C≤0.23 and CE ≤0.55 and R_e ≤450MPa and t≤32 mm, and as long as there is no accumulation of weldments or extensive local stiffening, there is no toughness requirement.	

Review of Current Practice and Code Requirements

Fabrication Standards for C-Mn Steel Pressure Vessels, Piping, and Offshore Structures

A survey was carried out in 1971 (Ref. 10) that showed that the requirements of various codes, in terms of the material thickness above which PWHT was required, varied considerably. Later work in 1980 (Ref. 11) showed that, while considerable harmonization had taken place, significant divergence remained. More recent work by Mohr (Ref. 12) and also by Salkin (Ref. 13), who reviewed the differences in thickness limits, in temperature ranges, and in hold times covering a range of steel types, has highlighted the limits and provisions for exemption from PWHT. These studies showed there was still some variation between codes. The results are included in Table 1, where the requirements of the U.S. codes relate to ASME P1 to P5 steels. The table has been extended to include requirements for Charpy test properties, and to cover a range of other codes and standards.

Several of the codes have a similar thickness limit, at ~32 mm, above which PWHT is required. Provision is made in several codes (Refs. 14, 18–20, 25) to extend this limit to 38 or 40 mm if certain conditions, generally the imposition of a preheat of the order of 93°C (200°F), are met. The notable exceptions are ASME B31.1 (Ref. 15) and B31.3 (Ref. 16), with a thickness limit of 19 mm, and EEMUA 158 (Ref. 28) that specifies a limit of 40 mm for nodes, with a limit of 50 mm applying

Table 1 — Continued

Code	ASME P1 Group 1/C-Mn, and BS EN Group 1	ASME P3 Groups 1 and 2, and BS EN Group 1.4	ASME P4 Groups 1 and 2, and BS EN Group 5.1	ASME P5 Group 1, and BS EN Group 5.2	Comments	
BS 2971 (22)	35 mm				No Charpy test requirement.	
BS 1113 (23)	30 mm, increase to 35 mm with 100°C preheat, C≤0.25%	13 mm, increase to 35 mm with 100°C preheat, C≤0.25%	≤13 mm thick and ≤127 mm diameter, C≤0.15%	≤13 mm thick and ≤127 mm diameter, C≤0.15%	C_v >40J	
BS EN 12952 (24)	<35 mm		<13 mm	<13 mm	C_v ≥ 27J for transverse specimens (preferred) or C_v≥ 35J for longitudinal.	T_{CV} ≤ lowest scheduled operating temperature (T_{CV}.20°C).
BS 2633 (25)	30 mm, increase to 35 mm 100°C preheat, C≤0.25%	≤12.5 mm thick and ≤127 mm diameter	≤12.5 mm thick and ≤127 mm diameter, 120°C preheat	≤12.5 mm thick and ≤127 mm diameter, 150°C preheat, C≤0.15%	No Charpy test required.	
PD 5500 (26)	35 mm, increase to 40 mm if C_v ≥ 27J at −20°C	12.5 mm, increase to 19 mm with 100°C preheat	PWHT required for all thicknesses	PWHT required for all thicknesses		
PD 5500 (26) (Service temperature <0°C)	40 mm, but see comments				R_e<450MPa, C_v≥ 27J R_e≥ 450MPa, C_v≥ 40J	T_{CV} = 2.94 (MDMT−10)°C (PD 5500 Annex D)
PrEN 13445 (27)	35 mm		≤15 mm thick, or ≤13 mm thick and ≤120 mm diameter	≤15 mm thick, or ≤13 mm thick and ≤120 mm diameter and design temperature <480°C	C_v≥ 27J or C_v≥ 40J	Test temperature depends on strength, toughness level, and design reference temperature.
EEMUA 158 (28)	Minimum design throat thickness: –40 mm nodes 50 mm plain regions				R_e≥ 275 MPa, C_v≥ 27J R_e≥ 355MPa, C_v≥ 36J R_e≥ 450MPa, C_v≥ 45J	C_v at −40°C, for assumed MDMT = −10°C.
BS 5950 (30) & BS 5400(31)	$t_{max} = k.50.(\frac{355}{fy})^{1.4}.(1.2)\,(\frac{MDMT-T_{27J}}{10})$				C_v required at MDMT, k = 2 for as-welded joints but reduces with stress concentrations precent.	

to other regions. The apparent harmony is, however, in part illusory, because the steels employed in the United States and the United Kingdom are generally different in chemical composition (an issue that is considered in more detail later), and may well have different inherent Charpy test properties.

It should be noted that the basic requirements of BS 1113 (Ref. 23) and BS 2633 (Ref. 25), which are shown in Table 1, relate to steels with ≤0.25%C, and those of Stoomwezen (Ref. 21) to steels with ≤0.23%C; in these standards, PWHT is required for steels with higher carbon contents. In BS 2633 (Ref. 25), PWHT is not required for steels ≤35 mm thick if the service temperature is above 0°C, while PD 5500 (Ref. 26) has the same requirement for steels up to 40 mm thick. In Pr EN 13445 (Ref. 27), PWHT is only necessary in special cases, for example in H_2S service. In some of the British Standards (Refs. 22, 25, 26), PWHT is required, even up the limiting thickness shown, if it is specified by the purchaser.

The general trends revealed by the tabulation are for the permitted thickness without PWHT to decrease with increasing alloy content of steels and/or for increased preheat to be required, together with reductions in maximum carbon level permitted. For low-alloy steels containing ≤1.5%Cr and ≤0.5%Mo (including ASME P4 groups 1 and 2 steels), and also for 2.25%Cr-1%Mo steels (including ASME P5 group 1 steels), there is greater uniformity among the standards, and there are some strong similarities between the BS 2633 requirements and those of ASME VIII and ASME B31.1 and B31.3.

In Table 1, it will be noted that in ASME VIII (Ref. 14), API 650 (Ref. 18), BS 1113 (Ref. 23), and BS 2633 (Ref. 25), there is a marginal increase in the thickness limit if a preheat at a minimum temperature of ~93°C (200°F) is used. The reason for this is not known, and has not been discovered in the contacts made with representatives of the fabrication industry. It may reflect an anticipated increase in toughness or avoidance of hard local brittle zones from a slight reduction in as-welded HAZ hardness, as well as a reduced likelihood of hydrogen-assisted fabrication cracking.

Fabrication Standards for Buildings and Bridges

The material thickness requirements for bridges and buildings, as specified in BS 5950: 2000 (Ref. 30) and BS 5400: 2000 Part 3 (Ref. 31), have been examined. These specifications are much less prescriptive regarding requirements for exemption from PWHT; most welded connections in bridges and buildings, including those in thick sections, are left in the as-welded condition, and the emphasis is on the use of materials with sufficient fracture toughness not to require PWHT. Indeed, BS 5950 does not consider PWHT at all. However, these codes do provide material thickness limits. Unlike some of the pressure vessel and piping codes examined previously, the limiting thickness requirements are dependent upon service temperature, yield strength, and Charpy impact properties.

A summary of strength and impact values for current European structural steel products is given in Ref. 5. All the new European structural steel grades are supplied to a minimum Charpy impact level. The minimum Charpy toughness requirements are 27 J at −50°C for most grades, with some requirements being 40 J at –20°C (which is approximately equivalent to 27 J at –30°C). However, there may be a limiting thickness up to which the impact toughness is guaranteed. For example, in BS EN 10025 (Ref. 32), this limiting thickness for nonalloyed grades is 250 mm for plates and 100 mm for sections.

The limiting thickness values in BS 5950 (Ref. 30) and BS 5400 (Ref. 31) are presented as general equations; the form of these equations is the same for both specifications, although differences exist in calculating the so-called k-factor.

The equations, the background to which is explained in more detail in Ref. 5, are shown below.

$T_{min} \geq T_{27J} - 20$ *BS 5950 and BS5400:*

$$t \leq 50k\left(\frac{355}{\sigma_y}\right)^{1.4} 1.2\left(\frac{T_{min} - T_{27J}}{10}\right)$$

$T_{min} < T_{27J} - 20$ *BS 5950:*

$$t \leq 50K\left(\frac{355}{\sigma_y}\right)^{1.4}\left(\frac{35 + T_{min} - T_{27J}}{15}\right)1.2\left(\frac{T_{min} - T_{27J}}{10}\right)$$

BS 5400: not permitted

where t is the maximum permitted thickness of the part under stress in mm; k is the k-factor (see below); σ_y is the nominal yield strength of the part; T_{min} is the design minimum temperature of the part in °C; T_{27J} is the temperature in degrees Celsius for which a minimum Charpy energy of 27 J is specified by the product standard for impact tests on longitudinal V-notch test pieces.

The k-factor is the product of four subfactors relating to susceptibility to brittle fracture, as follows:

$$k = k_d \cdot k_g \cdot k_\sigma \cdot k_s$$

and takes values ranging from <0.25 to 4. Low values of k denote higher susceptibility to brittle fracture, e.g., high applied stress, high strain rate, or the presence of stress concentrations. The subfactors each account for a different aspect of susceptibility to brittle fracture, as follows:

- k_d accounts for the weld detail, and takes values between 0.5 and 2, which can be increased by 50% if PWHT is applied.
- k_g accounts for the presence of gross stress concentrations and takes values up to 1.
- k_σ takes account of stress levels, with values ranging from 1 to 2.
- k_s takes account of high strain rates, with values of 0.5 (for areas likely to be loaded under impact) and 1 (for all other areas).

As an example, the maximum permitted thickness of a grade 355 steel in the as-welded condition, subjected to Charpy testing at the material design minimum temperature (MDMT), would be 50 mm for the condition k = 1, i.e., with simple weld details, quasi-static strain rates, and no gross stress concentrations. This is broadly comparable with the upper range of allowable thicknesses of Table 1. However, the limiting thickness for the same as-welded joint could be as low as 14 mm under the same applied stresses and strain rates, if gross stress concentrations and poor weld details are present. If high-strain-rate loading also applies, e.g., bridge parapets, it could be even lower at 7 mm. Conversely, for simple welded joints under low applied stress, the limiting thickness could be as high as 100 mm, and even 150 mm if the fabrication is subjected to PWHT.

The fracture avoidance rules given in BS 5400 Part 3 (Ref. 31) are based on fracture mechanics calculations, calibrated against other considerations such as the results of full-scale tests on simulated bridge details, and case histories of bridge failure. Details of these calculation methods are described in Ref. 5.

> The steels employed in the United States and the United Kingdom are generally different in chemical composition, and may well have different inherent Charpy test properties.

Eurocode 3 — Design of Steel Structures

The requirements of Eurocode 3 (Ref. 33) have also been examined. Note that the document examined is a draft for development (DD ENV), and so is subject to change before final issue as a Eurocode. The document contains a procedure based on fracture mechanics principles and the Master Curve correlation between fracture toughness and Charpy energy.

Basically, the procedure determines the required fracture toughness for a steel component, depending on factors such as steel strength grade, section thickness, loading speed, lowest service temperature, applied stress, application of PWHT, type of structural element, and consequences of failure.

The provisions of the draft Eurocode (Ref. 33) are fairly similar to those of BS 5400 (Ref. 31) (and therefore similar to the upper range of Table 1) for the case k = 1, i.e., where there are no gross stress concentrating features or fatigue-sensitive weld details. However, whereas under BS 5400 the maximum permitted thickness for the same as-welded joint under similar applied stress and at a similar strain rate could range from 14 to 50 mm, it would remain 50 mm throughout under the draft Eurocode.

The draft Eurocode (Ref. 33) and BS 5400-3 (Ref. 31) requirements are compared and contrasted in detail in Ref. 5, where concern is expressed at some of the potentially unsafe provisions of the former.

Review of Documentation for Low-Alloy Steels

Low-alloy steels in piping and pressure vessel codes, primarily from the United States and United Kingdom, have also been reviewed. The information is also summarized in Table 1. See Table 2 for the compositions of relevant ASME P numbers. For such steels, there are some strong similarities in the requirements relating to exemptions from PWHT between the U.S. and UK codes. In Table 1, BS 2633 (Ref. 25) stipulates a similar preheat to the U.S. codes. However, the requirements of ASME B31.3 (Ref. 16) differ from the other codes in that PWHT is not required for ASME P3 Grades 1 and 2 steels up to 19 mm thick, while this code requires a higher preheat for P4 Grades 1 and 2 and P5 Grade 1 steels. It should be recognized that the situation is appreciably more complex than these numbers in Table 1 suggest, as different recommendations apply to specific weldments. See, for example, the footnote to ASME VIII Division 1 Table UCS-56 (Ref. 14), which includes clauses relating to nozzle connections, and the welding of pressure parts to nonpressure parts. The additional requirement to gain exemption from PWHT for tubes less than or equal to 13-mm thickness and less than or equal to 120-mm diameter in P5-type steels in Pr EN 13445 (Ref. 27) is that the design temperature should exceed 480°C.

Table 2 — Summary of Information on Relevant ASME P Numbers

ASME P Number	Steel Type
P1 group 1	C-Mn
P3 groups 1 and 2	C-0.5%Mo; 0.5%Cr-0.5%Mo
P4 groups 1 and 2	C-0.5%Cr-1.25%Mn-Si;1%Cr-0.5%Mo;1.25%Cr-0.5%Mo-Si
P5 group 1	2.25%Cr-1%Mo; 3%Cr-1%Mo

Differences between Material Grouping Systems in the ASME, CEN, and British Standard Codes

The grouping of materials used for welding has been carried out under the auspices of the different code standards committees in both Europe, including the United Kingdom, and the United States. In the United States, steels have been allocated a P number or S number, but since 1998, materials used for welder qualification may conform to other national or international standards or specifications, provided that the requirements for mechanical properties and specified analysis limits of the P or S number are met. In the United Kingdom, materials have been given group numbers in BS 4870 (Ref. 34) (for welding procedures) and BS 4871 (Ref. 35) (for welder qualifications). Both of these standards have been superseded by European standards BS EN 288 (Ref. 36) and BS EN 287 (Ref. 37). A submission was made to the committee compiling CR TR 15608, the draft guidelines for a metallic material grouping system (Ref. 38) by Sperko (Ref. 39). In his proposed Annex to CR TR 15608, he attempted to unify the ASME and CRTR 15608 grouping. He examined 985 relevant U.S. steel specifications and found the following:

1) 196 steel compositions could be classified within an ASME P1 Group.

2) Of the 196, only 91 C-Mn steels could be given a CR TR 15608 group number.

This study has indicated that, in terms of an ASME or CEN grouping system, material grouping does not provide a basis for exemption from PWHT. It would clearly be of considerable benefit in moving toward more uniform PWHT requirements if steel producers were to extend the practice of dual, or even multiple, certification of steels, so that greater uniformity is achieved in the compositions of steels. The practice would also facilitate the eventual unification of standards.

Code Requirements

Although the fundamental details of the differences in the separate codes for pressure vessels and piping, in terms of preheat and other requirements, have not been included, Table 1 indicates that rationalization of the PWHT exemption of all the codes would not be easy to achieve. For C-Mn steels, a comparison of codes, in terms of maximum wall thickness where PWHT is not required and maximum carbon equivalent of material permitted, has suggested an even more widely spread divergence. The codes are for different engineering applications. Differences between these may include different design stress criteria, different inherent Charpy test requirements, and (through the inspection codes) different allowable defect sizes. The codes were drawn up by different professional bodies, based on extensive experience and engineering practice. Therefore, differences arose and inconsistent requirements ensued. The gross differences that have arisen are likely to preclude the issue of a unified code requirement giving exemption from PWHT.

Three of the main groups of steel users with an interest in obtaining exemption from PWHT are the petrochemical industry through the Engineering Equipment and Materials Users Association (EEMUA) Material Technology Committee, the power generation industry (through the Electricity Generators Welding Panel (EGWP)) and the general structural industry. The data covered in this review suggest that reconciliation of the requirements of these user groups may not be possible. It would clearly be of benefit to the power generation industry to increase the thickness threshold for PWHT, for example to the 40 mm embodied in EEMUA 158 (Ref. 28) for C-Mn steels. Examination of the data also raises questions about the need to give a PWHT to weldments covered by BS 1113 (Ref. 23) and BS 2633 (Ref. 25) when the carbon content exceeds 0.25%. This limitation appears questionable, in the absence of such a condition in the other codes, but should be considered in relation to the Charpy properties of the steels concerned.

C-Mn and Cr-Mo Steels

For C-Mn and Cr-Mo steels, the lower thickness threshold embodied in ASME B31.1 (Ref. 15) and B31.3 (Ref. 16), compared with the other standards, may reflect the likelihood that the welding will be carried out in the field, and that defect rates and defect sizes may be greater than for shop welds. Girth welds in steel pipes have been subjected to a fracture mechanics assessment by Mohr (Ref. 40), who assumed the presence of root defects, and who concluded that the fracture resistance of pipes thicker than 19 mm was at least equal to that of thinner walled pipes. As PWHT is not required by ASME B31.1 for thinner walled pipes, presumably because the fracture resistance has been found to be sufficient, Mohr questioned the need for PWHT of thicker walled pipe if a fixed (rather than a proportional) flaw size is assumed in the calculations. However, all of these considerations need to be seen in the context of the inherent Charpy properties of the materials concerned, and this is not explicitly treated in some of the codes involved.

The position of the general structural industry is that the scale and size of structures is so large that PWHT of the overall structure is impracticable, and PWHT is only considered for local sub-assemblies under exceptional circumstances. Virtually all welded connections in bridges and buildings, including those in thick sections, are left in the as-welded condition, and the emphasis is on the use of materials with sufficient fracture toughness not to require PWHT. Fracture mechanics calculations were used in defining the fracture avoidance rules given in BS 5400 Part 3 (Ref. 31), and these were calibrated against other information, including the results of full-scale tests on simulated bridge details, and case histories of bridge failure. The detailed history of the piping codes is not known, but it is likely that custom and practice made a greater contribution, no doubt with some experience of failures incorporated. Also, it is noted that ASME B31.1 (Ref. 15) and ASME B31.8 (Ref. 17) provide for nonimpact tested steels to be used. However, since the code development took place, steel-making technology has changed significantly, steel toughness levels have generally improved substantially, and (at least within Europe) steel specifications commonly incorporate impact toughness requirements. It is, therefore, likely that limiting thicknesses could be increased, and thus PWHT omitted, as was shown to be acceptable for the steel vessels subjected to an ECA by Leggatt et al. (Ref. 41).

General Discussion

In spite of the disparities between the PWHT requirements of the pressure vessel and piping standards depicted in Table 1, some rationalization could be effected by building on the similarities that do exist. One possible approach would be to define a modest limiting thickness, perhaps ~32 mm, for which there are few additional requirements and a minimum level of absorbed Charpy energy could be assumed for the steels concerned. A greater limiting thickness could then be accommodated if additional requirements were met. This is the approach adopted in PD 5500 (Ref. 26), where the additional requirement is a minimum Charpy impact toughness (of ≥ 27J at –20°C) for the higher level of limiting thickness of 40 mm. More extensive requirements for the same limiting thickness are imposed in Stoomwezen (Ref. 21). These are C ≤0.23%, IIW CE ≤0.45, R_e ≤370 N/mm^2, both C_V ≥ 27 J at –50°C and C_V ≥ 31 J at 0°C for the base steel, and C_V ≥ 31 J at 0°C for the weld metal. It will be noted that the codes do not mention explicitly as-welded HAZ toughness, even though this factor would probably be limiting if HAZ fracture toughness were to be measured and a detailed engineering critical assessment were to be carried out.

This present study has demonstrated that code classifications and material groupings do not provide avenues for a uniform approach across all the codes, at least for C and C-Mn steels, for the omission of PWHT following welding. PD 5500:2000 (Ref. 26) provides an Appendix that can be used to justify exemption from PWHT. The justification is based on a design reference temperature calculation. However, it appears that this philosophy has been adopted only in this pressure vessel code, and the approach may not gain wide acceptance in codes for other applications. A material properties, rather than code-based, approach might be more widely acceptable. What appears to be required is a knowledge base of weldment impact value/fracture toughness properties for welds deposited with known welding parameters. It may then be possible for codes to include HAZ toughness requirement for weldments.

Conclusions

Code requirements for permitting as-welded construction without PWHT have been reviewed for C and C-Mn steels and some low-alloy steels, and the requirements of different codes have been compared. The conclusions are as follows:

1) U.S. and UK code requirements are generally similar in the limiting thickness of C and C-Mn steels (including ASME P1 steels) beyond which PWHT is required for pressure vessels, piping, and storage tanks, at ~32 mm. However, differences in the chemical compositions of U.S. and UK steels influence PWHT requirements. The major exceptions in this area are ASME B31.1 and B31.3 (limiting thickness 19 mm). However, general structural codes, such as BS 5400 for bridges, BS 5950 for buildings, and EEMUA 158 for offshore structures, permit significantly higher thicknesses in the as-welded condition, linked to increasing Charpy energy requirements.

2) For low-alloy steels containing ≤1.5%Cr and ≤0.5%Mo (including ASME P4 groups 1 and 2 steels), and also for 2.25%Cr-1%Mo steels (including ASME P5 group 1 steels), there are some strong similarities between the BS 2633 requirements and those of ASME VIII and ASME B31.1 and B31.3. The general trends are for the permitted thickness without PWHT to decrease with increasing alloy content of steels and/or for increased preheat to be required, together with reductions in maximum carbon level permitted.

3) In view of the differences that exist in the chemical compositions of broadly comparable U.S. and UK steels and the lack of consistent requirements for Charpy test properties (as far as ASME and CEN are concerned), alignment by material grouping for C-Mn steels is not universally possible as a basis for exemption from PWHT.

4) Since the development of the earliest codes, steel-making technology has changed significantly, steel toughness levels have generally improved substantially, and (at least within Europe) steel specifications commonly incorporate impact toughness requirements. It is therefore likely that limiting thicknesses could be increased, and thus PWHT omitted.

5) UK code requirements for general structures such as bridges, buildings, and offshore structures permit significantly greater thicknesses to be used in the as-welded condition, linked to Charpy toughness requirements for different grades of steel, based on fracture mechanics analyses. The requirements can be expressed in terms of MDMT – T_{27J} (the temperature difference between the material design minimum temperature and the temperature for 27 J energy absorption in the Charpy test) and the yield strength of the steel, for given assumptions about flaw size and stress level.

Recommendations

1) Where the relevant fabrication codes require that a PWHT be carried out, consideration should be given to carrying out a fracture mechanics assessment, with the agreement of all interested parties, in order to extend the thickness beyond which PWHT is required.

2) Typical Charpy test data should be reviewed and collated in terms of thickness and material type and IIW CE for steels supplied against the various standards summarized in Table 1. Following completion of the review, consideration should be given to the following cases: C- and C-Mn steels that would potentially allow an increase in the ASME B31.1 and B31.3 threshold thickness level for PWHT, and C- and C-Mn steels with <0.25%C, to establish if the BS 1113 and BS 2633 requirements are justified.

3) Consideration should be given to the generation of toughness data for thicknesses >12.5 mm and where Charpy energy requirements are not unduly onerous, to see where the avoidance of PWHT can be justified.

4) Steel producers should be encouraged to extend the practice of dual, or even multiple, certification of steels, so that greater uniformity is achieved in the compositions of steels, thereby facilitating the eventual unification of standards.

5) Consideration should be given to introducing HAZ toughness requirements into fabrication codes.

Acknowledgments

Helpful discussions with C. S. Wiesner and other colleagues at TWI, and input from D. J. Allen of Powergen, B. Parry-Mills and M. Coleman of British Energy, and R. Carroll of Foster Wheeler Energy Limited are gratefully acknowledged. The work was carried out within the Core Research program of TWI, which was funded by Industrial Members of TWI.

References

1. ASME *Boiler and Pressure Vessel Code*, Section III, 2004. Rules for construction of nuclear facility components. American Society of Mechanical Engineers, N.Y., paragraph NB-4622.9, Temper bead weld repair.

2. ASME *Boiler and Pressure Vessel Code*, Section XI. 2004. Rules for service inspection of nuclear power plant components. American Society of Mechanical Engineers, N.Y., paragraph IWA-4623.1 Temper bead welding of similar materials — Shielded metal arc welding.

3. *National Board Inspection Code — A Manual for Boiler and Pressure Vessel Inspectors*, 2004 National Board of Pressure Vessel Inspectors, Columbus, Ohio.

4. Burdekin, F. M. 1981. Materials aspects of BS5400: Part 6, paper 4 in *The Design of Steel Bridges*, Ed. K. C. Rockey and H. R. Evans, Granada ISBN 0 24611339 1.

5. Ogle, M. H., Burdekin, F. M., and Hadley, I. 2003. Material selection requirements for civil structures. *Proc. IIW Int. Conf. on Welded Construction for Urban Infrastructure*, 56th Annual Assembly of the IIW, Bucharest, Romania, Ed. D. Dehelean, International Institute of Welding, pp. 201–229.

6. Spaeder, C. E., and Doty, W. D. 1995. Report No. 2, ASME postweld heat treating practices: An interpretive report. Welding Research Council Bulletin 407, pp. 50–65.

7. Hancock, P., Chubb, J. P., and Spurrier, J. 1995. A new perspective on the influence of thickness and post-weld heat treatment for large scale welded joints. *J Engineering Materials and Technology*, pp. 117, 209–214.

8. BS 7910: 1999. *Guide on Methods for Assessing the Acceptability of Flaws in Metallic Structures*, incorporating Amendment 1, now superseded by BS 7910: 2005: *Guide on Methods for Assessing the Acceptability of Flaws in Metallic Structures*.

9. BS 7448: Part 2: 1997. *Fracture Mechanics Toughness Tests — Method for Determination of K_{Ic}, critical CTOD, and Critical J Values of Welds in Metallic Material.*

10. Nicholson, S., and Brook, J. C. Review of codes. 1971. *Proc. Biennial Conf. On Heat Treatment.* Joint Committee Iron and Steel Inst., London.

11. Saunders, G. G. 1980. Residual stresses and their reduction. *Developments in Pressure Vessel Technology-3*, Applied Science Publishers Ltd.

12. Mohr, W. 1994. Post-weld heat treatment: A review. Inspection, assessment and repair of welded structures and components. *10th Annual North American Welding Research Conference*, Columbus, Ohio.

13. Salkin, R. V. 1988. The desirability of unifying ideas and codes on stress relief thermal heat treatments. *FWP Journal*, Part 1 Nov., pp. 27–34, Part 2 Dec., pp. 5–13.

14. ASME VIII Div. 1: 2004. *Rules for Construction of Pressure Vessels.*

15. ASME B31.1. 2004. ASME *Code for Pressure Piping, Power Piping.*

16. ASME B31.3. 2004. ASME *Code for Pressure Piping, Process Piping.*

17. ASME B31.8: 2003. ASME *Code for Pressure Piping, Gas Transmission and Distribution Piping Systems*.

18. API 650. 1998. Welded steel tanks for oil storage.

19. API 620. 2002. *Design and Construction of Large, Welded, Low-Pressure Storage Tanks.* American Petroleum Institute.

20. JIS B 8243. 1981. Construction of pressure vessels. Now supersede by JIS B 8265: 2003 and JIS B 8266: 2003.

21. *Rules for Pressure Vessels.* 1991. Vol. 2, Section W 0701. Heat treatment of unalloyed and low alloy steel, and Section W 0702 Heat treatment of unalloyed and low alloy steel pipes. Dienst voor het Stoomwezen, The Hague, (updated 1998.)

22. BS 2971: 1991. Specification for Class II arc welding of carbon steel pipework for carrying fluids. British Standards Institution, including amendment 1, February 1998.

23. BS 1113: 1999. *Design and Manufacture of Water-Tube Steam Generating Plant* (including superheaters, reheaters and steel tube economizers).

24. BS EN 12952: 2001. *Water Tube Boilers and Auxiliary Installations*, Part 2 — Materials for pressure parts of boilers and accessories, and Part 5 — Workmanship and construction of pressure parts of the boiler.

25. BS 2633: 1987. *Class 1 Arc Welding of Ferritic Steel Pipework for Carrying Fluids.*

26. British Standards Institution Published Document PD 5500, 2003. *Unfired Fusion Welded Pressure Vessels.*

27. BS EN 13445: 2002. *Unfired Pressure Vessels*, Part 4 — Manufacture.

28. EEMUA 158: 2000. *Construction Specification for Fixed Offshore Structures in the North Sea*.

29. AWS D1.1/D1.1M: 2002. *Structural Welding Code — Steel.* Miami, Fla.: American Welding Society.

30. BS 5950-1: 2000. *Structural Use of Steelwork in Building*. Code of practice for design — Rolled and welded sections.

31. BS 5400-3: 2000 (incorporating Corrigendum 1). *Steel, Concrete and Composite Bridges*, Part 3 — Code of practice for design of steel bridges.

32. BS EN 10025: 1993. *Hot Rolled Products of Non-alloy Structural Steels — Technical Delivery Conditions.*

33. DD ENV 1993-1-1:1992. Eurocode 3: *Design of Steel Structures*, Part 1.1 — General rules and rules for buildings.

34. BS 4870: 1981. *Approval Testing of Welding Procedures,* Part 1 — Fusion welding of steel. (Superseded by BS EN 288-1: 1992, and BS EN 288-3: 1992.)

35. BS 4871: 1992. *Approval Testing of Welders Working To Approved Welding Procedures*, Part 1 — Fusion welding of steel. (Superseded by BS EN 287-1: 1992.)

36. BS EN 288: Part 1: 1992. *Specification and Approval of Welding Procedures for Metallic Materials — General Rules for Fusion Welding*, and BS EN 288: Part 3: 1992. *Specification and Approval of Welding Procedures for Metallic Materials — Welding Procedure Tests for the Arc Welding of Steels.*

37. BS EN 287, Part 1: 1992. *Approval Testing of Welders for Fusion Welding — Steels.*

38. British Standards Institution, Published Document PD CR ISO 15608: 2000. *Welding — Guidelines for a Metallic Material Grouping System.*

39. Sperko, W. J. 1998. Assignation of ASME materials to the new grouping system CR TR 15608, CEN/TC 121/SC 1 N, p. 407.

40. Mohr, W. C. 1997. Fracture mechanics to justify the minimum thickness for PWHT: Girth butt-welded steel pipe. Edison Welding Institute Report for Research Members MR9708.

41. Leggatt, R. H., Muhammed, A., Smith, A. T., and Cheaitani, M. J. 1999. Using fracture mechanics to claim exemption from PWHT — Four case studies. TWI Report for Research Members 679/1999.

Automotive Resistance Spot Weld Quality

Production welded parts joined by resistance spot welding have continually changing weld quality characteristics. Tolerances must be established for the required quality to be consistent with the manufacturing process capabilities. The welding process must be controlled to maintain (or exceed) a minimum weld quality level.

A satisfactory weld has a nugget width or button greater than or equal to the minimum weld size and satisfies the other criteria shown below. Tool design and setup are based on a weld size larger than the minimum. As production welding continues, the weld size can vary down to the minimum value. When this deterioration becomes apparent, adjustment of the equipment or electrode maintenance, or both, is required to reestablish the weld dimensions near the setup weld size.

Size. The weld button or plug is that part of the weld joint that tears out in a peel or chisel test. The button size is the measurement of the maximum dimension (D_{MAX}) added to the measurement of the minimum dimension (D_{MIN}) and divided by 2: [Button size = $D_{MAX} + D_{MIN})/2$] — Fig. 1.

Nugget width is the measure of the fusion zone in the plane of the faying surfaces from a cross section — Fig. 2. The weld aspect ratio for asymetrical weld buttons should be 2.0 or less.

Location. A properly located weld has base metal surrounding the electrode imprint and is placed within the dimensional tolerance allowed on the product drawing. If no location tolerance is specified, a weld is properly located provided the product resembles the weld locations indicated on the drawing. A typical weld location tolerance is ±6.4 mm. Edge welds (Fig. 3) and mislocated welds (Fig. 4) are unacceptable.

Spacing. Spot welds that maintain minimum weld spaces as specified in a product drawing or equivalent are acceptable; however, overlapping welds (Fig. 5) or those with insufficient space (Fig. 6) are unacceptable.

Indentation. A weld with 30% or more electrode indentation depth in any sheet of the material stackup is unacceptable — Figs. 2, 7.

Distortion. Welds that distort the sheet surfaces less than twice the governing metal thickness are acceptable (Fig. 8), but excess distortion is unacceptable.

Appearance. Welds featuring cracks, holes, and whiskers are unacceptable — Figs. 9, 10.

Quantity. The number of acceptable welds in a group should equal the number of welds specified on the product drawing or be within the weld group quantity tolerance. Two adjacent unacceptable welds, or an insufficient or excessive number of acceptable welds in a group are unacceptable.

Penetration. Penetration is the ratio of the nugget's depth of fusion to the prewelded sheet thickness. It must exceed 20% of the prewelded sheet thickness into each sheet of the weldment — Fig. 2.

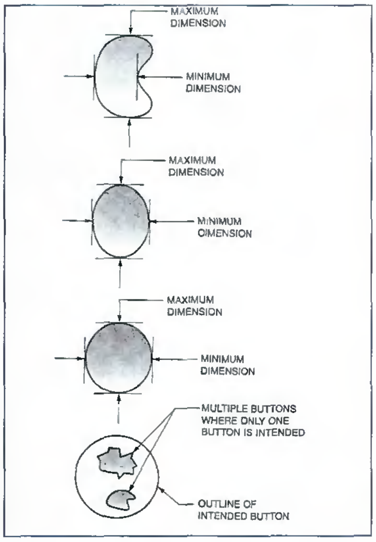

Fig. 1 — Measurement of weld size.

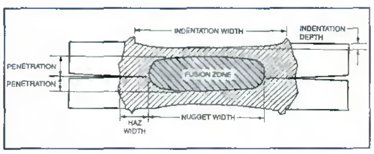

Fig. 2 — Attributes of a spot weld measured from a section through the center.

Fig. 3 — An edge weld.

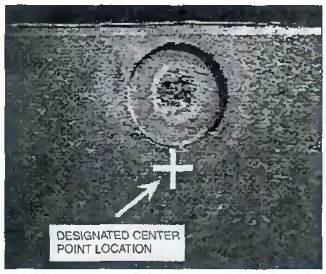

Fig. 4 — A mislocated weld.

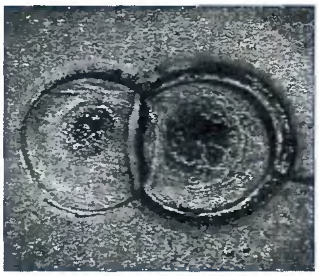

Fig. 5 — Overlapped welds.

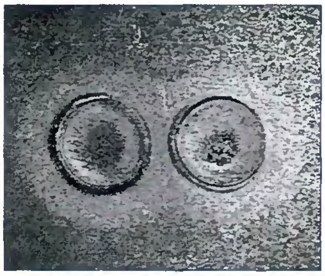

Fig. 6 — Potentially insufficiently spaced welds.

Fig. 7 — Excessive indentation.

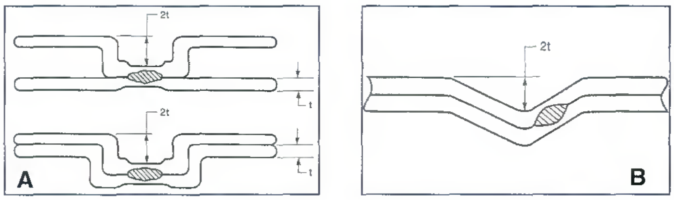

Fig. 8 — Weld distortion.

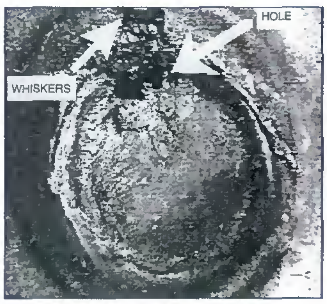

Fig. 9 — Holes and whiskers on a weld surface.

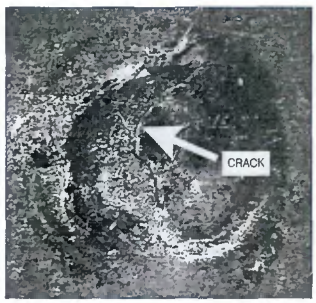

Fig. 10 — Surface cracks.

Excerpted from AWS D8.7M:2005, *Recommended Practices for Automotive Weld Quality — Resistance Spot Welding.*

This month's AWS Foundation spotlights:

Spotlight on a scholar

"My name is Nicole Dutruch and I was a recipient of the James A. Turner Jr. National Memorial Scholarship. I have been very fortunate and blessed to have been awarded the scholarship from 2002 through 2005. The James A. Turner Jr. Memorial Scholarship is awarded to students who are pursuing a career in business management. I was able to attend the University of Mobile in Mobile, Alabama, and would not have been able to do that without the help of the American Welding Society. At the University of Mobile, I chose to major in the field of communications with an emphasis in advertising and public relations. I graduated in December 2005. I am currently employed by Welding Engineering Supply Company and have been since 1999. My advice to students who are in need of financial assistance and want to pursue a career in the welding industry: you probably would not have to look any further than the American Welding Society. Without the generosity of such a prestigious organization, I would not have been able to attend the university of my choice."

Spotlight on a scholarship

The Jack R. Barckhoff Welding Management Scholarships are named for a person who has served the welding community and industry with great distinction. Jack Barckhoff's career of distinguished organizational leadership has enhanced the image and impact of the welding industry. He adheres to the principles of "giving forward" to provide more scholarships while supporting his involvement within the welding community, and welding as an "engineered science."

The American Welding Society Foundation has helped thousands of students who otherwise would be unable to afford a welding education. We are proud of the fact that we help hundreds of welding students annually by providing them with funding towards their education. In fact, we are the only industry foundation set up specifically to further educations and, in so doing, create the careers that sustain and grow our industry.

We get these funds from your contributions. So if you don't contribute, we will not be able to expand our work and our students' educations. And there is so much work to be done.

If you would like to make a scholarship contribution, or even set up your own Section or National Named Scholarship, contact the AWS Foundation at 1-800-443-9353, ext. 212.

Foundation, Inc.

Building Welding's Future through Education

For specific information on the Scholarship Programs, please visit our website at *www.aws.org/foundation.*

Circle No. 14 on Reader Info-Card

3rd International Brazing and Soldering Conference (IBSC)
April 23–26
San Antonio, Tex.

This special event will feature four days' worth of the best information available in the brazing and soldering fields. Join us beginning on Sunday, when we will feature our Short Courses. These courses have been extremely popular in the past, so we encourage you to plan accordingly as space is limited. Monday, Tuesday, and Wednesday will feature a phenomenal Technical Program comprised of two parallel tracks covering the latest advances in the field. Plus, as a complement to the technical program, a special Tabletop Exhibit will be organized — this is a great opportunity to network with vendors and learn about the latest products and services being offered.

We encourage you to mark your calendars and see us in the beautiful city of San Antonio — one of North America's most expressive and charming cities.

The 2006 IBSC event is sponsored by the American Welding Society and ASM International, the materials information society.

For more information, please contact the AWS Conferences and Seminars Business Unit at (800) 443-9353, ext. 223. You can also visit the Conference Department at *www.aws.org* for upcoming conferences and registration information.

Welding in Aircraft and Aerospace Conference
September 19 and 20
Dayton, Ohio

Welding is finally making a big play in the aircraft industry. Two technologies in particular, friction stir welding and additive manufacture, are leading the way. At the conference in Dayton, Ohio, attendees will learn the latest about the welding processes that are starting to replace rivets as the main means of joining aluminum and about the many systems now in use where various welding processes are being used to build high-performance parts "from the ground up."

Welding the New Materials for the Automotive Industry Conference
October 31
FABTECH International & AWS Welding Show
Atlanta, Ga.

Welding engineers are often being asked these days to figure out how to weld the avalanche of new materials targeted for use in tomorrow's automobiles. The lighter-weight steels have moved up several notches in strength. Here the engineers are looking at the advanced high-strength steels (AHSS), the TRIP steels, and the dual-phase steels. Aluminum is another relative newcomer. A new generation of resistance spot welding plus laser beam welding are very much in the running as the main joining processes for these new materials.

Quality Control in Welding Conference
November 1
FABTECH International & AWS Welding Show
Atlanta, Ga.

Quality control is something that must be kept up front in the planning of welds. It is not enough to rely solely on control charts, statistical process control, or Taguchi methods to get the job done properly. The human factor must take front seat. Here is where we get into such aids as certified material testing reports for electrodes and real-time sensing and control of welding processes. This is how weld quality can be assured the first time around.

Spot Welding Conference
November 2
FABTECH International & AWS Welding Show
Atlanta, Ga.

Resistance spot welding continues to dominate the automotive industry and other industries where sheet metal has to be joined. But recently, a host of new processes, all of which are capable of applying spot welds, are attracting all sorts of attention. This list includes the likes of laser weldbonding, ultrasonic welding, friction stir welding, and kinetic spot welding. Will these new methods make life difficult for the more established resistance welding systems? Resistance welding is fighting back with some innovations of its own.

NJC Technology Presented at ShipTech 2006

Several technologies under development at the Navy Joining Center (NJC) were presented at ShipTech 2006, January 24, 25, in Panama City Beach, Fla. The event is sponsored by the Office of Naval Research Navy Manufacturing Technology (ManTech) Program and The National Shipbuilding Research Program to promote the exchange of information on new technology for shipbuilding. The NJC presentations included the following projects.

Virtual Reality Welder Training

An aging welder workforce coupled with a reduction in new workers entering the field is creating a shortage of skilled welders for ship construction. This project developed an innovative welder training approach using state-of-the-art virtual reality (VR) technology. The VR approach for welder training has the potential to increase training effectiveness while significantly reducing labor and material costs, which are estimated to exceed $5 million/year in the shipbuilding industry alone.

The Navy Joining Center, General Dynamics Electric Boat (GDEB), and virtual reality developer VRSim partnered to develop a VR system that immerses the trainee into real-time simulations of the gas metal arc welding process. This first-of-its-kind welder training system features a mixed reality environment whereby the trainee holds a real welding torch while seeing and hearing a virtual weld bead being created. Hard and soft ghosting has also been developed and integrated into the system to guide the movements of the trainee to more rapidly acquire proper muscle memory.

The VR training system, which is available commercially, has been favorably evaluated by more than 100 welders from various shipyards.

Automated Prediction of Welding Fabrication Costs

The *Welding Procedure Estimator*™ has been developed on this ManTech project with GDEB to accurately predict welding fabrication times for manual, semiautomatic, and mechanized welding processes. This tool provides accurate data to assign production jobs and enable GDEB to easily compare the economic benefits of multiple welding processes, or to compare the advantages of semiautomatic vs. automated deployment of a single welding process. The *Welding Procedure Estimator*™ calculates welding time and other processing parameters inherent in welding operations.

The software is easy to use and very intuitive for the end user. This enables shop floor supervisors to more accurately estimate job duration and make more efficient use of personnel and equipment.

Panel Discussion — Collarless Construction

The Navy Joining Center also participated in a panel discussion titled Technology Transition from ManTech to Industry. The discussion emphasized the Surface Strike Affordability Initiative for the DD(X) program with a focus on the Collarless Construction project.

This project has determined an optimal "collarless" construction method to decrease fabrication costs and weight of the DD(X). Current Navy ship designs feature oversized rectangular openings cut from transverse stiffener webs to allow penetration of the longitudinal stiffeners. In order to restore the structural integrity of the transverse stiffeners, each opening is filled by a "collar" that is welded to the web of the longitudinal stiffener and to the web of the transverse stiffener. Fabricating and installing these collars is labor intensive and costly, as they require extensive fitting and welding time. The panel discussion highlighted the activity necessary for U.S. Navy acceptance to transition a collarless approach in building next-generation surface ships.

Contact **Larry Brown** at 614-688-5080, *larry_brown@ewi.org*, or visit *www.ewi.org* for more information on these and other NJC projects. ⇔

njc
Operated by
EWI

The Navy Joining Center
1250 Arthur E. Adams Dr.
Columbus, OH 43221
Phone: (614) 688-5010
FAX: (614) 688-5001
e-mail: *NJC@ewi.org*
www: *http://www.ewi.org*
Contact: Larry Brown

NOTE: A DIAMOND (♦) DENOTES AN AWS-SPONSORED EVENT.

Expo Manufactura. March 7–9. Cintermex, Monterrey, Mexico. Contact *www.ejkrause.com/expomanufactura/index.html.*

♦ Gas Shielded Arc Welding Conference. Las Vegas, Nev., March 7, 8. Contact American Welding Society, (800/305) 443-9353, ext. 223; or visit *www.aws.org/conferences.*

IIW Regional Congress, 'Welding and Inspection Technology for the Development of Southern Africa.' March 8–10. Stellenbosch, South Africa. Topics to include offshore oil and gas, power generation, construction, automotive, petrochemical, and food and beverage. Contact Southern African Institute of Welding at *congress@saiw.co.za; www.saiw.co.za.*

Shanghai Welding and Cutting Fair 2006. March 10–12, Shanghai, China. Specialized for shipbuilding, offshore platform, and petrochemical plant construction. Visit *www.cpexhibition.com.*

Corrosion/2006, NACE Int'l Annual Conference and Exhibition. March 12–16, San Diego Convention Center, San Diego, Calif. Visit *www.nace.org/c2006.*

Int'l Laser Safety Conf. (ILSC 2007). March 19–22, 2007, Airport Marriott, San Francisco, Calif. Visit *www.laserinstitute.org.*

METALFORM Regional Trade Show. March 21–23, Nashville, Tenn. Sponsored by the Precision Metalforming Assn. Visit *www.metalform.com.*

The Total Manufacturing Experience. March 27–30, Los Angeles Convention Center, Los Angeles, Calif. Co-locates WESTEC 2006, SME Summit and Annual Meeting, Automation and Assembly Conf. and Exhibits, Micro-Mfg. Conf., Metalworking Fluid Management Certificate Program, and Nano-Mfg. Conf. Contact Society of Manufacturing Engineers (313) 271-1500; *www.sme.org.*

FlowExpo China 2006 Int'l Exhibition on Fluid Engineering and Process Industry. March 29–31, Guangzhou, China. Organized by Guangzhou Flow Expo Co., Ltd., e-mail *yanqin627@163.com.*

6th Int'l Welding and Cutting Exhibition. March 29, 30, Exhibition Center, Pobediteley Ave., Minsk, Belarus. Visit *www.minskexpo.com.*

PICALO 2006, 2nd Pacific Int'l Conference on Applications of Lasers and Optics. April 3–5, Grand Hyatt, Melbourne, Australia. Visit *www.laserinstitute.org/conferences/picalo.*

Aerospace Testing Expo 2006 Europe. April 4–6, Hamburg, Germany. Contact *www.aerospacetesting.com.*

Japan Int'l Welding Show. April 12–15, Big Sight Exposition Center, Tokyo, Japan. Contact *www.weldingshow.jp/english.*

110th Metalcasting Congress. April 18–21. Columbus, Ohio. Sponsored by the American Foundry Society and North American Die Casting Assn. Visit *www.metalcastingcongress.org.*

♦ **3rd Int'l Brazing and Soldering Conference.** April 23–26. Crowne Plaza Hotel, San Antonio, Tex. Sponsored by AWS and ASM International. Contact Gladys Santana (800/305) 443-9353, ext. 223; *www.aws.org/conferences* to download exhibitors list.

Int'l Tube and Pipe Trade Fair. April 24–28, Düsseldorf, Germany. Contact Messe Düsseldorf North America at *www.mdna.com*.

5th Int'l Conference on NDE in Relation to Structural Integrity for Nuclear and Pressurized Components. May 10–12, San Diego, Calif. Contact EPRI at *www.epri.com*.

♦ **Sheet Metal Welding Conference XII.** May 10–12, VistaTech Center, Livonia, Mich. Sponsored by the AWS Detroit Section. Contact Mike Palko (313) 805-6199, or visit *www.awsdetroit.org*.

37th ISR Int'l Symposium on Robotics and 4th German Conference on Robotics: Robotik 2006. May 15–17, Int'l Congress Centre, Munich, Germany. Contact *www.isr2006.com*.

11th Beijing Essen Welding & Cutting Fair. May 16–19. China Int'l Exhibition Centre, Beijing, China. Contact *http://essen.cmes.org/en/index.htm*.

37th Int'l Steelmaking Seminar. May 21–24, Porto Alegre, Rio Grande do Sul, Brazil. Sponsored by ABM (Metallurgy and Materials Assn. of Brazil). E-mail Sandra Feraccini at *sandra.feraccini@abmbrasil.com.br*.

EASTEC 2006 Exposition and Conf. May 23–25, Eastern States Exposition, W. Springfield, Mass. Contact Society of Manufacturing Engineers (313) 271-1500; *www.sme.org*.

Rapid Prototyping and Manufacturing 2006, and 3-D Scanning: Reverse Engineering, Analysis, and Inspection. May 23, 24, Pheasant Run, Saint Charles, Ill. Contact Society of Manufacturing Engineers (313) 271-1500; *www.sme.org.*

♦**WELDMEX 2006.** May 31–June 2, Cintermex, Monterrey, Mexico. Contact Chuck Cross (410) 252-1322; *chuckcross17@msn.com.*

SURFEX 2006. June 21, 22, G-Mex Int'l Centre, Manchester, U.K. To feature surface coatings, adhesives, corrosion, printing inks, and construction chemicals. Contacts *info@orrest.com*; *www.orrest.com.*

2006 Annual Assembly and Int'l Conf. of the Int'l Institute of Welding (IIW). Aug. 27–Sept. 2, Québec City, Canada. E-mail the Organizing Committee *iiwassembly2006@cwbgroup.com,* or visit *www.iiw2006.com.*

♦**Welding in Aircraft and Aerospace Conference.** Sept. 19, 20. Dayton, Ohio. Contact American Welding Society, (800/305) 443-9353, ext. 223; or visit *www.aws.org/conferences.*

♦**FABTECH International AWS Welding Show.** Oct. 31–Nov. 2, Georgia World Congress Center, Atlanta, Ga. Contact American Welding Society, (800) 443-9353, ext. 462; *www.aws.org.*

♦**Conference on Ways to Weld New Materials in the Automotive Industry.** Oct. 31. Atlanta, Ga., at the FABTECH International & AWS Welding Show. Contact American Welding Society, (800) 443-9353, ext. 462; or visit *www.aws.org/conferences.*

♦**Quality Control in Welding Conference.** Nov. 1, Atlanta, Ga., at the FABTECH International & AWS Welding Show. Contact American Welding Society, (800) 443-9353, ext. 462; or visit *www.aws.org/conferences.*

♦**Spot Welding Conference.** Nov. 2, Atlanta, Ga., at the FABTECH International & AWS Welding Show. Contact American Welding Society, (800) 443-9353, ext. 462; or *www.aws.org/conferences.*

Aerospace Testing Expo North America. Nov. 14–16, Anaheim Convention Center, Anaheim, Calif. For information, visit *www.aerospacetesting-expo.com/northamerica/contact.html.*

Educational Opportunities

ASME Int'l — Section IX Welding Guide. March 13–15, Houston, Tex.; May 8–10, Atlanta, Ga. Walter J. Sperko, instructor. Visit *www.asme.org/education.*

Structural Welding: Design and Specification. March 28, Philadelphia, Pa.; April 4, New York, N.Y. Fee: $225, group discounts available. Visit *www.steelstructures.com.*

Steel Connections: Seismic Applications 2006. May 2, Los Angeles, Calif.; May 9, San Francisco, Calif. Fee: $225, group discounts available. Visit *www.steelstructures.com.*

Hands-On Welding Summer Workshop. July 10–14, Ball State University, Muncie, Ind. Fee: $300. Contact: William Ed Wyatt, instructor, (765) 289-0459; *wyatt.w@worldnet.att.net.*

Boiler and Pressure Vessel Inspectors Training Courses and Seminars. Columbus, Ohio. Contact Richard McGuire, (614) 888-8320, *rmcguire@nationalboard.org*, *www.nationalboard.org*.

CWI/CWE Course and Exam. This 10-day program prepares students for the AWS CWI/CWE exam. For schedule and entry requirements, contact Hobart Institute of Welding Technology (800) 332-9448, *www.welding.org*.

CWI Preparation. Courses on ultrasonic, eddy current, radiography, dye penetrant, magnetic particle, and visual at Levels 1–3. Meet SNT-TC-1A and NAS-410 requirements. On-site training available. T.E.S.T. NDT, Inc., 193 Viking Ave., Brea, CA 92821; (714) 255-1500; *ndtguru@aol.com*; *www.testndt.com*.

CWI Preparatory and Visual Weld Inspection Courses. Classes presented in Pascagoula, Miss., Houston, Tex., and Houma and Sulphur, La. Course lengths range from 40 to 80 hours. Contact Real Educational Services, Inc., (800) 489-2890; *info@realeducational.com*.

EPRI NDE Training Seminars. EPRI offers NDE technical skills training in visual examination, ultrasonic examination, ASME Section XI, and UT operator training. Contact Sherryl Stogner, (704) 547-6174, e-mail: *sstogner@epri.com*.

Fabricators and Manufacturers Assn., and Tube and Pipe Assn. Courses. Contact (815) 399-8775; *www.fmametalfab.org*; *info@fmametalfab.org*.

Fastening Technology and Bolted Joint Design Seminars. April 11, 12, Detroit, Mich.; August 23, 24, Baltimore, Md.; Nov. 8, 9, Chicago, Ill. For details visit *www.SeminarsForEngineers.com*.

2006 AWS Certification Schedule

Certification Seminars, Code Clinics and Examinations

Application deadlines are six weeks before the scheduled seminar or exam. Late applications will be assessed a $250 Fast Track fee.

Certified Welding Inspector (CWI)

Location	Seminar Date	Exam Date	Site Code
Miami, FL	EXAM ONLY	Mar. 16	HQ28606
Houston, TX	Mar. 12-17	Mar. 18	TX26706
Mobile, AL	EXAM ONLY	Mar. 18	AL29006
Rochester, NY	EXAM ONLY	Mar. 18	NY29306
San Francisco, CA	Mar. 19-24	Mar. 25	CA26906
Anchorage, AK	Mar. 19-24	Mar. 25	AK27006
York, PA	EXAM ONLY	Mar. 25	PA29406
Monterrey, Mex.	(contact *info@dalus.com*)		
	Mar. 27-31	Apr. 1	-----
Pittsburgh, PA	Apr. 2-7	Apr. 8	PA27106
San Juan, PR	Apr. 2-7	Apr. 8	PR27206
Miami, FL	EXAM ONLY	Apr. 20	HQ28706
Corpus Christi, TX	EXAM ONLY	Apr. 22	TX28906
Portland, ME	Apr. 23-28	Apr. 29	ME27306
Roanoke, VA	Apr. 23-28	Apr. 29	VA27406
Columbus, OH (at NBBPVI*)			
	Apr. 24-28	Apr. 29	OH29906
Bakersfield, CA	Apr. 30-May 5	May 6	CA27506
Milwaukee, WI	Apr. 30-May 5	May 6	WI27606
Waco, TX	EXAM ONLY	May 6	TX29806
Newark, NJ	May 7-12	May 13	NJ27706
Spokane, WA	May 7-12	May 13	WA27806
Long Beach, CA	May 7-12	May 13	CA27906
Monterrey, Mex.	(contact *info@dalus.com*)		
	May 15-19	May 20	-----
St. Louis, MO	May 21-26	May 27	MO28106
Miami, FL	May 21-26	May 27	FL28006
Atlanta, GA	May 21-26	May 27	GA28206
Beaumont, TX	Jun. 4-9	Jun. 10	TX03907
Sacramento, CA	Jun. 4-9	Jun. 10	CA04007
Fargo, ND	Jun. 4-9	Jun. 10	ND04107
Miami, FL	EXAM ONLY	Jun. 15	HQ07607
Philadelphia, PA	Jul. 9-14	Jul. 15	PA04207
Orlando, FL	Jul. 9-14	Jul. 15	FL04307
Corpus Christi, TX	EXAM ONLY	Jul. 15	TX08207
Monterrey, Mex.	(contact *info@dalus.com*)		
	Jul. 10-14	Jul. 15	-----
Miami, FL	EXAM ONLY	Jul. 20	HQ08107
Baton Rouge, LA	Jul. 16-21	Jul. 22	LA04407
Kansas City, MO	Jul. 16-21	Jul. 22	MO04507
Chicago, IL	Jul. 23-28	Jul. 29	IL04607
Portland, ME	Jul. 23-28	Jul. 29	ME04707
Albuquerque, NM	Jul. 30-Aug. 4	Aug. 5	NM04807
Columbus, OH (at NBBPVI*)			
	Jul. 31-Aug. 4	Aug. 5	OH09307
Memphis, TN	Aug. 6-11	Aug. 12	TN04907
Salt Lake City, UT	Aug. 6-11	Aug. 12	UT05007
Miami, FL	EXAM ONLY	Aug. 17	HQ07807
Houston, TX	Aug. 13-18	Aug. 19	TX05207
Charlotte, NC	Aug. 20-25	Aug. 26	NC05307
Rochester, NY	EXAM ONLY	Aug. 26	NY08607
Syracuse, NY	Sep. 10-15	Sep. 16	NY05507
Miami, FL	EXAM ONLY	Sep. 21	HQ07907
Minneapolis, MN	Sep. 17-22	Sep. 23	MN05607
Seattle, WA	Sep. 17-22	Sep. 23	WA05707
San Diego, CA	Sep. 17-22	Sep. 23	CA05807
Anchorage, AK	EXAM ONLY	Sep. 23	AK08407
Dallas, TX	Sep. 24-29	Sep. 30	TX05907
Detroit, MI	Sep. 24-29	Sep. 30	MI06007
Milwaukee, WI	Sep. 24-29	Sep. 30	WI06107
Denver, CO	Oct. 8-13	Oct. 14	CO06207
Phoenix, AZ	Oct. 8-13	Oct. 14	AZ06307
Miami, FL	EXAM ONLY	Oct. 19	HQ08007
Pittsburgh, PA	Oct. 15-20	Oct. 21	PA06407
Tulsa, OK	Oct. 15-20	Oct. 21	OK06507
San Antonio, TX	Oct. 15-20	Oct. 21	TX06607
Chicago, IL	Oct. 22-27	Oct. 28	IL06707
Atlanta, GA	Oct. 22-27	Oct. 28	GA06807
Reno, NV	Oct. 29-Nov. 3	Nov. 4	NV06907
Baltimore, MD	Oct. 29-Nov. 3	Nov. 4	MD07007
Long Beach, CA	Nov. 5-10	Nov. 11	CA07107
Beaumont, TX	Nov. 5-10	Nov. 11	TX07207
Portland, OR	Nov. 5-10	Nov. 11	OR07307
Monterrey, Mex.	(contact *info@dalus.com*)		
	Nov. 6-10	Nov. 11	-----
Louisville, KY	Nov. 12-17	Nov. 18	KY07407
St. Louis, MO	EXAM ONLY	Dec. 2	MO08507
Miami, FL	Dec. 3-8	Dec. 9	FL07507
Columbus, OH (at NBBPVI*)			
	Dec. 11-15	Dec. 16	OH09407
Corpus Christi, TX	EXAM ONLY	Dec. 16	TX08307

* Mail seminar registration and fees for Columbus seminars only to National Board of Boiler & Pressure Vessel Inspectors, 1055 Crupper Ave., Columbus, OH 43229-1183. Phone (614) 888-8320. Exam application and fees should be mailed to AWS.

9-Year Recertification for CWI and SCWI

Location	Seminar Dates	Exam Date	Site Code
Dallas, TX	Mar. 20-25	NO EXAM**	RSV215
Sacramento, CA	Apr. 3-8	NO EXAM**	RSV225
Pittsburgh, PA	Jun. 12-17	NO EXAM**	RSV235
San Diego, CA	Aug. 28-Sep. 2	NO EXAM**	RSV245
Dallas, TX	Nov. 13-18	NO EXAM**	RSV255
Orlando, FL	Dec. 4-9	NO EXAM**	RSV265

**For current CWIs needing to meet education requirements without taking the exam. If needed, recertification exam can be taken at any site listed under Certified Welding Inspector.

Certified Welding Supervisor (CWS)

Location	Seminar Dates	Exam Date	Site Code
Pittsburgh, PA	Apr. 3-7	Apr. 8	CWS6
Spokane, WA	May 8-12	May 13	CWS7
Beaumont, TX	Jun. 5-9	Jun. 10	CWS8
Portland, ME	Jul. 24-28	Jul. 29	CWS9
Salt Lake City, UT	Aug. 7-11	Aug. 12	CWS10
Milwaukee, WI	Sep. 25-29	Sep. 30	CWS11
Portland, OR	Nov. 6-10	Nov. 11	CWS12

Certified Radiographic Interpreter (RI)

Location	Seminar Dates	Exam Date	Site Code
Anchorage, AK	Mar. 20-24	Mar. 25	RIP13
Monterrey, Mex.	(contact *info@dalus.com*)		
	May 15-19	May 20	-----
Orlando, FL	Jul. 10-14	Jul. 15	RIP14
Chicago, IL	Jul. 24-28	Jul. 29	RIP15
Long Beach, CA	Nov. 6-10	Nov. 11	RIP16
Louisville, KY	Nov. 13-17	Nov. 18	RIP17

Certified Welding Educator (CWE)

Seminar and exam are given at all sites listed under Certified Welding Inspector. Seminar attendees will not attend the Code Clinic portion of the seminar (usually first two days).

Senior Certified Welding Inspector (SCWI)

Exam can be taken at any site listed under Certified Welding Inspector. No preparatory seminar is offered.

Certified Welding Engineer – (CWEng)

Exam can be taken at any site listed under Certified Welding Inspector. No preparatory seminar is offered. Two exam days are necessary for this certification.

Certified Welding Sales Representative (CWSR)

Exam can be taken at any site listed under Certified Welding Inspector. No preparatory seminar is offered.

Certified Welding Fabricator

This program is designed to certify companies to specific requirements in the ANSI standard AWS B5.17, *Specification for the Qualification of Welding Fabricators*. There is no seminar or exam for this program. Call Jeff Hufsey at ext. 264 for more information.

Code Clinics

D1.1, API-1104, Welding Inspection Technology, and Visual Inspection workshops are offered at all sites where the Certified Welding Inspector seminar is offered (usually first two days).

On-site Training and Examination

On-site training is available for larger groups or for programs that are customized to meet specific needs of a company. Call Jeff Hufsey at ext. 264 for more information.

For information on any of our seminars and certification programs, visit our website at **www.aws.org** or contact AWS at (800/305) 443-9353, Ext. 273 for Certification and Ext. 449 for Seminars.

Please **apply early** to save Fast Track fees. **This schedule is subject to change without notice.** Please verify the dates with the Certification Dept. Confirm your course status before making final travel plans. Please note that all **originally scheduled sites in New Orleans** have been canceled.

Circle No. 11 on Reader Info-Card

American Welding Society

Founded in 1919 to advance the science, technology and application of welding and allied processes including joining, brazing, soldering, cutting and thermal spray.

SOCIETY NEWS

BY HOWARD M. WOODWARD

Friction Stir Welding Is a Hot Topic Worldwide

Both AWS and the International Institute of Welding (IIW) technical committees are preparing new standards on friction stir welding.

The AWS D8 Committee on Automotive Welding is working on the first draft of AWS D8.17, *Specification for Automotive Weld Quality — Friction Stir Welding.* Its scope is, "To establish a specification for postweld acceptance criteria to be used for evaluating continuous friction stir welds and friction stir spot welds in automotive applications."

The D17 Committee on Welding in the Aircraft and Aerospace Industries is in the final balloting stages for a draft of AWS D17.3, *Specification for Friction Stir Welding of Aluminum for Aerospace Applications.* Its scope is, "This specification contains requirements for the friction stir welding of aluminum aerospace hardware. It is to be used in conjunction with the Engineering Authority's design handbooks or their accepted data." AWS D17.3 provides general requirements for friction stir welding of aluminum aerospace structures. Nonflight hardware, tooling, ground support equipment, and related nonconventional aerospace facilities may be designed and welded in accordance with the requirements of this specification.

The C6 Committee on Friction Welding has issued one published standard on friction welding, AWS C6.1, *Recommended Practices for Friction Welding,* and is currently developing AWS C6.2, *Specification for Qualification of Friction Welding,* expected to be published by early 2007. Its scope is, "This document specifies the requirements for the manufacture and quality assurance of friction weldments. It also contains requirements for the qualification of welding machines, welding procedures, and welding operators."

This specification is directly applicable to inertia, direct-drive, and friction stir variants of friction welding, but may also be used with orbital, angular reciprocating, and linear reciprocating variants.

If you are interested in assisting with the development of the D8 or D17 standards, contact **Annette Alonso**, *aalonso@aws.org.* To assist with the C6 standard, contact Selvis

— *Friction Stir continued on next page*

Resistance Welding Pros Meet in Miami

The RWMA (Resistance Welding Manufacturing Alliance), a new standing committee of the American Welding Society, held its Annual Meeting January 10–13 in Miami, Fla.

Larry E. Moss of Automation International, Danville, Ill., is the chairman, succeeding **David M. Beneteau,** CenterLine (Windsor) Ltd., Ont., Canada.

Michael Simmons, TG Systems, Inc., Greer, S.C., is vice chairman; and **Roger B. Hirsch,** Unitrol Electronics, Inc., Northbrook, Ill., is second vice chairman.

Founded in 1936, RWMA has served as the leading trade association for promoting the technical and economic advantages of the resistance welding process. As an AWS standing committee, RWMA members are required to be either an AWS Sustaining Member or a Supporting Member Company.

Great Incentive to Join Now

Until March 31, as an incentive to join RWMA now, the initiation fee to become an AWS Sustaining Member or Supporting Company Member will be waived. To take advantage of this special offer, contact **Susan Hopkins,** (305/800) 443-9353, ext. 295, before the deadline date.

RWMA Student Assistance

A remarkably diverse committee, RWMA offers scholarships to students majoring in welding engineering who are citizens of the United States or Canada, and meet other qualifications. The program operates under the direction of the AWS Foundation.

Emmet A. Craig School

Noteworthy too, RWMA sponsors an intensive two-day course designed to teach the basics of resistance welding. The renowned Emmet A. Craig Resistance Welding School is offered twice a year for training operators, production supervisors, engineers, and others who want to study the theory, applications, and equipment used in the resistance welding process. The course features one-on-one instruction with valuable hands-on exercises. The six instructors who present this program are accomplished professionals with a combined industry experience of 150 years.

Resistance Welding Manual

The *RWMA Resistance Welding Manual,* Revised Fourth Edition. The 468-page, profusely illustrated (308 figures, 85 tables), hard-bound volume is the

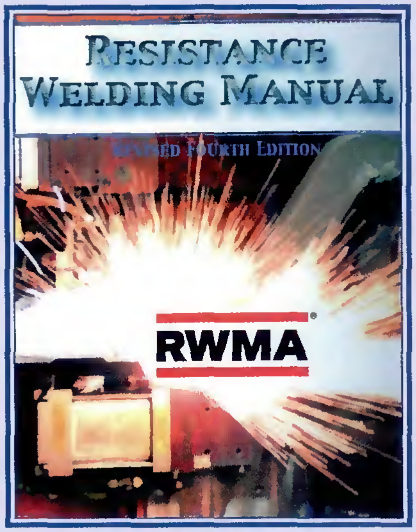

most complete compilation of basic information on resistance welding available anywhere.

It describes the entire resistance welding process, including theory, methods, materials, equipment, welding machines, electrodes, jigs, fixtures, transformers, controls, power supplies, and accessories. The fourth edition includes many new features, including updated weld schedules with the latest cal-

— *RWMA continued on next page*

New AWS Supporters

New Sustaining Members

Gayle Manufacturing Co.
1455 E. Kentucky Ave.
Woodland, CA 95776
www.gaylemfg.com
Representative: **Gary Glenn**

Gayle Manufacturing Co. is a major structural steel fabricator of commercial, hospital, and public works projects.The GMC team has become accustomed to implementing sophisticated systems and equipment combined with innovative technical solutions to increase productivity year after year. Its motto is "Performance through innovation."

White Construction, Inc.
11993 S. State Rd. 63
Clinton, IN 47842-7148
www.whiteconstruction.com
Representative: **Douglas A. Foli**

White Construction, Inc. (WCI), is a union contractor with its corporate headquarters located in Clinton, Ind. WCI prides itself on assisting its clients with quality service. It has been serving its customers for the past 60 years while specializing in the following areas: commercial/industrial site development and/or maintenance, heavy highway and public works construction, engineering, procurement, and construction (EPC) services, crane/heavy rigging service, equipment rentals, and wind power.

New Affiliate Companies

Arizona Steelfab & Supply, Inc.
5355 N. Dodge Ave.
Flagstaff, AZ 86004

International Tower Supply, LLC
1701 John Tipton Blvd.
Pennsauken, NJ 08110

Rosario Steel Works
PO Box 802
Camuy, PR 00627

Son Set Consultants
PO Box 489, 9045 N. 84th West Ave
Sperry, OK 74073

VA Tech Escher Wyss Flovel Ltd.
4915 Mathura Rd., Village Prithla
Tensil Palwal, Dist. Faridabad
Haryana 121 102, India

West Coast Weld Tech
19770 98th Ave.
Langley, BC, V1M 2X5, Canada

Wheeler Lumber, LLC
9330 James Ave. S.
Bloomington, MN 55431

New Educational Institutions

Big Bend Community College
7662 Chanute St.
Moses Lake, WA 98837

Central Oregon Community College
2030 SE College Loop
Redmond, OR 97701

El Paso Community College
919 Hunter
El Paso, TX 79915

Kentucky Tech Madison
PO Box 809, 703 N. Second St.
Richmond, KY 40476-0809

Los Angeles Trade Technical College
400 W. Washington Blvd.
Los Angeles, CA 90015

Rite of Passage Charter High School
100 Rosaschi Rd.
Yerington, NV 89447

Southeastern Illinois College
3575 College Rd.
Harrisburg, IL 62946

St. Cloud Technical College
1540 Northway Dr.
St. Cloud, MN 56303

Traviss Career Center
3225 Winter Lake Rd.
Lakeland, FL 33830

New Supporting Companies

NGK Metals Corp.
917 U.S. Hwy. 11 S.
Sweetwater, TN 37874

Phelps Dodge Specialty Copper Products
48–94 Bayway Ave.
Elizabeth, NJ 07202

Welform Electrodes
2147 Kenney Rd.
Warren, MI 48091 ♦

— *Friction Stir from previous page*

Morales, *smorales@ aws.org.*

The International Institute of Welding established Subcommission III-B (SC III-B) within IIW's Commission III (Resistance and Solid State Welding and Allied Joining Processes) in 2003. SC III-B was created to concentrate on friction-based welding processes. During the 2003 IIW Annual Assembly held in Bucharest, Romania, SC III-B proposed that working group B1 (WG-B1) be formed to write a standard for friction stir welding. This proposal was accepted the following year in Osaka and David Bolser, U.S.A., was approved as the leader. The members of WG-B1 represent ten nations.

The proposed title for the standard is *Friction Stir Welding of Aluminum — General Requirements.* The ISO designation will be ISO 25239.

The standard has five parts: vocabulary, design of weld joints, qualification of friction stir welding operators, specification and qualification of welding procedures, and quality and inspection requirements. The committee draft will be voted on later this year. ♦

— *RWMA from previous page*

culations for resistance welding processes, new graphic format for easier reading of weld schedules and information on newer metal alloys, hot dip galvanized, and electroplated steel. It sells for $125 list, $80 for RWMA members. To purchase, contact WEX, Ltd., (888) 935-3464; *www.aws.org/standards.*

RWMA Goals

To prepare and distribute the *Resistance Welding Manual* and other literature for the benefit of educators, producers, and users.

To encourage education pertaining to the resistance welding processes.

To promote the resistance welding processes and their advantages in the design and manufacture of assemblies for government and general consumption.

To represent the resistance welding industry and processes in the activities of other technical organizations.

To cooperate in the development of statistical and other information concerning the resistance welding industry and its use in the marketplace.

To encourage a high standard of ethics in the industry.

To encourage the adoption of practices that lead to increased efficiency of the resistance welding processes.

RWMA's next meeting will be in May. Contact RWMA at *rwma@aws.org* or (305/800) 443-9353, ext. 295. ♦

Member-Get-A-Member Campaign

Listed below are the January 16, 2006, standings for participants in the 2005–2006 Member-Get-A-Member Campaign. See page 83 of this *Welding Journal* for the rules and prize list. For complete information, contact the AWS Membership Department (800/305) 443-9353, ext. 480.

Winner's Circle

Members who have sponsored 20 or more new Individual Members, per year, since June 1, 1999. The superscript denotes the number of times the member has achieved Winner's Circle status if more than once.

J. Compton, San Fernando Valley^5
E. Ezell, Mobile^3
J. Merzthal, Peru^2
G. Taylor, Pascagoula^2
B. Mikeska, Houston
R. Peaslee, Detroit
W. Shreve, Fox Valley
M. Karagoulis, Detroit
S. McGill, Northeast Tennessee
T. Weaver, Johnstown/Altoona
G. Woomer, Johnstown/Altoona
R. Wray, Nebraska

President's Guild

Members sponsoring 20 or more new Individual Members between June 1, 2005, and May 31, 2006.

M. Haggard, Inland Empire — 20

President's Roundtable

Members sponsoring 11–19 new Individual Members between June 1, 2005, and May 31, 2006.

C. Daily, Puget Sound — 14
G. Fudala, Philadelphia — 11

President's Club

Members sponsoring 6–10 new Individual Members between June 1, 2005, and May 31, 2006.

J. Compton, San Fernando Valley — 10
J. Williams, Houston — 10
G. Gardner, Ozark — 9
G. Taylor, Pascagoula — 9
T. White, Pittsburgh — 9
D. Norum, North Texas — 8
D. Wright, Kansas City — 8
J. Christianson, Saginaw Valley — 7

President's Honor Roll

Members sponsoring 1–5 new Individual Members between June 1, 2005, and May 31, 2006. (Two or more listed.)

D. Wilson, Inland Empire — 4
R. Wright, Southern Colorado — 4
A. Mattox, Lexington — 3
J. Mendoza, San Antonio — 3
R. Merreighn, Mississippi Valley — 3
G. Merriman, Chicago — 3
R. Quintero, Corpus Christi — 3
R. Sands, Northwest — 3
J. Smutny, Spokane — 3
M. Tsai, Taiwan Int'l — 3
T. Alston, Sierra Nevada — 2
R. Bernstein, South Florida — 2
J. Cusick, Kansas — 2
J. Durbin, Tri-River — 2
W. Kuchta, Cleveland — 2
P. Newhouse, British Columbia — 2
R. Rux, Wyoming — 2
C. Schiner, Wyoming — 2
S. Siviski, Maine — 2
K. Stelzl, New York — 2
J. Vansambeek, Lakeshore — 2
H. Wilden, Reading — 2

Student Sponsors

Members sponsoring 3 or more new Student Members between June 1, 2005, and May 31, 2006.

C. Daily, Puget Sound — 85
G. Euliano, Northwestern Pa. — 61
R. Durham, Cincinnati — 39
R. Evans, Siouxland — 35
T. Kienbaum, Colorado — 32
D. Newman, Ozark — 26
M. Anderson, Indiana — 24
S. Siviski, Maine — 24
H. Hughes, Mahoning Valley — 23
A. Baughman, Stark Central — 22
J. Daugherty, Louisville — 20
C. Hobson, Olympic — 20
R. Boyer, Nevada — 19
D. Combs, Santa Clara Valley — 19
S. Robeson, Cumberland Valley — 18
G. Smith, Lehigh Valley — 18
W. Ketler, Willamette Valley — 17
R. Shrewsbury, Tri-State — 17
M. Arand, Louisville — 15
R. Munns, Utah — 15
B. Olson, Sangamon Valley — 15
C. Overfelt, Southwest Virginia — 15
T. Strickland, Arizona — 15
A. Stute, Madison-Beloit — 15
A. Mattox, Lexington — 14
C. Jones, Houston — 13
A. Reis, Pittsburgh — 13
M. Koehler, Milwaukee — 12
R. Olesky, Sangamon Valley — 12
J. Smith, Jr., Mobile — 12
T. Buchanan, Mid-Ohio Valley — 11
D. Griep, New Jersey — 11
H. Browne, New Jersey — 10
K. Paolino, Connecticut — 10
J. Pawley, Lexington — 10
M. Batchelor, Boston — 9
W. Galvery, Long Bch/Orange Cty — 9
R. Zabel, Southeast Nebraska — 9
C. Chancy, LA/Inland Empire — 8
J. McCarty, St. Louis — 8
G. Gammill, Northeast Mississippi — 7
T. Moffit, Tulsa — 7
A. Badeaux, Washington, D.C. — 6
J. Boyer, Lancaster — 6
J. Carney, Western Michigan — 6
C. Kipp, Lehigh Valley — 6
D. Kowalski, Pittsburgh — 5
R. Rux, Wyoming — 5
C. Schiner, Wyoming — 5
J. Smith, Tri-River — 5
R. Chase, LA/Inland Empire — 4
R. Hutchison, Long Bch/Orange Cty — 4
S. Stevenson, Cumberland Valley — 4
C. Bridwell, Ozark — 3
P. Carney, Lehigh Valley — 3
J. Cox, Northern Plains — 3
R. Haag, Wyoming — 3
D. Hamilton, Chattanooga — 3
M. Hill, Lexington — 3
J. Knapp, Tulsa — 3
T. Moore, New Orleans — 3
D. Vranich, North Florida — 3 ♦

Membership Counts

Member Grades	As of 2/1/06
Sustaining	439
Supporting	249
Educational	354
Affiliate	309
Welding distributor	52
Total corporate members	**1,403**
Individual members	43,873
Student + transitional members	4,989
Total members	**48,862**

Tech Topics

Technical Committee Meetings

AWS technical committee meetings are open to the public. If you want to attend a meeting, contact the committee secretary as listed below at (800/305) 443-9353. All meetings are for standards preparation and general business.

March 12, A5 Executive Subcommittee. Orlando, Fla. Contact R. Gupta, ext. 301.

March 13, 14, A5 Committee on Filler Metals and Allied Materials. Orlando, Fla. Contact **R. Gupta,** ext. 301.

March 13–17, D1 Committee on Structural Welding. Raleigh, N.C. Contact **J. Gayler,** ext. 472.

March 14, A5T Subcommittee on Filler Metal Procurement Guidelines. Orlando, Fla. Contact **R. Gupta,** ext. 301.

March 14, A5W Subcommittee on Moisture and Hydrogen. Orlando, Fla. Contact **R. Gupta,** ext. 301.

March 15, A5B Subcommittee on Carbon and Low-Alloy Steel Electrodes and Fluxes for Submerged Arc Welding. Orlando, Fla. Contact **R. Gupta,** ext. 301.

March 16, A5A Subcommittee on Carbon and Low-Alloy Steel Electrodes and Rods for Shielded Metal Arc and Oxyfuel Gas Welding. Orlando, Fla. Contact **R. Gupta,** ext. 301.

April 4, D14E Subcommittee on Welding of Presses. Miami, Fla. Contact **P. Howe,** ext. 309.

April 4, D14H Subcommittee on the Surfacing of Industrial Rolls and Equipment. Miami, Fla. Contact **P. Howe,** ext. 309.

April 5, D14B Subcommittee on General Design and Practices. Miami, Fla. Contact **P. Howe,** ext. 309.

April 5, D14C Subcommittee on Earthmoving and Construction Equipment. Miami, Fla. Contact **P. Howe,** ext. 309.

April 6, D14 Committee on Machinery and Equipment. Miami, Fla. Contact **P. Howe,** ext. 309.

April 6, D14G Subcommittee on Welding of Rotating Equipment. Miami, Fla. Contact **P. Howe,** ext. 309.

Standard for PINS

Development work has begun on the following new standard. Materially affected individuals are invited to contribute to its development. Participation on AWS Technical Committees and Subcommittees is open to all persons.

D8.9M:200X, *Test Methods for Evaluating the Resistance Spot Welding Behavior of Automotive Sheet Steel Materials.* This document contains several standardized test methods for evaluating the resistance spot welding behavior of coated and uncoated sheet steels in a laboratory environment. The test methods are designed to assess current range, electrode endurance, and weld properties of automotive sheet steels. The weld property tests include tests for hold time sensitivity, weld hardness, shear-tension strength, and cross-tension strength. Stakeholders are Automotive and Steel Industry (producers of automotive sheet steel). Revised standard. Contact **A. Alonso,** ext. 299.

Standards for Public Review

AWS was approved as an accredited standards-preparing organization by the American National Standards Institute (ANSI) in 1979. AWS rules, as approved by ANSI, require that all standards be open to public review for comment during the approval process. This column also advises of ANSI approval of documents. The following standards are submitted for public review. A draft copy may be obtained by contacting Rosalinda O'Neill (800/305) 443-9353, ext. 451, *roneill@aws.org.*

A2.4M/A2.4:200X, *Standard Symbols for Welding, Brazing, and Nondestructive Examination.* Revised standard — $111. Review expires 3/13/06.

A5.5/A5.5M:200X, *Specification for Low-Alloy Steel Electrodes for Shielded Metal Arc Welding.* Revised standard — $43.50. Review expired 2/6/06.]

B2.1-1-232:200X, *Standard Welding Procedure Specification (SWPS) for Argon Plus 25% Carbon Dioxide Shielded Gas Metal Arc Welding (Short Circuiting Transfer Mode) Followed by Argon Plus 25% Carbon Dioxide Shielded Flux Cored Arc Welding of Carbon Steel (M-1/P-1/S-1) Groups 1 and 2, ⅛ through 1½ in. Thick, ER70S-3 and E7XT-X, Flat Position Only, As-Welded or PWHT Condition, Primarily Pipe Applications.* New standard — $25. Review expired 2/13/06.

B2.1-1-233:200X, *Standard Welding Procedure Specification (SWPS) for Argon Plus 25% Carbon Dioxide Shielded Gas Metal Arc Welding (Short Circuiting Transfer Mode) Followed by Argon Plus 2% Oxygen Shielded Gas Metal Arc Welding (Spray Transfer Mode) of Carbon Steel (M-1/P-1/S-1) Groups 1 and 2, ⅛ through 1½ in. Thick, ER70S-3, Flat Position Only, As-Welded or PWHT Condition, Primarily Pipe Applications.* New standard — $25. Review expired 2/13/06.

B2.1-1-234:200X, *Standard Welding Procedure Specification (SWPS) for Argon Plus 25% Carbon Dioxide Shielded Flux Cored Arc Welding of Carbon Steel (M-1/P-1/S-1) Groups 1 and 2, ⅛ through 1½ in. Thick, E7XT-X, As-Welded or PWHT Condition, Primarily Pipe Applications.* New standard — $25. Review expired 2/13/06.

B2.1-1-235:200X, *Standard Welding Procedure Specification (SWPS) for Argon Plus 2% Oxygen Shielded Gas Metal Arc Welding (Spray Transfer Mode) of Carbon Steel (M-1/P-1/S-1) Groups 1 and 2, ⅛ through 1½ in. Thick, ER70S-3, Flat Position Only, As-Welded or PWHT Condition, Primarily Pipe Applications.* New standard — $25. Review expired 2/13/06.

C3.4M/C3.4:200X, *Specification for Torch Brazing.* Revised standard — $25.00. Review expired 2/20/06.

C3.5M/C3.5:200X, *Specification for Induction Brazing.* Revised standard — $25. Review expired 2/20/06.

Standards Approved by ANSI

A5.19-92, *Specification for Magnesium Alloy Welding Electrodes and Rods.* Reaffirmed date 11/29/05.

D1.6:1999, *Structural Welding Code — Stainless Steel.* Extended to 3/10/08.

ISO Draft Standards for Public Review

Copies of the following draft International Standard is available for review and comment through your national standards body, which in the United States is ANSI, 25 W. 43rd St., Fourth Floor, New York, NY 10036; (212) 642-4900. Any comments regarding ISO documents should be sent to your national standards body.

In the United States, if you wish to participate in the development of International Standards for welding, contact **Andrew Davis,** (305) 443-9353, ext. 466, *adavis @aws.org.*

ISO/DIS 13918, *Welding — Studs and Ceramic Ferrules for Arc Stud Welding.* ♦

SPECIAL OFFER FOR NEW AWS INDIVIDUAL MEMBERS – TWO YEARS FOR $135 (a $25 savings)

★ *PLUS... Get a popular welding publication for only $25 ($192 value)*

AWS MEMBERSHIP APPLICATION

4 Easy Ways to Join or Renew:

Mail this form, along with your payment, to AWS

Call the Membership Department at (800) 443-9353, ext. 480

Fax this completed form to (305) 443-5647

Join or renew on our website <www.aws.org/membership>

❑ Mr. ❑ Ms. ❑ Mrs. ❑ Dr. Please print • Duplicate this page as needed

Last Name ______

First Name ______ M.I. ______

Title ______ Birthdate ______

Were you ever an AWS Member? ❑ YES ❑ NO If "YES," give year____ and Member # ______

Primary Phone ( ) ______ Secondary Phone ( ) ______

FAX ( ) ______ E-Mail ______

Did you learn of the Society through an AWS Member? ❑ Yes ❑ No

If "yes," Member's name: ______ Member's # (if known): ______

ADDRESS

NOTE: This address will be used for all Society mail.

Company (if applicable) ______

Address ______

Address Con't. ______

City ______ State/Province ______ Zip/Postal Code ______ Country ______

PROFILE DATA

NOTE: This data will be used to develop programs and services to serve you better.

① Who pays your dues?: ❑ Company ❑ Self-paid ② Sex: ❑ Male ❑ Female

③ Education level: ❑ High school diploma ❑ Associate's ❑ Bachelor's ❑ Master's ❑ Doctoral

PAYMENT INFORMATION (Required)

ONE-YEAR AWS INDIVIDUAL MEMBERSHIP $80

TWO-YEAR AWS INDIVIDUAL MEMBERSHIP† ....~~$160~~ $135

SAVE $25 (New Members Only)

New Member? ___Yes ___No

If yes, add one-time initiation fee of $12 .... $______

Add $25 for book selection ($192 value), and save up to 87%††............ $______ (Optional)

(Note: applies to new Individual Members only – Book selections on upper-right corner)

TOTAL PAYMENT .... $______

AWS STUDENT MEMBERSHIP†††

❑ Domestic (Canada & Mexico incl.) $15

❑ International $50

TOTAL PAYMENT .... $______

NOTE: Dues include $18.70 for *Welding Journal* subscription and $4.00 for the AWS Foundation.

$4.00 of membership dues goes to support the AWS Foundation

Payment can be made (in U.S. dollars) by check or money order (international or foreign), payable to the American Welding Society, or by charge card.

❑ Check ❑ Money Order ❑ Bill Me

❑ American Express ❑ Diners Club ❑ Carte Blanche ❑ MasterCard ❑ Visa ❑ Discover ❑ Other

Your Account Number ______ Expiration Date (mm/yy) ______

Signature of Applicant: ______ Application Date: ______

Office Use Only

Check # ______ Account # ______

Source Code WJ ______ Date ______ Amount ______

American Welding Society

P.O. Box 440367

Miami, FL 33144-0367

Telephone (800) 443-9353

FAX (305) 443-5647

Visit our website: www.aws.org

†Two-year Individual Membership Special Offer: applies only to new AWS Individual Members. **††Discount Publication Offer:** applies only to new AWS Individual Members. Select one of the four listed publications for an additional $25. **Multi-Year Discount:** First year is $80, each additional year is $75. No limit on years (not available to Student Members). **†††Student Member:** Any individual who attends a recognized college, university, technical, vocational school or high school is eligible. Domestic Members are those students residing in North America (incl. Canada & Mexico). This membership includes the *Welding Journal* magazine. Student Memberships do not include a discounted publication. **Airmail Postage Option:** International Members may receive their magazines via Airmail by adding $99 to the annual dues amount.

Member Services Revised 4/10/05

BOOK/CD-ROM SELECTION

(Pay Only $25... up to a $192 value)

NOTE: Only *New* Individual Members are eligible for this selection. Be sure to add $25 to your total payment. **ONLY ONE SELECTION PLEASE.**

- ❑ NEW *Jefferson's Welding Encyclopedia (CD-ROM only)*
- ❑ *Design and Planning Manual for Cost-Effective Welding*
- ❑ *Welding Metallurgy*
- ❑ *Welding Handbook (9th Ed., Vol. 2)*

❑ New Member ❑ Renewal

A free local Section Membership is included with all AWS Memberships

Section Affiliation Preference (if known):

Type of Business (Check ONE only)

A ❑ Contract construction
B ❑ Chemicals & allied products
C ❑ Petroleum & coal industries
D ❑ Primary metal industries
E ❑ Fabricated metal products
F ❑ Machinery except elect. (incl. gas welding)
G ❑ Electrical equip., supplies, electrodes
H ❑ Transportation equip. — air, aerospace
I ❑ Transportation equip. — automotive
J ❑ Transportation equip. — boats, ships
K ❑ Transportation equip. — railroad
L ❑ Utilities
M ❑ Welding distributors & retail trade
N ❑ Misc. repair services (incl. welding shops)
O ❑ Educational Services (univ., libraries, schools)
P ❑ Engineering & architectural services (incl. assns.)
Q ❑ Misc. business services (incl. commercial labs)
R ❑ Government (federal, state, local)
S ❑ Other

Job Classification (Check ONE only)

01 ❑ President, owner, partner, officer
02 ❑ Manager, director, superintendent (or assistant)
03 ❑ Sales
04 ❑ Purchasing
05 ❑ Engineer — welding
20 ❑ Engineer — design
21 ❑ Engineer — manufacturing
06 ❑ Engineer — other
10 ❑ Architect designer
12 ❑ Metallurgist
13 ❑ Research & development
22 ❑ Quality control
07 ❑ Inspector, tester
08 ❑ Supervisor, foreman
14 ❑ Technician
09 ❑ Welder, welding or cutting operator
11 ❑ Consultant
15 ❑ Educator
17 ❑ Librarian
16 ❑ Student
18 ❑ Customer Service
19 ❑ Other

Technical Interests (Check all that apply)

A ❑ Ferrous metals
B ❑ Aluminum
C ❑ Nonferrous metals except aluminum
D ❑ Advanced materials/Intermetallics
E ❑ Ceramics
F ❑ High energy beam processes
G ❑ Arc welding
H ❑ Brazing and soldering
I ❑ Resistance welding
J ❑ Thermal spray
K ❑ Cutting
L ❑ NDT
M ❑ Safety and health
N ❑ Bending and shearing
O ❑ Roll forming
P ❑ Stamping and punching
Q ❑ Aerospace
R ❑ Automotive
S ❑ Machinery
T ❑ Marine
U ❑ Piping and tubing
V ❑ Pressure vessels and tanks
W ❑ Sheet metal
X ❑ Structures
Y ❑ Other
Z ❑ Automation
1 ❑ Robotics
2 ❑ Computerization of Welding

SECTION NEWS

DISTRICT 1

Director: Russ Norris
Phone: (603) 433-0855

BOSTON

JANUARY 9
Activity: The Section members toured the B. E. Peterson facilities in Avon, Mass., to study the fabrication, welding, and machining of various parts made from stainless steels, high-alloy steels, duplex steels, and nickel alloys. **Mike Nolan,** plant manager, conducted the tour.

CONNECTICUT

NOVEMBER 19
Activity: Section Vice Chair **John Gullotti,** welding engineer, General Dynamics, Electric Boat Division, Groton, Conn., conducted a seminar on Welding Metallurgy. The event was held at Ironworkers Training Center.

JANUARY 17
Speaker: **Kai Moellendorf,** director of manufacturing
Affiliation: TRUMPF, Inc.
Topic: Laser beam cutting
Activity: Following the technical session, the Connecticut Section members toured the TRUMPF facility in Farmington, Conn., to study its integrated automated laser beam cutting and punching machinery. **Larry Johnson** led a tour of the welding department. **Micky Lawson** demonstrated some of the laser equipment capabilities.

GREEN & WHITE MOUNTAINS

JANUARY 12
Speaker: **Eric Bauer,** owner
Affiliation: Bauer Fabrication
Topic: Thermal spray
Activity: Bauer detailed his patented use of the thermal spray process for cast-in-place applications to produce sculptural works of art as an alternative to making large castings.

MAINE

JANUARY 18
Speaker: **Tom Cormier,** vice chairman
Affiliation: Metso Paper
Topic: The upcoming SkillsUSA weld test
Activity: **Mike Gendron** shared his ideas about the blueprints he is preparing for the SkillsUSA welding test. **Scott Lee** discussed processes and consumables that will be used. The meeting was held at Metso Paper in Biddeford, Maine.

DISTRICT 2

Director: Kenneth R. Stockton
Phone: (732) 787-0805

NEW JERSEY

OCTOBER 18
Activity: The Section members toured the Welco/CGI facility in Newark, N.J., to study the manufacture and bottling of industrial gases used in the Newark-New York City area. The tour was conducted by **John Smith.**

DISTRICT 3

Director: Alan J. Badeaux, Sr.
Phone: (301) 934-9061

LANCASTER

JANUARY 10
Speaker: **Pat Belsole**
Affiliation: Hypertherm Corp.
Topic: Plasma arc cutting
Activity: The program was held at Lancaster County Career and Technology Center in Mt. Joy, Pa. The dinner was prepared by the school's culinary department. Following the talk, the Section members had hands-on opportunities to use the plasma cutting equipment.

READING

NOVEMBER 19
Speaker: **Ed Starkey**
Affiliation: AlcoTec
Topic: The history of aluminum and aluminum welding — Part 1
Activity: The program was held at Super King Buffet in Reading, Pa. Starkey is scheduled to present Part 2 of his lecture on aluminum at a future meeting.

YORK-CENTRAL PA.

JANUARY 5
Activity: The Section members visited the Airgas facility in Harrisburg, Pa., for a hands-on tour conducted by **Charlie Minnach** and **Tim Stott,** both from Miller Electric Co. **Russell Stine** won the raffle prize, a 75th anniversary mini chopper donated by Miller Electric. See the photograph on next page.

Tom Ferri (left), Boston Section vice chair, is shown with Mike Nolan during the B. E. Peterson plant tour in January.

Speaker Ed Starkey (left) is shown with Reading Section Chair Chris Ochs (center), and Vice Chair David Butkus.

DISTRICT 4

Director: Ted Alberts
Phone: (540) 674-3600, ext. 4314

DISTRICT 5

Director: Leonard P. Connor
Phone: (954) 981-3977

Shown at the York-Central Pennsylvania Section program are (from left) Charlie Minnach and Tim Stott receiving their speaker gifts from Vice Chair Margaret Malehorn.

Gordon Smith (right) accepts the Cincinnati Section speaker gift from Uwe Achemeier, Section secretary.

Mark Lozev (left) receives a speaker gift from Jerry Van Meter, Columbus Section chair.

Shown are the top welding students with their awards displayed at the Johnstown-Altoona Division program in April.

SOUTH FLORIDA

DECEMBER 8
Speaker: **Rich DePue,** managing director, AWS education services
Affiliation: American Welding Society
Topic: Welding inspection around the world, including a weapons manufacturing facility in Turkey and at Ground Zero after 9/11
Activity: The program was held at McFatter Technical High School in Davie, Fla., for 30 attendees.

DISTRICT 6

Director: Neal A. Chapman
Phone: (315) 349-6960

NORTHERN NEW YORK

DECEMBER 6
Activity: The Section held a round table meeting. **Bob Christoffel** presented **Bob Dybas** his Gold Membership Certificate Award for 50 years of membership in the Society.

DISTRICT 7

Director: Don Howard
Phone: (814) 269-2895

CINCINNATI

JANUARY 17
Speaker: **Gordon Smith,** manager
Affiliation: Materials Joining Consultants
Topic: Forensic analysis of weld failures
Activity: The meeting was held at Corinthian Restaurant in Cincinnati, Ohio.

COLUMBUS

JANUARY 12
Speaker: **Mark Lozev,** chief engineer
Affiliation: Edison Welding Institute
Topic: Typical ultrasonic testing compared with phased array technology
Activity: The program was held at Edison Welding Institute in Columbus, Ohio.

JOHNSTOWN-ALTOONA Div.

APRIL 21
Speaker: **John Slagel,** human resources director
Affiliation: Johnstown Welding & Fabrication Industries
Topic: Opportunities in welding
Activity: The Division hosted its students' day program in Johnstown, Pa. Awards were presented to the top welding students from six local high schools.

MAY 27
Activity: The Johnstown-Altoona Division members competed with Pittsburgh

Section members during their 38th annual golf outing. The event was held at Tom's Run Golf Course in Blairsville, Pa.

SEPTEMBER 29
Activity: The Division toured Concurrent Technologies Corp., in Johnstown, Pa. **Kevin Klug,** senior materials scientist, spoke on titanium welding then conducted the tour with **Bruce Williams,** welding manager. **Don Howard,** District 7 director, made a presentation on AWS activities and opportunities for welding scholarships.

OCTOBER 18
Activity: The Johnstown-Altoona Division members toured the Colver Power Project to study how the facility uses waste coal products to generate power for metal refining and distribution. The tour guides were **Carl Yusko,** quality manager, and **Jason Burba,** operating technician.

NOVEMBER 29
Activity: **Bill Krupa,** area manager, conducted the Johnstown-Altoona Division members on a tour of the Freight Car America plant in Johnstown, Pa. Highlighted was the production line operations for building the Autoflood III, an aluminum coal-carrying freight car widely used in the industry. Twenty-seven members attended the event.

A few of the Johnstown-Altoona Division members pose in front of an Autoflood III rail car during their tour of Freight Car America in November.

PITTSBURGH

JANUARY 10
Speaker: **Damian Kotecki,** AWS president
Affiliation: The Lincoln Electric Co., technical director for stainless and high-alloy product development
Topic: How to convert good austenitic stainless steel filler metal into bad welds
Activity: The Section honored its past chairmen at this program. Kotecki presented **Richard LaFave** and **Joseph Mammarelli** their AWS Life Membership Awards for 35 years of service to the Society.

Fifteen past chairs of the Pittsburgh Section assembled for this group shot taken at the January 10 program.

Richard LaFave (right) accepts his Life Membership Award from AWS President Damian Kotecki at the Pittsburgh Section program in January.

Joseph Mammarelli (right) receives his Life Membership Award from Damian Kotecki, AWS president, at the Pittsburgh Section meeting.

DISTRICT 8

Director: Wallace E. Honey
Phone: (256) 332-3366

DISTRICT 9

Director: John Bruskotter
Phone: (504) 394-0812

DISTRICT 10

Director: Richard A. Harris
Phone: (440) 338-5921

MAHONING VALLEY

JANUARY 29
Speakers: **John Steel,** president; and **Chris Holt,** secretary
Affiliation: Pittsburgh Area Artist Blacksmiths Assoc.
Topic: Blacksmithing
Activity: Members of the Warren, Ohio, Chapter of ASM International attended this meeting.

Shown at the Mahoning Valley Section program are (from left) blacksmiths John Steel and Chris Holt receiving a speaker gift from Richard Polenicik, ASM International chapter chair.

DISTRICT 11

Director: Eftihios Siradakis
Phone: (989) 894-4101

Racine-Kenosha Section members and welding students from Gateway Technical College are shown during their tour of Lynch Display Vans in December.

Louie Rowe (right) accepts his Silver Membership Award from Jess Hunter, District 13 director, at the Blackhawk Section meeting.

Ginny Kowalski accepts a speaker gift from Don DeCorte, Detroit Section chairman, at the January program.

Jess Hunter (left), District 13 director, presents the Life Membership Award to Darrell McLaughlin at the Blackhawk Section program in November.

Racine-Kenosha Section Chair Ken Karwowski (left) thanks Nathan Goetsch for conducting the tour of Lynch Display Vans.

DETROIT

January 12
Activity: The Section members toured the William D. Ford Career Technical Center in Westland, Mich. **Ginny Kowalski,** principal and director of the facility, described how the center's 21 programs benefit the community. She highlighted the center's modern welding-fabrication technology facility.

WESTERN MICHIGAN

January 16
Speaker: **Lon Goble,** sales engineer
Affiliation: Central Metallizing & Machine, Inc.
Topic: Thermal spray coatings
Activity: The meeting was held at O'Malley's Grill & Pub in Grand Rapids, Mich. Plans were made for the Section's tour of Flex-Cable in February.

DISTRICT 12

Director: Sean P. Moran
Phone: (920) 954-3828

RACINE-KENOSHA

December 12
Activity: The Section members were joined by welding students from Gateway Technical College for a tour of Lynch Display Vans in Burlington, Wis., to study the fabrication of custom vehicles. **Nathan Goetsch,** plant facilities manager, conducted the tour.

DISTRICT 13

Director: Jesse L. Hunter
Phone: (309) 359-3063

BLACKHAWK

November 19
Activity: District 13 Director **Jess Hunter** presented **Darrell McLaughlin** the Life Membership Award for 35 years of membership in the Society. **Louie W. Rowe** received the Silver Membership Award for 25 years of service to AWS.

CHICAGO

January 18
Activity: Thirty-seven Chicago Section members toured the 200,000 sq-ft Pipefitters Union Local 597 Training Center in Mokena, Ill. **John Leen,** training director, made a presentation on its four-year apprenticeship program and continuing education courses for journeymen. The Center currently has enrolled 600 apprentices between the ages of 18 and 55. The talk was followed by a tour of the facilities and a meeting of the Section board members.

DISTRICT 14

Director: Tully C. Parker
Phone: (618) 667-7744

John Leen (left) accepts a speaker gift from Chuck Hubbard, Chicago Section chairman, at the Pipefitters Local 597 Training Center.

Shown at the St. Louis Section program are (front row, from left) Vince Suria, Bud Payton, Rick Suria, Jerry Bickel, and Jerry Simpson.

INDIANAPOLIS

DECEMBER 9

Activity: The Section held its Christmas party for 72 attendees at Beef and Boards Dinner Theater in Indianapolis, Ind.

ST. LOUIS

JANUARY 19

Activity: Forty Section members toured Jerry Bickel Race Cars in Moscow Mills, Mo., to study its welding and fitup operations. **Bud Payton** and owner **Jerry Bickel** discussed the facility's procedures and conducted the tour.

DISTRICT 15

Director: Mace V. Harris
Phone: (952) 925-1222

DISTRICT 16

Director: Charles F. Burg
Phone: (515) 233-1333

KANSAS

2005 UPDATE

Activities: The Section's initial goal for establishing a scholarship fund was achieved in September with the help of Airgas, Crowley College, Falcon Ind., Kice Ind., Linweld, Pac-Mig, Ward Welding, Inspection Services, Carl Harris Co., Wichita Welding Supply, Lampton Welding Supply, Tindle Construction, J.R.Custom Fab, Metal Finishing Co., Tec Weld Automation,Thompson Brothers, Miller Mfg., Wyldewood Cellers Winery, and Gracepoint Church. The Section hosted a successful career night program at Winfield High School. A tour of Wichita State University provided a look into the future of welding processes. The Section also toured Big Dog Motorcycles. The

Shown at the Nebraska Section program are (from left) Mike Naccarato, Amber Dewitt, Leo Dewitt, and Ron Oates.

year 2006 activities are looking good. Contact **Mark A. Ward,** Kansas Section chair at ward@cowley.edu.

NEBRASKA

JANUARY 19

Speaker: Mark V. Holland, chief engineer

Affiliation: Paxton Vierling Steel

Topic: Tolerances for structural steel

DISTRICT 17

Director: Oren P. Reich
Phone: (254) 867-2203

CENTRAL TEXAS

DECEMBER 6

Activity: The Section hosted its Christmas social and meeting at Olive Garden Restaurant in Waco, Tex. **Oren Reich,** District 17 director, updated everyone on recent events in AWS.

NORTH TEXAS

JANUARY 16

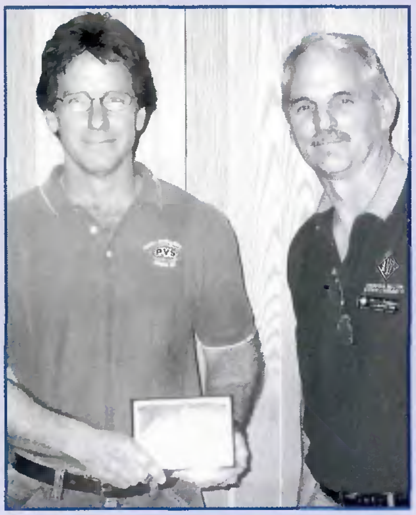

Mark Holland (left) accepts a speaker gift from Monty Rogers, Nebraska Section chair.

Activity: The Section members toured Martin Brothers Motorcycle Shop in Duncanville, Tex. Owners **Jason** and **Joe Martin** discussed the design and welding of their custom-made bikes and the specialized welding equipment used. See photo on next page.

OZARK

JANUARY 19

Speaker: **Dick Cady,** training manager

Affiliation: Kirk Welding Supply, Inc., Kansas City, Mo.

Topic: Welding gases

Activity: The program was held in Springfield, Mo. The subject for discussion was a new gas mixture for enhancing short arc, spray transfer, and pulsed spray for use with stainless steels.

DISTRICT 18

Director: John L. Mendoza
Phone: (210) 353-3679

The newly chartered Stanwood High School Student Chapter members pose at the Puget Sound Section program. Shown are (from left) Advisor Darryl Main, J. R. Winckler, Kyle Jacobson, Lena Rink, Julie Bryant, Tom Byers, Brandon Heichle, Todd Jacobson, and Matt Kline.

Shown during the North Texas Section tour of Martin Brothers Motorcycle Shop are (from left) Jason Martin, Section Chair Howie Sifford, and Joe Martin.

Some of the attendees posed at the Puget Sound Section program. Shown are (from left) District 19 Director Phil Zammit, students Marcus Williams and Tim Gramly, Vice Chair Ken Johnson, Section Chair Chris Sundberg, speaker Elaine Thomas, AWS President Damian Kotecki, and Matt Kuffel.

Speaker Jim Richardson (left) is shown with Puget Sound Chair Ken Johnson at the January program.

Winners in the Utah Section's annual Section 59 Turkey Shoot proudly display their awards.

DISTRICT 19

Director: Phil Zammit
Phone: (509) 468-2310 ext. 120

PUGET SOUND

DECEMBER 8
Speaker: **Elaine Thomas**
Topic: Duplex stainless steels
Activity: The Stanwood High School welding students were chartered as an AWS Student Chapter at this program. Welding instructor **Darryl Main** will serve as the Chapter advisor. **Damian Kotecki,** AWS president, and **Phil Zammit,** District 19 director, attended the program.

JANUARY
Speaker: **Jim Richardson**
Topic: Titanium materials and welding development

DISTRICT 20

Director: Nancy M. Carlson
Phone: (208) 526-6302

UTAH

November 15

Activity: The Section hosted its annual Section 59 Turkey Shoot at Impact Guns in Ogden, Utah. Section Chairman **Wayne Western,** of Ogden-Weber Applied Technology College, presented a talk on welding fun.

DISTRICT 21

Director: Jack D. Compton
Phone: (661) 362-3218

DISTRICT 22

Director: Kent S. Baucher
Phone: (559) 276-9311

NEVADA

November—January

Activities: The Nevada Section members toured three welding educational facilities in the area. First, the members visited Southern Nevada Vo-Tech Center, Las Vegas, Nev., for a tour guided by **Rick Boyer,** welding program instructor. **Henry Leaty** was presented his Life Membership Award for 35 years of service to the Society. A second outing toured the Area Technical Trade Center, North Las Vegas, directed by **Brian Stout,** a pipe fitter. A third meeting was held at the Community College of Southern Nevada, Henderson Campus, an AWS Educational Member. **Tony Adams** and **Shannon Girard** explained the school's two-year associate's degree in welding program. The Section has planned an awards-presentation program at Clark County Nevada Building Department, Building Services Div., to by hosted by CWI **Mark Hayer,** a fabrication inspector for the county. Contact **Gary Rogers** at *gmacarthur5@aol.com,* for more information about the Section's upcoming events.

Rick Boyer conducted the Nevada Section members on a tour of Southern Nevada Vo-Tech Center.

SAN FRANCISCO

January 4

Speaker: **Douglas E. Williams,** P.E.

Affiliation: Douglas E. Williams Consulting Engineer

Topic: "Per D1.1 Code?"

Activity: Following the talk, Williams conducted the Section members in a hands-on exercise using fillet gauges to examine weld specimens. The meeting was held at Spenger's Restaurant in Berkeley, Calif.

San Francisco Section Chair Robert Mertz (left) is shown with speaker Douglas Williams.

SANTA CLARA VALLEY

January 10

Speaker: **Brian Ahrens,** western regional manager

Affiliation: D. L. Ricci Corp.

Topic: Portable machining applications for pipe welding industry

Activity: **Ken Baucher,** District 22 director, presented appreciation awards to **Lou DeFreitas** and **Durella Combs** for their contributions to the Section.

INTERNATIONAL SECTION

TAIWAN

December 22

Activity: The International Section hosted a CWI training and testing program in Taipei, Taiwan. During the event, Section Chairman **Chon-Liang Tsai** presented the AWS Life Membership Award and pin to **Hsin-Zih Lin.** Lin is president of Jian King Enterprise Co., Ltd., a company specializing in welding repairs of marine and land-based diesel engines, pumps, valves, and other precision machinery parts.

Shown at the Taiwan International Section's CWI training and testing program are candidates and Section members. Chairman Tsai (front, center right) appears with Life Member Lin (front, center, left).

Committee Pros Sought

www.aws.org/join_a_committee

Welding Rotating Elements

The D14G Subcommittee on Welding of Rotating Equipment seeks volunteers to help revise AWS D14.6, *Specification for Welding of Rotating Elements of Equipment.* Needed are users and makers of such equipment, including crushers, fans, crankshafts, flywheels, centrifugal impellers, blowers, etc. For information, contact **Peter Howe,** *phowe@aws.org,* (800/305) 443-9353, ext. 309, or the Web site.

Welding Presses

The D14E Subcommittee on Welding of Presses seeks volunteers to help update AWS D14.5, *Specification for Welding of Presses and Press Components.* For information, contact **Peter Howe,** *phowe@aws.org,* (800/305) 443-9353, ext. 309, or the Web site.

Guide to AWS Services

550 NW LeJeune Rd., Miami, FL 33126
Phone (800) 443-9353; (888) WELDING; FAX (305) 443-7559
Internet: *www.aws.org*
Phone extensions appear in parentheses.

AWS PRESIDENT

Damian J. Kotecki
Damian_Kotecki@lincolnelectric.com
The Lincoln Electric Co.
22801 St. Clair Ave.
Cleveland, OH 44117-1199

ADMINISTRATION

Executive Director
Ray W. Shook.. *rshook@aws.org* ....(210)

CFO/Deputy Executive Director
Frank R. Tarafa.. *tarafa@aws.org* ....(252)

Deputy Executive Director
Jeffrey R. Hufsey .. *hufsey@aws.org* ....(264)

Associate Executive Director
Cassie R. Burrell.. *cburrell@aws.org* ....(253)

Associate Executive Director
Jeff Weber.. *jweber@aws.org* ....(246)

Executive Assistant for Board Services
Gricelda Manalich.. *gricelda@aws.org* ..(294)

COMPENSATION and BENEFITS

Director
Luisa Hernandez.. *luisa@aws.org* ......(266)

DATABASE ADMINISTRATION

Corporate Director
Jim Lankford.. *jiml@aws.org* ....(214)

INT'L INSTITUTE OF WELDING

Senior Coordinator
Sissibeth Lopez .. *sissi@aws.org* ......(319)
Provides liaison services with other national and international professional societies and standards organizations.

GOVERNMENT LIAISON SERVICES

Hugh K. Webster. ...... *hwebster@wc-b.com*
Webster, Chamberlain & Bean
Washington, D.C.
(202) 466-2976; FAX (202) 835-0243
Identifies funding sources for welding education, research, and development. Monitors legislative and regulatory issues of importance to the industry.

Brazing and Soldering Manufacturers' Committee

Jeff Weber.. *jweber@aws.org* ....(246)

RWMA — Resistance Welding Manufacturing Alliance

Jeff Weber.. *jweber@aws.org* ....(246)

WEMCO — Welding Equipment Manufacturing Committee, and WIN — Welding Industry Network

Jeff Weber.. *jweber@aws.org* ....(246)

CONVENTION and EXPOSITIONS

Exhibiting Information .... (242, 295)

Associate Executive Director/Sales Director
Jeff Weber.. *jweber@aws.org* ....(246)

Director, Education and Convention Services
John Ospina.. *jospina@aws.org* ....(462)
Responsible for the budget, operations, and logistics of convention activities at the FABTECH International & AWS Welding Show.

PUBLICATION SERVICES

Department Information ....(275)

Managing Director
Andrew Cullison.. *cullison@aws.org* ....(249)

Welding Journal

Publisher/Editor
Andrew Cullison.. *cullison@aws.org* ....(249)

National Sales Director
Rob Saltzstein.. *salty@aws.org* ....(243)

Society and Section News Editor
Howard Woodward.. *woodward@aws.org* (244)

Welding Handbook

Welding Handbook Editor
Annette O'Brien.. *aobrien@aws.org* ....(303)

Publishes the Society's monthly magazine, *Welding Journal*, which provides information on the state of the welding industry, its technology, and Society activities. Publishes *Inspection Trends*, the *Welding Handbook*, and books on general welding subjects.

MARKETING COMMUNICATIONS

Director
Ross Hancock.. *rhancock@aws.org* ....(226)

Senior Manager, Marketing
Linda Henderson... *lindah@aws.org* ....(298)

Senior Manager
George Leposky.. *gleposky@aws.org* ...(416)

MEMBER SERVICES

Department Information ....(480)

Associate Executive Director
Cassie R. Burrell.. *cburrell@aws.org* ....(253)

Director
Rhenda A. Mayo... *rhenda@aws.org* ....(260)
Serves as a liaison between Section members and AWS headquarters. Informs members about AWS benefits and activities.

EDUCATION SERVICES

Director, Education and Convention Services
John Ospina.. *jospina@aws.org* ....(462)
Responsible for the budget, operations, and logistics of all conference, seminar, and education services.

Managing Director
Richard J. DePue.. *rdepue@aws.org* ....(237)

Director, Educational Product Development
Christopher Pollock.. *cpollock@aws.org* (219)
Oversees review and development of educational materials for AWS seminars and conferences. Serves as Secretary to the AWS Product Development and Conference Committees. Coordinates in-plant seminars and workshops.

AWS AWARDS, FELLOWS, COUNSELORS

Managing Director
Wendy S. Reeve.. *wreeve@aws.org* .....(293)
Coordinates AWS awards and AWS Fellow and Counselor nominees.

CERTIFICATION OPERATIONS

Department Information ....(273)

Deputy Executive Director
Jeffrey R. Hufsey... *hufsey@aws.org* ....(264)

Director, Certification Programs
Tina Burke . . *tburke@aws.org* ....(215)

Director, Operations
Terry Perez.. *tperez@aws.org* ....(470)

Director, Int'l Business Accreditation and Welder Certification
Walter Herrera.. *walter@aws.org* ....(475)
Provides information on personnel certification and accreditation services.

TECHNICAL SERVICES

Department Information ....(340)

Managing Director
Andrew R. Davis.. *adavis@aws.org* .....(466)
Int'l Standards Activities, American Council of the International Institute of Welding (IIW)

Director, National Standards Activities
Peter Howe.. *phowe@aws.org* ....(309)
Machinery and Equipment Welding, Robotic and Automatic Welding, Computerization of Welding Information

Manager, Safety and Health
Stephen P. Hedrick.. *steveh@aws.org* ..(305)
Metric Practice, Personnel and Facilities Qualification, Safety and Health, Joining of Plastics and Composites

Technical Publications

AWS publishes about 200 documents widely used in the welding industry.
Senior Manager
Rosalinda O'Neill.. *roneill@aws.org* ....(451)

Staff Engineers/Committee Secretaries
Annette Alonso.. *aalonso@aws.org* .....(299)
Welding in Sanitary Applications, Automotive Welding, Resistance Welding, High-Energy Beam Welding, Aircraft and Aerospace, Oxyfuel Gas Welding and Cutting

John L. Gayler.. *gayler@aws.org* ....(472)
Structural Welding, Welding Iron Castings

Rakesh Gupta.. *gupta@aws.org* ....(301)
Filler Metals and Allied Materials, Int'l Filler Metals, Instrumentation for Welding, UNS Numbers Assignment

Cynthia Jenney .. *cynthiaj@aws.org* ....(304)
Definitions & Symbols, Brazing & Soldering, Brazing Filler Metals & Fluxes, Technical Editing

Brian McGrath . *bmcgrath@aws.org* ....(311)
Methods of Inspection, Mechanical Testing of Welds, Thermal Spray, Arc Welding and Cutting, Welding in Marine Construction, Piping and Tubing, Titaniu....m and Zirconium Filler Metals, Filler Metals for Naval Vessels

Selvis Morales.... *smorales@aws.org* ...(313)
Welding Qualification, Friction Welding, Joining of Metals and Alloys, Railroad Welding

Note: Official interpretations of AWS standards may be obtained only by sending a request in writing to the Managing Director, Technical Services. Oral opinions on AWS standards may be rendered. However, such opinions represent only the personal opinions of the particular individuals giving them. These individuals do not speak on behalf of AWS, nor do these oral opinions constitute official or unofficial opinions or interpretations of AWS. In addition, oral opinions are informal and should not be used as a substitute for an official interpretation.

AWS WEB SITE ADMINISTRATION

Web Site Coordinator
Natalie Tapley.. *tapley@aws.org* ....(456)

Nominees for National Office

Only Sustaining Members, Members, Honorary Members, Life Members, or Retired Members who have been members for a period of at least three years shall be eligible for election as a director or national officer.

It is the duty of the National Nominating Committee to nominate candidates for national office. The committee shall hold an open meeting, preferably at the Annual Meeting, at which members may appear to present and discuss the eligibility of all candidates.

To be considered a candidate for the positions of president, vice president, treasurer, or director-at-large, the following qualifications and conditions apply:

President: To be eligible to hold the office of president, an individual must have served as a vice president for at least one year.

Vice President: To be eligible to hold the office of vice president, an individual must have served at least one year as a director, other than executive director and secretary.

Treasurer: To be eligible to hold the office of treasurer, an individual must be a member of the Society, other than a Student Member, must be frequently available to the national office, and should be of executive status in business or industry with experience in financial affairs.

Director-at-Large: To be eligible for election as a director-at-large, an individual shall previously have held office as chairman of a Section; as chairman or vice chairman of a standing, technical or special committee of the Society; or as District director.

Interested parties should write a letter stating which office they seek, including a statement of qualifications, their willingness and ability to serve if nominated and elected, and 20 copies of their biographical sketch.

This material should be sent to James E. Greer, Chairman, National Nominating Committee, American Welding Society, 550 NW LeJeune Rd., Miami, FL 33126.

The next meeting of the National Nominating Committee is scheduled for October 2006. The term of office for candidates nominated at this meeting will commence January 1, 2008.♦

Honorary Meritorious Awards

The Honorary-Meritorious Awards Committee makes recommendations for the nominees presented for Honorary Membership, National Meritorious Certificate, William Irrgang Memorial, and the George E. Willis Awards. These awards are presented during the AWS Exposition and Convention held each spring. The deadline for submissions is December 31 prior to the year of awards presentations. Send candidate materials to Wendy Sue Reeve, Secretary, Honorary-Meritorious Awards Committee, 550 NW LeJeune Rd., Miami, FL 33126. Descriptions of the awards follow.

National Meritorious Certificate Award: This award is given in recognition of the candidate's counsel, loyalty, and devotion to the affairs of the Society, assistance in promoting cordial relations with industry and other organizations, and for the contribution of time and effort on behalf of the Society.

William Irrgang Memorial Award: This award is administered by the American Welding Society and sponsored by The Lincoln Electric Co. to honor the late William Irrgang. It is awarded each year to the individual who has done the most to enhance the American Welding Society's goal of advancing the science and technology of welding over the past five-year period.

George E. Willis Award: This award is administered by the American Welding Society and sponsored by The Lincoln Electric Co. to honor George E. Willis. It is awarded each year to an individual for promoting the advancement of welding internationally by fostering cooperative participation in areas such as technology transfer, standards rationalization, and promotion of industrial goodwill.

International Meritorious Certificate Award: This award is given in recognition of the candidate's significant contributions to the worldwide welding industry. This award should reflect "Service to the International Welding Community" in the broadest terms. The awardee is not required to be a member of the American Welding Society. Multiple awards can be given per year as the situation dictates. The award consists of a certificate to be presented at the awards luncheon or at another time as appropriate in conjunction with the AWS President's travel itinerary, and, if appropriate, a one-year membership in the American Welding Society.

Honorary Membership Award: An Honorary Member shall be a person of acknowledged eminence in the welding profession, or who is accredited with exceptional accomplishments in the development of the welding art, upon whom the American Welding Society sees fit to confer an honorary distinction. An Honorary Member shall have full rights of membership.♦

NEW CONTACT

Publications Sales/Orders

World Engineering Xchange (WEX), Ltd.
Toll-free (888) 935-3464 (U.S., Canada)
(305) 824-1177; FAX (305) 826-6195
www.aws.org/standards

Journal Reprints

Order quality custom reprints from
Claudia Stachowiak, FosteReprints
Toll-free (866) 879-9144, ext. 121
sales@fostereprints.com

AWS Foundation, Inc.

The AWS Foundation is a not-for-profit corporation established to provide support for educational and scientific endeavors of the American Welding Society. Information on gift-giving programs is available upon request.

550 NW LeJeune Rd., Miami, FL 33126
(305) 445-6628; (800) 443-9353, ext. 293
e-mail: *vpinsky@aws.org*
general information:
(800) 443-9353, ext. 689

AWS Mission Statement

The mission of the American Welding Society is to advance the science, technology, and application of welding and allied processes, including joining, brazing, soldering, cutting, and thermal spraying.

It is the intent of the American Welding Society to build AWS to the highest quality standards possible. The Society welcomes your suggestions. Please contact any staff member, or AWS President Damian J. Kotecki, as listed on the previous page.

Hobart Institute Offers New Training Materials Catalog

The 2006 Hobart Institute Welding Training Materials Catalog outlines and provides details for all of the institute's courseware and publications.

Hobart Institute of Welding Technology 114
400 Trade Square East, Troy, OH 45373

Catalog Details Laser Safety Courses

The 16-page, full-color 2006 Laser Safety Training Catalog details the certificate courses titled laser safety officer, in-house laser safety training, medical laser safety officer, advanced concepts in laser safety, laser safety in the lab, industrial lasers and safety online training, laser safety in educational institutions online training, OSHA laser safety seminar, and laser safety auditing for medical facilities. Each course description includes dates and locations, course overview, who should attend, course instructors' names and qualifications, supplies provided, and registration fees. Texts provided include ANSI Z136.1, *Safe Use of Lasers,* the Laser Institute of America (LIA) *Laser Safety Guide,* and the LIA *Guide for Selection of Laser Eye Protection.*

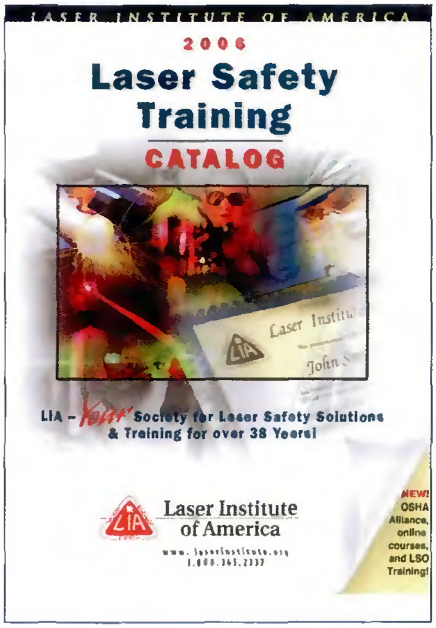

Laser Institute of America 115
13501 Ingenuity Dr., Ste. 128, Orlando, FL 32826

ASM Catalog Details Many New Publications

The 64-page, full-color January 2006 ASM Catalog details its books, CDs, journals, online information, training courses and seminars. Among the many new titles described are *Failure Analysis; Gear Materials, Properties, and Manufacture; Practical Heat Treating; Fatigue and Durability; Lead-Free Solder Interconnect Reliability; Principles of Brazing; Principles of Soldering;* and *Steels Processing, Structure and Performance.* The 2006 Seminar schedule is displayed in a calendar format for 33 course titles, with cross references to the complete course descriptions and fees.

ASM International 116
9639 Kinsman Rd., Materials Park, OH 44073-0002

Laser Cutting System Pictured in Brochure

A 4-page, full-color brochure presents a photo lineup displaying the features and operating parameters of the TLV series

of 3-axis, 2-dimensional CO_2 bridge-style laser beam cutting systems. Detailed are four energy options and five model sizes including a 6-kW unit with cutting speeds to 787 in. per minute ±0.0005 in. per 12 in. of movement accuracy, and a work envelope 246 x 86 in.

NTC America Corp., Laser Group 117
24495 Hathaway Dr., Farmington Hills, MI 48335

National Standard for Hand Protection Updated

The International Safety Equipment Association (ISEA), Arlington, Va., has released ANSI/ISEA 105-2005, *American National Standard for Hand Protection Selection Criteria,* which replaces the 2000 edition. New in this document is a numeric-scale method for manufacturers to rate their gloves against certain contaminants and exposures. Performance and pass/fail criteria are given for cut, puncture, and abrasion resistance, chemical permeation and degradation, hole detection, and heat and flame resistance. Also new are tests and glove selection criteria

— *continued on page 97*

— *continued from page 95*

for vibration reduction and dexterity. The test methods and classification levels for product characteristics now include the newest materials, performance, and technology, to bring the standard into harmony with current industrial requirements. The document is available from ISEA for $30, $20 for ISEA members. Download the order form from *www.safetyequipment.org*, or call (703) 525-1695.

'Essentials' Offered in New AWS Catalog

This compact (6- x 11-in.) catalog details in its 44, full-color pages all of the essential standards plus numerous other publications developed by the American Welding Society. The first few pages detail all of the new publications, followed by listings of new editions of existing specifications and standards. Included are listings of all of the qualification and welding procedure specifications presented in chart form for sheet metal, pipe, plate, welding and cutting processes, training documents, filler metals, etc. An extensive subject index simplifies determining all of the documents pertaining to each need. Included are details about AWS conferences for 2006, and general information about AWS and its services. *www.aws.org/catalog*

American Welding Society **118**
550 NW LeJeune Rd., Miami, FL 33126

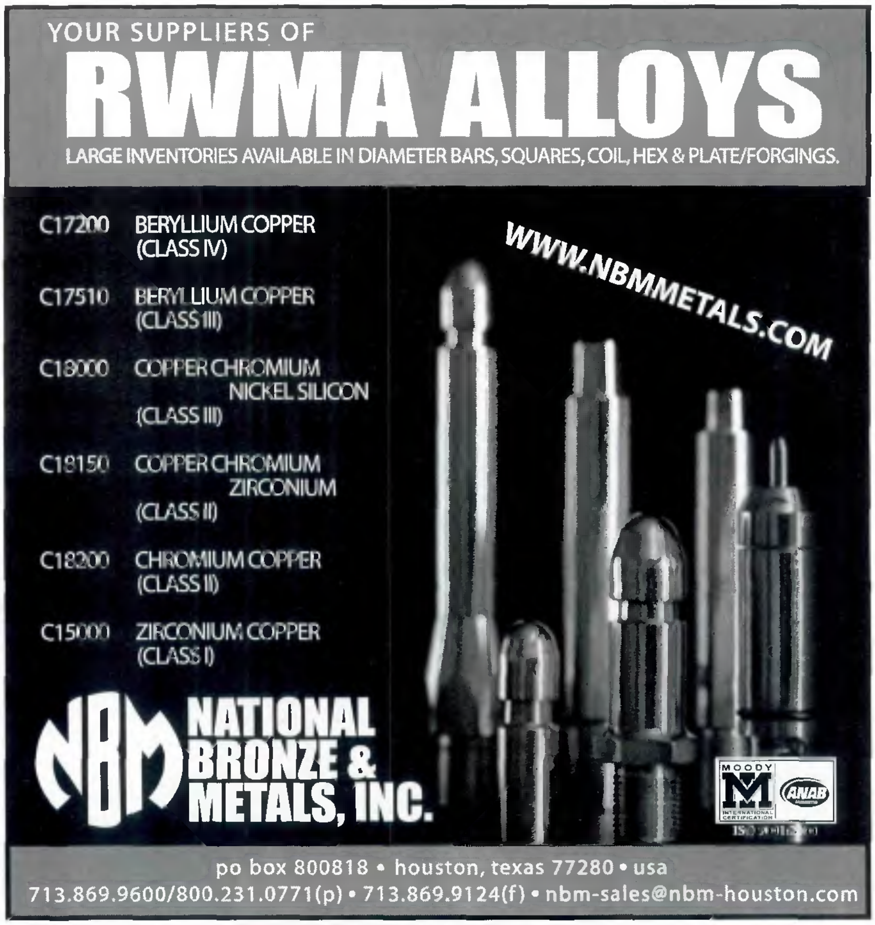

Circle No. 45 on Reader Info-Card

Circle No. 54 on Reader Info-Card

VP Named at Rankin Industries

Strong Welding Products Inc., Rancho Cucamonga, Calif., has appointed **William Shum** vice president and managing director of Rankin Industries, San Diego, Calif., a producer of hardfacing products. Shum, with the company for ten years, previously served as director of research and development.

Sabel Retires from Hobart

Gene Sabel, vice president of sales, Hobart Brothers Co., Troy, Ohio, retired December 23. Sabel began his career in the welding industry in 1963 at the A. O. Smith Corp., Welding Products division, which later became Alloy Rods Corp. In 1993, he left the company to join Hobart Brothers as vice president of sales.

Wall Colmonoy Appoints Marketing and Sales Manager

David Hart

David Hart has been appointed marketing and sales manager for Wall Colmonoy Corp., based at the corporate office in Madison Heights, Mich. Hart has 25 years of experience in the hardfacing and brazing industries in Australia, Canada, and the United States.

FKI Logistex Appoints President

Bob Duplain

FKI Logistex North America, Cincinnati, Ohio, has promoted **Bob Duplain** to president, Warehouse and Distribution division. Previously, Duplain was the acting division president. He succeeds **John Westendorf,** who now serves as president, FKI Hardware Group.

Lincoln Electric Elects Three to Key Posts

The Lincoln Electric Co., Cleveland, Ohio, has elected **Gabriel Bruno,** vice president, corporate controller; **Michele Kuhrt,** vice president, corporate tax; and **David Nangle,** vice president and group president of brazing, cutting, and retail subsidiaries. Bruno previously served as corporate controller and director of information technology. Kuhrt formerly was director of taxes and financial administration. Nangle, with the company since 1979, most recently served as president of Welding, Cutting, Tools and Accessories, Inc., and president of J. W. Harris Co., two subsidiaries of the company.

worked as head of the laser business unit for a Swiss optics company. Bleher previously served as managing director of TRUMPF Laser Marking Systems AG in Switzerland.

Welding division based in South Windsor, Conn. He succeeds **Robert Sanborn.** Wiegard previously served as vice president of operations for The Miller Co., a manufacturer of copper-based alloys.

SME Elects President for 2006

William J. Geary

William J. Geary has been elected president of the Society of Manufacturing Engineers (SME) for 2006. Geary is chief engineer, aircraft interiors, 737 program, at The Boeing Co., Seattle, Wash. Geary has served on the SME board of directors since 2001, and most recently as SME's president-elect. In 1990, he received the SME Outstanding Young Manufacturing Engineer Award.

Koike Aronson Names National Sales Manager

Brad Williams

Brad Williams has been appointed national sales manager for Koike Aronson, Inc., Arcade, N.Y. With the company for 30 years, Williams most recently served as sales training specialist.

TRUMPF Notes Laser Management Changes

Peter Grollmann

TRUMPF Inc., Farmington, Conn., has appointed **Peter Grollmann** product manager for laser marking products for North America, and **Jens Bleher,** managing director of TRUMPF Laser- und Systemtechnik, GmbH, Ditzingen, Germany. Most recently, Grollmann

Dynamic Materials Names Welding Division President

Dynamic Materials Corp., Boulder, Colo., has named **Harold Wiegard** president and general manager of its AMK

Tricon Metals Names VP of Operations

Tricon Metals & Services, Inc., Birm-

— continued on page 104

American Welding Society

Friends and Colleagues:

I want to encourage you to submit nomination packages for those individuals whom you feel have a history of accomplishments and contributions to our profession consistent with the standards set by the existing Fellows. In particular, I would make a special request that you look to the most senior members of your Section or District in considering members for nomination. In many cases, the colleagues and peers of these individuals who are the most familiar with their contributions, and who would normally nominate the candidate, are no longer with us. I want to be sure that we take the extra effort required to make sure that those truly worthy are not overlooked because no obvious individual was available to start the nomination process.

For specifics on the nomination requirements, please contact Wendy Sue Reeve, at AWS headquarters in Miami, or simply follow the instructions on the Fellows nomination form in this issue of the *Welding Journal*. Please remember, we all benefit in the honoring of those who have made major contributions to our chosen profession and livelihood. The deadline for submission is July 1, 2006. The Committee looks forward to receiving numerous Fellow nominations for 2007 consideration.

Sincerely,

Nancy C. Cole
Chair, AWS Fellows Selection Committee

(please type or print in black ink)

CLASS OF 2007

FELLOW NOMINATION FORM

DATE________________NAME OF CANDIDATE____

AWS MEMBER NO.______________________YEARS OF AWS MEMBERSHIP______________________

HOME ADDRESS____

CITY______________________________STATE______ZIP CODE________PHONE______________

PRESENT COMPANY/INSTITUTION AFFILIATION________________________________

TITLE/POSITION____

BUSINESS ADDRESS____

CITY______________________________STATE______ZIP CODE________PHONE______________

ACADEMIC BACKGROUND, AS APPLICABLE:

INSTITUTION____

MAJOR & MINOR____

DEGREES OR CERTIFICATES/YEAR____

LICENSED PROFESSIONAL ENGINEER: YES________NO________ STATE______________________

SIGNIFICANT WORK EXPERIENCE:

COMPANY/CITY/STATE____

POSITION____YEARS______________

COMPANY/CITY/STATE____

POSITION____YEARS______________

SUMMARIZE MAJOR CONTRIBUTIONS IN THESE POSITIONS:

____

____

____

IT IS MANDATORY THAT A CITATION (50 TO 100 WORDS, USE SEPARATE SHEET) INDICATING WHY THE NOMINEE SHOULD BE SELECTED AS AN AWS FELLOW ACCOMPANY NOMINATION PACKET. IF NOMINEE IS SELECTED, THIS STATEMENT MAY BE INCORPORATED WITHIN THE CITATION CERTIFICATE.

SEE GUIDELINES ON REVERSE SIDE

SUBMITTED BY: PROPOSER________________________________AWS Member No.______________
Print Name________________________________

The Proposer will serve as the contact if the Selection Committee requires further information. Signatures on this nominating form, or supporting letters from each nominator, are required from four AWS members in addition to the Proposer. Signatures may be acquired by photocopying the original and transmitting to each nominating member. Once the signatures are secured, the total package should be submitted.

NOMINATING MEMBER:______________________ NOMINATING MEMBER:______________________
Print Name______________________ Print Name______________________
AWS Member No.__________ AWS Member No.__________

NOMINATING MEMBER:______________________ NOMINATING MEMBER:______________________
Print Name______________________ Print Name______________________
AWS Member No.__________ AWS Member No.__________

SUBMISSION DEADLINE JULY 1, 2006

American Welding Society

Fellow Description

DEFINITION AND HISTORY

The American Welding Society, in 1990, established the honor of Fellow of the Society to recognize members for distinguished contributions to the field of welding science and technology, and for promoting and sustaining the professional stature of the field. Election as a Fellow of the Society is based on the outstanding accomplishments and technical impact of the individual. Such accomplishments will have advanced the science, technology and application of welding, as evidenced by:

* Sustained service and performance in the advancement of welding science and technology
* Publication of papers, articles and books which enhance knowledge of welding
* Innovative development of welding technology
* Society and chapter contributions
* Professional recognition

RULES

1. Candidates shall have 10 years of membership in AWS
2. Candidates shall be nominated by any five members of the Society
3. Nominations shall be submitted on the official form available from AWS Headquarters
4. Nominations must be submitted to AWS Headquarters no *later than July 1 of the year prior* to that in which the award is to be presented
5. Nominations will remain valid for three years
6. All information on nominees will be held in strict confidence
7. No more than two posthumous Fellows may be elected each year

NUMBER OF FELLOWS

Maximum of 10 Fellows selected each year.

AWS Fellow Application Guidelines

Nomination packages for AWS Fellow should clearly demonstrate the candidates outstanding contributions to the advancement of welding science and technology. In order for the Fellows Selection Committee to fairly assess the candidates qualifications, the nomination package must list and clearly describe the candidates specific technical accomplishments, how they contributed to the advancement of welding technology, and that these contributions were sustained. Essential in demonstrating the candidates impact are the following (in approximate order of importance).

1. Description of significant technical advancements. This should be a brief summary of the candidates most significant contributions to the advancement of welding science and technology.
2. Publications of books, papers, articles or other significant scholarly works that demonstrate the contributions cited in (1). Where possible, papers and articles should be designated as to whether they were published in peer-reviewed journals.
3. Inventions and patents.
4. Professional recognition including awards and honors from AWS and other professional societies.
5. Meaningful participation in technical committees. Indicate the number of years served on these committees and any leadership roles (chair, vice-chair, subcommittee responsibilities, etc.).
6. Contributions to handbooks and standards.
7. Presentations made at technical conferences and section meetings.
8. Consultancy — particularly as it impacts technology advancement.
9. Leadership at the technical society or corporate level, particularly as it impacts advancement of welding technology.
10. Participation on organizing committees for technical programming.
11. Advocacy — support of the society and its technical advancement through institutional, political or other means.

Note: Application packages that do not support the candidate using the metrics listed above will have a very low probability of success.

Supporting Letters

Letters of support from individuals knowledgeable of the candidate and his/her contributions are encouraged. These letters should address the metrics listed above and provide personal insight into the contributions and stature of the candidate. Letters of support that simply endorse the candidate will have little impact on the selection process.

Return completed Fellow nomination package to:

Wendy S. Reeve
American Welding Society
550 N.W. LeJeune Road
Miami, FL 33126

Telephone: 800-443-9353, extension 293

SUBMISSION DEADLINE: July 1, 2006

NEW PRODUCTS

— *continued from page 27*

company's Versagraph Millennium model machines. It makes a clean, bevel cut in a single pass with less residual slag. It provides 360 deg of continuous rotation without wind up of the plasma torch leads or interconnecting cables and performs contour bevel angles to +45 and –40 deg. It is mounted to the Versagraph Millennium's rigid master carriage. The unit is compatible with Innerlogic Fineline 260 and Proline 2260 plasma cutting systems for production cutting of mild steel to 1¼ in. thick. In addition, it features integrated initial height sensing using ohmic contact as well as real-time arc voltage detection technology with arc voltage tracking within 0.1 arc volts.

Koike Aronson, Inc. **110**
635 W. Main St., PO Box 307, Arcade, NY 14009

Gas Blender Mixes Shielding Gases on Site

The BlendMaster™ 1000 Series enables users to create custom-blended gas mixtures on site for GTA and GMA industrial welding applications. Utilizing pure gases such as argon, carbon dioxide, helium, and oxygen, it enhances quality by maintaining a ±1.5% accuracy. EquiBlend™ technology allows for full flow regardless of the mix or blend ratio. A pressure equalization system minimizes inlet pressure fluctuations to stabilize the mix, broadening the inlet pressure range difference between the major and minor component gases. It is available as a wall- or floor-mounted unit for installation and maintenance flexibility, and provides up to 1000 ft^3/h at delivery pressures from 10 to 45 lb/in.^{2}. A lockable enclosure assures process control, and an integral line regulator supports flowmeters, regulators, and flowmeter installations. Power requirements are 110 or 220 VAC, and ambient atmosphere and gas supply temperature requirements are 32° to 100°F.

CONCOA **111**
1501 Harpers Rd., Virginia Beach, VA 23454

Metal Cored Electrodes Feature Smooth Spray Transfer, Low Fume Levels

The Select 70C-6LS is a carbon steel,

gas-shielded, composite metal cored electrode that produces fewer slag islands. It also delivers weld bead appearance with tie-in, a smooth spray transfer, and virtually no spatter. The Select 70C-7 features a smooth arc transfer and a low spatter level to minimize postweld cleanup, making it suited for weldments that require painting. Its low fume levels reduce worker exposure in more difficult-to-weld areas. Typical applications for both electrodes include car and truck frames, thin-walled tanks, structural steels, and earth-moving equipment.

Select-Arc, Inc. 112
PO Box 259, Fort Loramie, OH 45845-0259

Accessories Added to Hand-held Plasma Cutting Systems

Three items have been added to the company's line of accessories for Powermax hand-held plasma arc cutting systems. The basic circle cutting guide allows Powermax hand torches to be used for performing straight cuts, circle cuts as large as 22 in. in diameter and as small as 4 in. in diameter, and bevel cuts. The guide package includes an adjustable point pivot, stabilizing wheels, and a torch-head bushing to cut accurate circles on any workpiece. The multipurpose operator face shield delivers face and eye protection during any Powermax plasma cutting application. It comes with an adjustable head strap, a clear face shield, plus an AWS #8 shade filter that can be lowered during cutting. The Powermax dust covers are designed to help protect the power supply when the system is not in use. They are constructed of durable denim fabric with a polyurethane coating and are available in four sizes for any Powermax system.

Hypertherm, Inc. 113
Etna Rd., PO Box 5010, Hanover, NH 03755

Personnel

— *continued from page 99*

Greg Boggis

ingham, Ala., has promoted **Greg Boggis** to senior vice president of operations for the Birmingham, Chicago, Ill., and Elko, Nev., plants. Boggis has served the company in various positions for 15 years.

EWI Names Human Resources Director

Mark Matson

Edison Welding Institute has appointed **Mark Matson** as human resources director. Before joining the institute, Matson was corporate human resources director at OCLC, Online Computer Library Center, Inc.

Polymet Names Hardfacing Sales Manager

Richard Cook

Polymet Corp., Cincinnati, Ohio, has appointed **Richard Cook** as sales manager for industrial hardfacing products. Cook has more than 30 years' experience in product management, technical sales, and other management positions for Stoody and other companies serving the welding and hardfacing industries.

Member Milestone

Smith Named Outstanding Faculty Member at West Virginia

Carl Smith recently received the

Carl Smith is shown with President Marie Foster Gnage as he received the Waller C. Hardy Outstanding Faculty Member of the Year Award at West Virginia University at Parkersburg.

Waller C. Hardy Outstanding Faculty Member of the Year Award from **Marie Foster Gnage,** president, West Virginia University at Parkersburg. Smith, an associate professor of welding at the university, sits on the AWS Education Committee, is chairman of the Tri-State Section (District 7), and serves as quality manager at Kanawha Mfg. Co. based in Charleston and Buffalo, W.Va. Earlier in 2005, Smith was cited to receive the National Institute for Student and Organizational Development Award.

OBITUARY

Leonard Francis Wood

Leonard Francis Wood, 87, died November 22 in Longmeadow, Mass. Mr. Wood joined AWS in 1974. He served the Boston Section in many offices, including Certification Committee chair (1986–91).

L. F. Wood

Mr. Wood worked as a welding engineer for Bethlehem Steel Corp. of Boston for 34 years until he retired in 1973. Later, he taught metallurgy and welding at Wentworth College and served as the Northeastern Regional Test Supervisor for welding inspectors exams.

A veteran of World War II, he was a member of VFW Post 2490 and the Eighth Air Force Historical Society. He played trumpet and trombone in the USO Band while stationed in France, and at home he performed in local bands and orchestras.

He also served as a Technical Committee member for Vocational Industrial Club of America (VICA), currently named SkillsUSA.

Mr. Wood attended Northeastern University and earned his teaching certificate in metal fabrication at Fitchburg State College.

He is survived by his wife, Loretta, three sons, three daughters, one stepdaughter, and 18 grandchildren.

CAREER OPPORTUNITIES

Maintenance Manager

needed for Steel Processing/Welding Co. Job duties: Supervise maintenance technicians for all aspects of maintenance, repair and new installations of automated plant equipment and lasers for welding including Allen Bradley PLC's (Programmable Logic Controllers), ABB Robotics, Indramat Servo Drives, Trumpf/Haas Nd/YAG lasers, AD and DC variable speed drives, power distribution systems and NEC; establish and supervise plant-wide preventive maintenance programs. Maintain inventory levels of spare parts and equipment for the facility. Two years experience in job duties or 2 years experience in working with Allen Bradley PLC (or Siemens PLC), ABB Robotics (or Motoman Robotics), Indramat Servo Drives (or Allen Bradley Servo Drives), and Trumpf/Haas Nd: YAG lasers (or Unitek Miyachi Md: YAG lasers). Résumés to HR Dept., Shiloh Industries/Jefferson Blanking Division, 234 W. Holland Dr., Pendegrass, GA 30567. No calls. EOE.

Welding Engineer

Hobart Brothers, an ITW Co., located just North of Dayton in Troy, OH seeks a hands-on Welding Engineer. Responsibilities with tubular welding wire include: Productivity & quality improvements, product conversions, evaluate wire for new product development and marketing, respond to technical inquiries, troubleshoot customer welding issues. May involve up to 25% domestic and international travel. Seeking candidates with a BS in Welding Technology/Engineering and min. 1 yr. of related experience. Knowledge of PLC programming as well as robotic and automatic welding experience is a plus. We offer a competitive salary and benefits package. Please reply with a resume and salary requirements to:

Hobart Brothers Company
101 Trade Square East
Troy, OH 45373
ATTN: Welding Engineer
Fax: (937) 332-5178
E-mail: aboulmi@hobartbrothers.com
www.hobartbrothers.com
www.itw.com
EOE M/F/D/V

Structural Fabrication Inspector

$18.68 - $25.89/hour; $39,004 - $54,058/year MN Department of Transportation has a permanent full time vacancy at MN/DOT in Oakdale, MN. Provide QA inspection during steel bridge and structure fabrication to comply w/codes, standards & specs. 40% out-of-state travel required. Must have AWS Certified Welding Inspector certificate & Class D driver's license. For further info & to apply, go to: http://www.doer.state.mn.us/employment.htm and click on Job #05DOT000523. Questions, contact Barb Kochevar at 651-296-1360 or Barbara.kochevar@dot.state.mn.us. EOE.

Welding Engineer

Highly visible position is responsible for the planning, organizing and directing of the technical aspects of all types of welding processes and training. Crenlo is a metal fabricator of enclosures and of cabs for the ag/construction industries. Over 240 different welding machines. Visit our website for more information www.crenlo.com. Crenlo, HR, 1600 4th Avenue NW, Rochester, MN 55901. Tele (507) 287-3614. Fax (507) 280-2350. E-mail hr@crenlo.com. EOE.

Assistant or Associate Professor

A tenure-track faculty position at the Assistant or Associate Professor level is available in the Department of Materials and Metallurgical Engineering at the South Dakota School of Mines and Technology. A Ph.D. in Metallurgical Engineering or a closely related discipline is required at the time of the appointment. The successful candidate is expected to teach undergraduate and graduate courses, and initiate and/or sustain sponsored research and graduate education programs. The department participates in materials engineering and science and nanoscience/nanoengineering graduate programs. Individuals with specific research and teaching interests in welding/joining technology and other related metallurgical engineering areas are strongly encouraged to apply. The department requires a close collaboration with the Advanced Materials Processing Center (http://ampcenter.sdsmt.edu). For more information regarding the university, visit http://www.sdsmt.edu. Interested candidates need to send a letter of application, curriculum vitae, teaching interests, research plans, graduate transcript(s), and contact information for three professional references to:

Dr. Jon Kellar, Chair of the Search Committee
College of Engineering
South Dakota School of Mines and Technology
501 East Saint Joseph Street
Rapid City, SD 57701-3995

Review of the applications will begin April 1, 2006, and will continue until the position is filled.

South Dakota School of Mines and Technology does not discriminate on the basis of race, color, national origin, military status, gender, religion, age, sexual orientation, political preference, or disability in employment or the provision of service.

Inspectors

Consolidated Engineering Labs, a top construction materials inspection firm with a long history of success in California and Utah is hiring qualified certified construction inspectors with AWS / UT / MT certifications. Work consists of shop and job site locations including schools, hospitals, bridges, large commercial and private structures. Union pay scales plus generous fringe benefits. 5 openings. US residents only. Relocation assistance may be available.

Apply to Bill Drouin
Consolidated Engineering Labs
2001 Crow Canyon Road, Suite 100
San Ramon, CA 94583
email: awd@ce-labs.com>awd@ce-labs.com
Phone: 925-314-7100
Fax: 925-855-7140

Welding Engineer

PK Mfg. is an Oilfield Fabrication company in the Houston, Texas area. We are looking for a degreed or certified Welding Engineer to develop, write and maintain our weld procedures as well as handle other weld issues. Candidate should be familiar with ASME, AWS, API, DNV, and PED code requirements. Please email resume to rkennedy@pkmfg.com or fax to (281)807-4774.

CAREER OPPORTUNITIES

Job Opportunity

American Tank & Vessel, a manufacturer of API storage tanks and ASME pressure vessels has an opening for an API Tank Building Instructor. Candidate must have a minimum of 15 years experience in API tank construction. AT&V will also consider retired experienced tank building candidates.

Candidate will be required to teach new and existing employees basic and advanced tank building methods in accordance with API codes. Candidate must have good communication and teaching skills. Training programs will require classroom and hands on instruction. AT&V offers Health insurance and 401(k).

To apply, submit your resume to
sbrown@atvluc.com or
Fax to 601-947-6453.

For additional information about AT&V
go to www.at-v.com.

BUSINESS FOR SALE

Business for Sale

DIVERSIFY - Small 23-year-old business for sale. Manufacture stored energy micro welding equipment. Pulse arc, spot, tack and fusion percussion welders used in the jewelry, crafts, medical, electronic, and automotive assembly industries. Owners retiring.

Confidential, please write:

Business 4 Sale
PO Box 893
E. Greenwich, RI 02818

EQUIPMENT FOR SALE OR RENT

Portable System Stops Distortion up to 90% Better

"A natural for welders"

www.Bonal.com

1-800-638-2529

EQUIPMENT FOR SALE OR RENT

WELD PLUS

JUST IN!! Pandjiris Mig Pipe Welding Station. Includes a Pandjiris 4' x 4' Manipulator on a Travel Car, 2 Pandjiris Headstocks with TJ-20 Chucks, Pandjiris Pipe Supports on Manual Travel Cars, Miller Mig Welding Package and a set of 50' tracks.

"WE KNOW WELDING"
TALK TO US!! ** COME VISIT US!!**

www.weldplus.com
E-mail: Melissa@weldplus.com
800-288-9414
Fax: 513-467-3585

ATTENTION!

Welding Equipment Sales Personnel. We pay you for finding us good used welding systems, seamers, positioners, manipulators, turning rolls, etc. We will buy your customers' trade-ins.

WELD PLUS, INC.
1-800-288-9414

robots4welding .com

Toll free: 1-800-762-6862

We Buy & Sell Surplus
Welding Rod & Wire
All types, sizes & Quantities

Liberty Alloys INC

Call us first!

800-523-2791
PA: 610-825-1250
FAX: 610-825-1553

RED-D-ARC®

Quality-Checked™ Used Equipment

www.red-d-arc.com

An Excellent Selection of Used Welding and Positioning Equipment for Sale

1-800-245-3660
Service Centers Across North America

VERSA-TIG™
MULTIPLE TIG TORCH SELECTORS
www.versa-tig.com

We buy and sell
WELDING RODS & WIRE
••ALL TYPES•• ALL SIZES••
ALL QUANTITIES

Excess Welding Alloys, Inc.
A division of Weld Wire Company Inc.

800-523-1266 FAX 610-265-7806
www.weldwire.net

Welding Positioners & Turning Rolls
New and Used

Large selection in stock for immediate delivery.

www.allfabcorp.com

Call, Fax or Email for a free catalog.

All-Fab Corp.

Email: sales@allfabcorp.com
Web: www.allfabcorp.com
Phone: 269-673-6572
Fax: 269-673-1644

Turning Rolls
Positioners
& Manipulators
New and Used

Joe Fuller LLC
@ www.joefuller.com
or email joe@joefuller.com

Phone: 979-277-8343
Fax: 281-290-6184

cash4usedrobots .com

We buy and sell
740-383-8383

CERTIFICATION & TRAINING

The AWS Certification Committee

Is seeking the donation of sets of Shop and Erection drawings of high-rise buildings greater than ten stories with Moment Connections including Ordinary Moment Resistant Frame (OMRF) and Special Moment Resistant Frame (SMRF) for use in AWS training and certification activities. Drawings should be in CAD format for reproduction purposes. Written permission for unrestricted reproduction, alteration, and reuse as training and testing material is requested from the owner and others holding intellectual rights.

For further information, contact:

Joseph P. Kane
631-265-3422 (office)
516-658-7571 (cell)
joseph.kane11@verizon.net

SERVICES

ADVERTISER INDEX

WELDING RESEARCH

SUPPLEMENT TO THE *WELDING JOURNAL,* MARCH 2006
Sponsored by the American Welding Society and the Welding Research Council

Design of Experiment Analysis and Weld Lobe Estimation for Aluminum Resistance Spot Welding

A systematic experimental study reveals how welding parameters and abnormal process conditions affect the quality of aluminum resistance spot welds

BY Y. CHO, W. LI, AND S. J. HU

ABSTRACT. The effects of various process conditions on weld quality were studied for aluminum resistance spot welding. Along with major welding process parameters including current, time, and electrode force, abnormal process conditions such as poor fitup, axial misalignment, and angular misalignment were also examined using a systematic design of experiment method. The combinations of two and three levels of these factors were tested in the experiment and the corresponding weld button diameters were evaluated with peel tests. As an experimental method to estimate the weld lobe and quality, the two-stage, sliding-level design of experiment was used to consider the linear and quadratic effects of the process parameters. Through the analysis, mathematical models were established, based on which the influences of the welding parameters on the weld lobes and weld size were discussed. The significance of the process abnormalities and the recommendations for better weld quality were also presented.

Introduction

As the demand for lightweight and highly fuel-efficient automobiles increases, joining of aluminum alloy has become an important issue in the automotive industry. Aluminum alloy offers high strength-to-weight ratio and excellent corrosion resistance. It is therefore considered a substantial weight-saving alternative to traditional mild steels for vehicle body structures. For several decades, the joining of mild steel body structures has been done using resistance spot welding (RSW). Unlike other methods such as mechanical fastening and riveting, the RSW process is fast, flexible, and easy to maintain. Moreover, it is a well-established process in the automotive industry. As a result, there is a strong preference to using RSW in joining aluminum sheet metal parts. However, a serious concern exists on the quality of aluminum spot welds due to the difference between the RSW of steel and aluminum (Ref. 1). Compared to steel, aluminum has higher electrical and thermal conductivities, a narrower range between the solidus and liquidus temperatures (about 30°C), and a lower melting temperature around 670°C (Ref. 2). Aluminum also forms nonconductive films on its surfaces when exposed to air. All these properties make the RSW process of aluminum harder to control. Consequently, detailed studies are needed on the quality variation of the aluminum RSW process to achieve consistency in high-volume production (Ref. 3).

Most of the previous research on aluminum RSW was concentrated on the effects of major process parameters such as electrode force, current, time, electrode type, and surface conditions (Refs. 4–7). Shear strength and weld button diameter were used as measures of the weld quality. Early work on RSW of high-strength aluminum alloys in the aerospace industry has shown that riveting performed better in terms of the fatigue strength (Ref. 8). Later, high-strength spot-welded aluminum structures have been demonstrated in the automotive industry (Ref. 9). Among various methods of analyzing the effects of welding parameters, the weldability lobe diagram is one of the most powerful techniques that can be used to illustrate the effects of welding current and time. Kaiser et al. (Ref. 10), and Han et al. (Ref. 11), employed the lobe diagram to investigate the acceptable welding current and time for high-strength steel. The weld lobe diagram was also used to examine the coating effects of various types of coated steels, e.g., hot-dipped galvanized steel, electrogalvanized steel, and galvannealed steel (Refs. 12–14). Weld lobe diagrams are usually developed in a lab environment with nominal process settings and then extended to production. In a production environment, however, there are many abnormal process conditions that may result in large weld quality variation. The effects of the abnormal process conditions have been discussed by a number of researchers. Nagel and Lee considered abnormal conditions in order to develop a new automatic process control approach (Ref. 15). Karagoulis studied the effect of electrode misalignment in a plant environment and reported that a shift of the weldability lobe curves was observed because of the electrode misalignment (Ref. 16). Li, et al. conducted a systematic study on the effects of both normal and abnor-

KEYWORDS

Aluminum Alloy
Resistance Spot Welding
Two-stage, Sliding-level
Design of Experiment
Regression Analysis
Weld Lobe
Quality Estimation
Weld Quality

Y. CHO and S. J. HU are with Department of Mechanical Engineering, The University of Michigan, Ann Arbor, Mich. W. LI is with Department of Mechanical Engineering, University of Washington, Seattle, Wash.

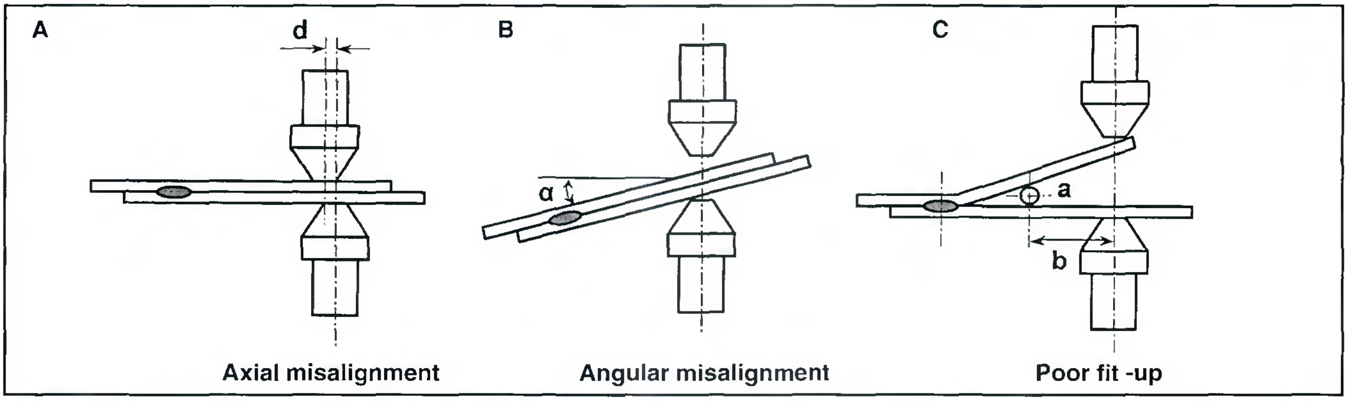

Fig. 1 — Abnormal process conditions in aluminum resistance spot welding.

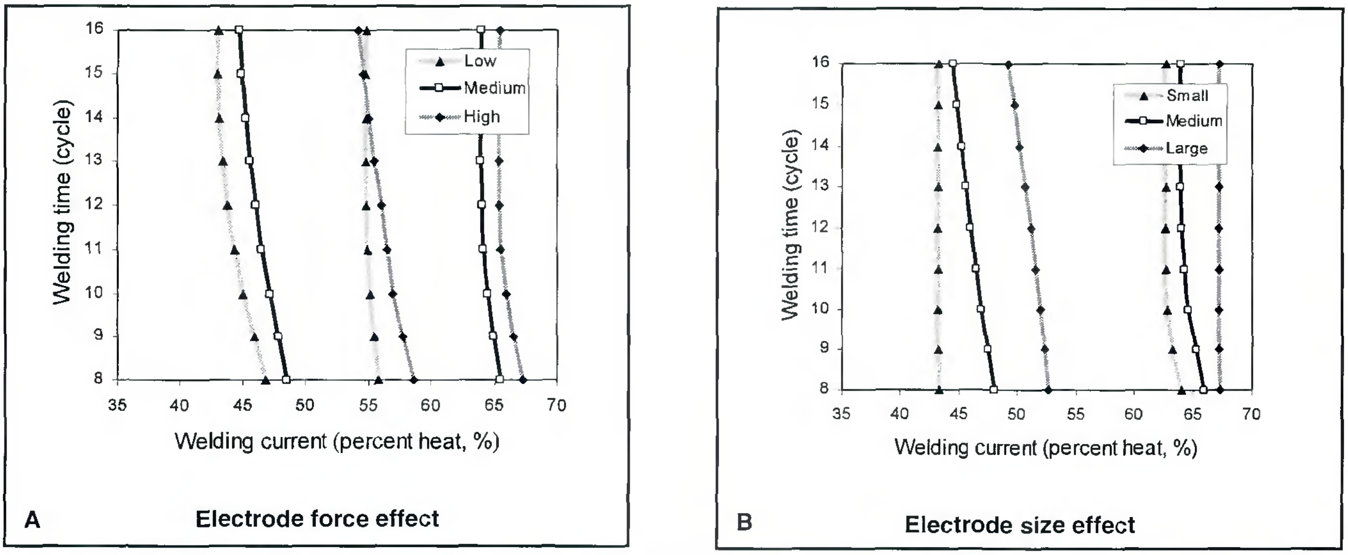

Fig. 2 — Effect of the major welding parameters on the weld lobes. A — Electrode force effect; B — electrode size effect.

Table 1 — Design Factors of the Experiment

Design Factors	Low	Medium	High
Current I (A)	Determined accordingly (sliding level)		
Time T (cycle)	8	12	16
Electrode force F (kN)	5.1	6.3	7.5
Electrode size S (mm)	25	50	75
Poor fitup Fit (mm)	0	—	5
Axial misalignment Ax (mm)	0	—	1.5
Angular misalignment Ang (°)	0	—	10

mal welding conditions (Ref. 17). Mathematical models were developed for process analysis and improvement. All the above research, however, was focused on the RSW of mild steels. A systematic study on the effects of various process conditions for the aluminum RSW process has not been reported.

In this study, the effects of various welding conditions on the quality of aluminum welds were investigated using the design of experiment and statistical modeling approach. Both process parameters and abnormalities, such as electrode misalignment and poor fitup, were examined. Because of the complexity of the combinations and the interdependency among the process parameters, a newly developed two-stage, sliding-level experiment (Ref. 17) was used for the experimental design and analysis. Mathematical models were developed for estimating the weld size and weldability lobe curves, both of which were used as response variables to analyze the effects of the process conditions. The proprieties of the models and recommendations for better weld quality were also presented.

Experimental Procedure

The experiments were performed using 2.0-mm commercial aluminum Alloy AA5754 on a mid-frequency DC welding machine. The electrodes were dome-type with a spherical surface. Welding parameters, such as welding current, time, and electrode force, were examined with a number of abnormal process conditions. The abnormal conditions considered in this study were recommended by a group of experienced welding engineers. These conditions included axial misalignment, angular misalignment, and poor fitup, as shown in Fig. 1. Axial misalignment Ax in Fig. 1A indicates that the axes of the upper and lower electrodes deviate

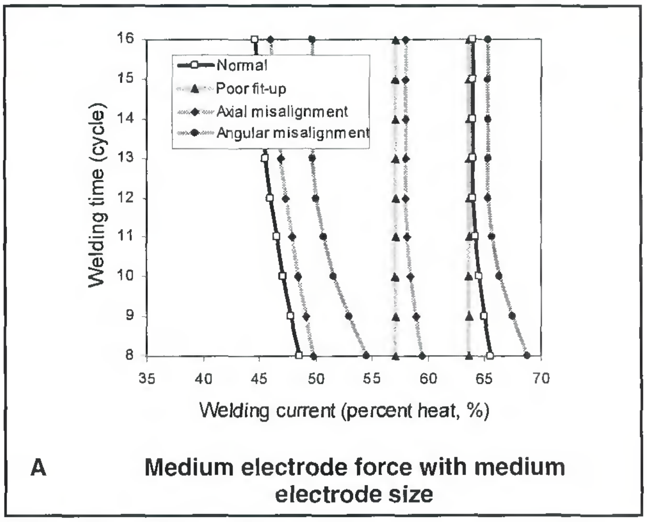

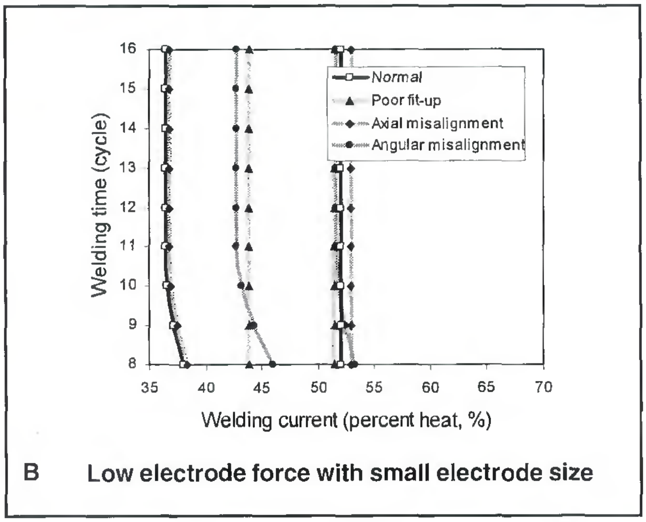

from each other by a distance *d*. Figure 1B shows the angular misalignment condition *Ang* in which the parts are tilted relative to the axis of the electrode by an angle of α. When the two sheet metal parts separate, a poor fitup condition *Fit* exists. This condition was created by inserting a piece of wire with a diameter of *a* at a distance *b* from the centerline of the electrodes, as shown in Fig. 1C. A specially designed fixture was used to produce the above abnormal conditions.

In the design of experiment, the factors considered were the abnormal process conditions and the major welding parameters, including welding current *I*, time *T*, and electrode force *F*. In case of electrode wear, electrode size *S* (spherical radius) was used since it was assumed that the electrode wear affected the process through the change of the electrode face diameter. The settings of these factors in the experiment were determined based on previous process knowledge. Two levels were used for the abnormal process conditions and three levels for the major welding parameters and electrode size. The settings of the factors in the experiment are listed in Table 1.

In order to study the effects of the abnormal process conditions with various welding parameters, the two-stage, sliding-level method was employed in the design and analysis of the experiment. This method was necessary because of the interdependency among the variables in the resistance spot welding process. Specifically, there is an acceptable range for the welding current as shown in a typical weld lobe diagram. As such, the experiment had to be conducted in two stages. The first stage was used to determine the suitable current range under each designed experimental condition; and the second stage was used to perform test welds on the settings determined at the first stage.

The experiment matrix is shown in Table 2. The first three columns are for the three-level factors. The levels are low, medium, and high, represented by 1, 2, and 3, respectively. The last three columns are for the two-level factors whose levels are described as –1 and 1, with –1 indicating the low level and +1 indicating the high level. For each of these settings, a current range was determined based on a standard weld lobe development procedure (Ref. 18). After the current ranges were found, the experiment was carried out based on the results from the first stage to evaluate the weld quality. The welded samples were peeled and the diameters of the weld buttons measured following a standard weld quality evaluation procedure (Ref. 19).

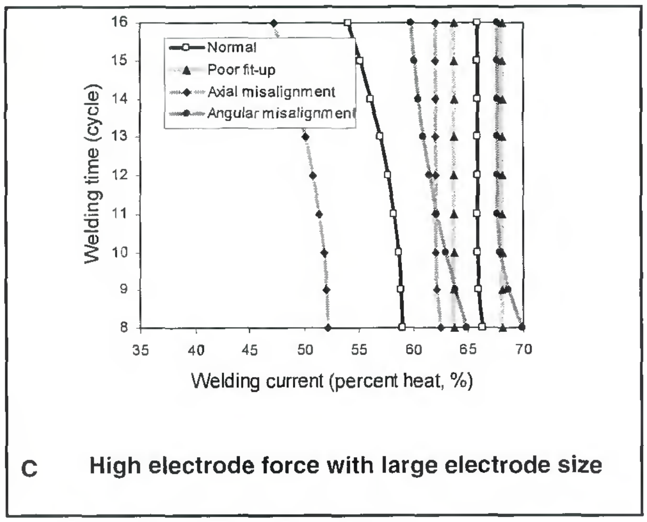

Fig. 3 — Examples of effects of the abnormal conditions on the weld lobes. A — Medium electrode force with medium electrode size; B — low electrode force with small electrode size; C — high electrode force with large electrode size.

Response Modeling

A statistical regression analysis was performed to analyze the quality of aluminum resistance spot welds in terms of the weld lobe and weld diameter. The relationships among the acceptable current range, weld diameter, and the welding parameters were characterized using mathematical models. The response variables of the models were different at different stages of the experiment. At the first stage, the current range was selected as the response variable. In order to facilitate the analysis, the current range of the weld lobe was converted into two independent response variables, the center of the current range I_C and the length of the current range I_L. At the second stage, the response variable was the weld button size.

In this study, two groups of factors were used to construct the response models through a regression analysis. One group was the two-level factors such as poor fitup, axial misalignment, and angular misalignment. The other group was the three-level factors consisting of electrode force, welding time, and electrode size. In the regression analysis, the first group of variables contributed to the first-order regressors. The second group contributed to both the first- and second-order regressors. In addition, the interactions among the independent regressors were also included in the response models. In order to avoid inaccurate estimation due to co-linearity among the above terms, an orthogonal coding system was introduced. For the three-level variables, the physical values were normalized to [–1 0 –1] for the first-order linear effect x_l and to [1 –2 1] for the second-order qua-

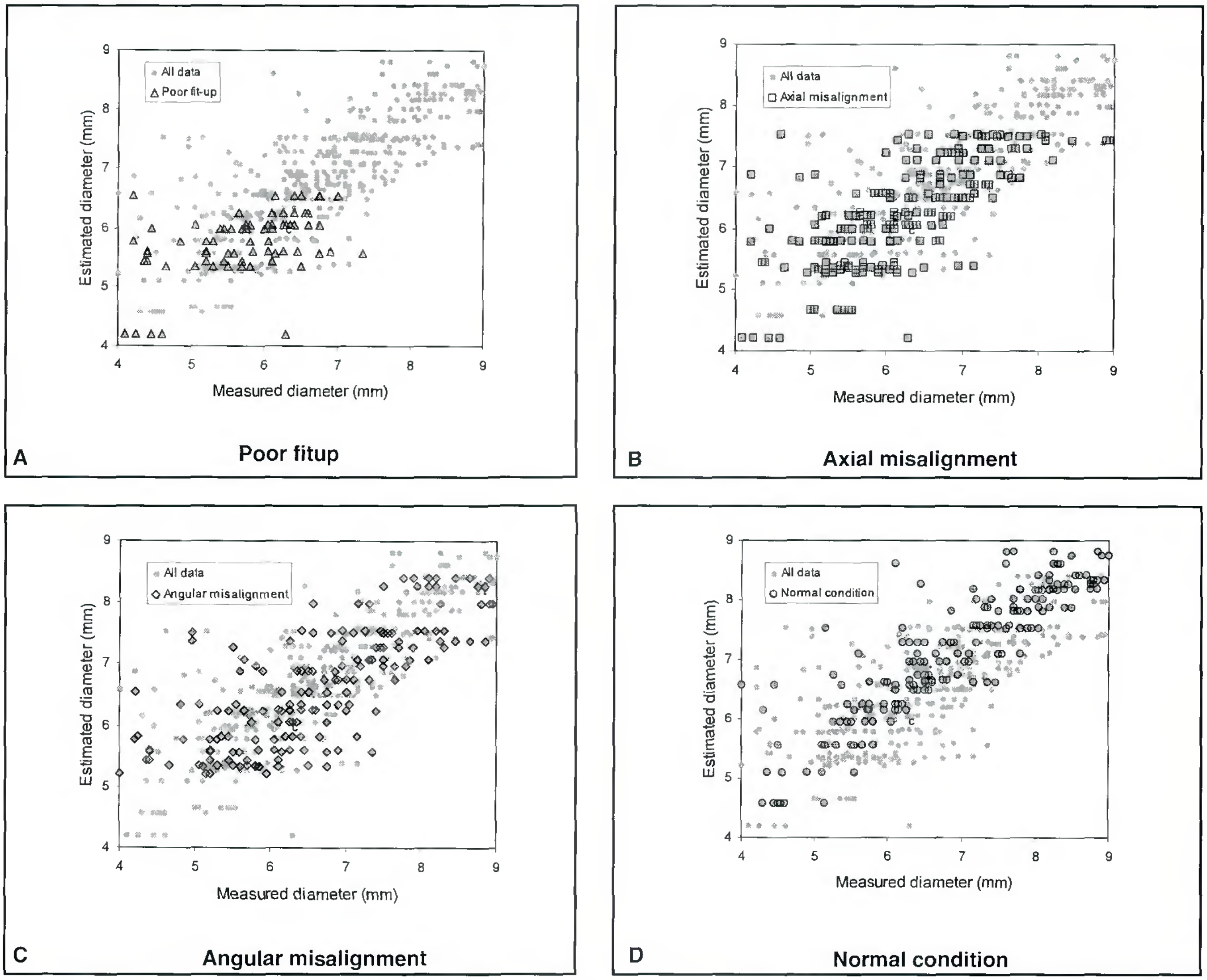

Fig. 4 — Relationship between measured and estimated weld diameter. A — Poor fitup; B — axial misalignment; C — angular misalignment; D — normal condition.

dratic effect x_2. The normalizations are defined in the following equations.

$$x_1 \begin{Bmatrix} \dfrac{x-x_l}{x_m-x_l}-1, & x_l \le x \le x_m \\ \dfrac{x-x_m}{x_n-x_m}, & x_m \le x \le x_n \end{Bmatrix} = \begin{cases} -1, & x=x_l \\ 0, & x=x_m \\ 1, & x=x_n \end{cases} \quad (1)$$

$$x_2 = \vec{x}\cdot\left(\vec{X}^T\cdot\vec{X}\right)^{-1}\cdot\vec{X}^T\cdot\vec{Y} = \begin{cases} 1, & x=x_\ell \\ -2, & x=x_m \\ 1, & x=x_n \end{cases} \quad (2)$$

where x_l, x_m, and x_n are the settings for low, medium, and high values of the factors, respectively. Due to the difference of response variables in the two stages of the experiment, current range and weld size were analyzed separately during the regression analysis.

Current Range Analysis

Before performing the regression analysis, the correlation coefficients between the dependent variables including the center and the length of the current range and the independent variables including the linear and quadratic effects of electrode size, force, and welding time and the linear effects of poor fitup, axial misalignment, and angular misalignment were calculated and listed in Table 3. Subscript 1 stands for the linear effect. Subscript 2 stands for the quadratic effect. From the table, it can be seen that electrode force, followed by electrode size, is the most dominant factor affecting the center of the current range. The abnormal conditions themselves do not play an important role on the center of the current range. However, they have strong influences on the length of the current range, e.g., the poor fitup condition *Fit* has a correlation coefficient of –0.840 with I_L. In general, the second-order quadratic effects have lower correlation than the first-order linear effects. Nonetheless, they significantly affect the center and length of the current range when their interactions with other factors are considered. This can be seen in Equations 3 and 4, where the interaction terms such as T_2*Fit* and F_2*Ax* are included in the response models.

Usually, the larger the correlation coefficient is, the larger the effect a variable will have. However, because the correlation coefficient depends only on the linear relationship between the response and the variable, a more advanced regressor selection procedure is required. To develop more reliable models, a stepwise regression method (Refs. 20, 21) was applied in this study. The regressors were selected from the independent variables including the linear, quadratic effects of the variables and the interactions among them. The independent variables were entered into the regression model one by one depending on their probabilistic significance to the response variable. The obtained models are as follows:

$$I_C = 57.39 + 4.17*F_1 - 3*T_1*S_1 + 2.5*S_1 - 2*Fit*Ang - 1.167*Ax - 1.5*F_1*Ax - 0.92*T_1*S_1 - 0.67*T_2*Fit + 0.5*S_2 + 0.33*T_2*Ang + 0.583*T_1*S_2 - 0.25*T_2*S_1 + 0.03*T_2*S_2 \quad (3)$$

$$I_L = 8.139 - 4.417*Fit + 2.0*Ax*Ang + 1.833*F2*Ax - 1.000*T1*Fit - 0.833*Ang + 1.167*F1*T2 + 0.667*S_1*Ang + 1.667*T_1*S_1 + 0.139*T_2 - 0.500*\mathrm{Fit}*\mathrm{Ax} - 0.667*\mathrm{S}_1 - 0.250*T_2*\mathrm{Fit} - 0.111*\mathrm{S}_2 - 0.167*T_1*Ang \quad (4)$$

The standardized regression coefficients are listed in Tables 4 and 5. These coefficients can be used to interpret the significance of individual regressors. As can be seen from these tables, the linear effects of electrode force F_1 and electrode size S_1 have the most significant influence on the center of the current range I_C. The interaction between welding time and electrode size T_1*S_1 and that between poor fitup and angular misalignment $Fit*Ang$ also play an important role. In case of the length of the current range I_L, poor fitup Fit shows the strongest influence, followed by the interactions between the quadratic effect of electrode force and axial misalignment F_2*Ax and that between axial misalignment and angular misalignment $Ax*Ang$.

Table 2 — Experiment Matrix

	Electrode Force (F)	Time (T)	Electrode Size (S)	Poor fitup (Fit)	Axial Misalignment (Ax)	Angular Misalignment (Ang)
1	1	1	1	-1	-1	-1
2	1	1	2	-1	1	-1
3	1	1	3	-1	-1	1
4	1	2	3	1	-1	1
5	1	3	1	1	1	1
6	1	3	3	1	1	-1
7	2	1	1	1	1	-1
8	2	1	2	1	1	1
9	2	2	1	-1	-1	1
10	2	2	2	-1	-1	-1
11	2	2	3	-1	1	-1
12	2	3	1	1	-1	1
13	3	1	2	1	-1	1
14	3	2	2	1	1	-1
15	3	2	3	1	1	1
16	3	3	1	-1	1	-1
17	3	3	2	-1	-1	1
18	3	3	3	-1	-1	-1

Table 3 — Correlation Coefficients of Welding Current and Independent Variables

	F_1	F_2	T_1	T_2	S_1	S_2	Fit	Ax	Ang
I_C	0.594	0.234	0.297	-0.093	0.513	-0.187	-0.022	-0.176	0.132
I_L	0.164	0.013	0.140	-0.027	-0.164	-0.067	-0.840	-0.305	-0.458

Weld Button Size Analysis

A similar procedure was also performed to develop an estimation model for the weld button size. In addition to the factors for the current range analysis, two new variables, the linear and quadratic effects (I_1 and I_2) of the given welding current, and their interactions with other variables were added to the button size analysis. Equation 5 shows the result of the analysis. The coefficient of determination R^2 is 0.944 and the standard error of the estimation is 0.3014. Therefore, more than 94.4% of the button size variance can be explained by the model.

$$\mathrm{Dia} = 6.214 - 0.477*Fit + 0.665*I_1 + 0.554*F_1 - 0.42*Fit*I_1 - 0.317*S_1*Fit - 0.241*Ax - 0.439*\mathrm{S}_1*Ax - 0.185*T_2 + 0.276*\mathrm{F}_1*Ang - 0.082*I_2 + 0.071*Fit*\mathrm{I}_2 + 0.0963*Ax*Ang \quad (5)$$

Standardized regression coefficients in Table 6 show that poor fitup Fit, the linear effect of welding current I_1, the linear effect of electrode force F_1, the interaction effect between poor fitup and welding current $Fit*I_1$, and the interaction effect between electrode size and axial misalignment S_1*Ax are the dominant factors in the button size estimation model.

Results and Discussion

Using the response models described in Equations 3–5, the effects of various welding parameters can be discussed based on the predictions of the weld lobes and the weld button diameters. Figure 2 shows the effects of electrode force and size on the weld lobe under normal and medium electrode size or force conditions. In Fig. 2A, the black lines with rectangular marks show the lobe curves when the medium electrode force level (6.3 kN) is used. It is seen that acceptable welds can be made in a range between 48% and 65% of heat when the welding time is 8 cycles. Percentage heat is a measure of the welding current. In this case, 50% heat is corresponding to 21.2 kA. When the electrode force becomes lower or higher, the current ranges both become narrower. In case of the low electrode force of 5.1 kN (shown in light-gray lines with triangles), the upper boundary of the lobe shifts to the left, indicating early expulsions caused by insufficient electrode force. The lower boundary also shifts slightly to the left, showing an early nugget formation due to the high initial contact resistance caused by the low electrode force. When the high electrode force of 7.5 kN is used, a different type of change of the lobe curves is observed as shown in the dark-gray lines with diamonds in the figure. The lower boundary is moved to the right, which indicates that excessive electrode force can cause the initial contact resistance to decrease due to the early collapse of asperities on the contact surfaces. The decreased contact resistance requires a higher welding current to produce enough heat in order to form a nugget. However, it is interesting to see that the upper boundary of the lobe does not shift to the right as much. This implies that using a higher electrode force does not help increase the expulsion limit.

The effects of electrode size are shown in Fig. 2B. The lobe curve shifts are also

Table 4 — Standardized Regression Coefficients for I_C

F_1	T_1*S_1	S_1	Fit*Ang	Ax	F_1*Ax	T_1*S_1	T_2*Fit	S_2	T_2*Ang	T_1*S_2	T_2*S_1	T_2*S_2
0.674	-0.396	0.405	-0.374	-0.231	-0.243	-0.121	-0.187	0.140	0.093	0.128	-0.055	0.011

Table 5 — Standardized Regression Coefficients for I_L

Fit	Ax*Ang	F_2*Ax	T_1*Fit	Ang	F_1*T_2	S_1*Ang	T_1*S_1	T_2	Fit*Ax	S_1	T_2*Fit	S_2	T_1*Ang
-0.759	0.324	0.445	-0.140	-0.143	0.214	0.094	0.191	0.034	-0.081	-0.094	-0.061	-0.027	-0.023

Table 6 — Standardized Regression Coefficients for Weld Button Diameter

Fit	I_1	F_1	$Fit*I_1$	S_1*Ax	Ax	S_1*Fit	T_2	F_1*Ang	I_2	$Fit*I_2$	Ax*Ang
-0.430	0.489	0.407	-0.306	-0.323	-0.217	-0.234	-0.235	0.203	-0.104	0.090	0.082

Table 7 — Estimation Results in Terms of Correlation Coefficients and Standard Errors

	Poor fitup		Axial misalignment		Angular misalignment		Normal condition	
	R	Er	R	Er	R	Er	R	Er
All data	0.552	0.499	0.731	0.581	0.774	0.605	0.870	0.555

observed when the electrode size varies. When smaller electrodes are used, the weld lobe shifts to the left (light-gray lines with triangles), showing that less current is needed to produce an acceptable weld. This is because the current density through the faying surface increases as the electrode size decreases. On the other hand, as larger electrodes are used (dark-gray lines with diamonds), more current is required to produce an acceptable weld. In this case, the upper boundary does not shift as much as the lower one. This means that an excessive electrode size can cause unwanted decrease in the length of the current range. Although the small electrode size yields a slightly wider weld lobe, the current density will be much higher when using smaller electrodes to make the same sized welds. Using small electrodes could accelerate the electrode wear, which should always be avoided in production.

Figure 3 shows the effects of the three abnormal process conditions on the weld lobes. The effects of the abnormal conditions at the medium electrode force and size are shown in Fig. 3A. As can be seen, the widest acceptable current range is obtained under the normal condition (black lines with rectangles). In the case of poor fitup condition (light-gray lines with triangles), the lower boundary of the weld lobe shifts to the right dramatically, while the upper boundary remains more or less the same as the normal condition. This has resulted in a much narrower current range and thus a less robust welding process. When axial misalignment exists (mid-gray lines with diamonds), expulsions occur with less heat input. However, there is no significant difference in the minimum heat to obtain an acceptable weld. Angular misalignment causes a slight shift of the lower boundary toward the right (dark-gray lines with circles), indicating an increase in the minimum current requirement. However, the upper boundary also increases slightly. Figure 3B shows the effects of abnormal conditions at low electrode force and small electrode size. In general, the acceptable current ranges tend to move toward the low current side comparing to the case for medium electrode force and size. Especially, the upper boundaries are around 50–55% of heat, suggesting that the current required to produce an acceptable weld is much smaller. Poor fitup and angular misalignment makes the current ranges narrower. There is almost no effect by the axial misalignment. The case for high electrode force and large electrode size is shown in Fig. 3C. Overall, the lobe curves move toward the high current side and the acceptable current ranges become narrower, too. Compared to the other abnormal conditions, the axial misalignment requires less current to form an acceptable weld. This is because axial misalignment reduces the effective contact area for current flow at the faying surface, which in turn results in increased current density and earlier nugget formation.

The effects of the abnormal conditions on the weld diameter are shown in Fig. 4. The estimated weld diameters are plotted against the measured ones for all the abnormal and normal process conditions. In these plots, each experimental data point including its replicates is represented with a gray dot. The data points corresponding to individual abnormal and normal conditions are indicated using special marks, triangles for poor fitup in Fig. 4A, squares for axial misalignment in Fig. 4B, diamonds for angular misalignment in Fig. 4C, and circles for the normal condition in Fig. 4D. By representing the experimental data this way, the effects of abnormal conditions can be visualized clearly with respect to the overall data set.

Figure 4A shows the effect of the poor fitup condition. Comparing to the measured weld diameters across all the conditions, poor fitup gives rise to smaller weld nuggets. This may mean that the poor fitup condition has the strongest detrimental effect on the weld size. The correlation between the estimated and measured weld diameters does not follow a good linear trend, which indicates that the statistical model does not predict the weld diameter well under the poor fitup condition. Figure 4B shows the effect of axial misalignment. It is seen that large weld diameters up to 8–9 mm can still be made under this abnormal process condition. The correlation between the measured and estimated weld diameters is reasonably strong. Similarly, large welds can also be made under the angular misalignment condition and the statistical model predicts the weld diameter fairly well, as shown in Fig. 4C. Figure 4D shows the weld diameters under the normal condition. The correlation between the measured and estimated seems to be the best among all the process conditions. This result is expected since the variation caused by the abnormal conditions is excluded.

The correlations between the estimated and measured weld diameters and the estimated errors for each of the process conditions are presented in Table 7. The correlation coefficient is represented as R and standard error of the estimation as Er. The correlation coefficients agree with the observations from Fig. 4, with the lowest for the poor fitup condition (0.552) and the highest for the normal condition (0.870). The standard errors are comparable among all the cases, which is about 0.5–0.6 mm.

Conclusions

The effects of various welding parameters in aluminum resistance spot welding were investigated using a systematic two-stage, sliding-level design of experiment approach. The following conclusions are obtained from this study:

1) From the statistical models, it is shown that the linear effects of electrode force and size have the most significant influence on the center of the current range. The poor fitup condition and the interaction between the quadratic effect of electrode force and axial misalignment have significant effects on the length of the current range.

2) When a medium electrode force is applied, the acceptable current range is the widest. Both lower and higher electrode force will reduce the length of the current range, which means a less robust welding process.

3) Among the abnormal process conditions, the poor fitup condition has the strongest detrimental effect on the quality of aluminum resistance spot welding. It causes small weld diameters and thus weak joints. In addition, the effect of poor fitup is hard to characterize using a statistical model.

4) In general, abnormal process conditions cause narrower weld lobes. In order to minimize the effects of these abnormalities, more heat input is recommended within the limits of acceptable current ranges to avoid expulsion.

Acknowledgments

This work was supported by NIST/ATP Intelligent Resistance Welding through Auto Body Consortium. Support for Cho's postdoctoral fellowship program from the Korea Science and Engineering Foundation (KOSEF) is also gratefully acknowledged.

References

1. Senkara, J., and Zhang, H. 2000. Cracking in spot welding aluminum alloy AA5754. *Welding Journal* 79(7): 194-s to 201-s.

2. Urech, W., and Gordon, H. F. 1986. Aluminum projection welding in industrial-scale production. *AWS Sheet Metal Conference II*, Paper No. 17.

3. Newton, C. J., Browne, D. J., Thornton, M. C., Boober, D. R., and Keay, B. F. P. 1994. The fundamentals of resistance spot welding aluminum, *Sheet Metal Conference VI*, Paper E2.

4. Hoglund, G. O., and Bernard, G. S., Jr. 1938. The effect of current, pressure and time on the shear strength and structure of spot welds in the aluminum alloys. *Welding Journal* 17(11): 45-s to 54-s.

5. Keller, F., and Smith, D. W. 1944. Correlation of the strength and structure of spot welds in aluminum alloys. *Welding Journal* 23(1): 23-s to 26-s.

6. Roset, C. A., and Rager, D. D. 1974. Resistance welding parameter profile for spot welding aluminum. *Welding Journal* 53(12): 529-s to 536-s.

7. Rönnhult, T., Rilby, U., and Olefjrd, I. 1980. The surface state and weldability of aluminum alloys. *Mat. Sci. Eng.* 42: 329 – 336.

8. Welter, O., and Croquet, A. 1954. Stress distribution and fatigue resistance of ALCLAD 24ST multiple spot welds. *Welding Journal* 33(2): 91-s to 98-s.

9. Thornton, P. H., Krause, A. R., and Davies, R. G. 1996. The aluminum spot weld. *Welding Journal* 75(3): 101-s to 108-s.

10. Kaiser, J. G., Dunn, G. J., and Eagar, T. W. 1982. The effect of electrical resistance on nugget formation during spot welding. *Welding Journal* 61(6):167-s to174-s.

11. Han, A., Indacochea, J. E., Chen, C. H., and Bhat, S. 1993. Weld nugget development and integrity in resistance spot welding of high-strength cold-rolled sheet steels. *Welding Journal* 72(5): 209-s to 265-s.

12. Gould, J. E., and Peterson, W. A. 1989. A detailed examination of weldability lobes for a range of zinc-coated steels, *SAE Technical Paper No. 880279.*

13. Howe, P., and Kelley, S. C. 1989. A comparison of the resistance spot weldability of bare, hot-dipped, galvannealed, and electrogalvanized DQSK sheet steels, *SAE Technical Paper No. 880280.*

14. Bowers, R. J., Sorensen, C. D., and Eagar, T. W. 1990. Electrode geometry in resistance spot welding. *Welding Journal* 69(2): 45-s to 51-s.

15. Nagel, G. L., and Lee, A. 1988. A new approach to spot welding feedback control. *SAE Technical Paper No. 880371.*

16. Karagoulis, M. 1992. Control of materials processing variables in production resistance spot welding. *Proc. AWS Sheet Metal Welding Conference V*, Detroit, Mich., Paper No. B5.

17. Li, W., Cheng, S., Hu, S., and Shriver, J. 2001. Statistical investigation of resistance spot welding quality using a two-state, sliding-level experiment. *ASME Journal of Manufacturing Science and Engineering*, 123: 523–520.

18. General Motors Corp. 1985. *Specifications and Procedures for Determining the Weldability of Body Steel Materials.*

19. Auto/Steel Partnership (A/SP). 1995. *Weld Quality Test Method Manual*, Standardized Test Method Task Force.

20. Montgomery, D. C. 2001. *Design and Analysis of Experiments*, 5th edition, John Wiley.

21. Hamada, M., and Wu, C. F. J. 1992. Analysis of designed experiments with complex aliasing. *Journal of Quality Technology* 24(3): 130–137.

Arc Behavior and Melting Rate in the VP-GMAW Process

Droplet melting analysis performed using high-speed video synchronized with high-speed data acquisition was used to evaluate arc behavior and melting rate

D. D. HARWIG, J. E. DIERKSHEIDE, D. YAPP, and S. BLACKMAN

ABSTRACT. This paper evaluates the arc behavior and melting rate in the variable polarity (VP) gas metal arc welding (GMAW) process. Droplet melting analysis was performed using high-speed video that was synchronized with high-speed data acquisition. Melting rate measurements were found to be very dependent on current waveform, polarity, droplet size, and metal transfer, if it occurred, for each waveform period. The transient conditions of current waveform and metal transfer produced rapid changes in arc behavior that influenced the melting at the electrode tip and growing droplet. The concentrated melting theory was developed to explain the significant increase in electrode extension burnoff and droplet growth rate that occurred at short electrode negative (EN) time as a function of current, and during electrode positive (EP) peak pulse when the prepulse droplet volume was small. The highest electrode extension burnoff and droplet growth rate occurred when the arc was permitted to climb over the solid electrode tip producing rapid concentrated melting. Likewise, large molten droplets were found to promote a negative electrode extension burnoff and a decreased droplet growth rate. The arc rooted on large droplets providing additional heating but limited electrode melting. The droplet burnoff rate (DBR) method was developed and found to yield good experimental measurements for the arc melting and resistive heating coefficients used in a second-order melting rate equation developed for a complex waveform process, like VP-GMAW. For the EN period, the EN time affected the melting rate as a function of EN current. The greater melting rate that occurred at low EN time was measured by the changes in the resistive heating coefficient. Concentrated arc melting of the electrode extension at low EN time caused the slope of the burnoff diagram to increase, which represented the resistive heating coefficient. The melting rate of the EP pulse was related to the prepulse droplet volume. Large prepulse droplets decreased the arc melting coefficient, which could be negative, which meant the electrode extension was increasing and the arc length was decreasing in that waveform period.

D. D. HARWIG is with Thermadyne Industries, West Lebanon, N.H. J. E. DIERKSHEIDE is with Northrop Grumman Newport News, Newport News, Va. D. YAPP and S. BLACKMAN are with Cranfield University, Bedfordshire, UK.

KEYWORDS

Metal Transfer
Droplet
Drops
Arc Behavior
Melting Rate
GMAW
Variable Polarity

Introduction

Gas metal arc welding (GMAW) technology has advanced considerably over the past two decades due to the development of microprocessor-controlled, solid-state power supplies. Currently, power supplies are designed for constant voltage (CV) GMAW, pulse GMAW (GMAW-P), and pulse short circuit GMAW (Refs. 1–4), and more recently variable polarity (VP) GMAW (Refs. 5–11). However, there was a lack of understanding of VP-GMAW principles. The limited research was mostly from Japan, where the process was introduced in 1988 (Refs. 5–7). Since the early 1990s, several hundred power supplies have been sold in the United States. Unfortunately, many industrial users do not understand the benefits of this technology since limited research has been published in the United States (Refs. 3, 4, 10, 11). This has deterred wide-scale implementation of VP-GMAW throughout industry. The power supplies offered by the Japanese manufacturers have preprogrammed algorithms and are presently limited to welding of mild steel, stainless steel, and aluminum at currents up to 350 A where the benefit has been the welding of thin-gauge structures with large root openings (Refs. 10–12).

The metal transfer process for VP-GMAW begins with droplet formation in the EN period where large droplets form on the end of the electrode — Fig. 1. The waveform switches to the electrode positive background (EPB) period to maintain the arc at low current. The electrode positive peak (EPP) period is used to transfer the droplets by using a high-current pulse that squeezes the droplet off the electrode tip forming a drop. The drops transfer across the arc into the weld pool. The VP-GMAW waveform can be designed to provide a range of heat inputs for a given wire feed speed, thus allowing optimization of the travel speed for different weld deposit size applications.

There are many factors that affect the droplet formation and transfer process that are not understood. The behavior of VP-GMAW arcs and metal transfer had not been published in the literature (Ref. 12). Based on this, there appeared to be a technology gap on the principles controlling melting rate, metal transfer, and arc behavior of the VP-GMAW process. The general melting rate equation for DC GMAW was developed by Lesnewich (Ref. 13). Based on his research, a well-accepted form of the melting rate equation has been established for a given electrode type and diameter for spray metal transfer modes as follows:

$$MR_{dc} = \alpha I + \beta L I^2 \qquad (1)$$

where MR_{dc} = (mm/s), α = arc melting coefficient (mm/s-amp), I = current (amps), β = resistive heating coefficient (amps^2-s)$^{-1}$, and L = electrode extension (mm).

The first term of this equation (αI) represents the contribution from arc melting, and the second term of the equation ($\beta L I^2$) represents the contribution from electrode extension resistance heating. The arc melting term is dependent on the polarity, and electrode type and size. For EN heating, the arc melting term is also a

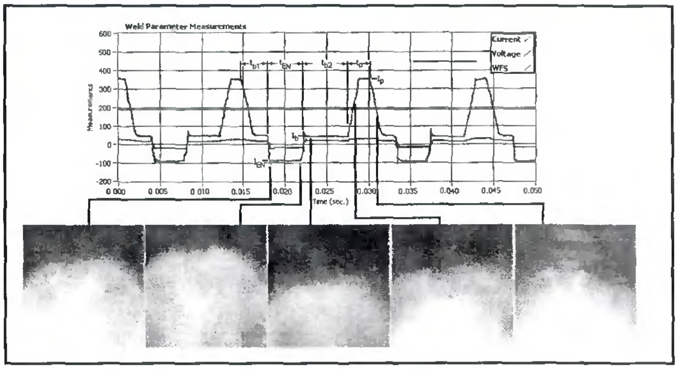

Fig. 1 — VP-GMAW waveform and droplet growth transfer process.

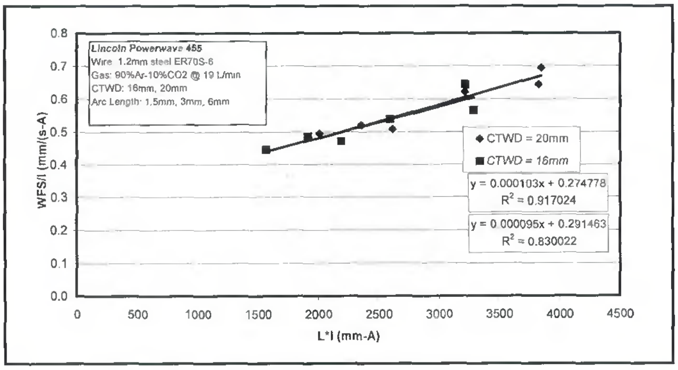

Fig. 2 — Burnoff diagram for spray metal transfer using a EP CV power supply for 1.2-mm steel electrode at various arc lengths and 16- and 19-mm CTWD. Note: equations are ordered in the same vertical order as the legend symbols.

function of shielding gas and electrode activation. The resistive heating term is based on I^2R heating that occurs in the electrode extension.

Allum (Ref. 14) and Richardson (Ref. 15) both attempted to use this fundamental melting rate equation to explain the behavior of GMAW-P. Their research assumed the current waveform was totally responsible for changes in melting rate. Under this assumption, α and β coefficients were believed to be constant for each electrode polarity, type, and size. The improved melting rate was solely attributed to increases in I^2R heating in the electrode extension due to the high current pulse. The research performed here showed the transient behavior of the arc at the electrode tip has a significant effect on melting rate for identical peak pulse waveforms. The resistive heating (I^2R) effect was secondary in importance compared to the arc melting effect using pulsed waveforms.

Richardson showed that the burnoff diagram (BD) technique can be used to determine empirically the α and β coefficients for GMAW processes, especially CV processes that have uniform metal transfer. The burnoff diagram (Fig. 2) plots the burnoff rate (MR/I) against the electrode extension heating factor, $F_L = (L * I)$ providing a line for a given electrode polarity, type, and size over a range of wire feed speeds (WFS), electrode extensions, and arc lengths. When the BD was applied to GMAW-P waveforms, both Allum and Richardson used an effective current parameter to make the data fit the burnoff diagram. This approach made quantitative prediction of melting rate using different waveforms very difficult and accuracy was marginal. In this investigation, it was decided to use the BD to study electrode melting rate based on the droplet growth and electrode extension position in each period of VP-GMAW waveforms. This approach gave a good data fit and allowed characterization of arc and melting rate behavior in complex waveforms.

To establish working pulse parameters, researchers (Refs. 14, 16–18) established a detachment parameter that described the GMAW-P pulse energy requirements for metal transfer. The detachment parameter was believed to satisfy the relationship for improved resistive heating for pulse waveforms. The detachment parameter was based on the energy required to achieve one drop per pulse conditions. However, industry has been plagued with cases that show that a simple relationship like this and others (Ref. 19) cannot be used to predict melting rate and metal transfer stability. In fact, most modern power supplies have empirically developed pulse parameters that are not based on a well-defined algorithm (Ref. 20). To remedy the technology gap, most power supply manufacturers provide waveform parameter development tools that allow the user to optimize metal transfer stability for a given melting rate. The user lacking fundamental knowledge usually develops pulse parameters through trial and error. This investigation showed that the EN period and/or EP background period controlled the EP prepulse droplet volume. The melting rate of identical EP pulses was dependent on the prepulse droplet size. Based on these observations, the detachment parameter can only be used under a small range of pulse waveforms that have a similar prepulse droplet size. Wide changes in pulse parameters that affect droplet size will surely lead to errors using the detachment parameter approach.

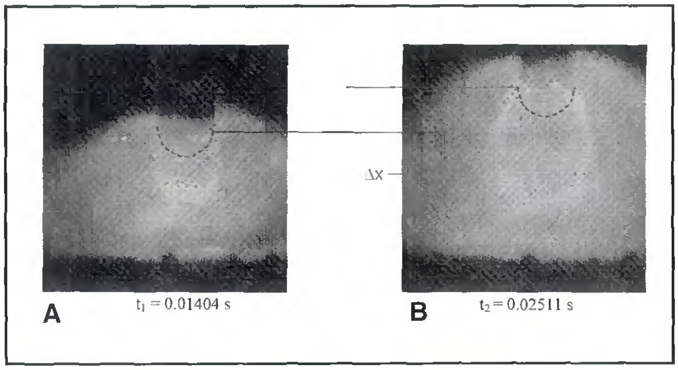

Fig. 3 — Electrode extension burnoff during droplet growth in EN period.

For VP-GMAW, the research reviewed (Refs. 4–11, 21–33) has focused on the development of power supplies that permit waveform control, working VP pulse parameters, and commercialization of equipment. The arc behavior and its interactive effects on melting rate were not understood for VP-GMAW waveforms. Engineering relationships were needed to provide an analytical approach for designing waveforms and predicting the resulting melting rate. This technology will promote deployment of VP-GMAW in applications, like welding sheet steel and cladding vessels that can benefit from the lower heat input and higher melting rates of this process.

Experimental Procedure

The objectives of this investigation were as follows:

1) Develop an electrode melting rate measurement method that can accurately solve for the α and β coefficients of advanced waveform processes, like VP-GMAW and GMAW-P.

2) Determine the effects of VP-GMAW waveform on electrode melting, and the droplet growth and detachment process.

3) Measure the change in α and β coefficients for a full range of VP-GMAW waveforms and determine the underlying mechanisms for differences due to polar-

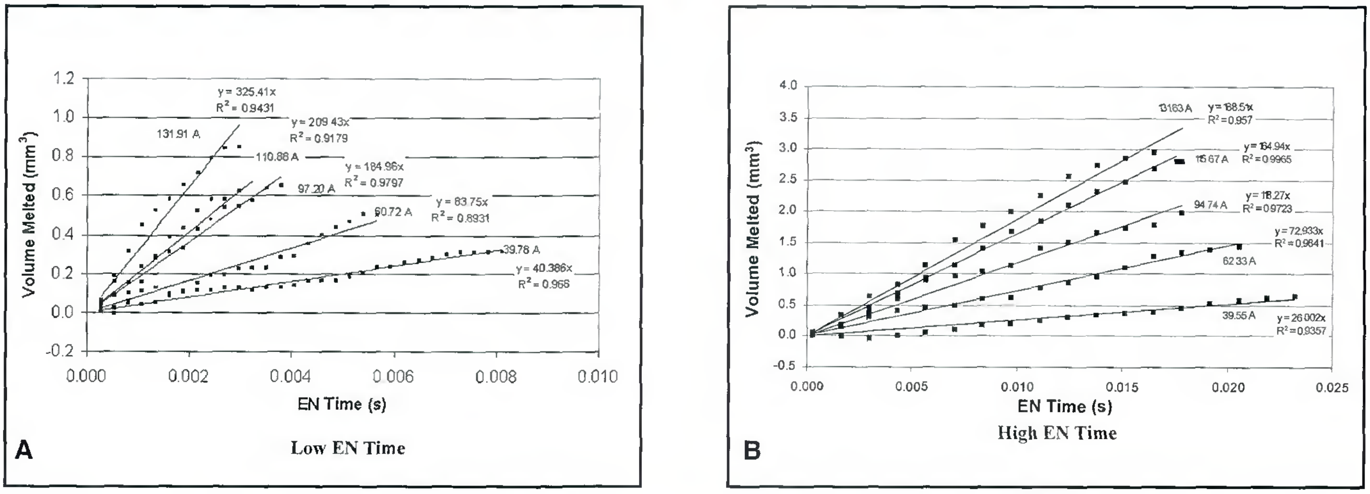

Fig. 4 — Droplet growth during the EN period at minimum and maximum time measured using high-speed video tests. A — Low EN time; B — high EN time.

Table 1 — DBR Measurements for EN Waveform Parameters

Weld No.	WFS_{DAQ} (mm/s)	Δx (mm)	t_{EN} (s)	$\Delta x/t_{EN}$ (mm/s)	MR_{EN} (mm/s)	V_d (mm^3)	V_D (mm^3/s)	I_{EN} (A)	BR (mm/(s A))	F_L (mm A)	f (Hz)	%EN (%)
0–42	39.32	–0.074	0.0083	–8.896	30.42	0.258	31.22	40.03	0.761	513.92	41.75	34.57
30–42	39.01	–0.005	0.0113	–0.451	38.56	0.446	39.57	39.81	0.968	512.48	44.04	49.63
60–42	38.26	0.020	0.0143	1.423	39.68	0.581	40.71	39.68	1.001	511.26	45.31	64.70
90–42	38.52	–0.097	0.0173	–5.582	32.93	0.584	33.79	39.56	0.833	507.45	39.51	68.31
120–42	38.96	–0.010	0.0202	–0.503	38.45	0.797	39.45	39.55	0.972	509.01	39.01	78.76
150–42	38.95	–0.041	0.0232	–1.752	37.20	0.885	38.17	39.55	0.941	508.40	34.72	80.52
0–63	59.28	0.076	0.0056	13.553	72.83	0.420	74.73	60.72	1.201	784.08	66.94	37.64
30–63	59.28	0.127	0.0086	14.767	74.04	0.653	75.97	62.30	1.189	806.07	66.07	56.82
60–63	59.28	0.157	0.0116	13.623	72.90	0.865	74.80	62.33	1.169	807.41	57.80	66.82
90–63	59.28	0.155	0.0145	10.663	69.94	1.043	71.76	62.39	1.121	808.10	50.03	72.69
120–63	59.28	0.366	0.0175	20.877	80.15	1.441	82.24	62.49	1.283	815.99	42.98	75.30
150–63	59.28	0.152	0.0205	7.423	66.70	1.405	68.44	62.33	1.070	807.25	36.90	75.76
0–85	80.34	0.276	0.0040	68.415	148.76	0.616	152.64	97.20	1.528	1264.92	74.03	29.89
30–85	83.01	0.502	0.0070	71.409	154.42	1.113	158.46	96.24	1.603	1263.26	71.78	50.43
60–85	81.65	0.592	0.0100	58.946	140.60	1.448	144.27	95.36	1.474	1255.96	61.51	61.76
90–85	81.83	0.528	0.0130	40.703	122.54	1.632	125.73	95.07	1.289	1249.17	51.00	66.20
120–85	81.96	0.478	0.0159	30.014	111.98	1.828	114.90	95.05	1.178	1246.48	43.99	69.99
150–85	81.25	0.546	0.0189	28.833	110.08	2.139	112.95	94.91	1.160	1247.83	38.90	73.68
0–106	102.24	0.218	0.0032	68.476	170.72	0.559	175.17	110.61	1.546	1436.18	91.04	29.04
30–106	102.24	0.650	0.0062	105.217	207.46	1.316	212.87	112.90	1.837	1490.29	74.98	46.34
60–106	102.24	0.737	0.0092	80.503	182.74	1.716	187.51	115.19	1.587	1525.50	60.99	55.81
90–106	102.24	0.785	0.0121	64.864	167.10	2.075	171.46	115.64	1.445	1534.25	51.00	61.71
120–106	102.24	0.897	0.0151	59.300	161.54	2.506	165.75	115.60	1.397	1540.17	42.19	63.79
150–106	102.24	0.970	0.0181	53.666	155.91	2.892	159.97	115.67	1.348	1545.37	37.12	67.11
0–127	123.28	0.426	0.0031	136.979	260.26	0.831	267.05	133.60	1.948	1748.63	91.09	28.34
30–127	123.49	0.754	0.0061	123.265	246.76	1.550	253.20	133.30	1.851	1766.52	71.83	43.96
60–127	123.55	0.813	0.0091	89.319	212.87	1.988	218.43	132.00	1.613	1753.14	58.06	52.83
90–127	123.31	0.914	0.0121	75.695	199.01	2.467	204.20	131.37	1.515	1751.45	49.68	60.01
120–127	123.21	0.554	0.0150	36.964	160.17	2.462	164.35	131.88	1.214	1734.47	43.60	65.31
150–127	123.94	0.777	0.0181	42.989	166.93	3.097	171.29	131.63	1.268	1745.89	38.06	68.81

Note: Weld No. = %EN pendant setting, wire feed speed setting.

ity and waveform.

4) Compare the measured α and β coefficients to measurements made by prior researchers to determine the validity of the DBR method that employed the BD to solve for the coefficients.

Constant arc length, contact tip-to-work distance (CTWD), and deposit area tests were used to study the effects of VP-GMAW waveform (Fig. 1) on melting rate. The power supply was an OTC AC/MIG 200. The machine was set up to use the preprogrammed waveform algorithms for 1.2-mm mild steel electrodes. The filler metal was 1.14-mm- (0.045-in.-) diameter ER70S-6 uncoated steel wire used with 90Ar-10CO_2 shielding gas at 18.8 L/min. The steel electrode was manufactured by National Standard per AWS A5.18 by the trade name of NS-115. The diameter of the electrode was measured with a micrometer prior to welding since the diameter was used to calibrate the high-speed video (HSV) dimensional analysis software in each test. High-speed video synchronized with high-speed data acquisition (DAQ) was used to capture

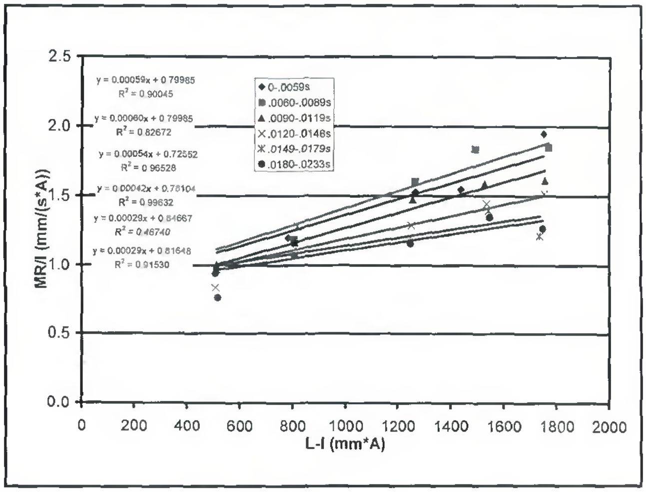

Fig. 5 — Burnoff diagram for EN waveforms for 1.2-mm steel electrode at 3-mm arc length and 16-mm CTWD. Note: equations are ordered in the same vertical order as the legend symbols.

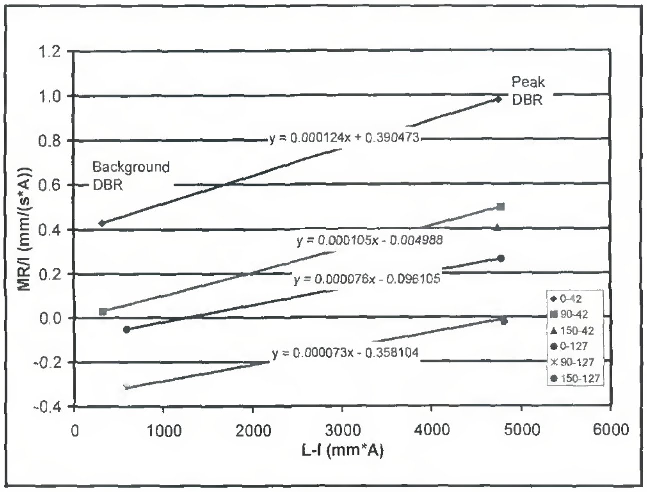

Fig. 6 — Burnoff diagram for EP waveforms for 1.2-mm steel electrode at 3-mm arc length and 16-mm CTWD.

the wire feed speed, current, voltage, and metal transfer of each waveform test.

The test matrix was designed to characterize a range of waveforms that varied the percent EN at five wire feed speeds ranging from 40 to 123 mm/s (Table 1). The EN current was increased from 40 to 133 A as the wire feed speed was increased from 40 to 123 mm/s, respectively. The actual DAQ wire feed speed varied slightly from the machine test setting. The EN current strategy was almost linear over this wire feed range since it was approximately 1 to 1.1 A EN to each mm/s of wire feed speed, respectively. The power transferred to the work was controlled by setting the percent EN, which changed the pulse frequency, f, and the EN time. On the AC/MIG 200 power supply, the percent EN pendant setting ranged from –150 to 150. The waveforms generated using the percent EN setting from 0 to –150 were GMAW-P type waveforms, therefore, these settings were not studied in detail. Percent EN increased as the pendant setting increased from 0 to 150 at each WFS. The arc length trim feature varied pulse frequency by varying EPB time, to control arc length.

Droplet Burnoff Rate Method

The droplet burnoff rate (DBR) method was based on measuring the droplet melting rate (mm/s) during each period, corresponding waveform (current and time), and electrode/droplet dimensions that affect these measurements. These data were then used to create burnoff diagrams (BDs) to solve for the melting rate coefficients. The BD plots electrode burnoff rate, BR (mm/s-A) vs. the electrode extension heating factor, F_L (mm-A). The Fig. 2 BD was for CV spray metal transfer with an ER70S-6 electrode. Here, a matrix of spray welding conditions was found to yield a linear relationship demonstrating the validity of the BD method. The intercept and slope of the line made with this diagram equaled the α and β coefficients. This approach was applied to each waveform period.

A Phantom V5.0 high-speed video camera, which used a complementary metal oxide semiconductor (CMOS) array, was set up to allow viewing of the growing droplet at the electrode tip and subsequent drop detachment. Shutter speed was adjusted to allow viewing of the metal transfer without using laser backlighting. The shutter speed was optimized for the waveform period being studied and for measuring arc length. The shutter settings for DBR measurements were 70 microsecond exposure and 10 microsecond extreme dynamic range. The latter feature switched the shutter speed to the higher speed to compensate for the very bright arc flash during pulse welding. The arc length was trimmed using the control pendant to 3 mm nominal at drop detachment between the electrode tip and weld pool surface. The high-speed video sampling frequency was nominally set at 3700 Hz. This frequency optimized the image size for measuring the droplet growth and electrode extension providing 512 x 512 pixel resolution. The HSV images were used to measure change in electrode extension (Δx) during each waveform period. Graphical software tools were used to calibrate distance measurements by marking and entering the wire diameter dimension in the first frame prior to measuring electrode extension changes. The electrode solid-liquid droplet interface position was measured in the first and last frame of this period to calculate $\varnothing x$ as shown in Fig. 3. During droplet formation, the electrode extension length either burned off or increased in length, with the current waveform to balance the melting rate. For this project, the electrode melting rate (MR) for each period of the waveform was determined empirically by adding the electrode extension burnoff rate to the WFS_{DAQ}. The MR for each waveform period (EN, EPB, EPP) was

$$MR_{(EN,EPP,EPB)} = \frac{\Delta x}{t_2 - t_1} + WFS_{DAQ} \quad (2)$$

where Δx is the electrode extension

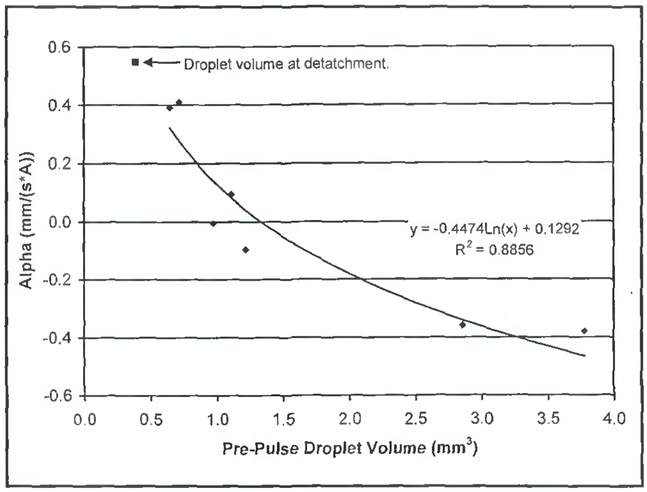

Fig. 7 — EP prepulse droplet volume effects on arc melting coefficient.

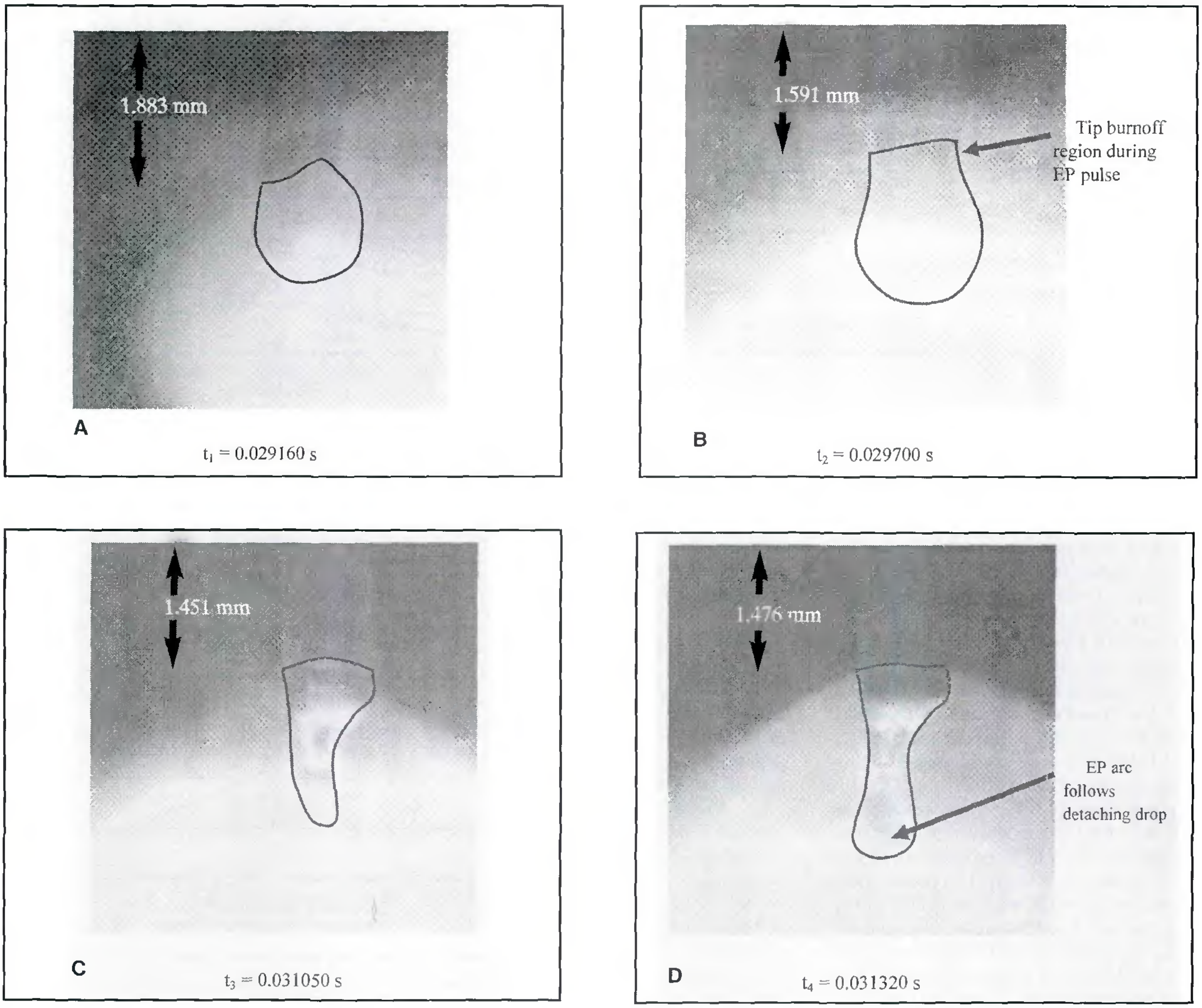

Fig. 8 — High-speed video image showing small prepulse droplet volume effect on EPP arc. A — $t_1 = 0.029160$ s; B — $t_2 = 0.029700$ s; C — $t_3 = 0.031050$ s; D — $t_4 = 0.031320$ s.

burnoff, which equals the length of change in solid-liquid interface position from initial time (t_1) to final time (t_2) and WFS_{DAQ} is wire feed speed measured with the data acquisition during that period. The Δx was measured by calibrating the high-speed video frames to the wire diameter (1.14 mm) and recording the droplet-electrode interface position at initial and final times for each period. The sign convention used for Δx required that positive interface growth be upward (toward the solid wire). Figure 3A shows the interface position at the beginning of the EN cycle. Figure 3B shows the interface position at the end of the EN cycle. In this case, the time elapsed throughout the cycle is 0.01107 s and growth is in the positive direction ($\Delta x > 0$). The droplet volume growth rate is proportional to the melting rate defined by Equation 2 and the wire area, A_w, which was 1.02 mm^2 (0.00159 in.^{2}), assuming the solid-liquid droplet interface shape does not change. Therefore, the droplet volume growth rate (V_D) in each period was

$$V_D = \left(\frac{\Delta x}{t_2 - t_1} + WFS_{DAQ} \right) \cdot A_w \qquad (3)$$

The electrode extension heating factor (F_L) for each waveform period was determined as follows:

$$F_{L(EN,EPB,EPP)} = L \cdot I_{EN,EPB,EPP} \qquad (4)$$

The average electrode extension was based on the change in electrode extension length, Δx, relative to the initial electrode extension, Lo, during the period of evaluation:

$$L_{EN,EPB,EPP} = Lo + \frac{\Delta x}{2} \qquad (5)$$

The average melting rate can be determined by summing the MR for each period and multiplying the waveform frequency, f, with the following equation:

$$MR_{AVG} = \left(\left(MR_{(EN)} \cdot t_{EN} \right) + \left(MR_{(EPB)} \cdot t_{EPB} \right) + \left(MR_{(EPP)} \cdot t_{EPP} \right) \right) \cdot f \qquad (6)$$

The MR_{AVG} should equal the wire feed speed for a stable VP-GMAW waveform. The percent EN of each waveform based on time was determined from the waveform DAQ. The percent EN was deter-

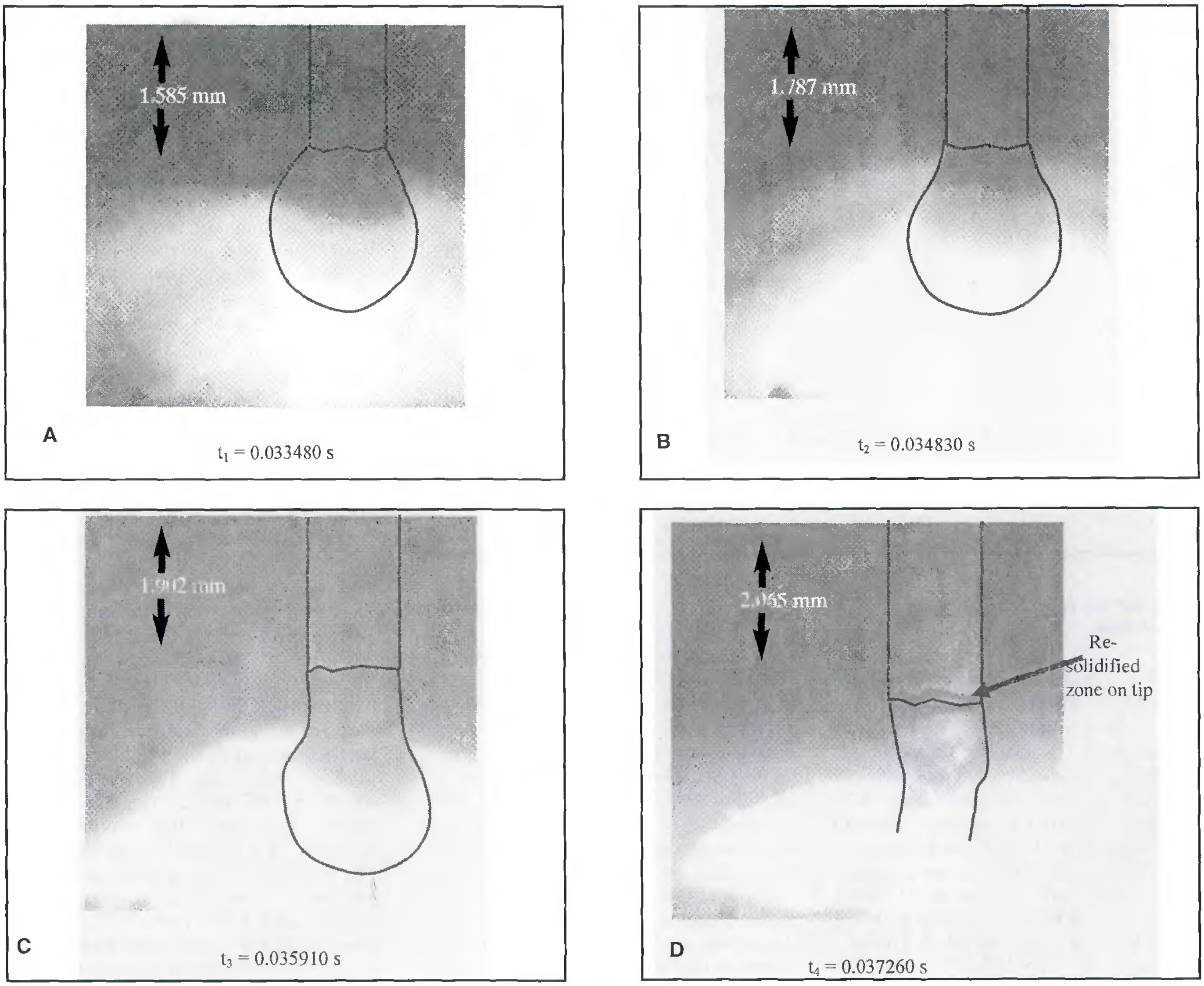

Fig. 9 — High-speed video image showing large prepulse droplet volume effect on EPP arc. A — t_1 = 0.033480 s; B — t_2 = 0.034830 s; C — t_3 = 0.035910 s; D — t_4 = 0.037260 s.

mined using the following equation:

$$\%EN = (f \cdot t_{EN}) \cdot 100\% \qquad (7)$$

where f is the pulse frequency and t_{EN} is time spent in EN polarity. Percent EN was related to waveform parameters to determine relationships for process stability, such as the effects of I_{EN} and t_{EN} on melting rate. The EN ratio was calculated on some tests to compare the arc melting potency with different waveforms as follows:

$$ENratio = \frac{I_{EN}t_{EN}}{\left(I_p t_p\right)+\left(I_b t_b\right)+\left(I_{EN}t_{EN}\right)} \qquad (8)$$

Once the melting rate, waveform, and other DBR measurements were made for each period, the BD was used to empirically determine α and β. The BD was demonstrated by Richardson (Ref. 15) as an efficient way to empirically determine the melting rate coefficients. A single line is yielded for CV processes (Fig. 2) that have a constant mode of transfer, like spray transfer, for a full range of operating conditions. The line produced on the BD for CV processes characterizes the effects of electrode extensions, wire feed speeds, and currents for that mode of transfer and electrode conditions. For the VP-GMAW process, this investigation showed that multiple BD lines were needed for each polarity depending on the waveform conditions. A separate burnoff diagram was created for each polarity, EN and EP, for the AC/MIG 200 power supply using the 1.14-mm steel electrode and 90%Ar-10%CO_2 shielding gas. For the EP period of different VP-GMAW waveforms, the lines were fitted between DBR measurements made in EPB and EPP periods. The coefficients measured in each waveform period were compared to prior research for EP heating, and used to establish the melting rate properties of EN, EPB, and EPP periods in VP-GMAW.

Results

The DBR method was used to measure the melting rate properties of each waveform period. The main focus was the EN period and waveform effects. Many measurements were taken to capture the relationship between I_{EN} and t_{EN} on the melting rate. Droplet burnoff rate measurements were also taken for the EP period, which used a constant pulse waveform. Here, separate DBR measurements were taken during the EPB and EPP periods until droplet detachment.

Table 2 — Summary of Melting Rate Coefficients for Steel Electrodes

Process	Electrode Diameter (mm)	Polarity	EN Time (ms)	α (mm-A^{-1}s^{-1})	β (10^{-4}, A^{-2}s^{-1})	Reference
CV Spray	0.8	EP		0.56	2.9	Lesnewich[13]
CV Spray	1.14	EP		0.25	0.7	Lesnewich
GMAW-P	0.8	EP		0.55	3.5–3.7	Richardson[15]
GMAW-P	1.0	EP		0.47	0.91	Richardson
GMAW-P	1.2	EP		0.27	0.59	Richardson
VP-GMAW	1.14	EN	0.0–5.9	0.80	5.9	
			6.0–8.0	0.80	6.0	
			9.0–11.9	0.72	5.4	
			12.0–14.8	0.78	4.2	
			14.9–17.9	0.85	2.9	
			18.0–23.3	0.82	2.9	
CV Spray	1.14	EP		0.28	0.9–1.0	
VP-GMAW	1.14	EP		–0.35–0.55	0.7–1.2	

EN Time Effects on Droplet Volume Growth Rate

Five I_{EN} and WFS combinations were studied to assess the effects of t_{EN}. The I_{EN} was constant for each WFS per Table 1 based on the pendant setting. The five different WFSs (42, 63, 84, 106, and 127 mm/s) were characterized at low %EN, which ranged from a minimum of 28 to 38%, to the highest %EN ranging from 67 to 81%. The AC/MIG 200 pendant settings for these times corresponded to 0 for low t_{EN} and 150 for the maximum t_{EN}. The lowest EN times were 3.1 and 8.3 ms at a 0 setting for WFSs of 127 and 42 mm/s, respectively. The highest t_{EN} were 18 and 23 ms at the 150 setting for the same WFS. The EN times were higher at the lower WFSs since the pulse frequency was lower. High-speed video was used to measure the droplet volume, V_d, as a function of t_{EN} at each WFS and I_{EN} combination. The EN droplet volumes (Table 1) were measured by averaging 0.5 s of image data at 3700 frames/s. Typically, 10 droplets per condition were used for DBR measurements depending on the stability of the waveform and metal transfer. Pulse frequency at each WFS decreased as the %EN increased. The f range was small, only 35 to 42 Hz, at the low WFS of 40 mm/s. At 123 mm/s WFS, the f ranged from 38 to 91 Hz. The number of droplets available for measurement for each EN waveform condition, therefore, varied from 17 to 45 droplets since only 0.5 s of data were taken.

From the data in Table 1, there appeared to be a nonlinear relationship between Δx and V_d, as a function of t_{EN}. At long t_{EN}, the Δx saturated on average at about 10 ms of t_{EN} for wire feed speeds greater than 63 mm/s. The V_d continued to grow but at a slower rate once saturated. The change in droplet growth rate, V_D, was related to t_{EN} by evaluating the droplet volume growth rate. The V_D was typically higher at short t_{EN} for constant I_{EN}. This was especially true for the higher WFS tests. The melting rate for the EN period was heavily dependent on Δx. Here, Δx was a larger part of the MR at short t_{EN}. Since there was a nonlinear relationship between I_{EN} and MR as a function of t_{EN}, additional image analysis was performed on three droplets from the low and high t_{EN} from each WFS test group. The droplets that were selected had uniform arc initiation and were considered ideal. The V_d was graphed during the whole EN period by continuously accounting for the WFS and Δx in each high-speed video frame as a function of time. The graphs shown in Fig. 4A and B were plotted to evaluate how V_d grows with time; the magnitude of growth rate, V_D, and compare the effects of t_{EN} at constant I_{EN}. The results from three drops were averaged and plotted in Fig. 4A (low t_{EN}) and 4B (high t_{EN}) for each WFS and I_{EN} combination. The line fitted in each graph was the average incremental droplet volume over time. The slope of the line equaled the droplet volume growth rate, V_D. At WFS of 42 mm/s, V_D was 40.4 and 26 mm^3/s for low and high t_{EN}, respectively, as shown in Fig. 4A. I_{EN} for this WFS was 40 A. The V_D increased to 325.4 and 188.5 mm^3/s at low and high t_{EN}, respectively, for 123 mm/s WFS and I_{EN} = 133 A, as shown in Fig. 4B. In all these tests, the low t_{EN} produced a higher V_D compared to long t_{EN}, at the same current. These data were similar to the Table 1 measurements, which averaged a 0.5 s of high-speed video data, especially for the higher WFS test groups. The line slopes measured from the Fig. 4 graphs, which equaled the V_D rate, had an average coefficient of multiple determination (R^2) of 0.957, which indicated a good data fit.

DBR Measurements for the EN Period

The DBR method was used to measure the MRs for the test matrix in Table 1, which had five different WFSs (42, 63, 84, 106, and 127 mm/s) at six different %EN levels. The corresponding pendant settings were 0, 30, 60, 90, 120, and 150. Since the melting rates were sensitive to t_{EN}, the results were separated into groups for plotting. The t_{EN} groups were 3 to 5.9, 6.0 to 8.9, 9.0 to 11.9, 12.0 to 14.8, 14.9 to 17.9, and 18.0 to 23.2 ms. These were basically 3-ms groupings except for the last. The average MR_{EN}, L_{EN}, and I_{EN}, and time at each waveform condition were used to calculate the BR and F_L. These results were plotted to construct the BD (Fig. 5), which was used to solve for the melting rate coefficients. The y-axis intercept was equal to the arc melting coefficient, α_-, and the slope of each line was equal to the resistive heating coefficient, β_-. The overall shape of this graph showed a burnoff rate range that increased as F_L increased instead of a single line. This was the opposite of a CV BD where a single line is produced describing the melting rate behavior of a GMAW consumable set. The lines in Fig. 5 were fitted to the data and were based on the 3-ms t_{EN} increments at each EN current. This approach was used based on the dependency on V_D to t_{EN} that was established during data analysis. The highest burnoff rates as a function of heating factor, F_L, were achieved at the lowest t_{EN}. Likewise, long t_{EN} showed a decrease in BR. Comparing the equations that were solved for each line shows β_- varied from 2.9 to 6.0 x 10^{-4}, A^{-2}s^{-1}.

These units were large for β. This was not expected since polarity should not affect the resistivity of the electrode. A theory was developed to explain why β_- was dependent on t_{EN} for the EN period. The increase in melting rate at short t_{EN} was believed to be due to a concentrated melting effect. Careful observation of the high-speed video data showed that the EN arc rapidly climbed the electrode tip; the extent depended on the current level. The electrode tip that was covered by the EN arc rapidly melted and promoted higher V_D in the initial part of the EN period. The Δx saturated as the t_{EN} increased at constant I_{EN} and WFS. The large droplet that was formed decreased the melting effect of the cathode arc at long t_{EN} since the arc concentrated on it. This theory was supported by Norrish (Ref. 34) who observed

Table 3 — BDR Measurements for EP Waveforms

Weld No.	WFS_{DAQ} (mm/s)	Δx (mm)	t_p or t_b (s)	$\Delta x/t_p$ or $\Delta x/t_b$ (mm/s)	MR (mm/s)	V_d (mm^3)	V_D (mm^3/s)	I_p or I_b (A)	BR (mm/(s A))	F_L (mm A)	f (Hz)	EPP or EPB Period (%)	V_{pp}- (prepulse) (mm^3)
B-0-42	39.09	−0.273	0.0119	−22.890	16.20	0.198	16.62	25.19	0.430	320.88	41.75	49.81	0.39
B-90-42	38.94	−0.057	0.0015	−37.708	1.23	0.002	1.27	24.81	0.028	318.72	39.51	5.97	0.39
B-0-127	123.28	−0.115	0.0009	−125.521	−2.24	−0.002	−2.30	46.46	−0.051	595.50	91.09	8.36	0.39
B-90-127	123.31	−0.221	0.0016	−141.286	−17.97	−0.029	−18.44	46.12	−0.315	588.69	49.68	7.78	0.39
P-0-42	39.09	0.500	0.0016	303.535	342.63	0.579	351.56	362.08	0.980	4752.26	41.75	6.87	0.78
P-90-42	38.94	0.424	0.0030	142.661	181.60	0.553	186.34	365.32	0.497	4780.87	39.51	11.73	1.05
P-150-42	38.84	0.184	0.0023	81.325	120.17	0.280	123.30	365.39	0.407	4738.09	34.72	7.87	1.38
P-0-127	123.28	−0.130	0.0053	−24.338	98.95	0.541	101.53	373.14	0.267	4779.97	91.09	48.56	1.11
P-90-127	123.31	−0.556	0.0044	−125.595	−2.28	−0.010	−2.34	381.48	−0.008	4805.50	49.68	21.99	2.86
P-150-127	123.97	−0.617	0.0047	−132.507	−8.56	−0.041	−8.79	382.26	−0.022	4803.67	38.20	17.79	3.78

Notes:
1) Weld No. code defines EP period — pendant setting, wire feed speed (mm/s).
2) For EP period: B indicates background period and P indicates peak period from that test.
3) The pendant setting of 150 had no background period to measure.
4) Prepulse droplet volume, V_{pp}, was measured from high-speed video DBR plus postpulse remainder of 0.39 mm^3.

that a constant voltage EN arc can oscillate between a multispot and single-spot cathode as the droplets form and detach, respectively.

The burnoff rate in Fig. 5 was heavily dependent on the Δx based on the measurements in Table 1. The electrode extension burnoff was up to 50% of the total melting rate at low t_{EN}, especially at the higher I_{EN} and WFSs. Since higher BR results in large changes in line slope, the effect was measured by the β_- coefficient. Since the electrode extension became shorter when including the burnoff effect, F_L decreased. This would increase the slope of the lines too. Therefore, Δx acts to increase the slope of the burnoff diagram based on its effect on both graph parameters, BR and F_L.

Melting Rate Measurements for the EP Period

Burnoff diagrams for a given electrode type and diameter are linear for EP constant voltage processes for a large range of currents, arc length, and CTWDs. This is true as long as the metal transfer mode is constant, especially for the spray transfer mode since it develops a very stable electrode tip that is covered by the arc and employs free-flight metal transfer. A separate set of spray GMAW tests were performed to verify the relationships that were established by Lesnewich and Richardson (Refs. 13, 15). This set of experiments simply tested the effects of several WFSs and arc lengths at 16 and 19 mm CTWD. The BD from these tests was plotted and found to yield a linear relationship for the entire group of tests — Fig. 2. Here, the α was 0.28 $mm\text{-}A^{-1}s^{-1}$ and the β was 0.9 to 1.0 x 10^{-4}, $A^{-2}s^{-1}$. The α and β coefficients were in good agreement with the measurements provided by Lesnewich (Ref. 13) for spray as shown in Table 2. This simple set of tests reinforced the use of the BD for solving melting rate relationships.

DBR Measurements for EP Pulse

Measurements made on the EP period of the VP-GMAW waveforms were found to be difficult. The major challenge was accommodating the wide range in light intensity during the current pulse, the EPP period, while following the position of the electrode extension-droplet neck. The image analysis software helped filter the light intensity of recorded images, but the contrast was too great during the full peak current to locate the solid-liquid interface if the arc expanded over the droplet. Even though improvement can still be made to the high-speed video equipment, enough good images were obtained at several waveforms to study the EPP period in VP-GMAW. Visual observation of the melting process yielded some important results. The EPP pulse arc rapidly climbed the electrode tip above the droplet when the droplet was small. As the arc covered the electrode, rapid melting occurred. An entire column of electrode above the droplet was observed to melt and mix with the droplet on pulses where the arc grew on the electrode extension. The droplet started to neck in most cases before finishing the EPP period. Likewise, different arc behavior was observed when the droplet size was large. Here, the EPP pulse arc rooted and could not expand over the bottom of large droplets. Once the neck started for droplet detachment, the peak current arc followed the detaching drop toward the weld pool. This resulted in some solidification at the electrode tip as the neck broke and before arc reattachment to the electrode tip. Therefore, the melting efficiency of the EP period was largely related to the prepulse droplet size. This behavior influenced MR_{EP} and Δx where the values were negative for large prepulse droplets (Table 3).

Detailed DBR measurements for EP periods were performed on 10 different conditions (Table 3). The WFS conditions represented the range of background and peak conditions that were observed with the VP-GMAW waveforms. The EN pendant settings of 0, 90, and 150 resulted in %EN range of 34 to 81% for 42 mm/s, and 28 to 69% for 127 mm/s tests. An EPB period was only measured on EN pendant settings of 0 and 90. At both WFSs, the 150 pendant setting resulted in a waveform that had no EPB time and alternated between EPP and EN pulses. The DBR measurements were calculated for both the EPB and EPP periods. The background time t_b was equal to the time for that period. For the EPP period, the time t_p was from the period beginning until drop detachment of the first drop per Fig. 1. This was factored to accommodate the large change in electrode melting rate that occurred during the current pulse and at drop detachment. The BD was plotted from the data in Table 3 and used to solve the arc and resistive heating coefficients — Fig. 6. Lines were fitted between DBR measurements that had both EPB and EPP periods for that waveform. The points on the left side of this figure were from EPB measurements and the right side were from EPP measurements. From these lines it was obvious that EP pulse melting rate coefficients were not constant. The change in α_+ coefficients was related to the prepulse droplet volume — Fig. 7. The droplet volume immediately after detachment was measured and approximated to be 0.39 mm^3 for most waveforms. The droplet was approximately equal to a half hemisphere based on the wire diameter immediately after detachment and starting into a new period. This assumption was made to account for the arc behavior observed in the high-speed video images.

Discussion

As shown in Fig. 2, the BD for EP constant voltage produced a linear burnoff relationship for a range of electrode extensions, WFSs, and current conditions. The second-order melting rate relationship described by Equation 1, which was developed by Lesnewich (Ref. 13) and verified by Richardson (Ref. 15), was verified here too. Based on these data, the BD can be used to determine melting rate coefficients for GMAW processes that have a stable mode of transfer, like spray transfer.

The DBR method evaluated the direct relationship between the arc current waveform and electrode droplet melting rate. Synchronized high-speed video was used to measure droplet melting, growth, and detachment in each waveform period, EN, EPB, and EPP. Best fit lines were used to trend the data on the BD for the EN period as a function of t_{EN} range (Fig. 5), and for the EP pulse period as a function of prepulse droplet volume — Figs. 6 and 7. This was performed to explain the variation in electrode melting rate with VP-GMAW waveforms.

A summary of arc and resistive heating coefficients was prepared for comparison (Table 2). For GMAW-P, Richardson determined the resistive heating coefficient, β_+, equaled 0.59 x 10^{-4}, $A^{-2}s^{-1}$ for 1.2-mm steel electrodes. For CV GMAW, Lesnewich determined β_+ to equal approximately 0.7 x 10^{-4}, $A^{-2}s^{-1}$ for steel at this wire diameter. The resistive heating coefficient is dependent on electrode cross section and resistivity, so different values would be expected if different sizes and types of electrodes were tested. However, it was not expected that β values would be different for EN and EP periods with constant electrode conditions. At the very longest t_{EN} groups shown in Table 2, the β_- values for the EN period decreased enough that they were near the values measured by Richardson for GMAW-P for smaller electrodes. Overall, the β_- coefficients were three to six times greater than the values reported by Lesnewich for CV GMAW. Since β_- varied in these tests, the results from the BD based on the DBR method were physically not linked to the arc melting and resistive heating coefficients as defined per Equation 1 by Lesnewich. Here, the BD provided a simple tool for solving for coefficients used in second-order polynomials for each period. It was not believed that resistive heating changed with polarity. The slope of the lines in Fig. 5, which equal β_-, increased since BR increased and F_L decreased when t_{EN} decreased at constant I_{EN}. This behavior was related to the concentrated melting theory that is based on the transient behavior between the growing droplet and the arc. The arc heat used for melting changed based on the conditions between the forming droplet and the arc, but the BD measures these changes by slope changes. The β_- data fit was good except at the lower WFSs and I_{EN}s as shown in Fig. 5. Linear lines were used to simply solve for the melting rate coefficients. A higher-order polynomial may have provided better fit for the lower I_{EN} data. Ignoring the low I_{EN} data, the intercept of the lines for the EN burnoff diagram varied little. The variation in data line fit was attributed to grouping t_{EN} into 3-ms groups. This data grouping was based on fitting the measured t_{EN} from incremental %EN pendant test settings that were used at each WFS.

The α_- (intercepts in Fig. 5) were significant and were almost constant for all the t_{EN} groups. Average α_- was approximately 0.8 mm-$A^{-1}s^{-1}$ and ranged from 0.72 to 0.85 mm-$A^{-1}s^{-1}$ (Table 2). For comparison, α_+ for GMAW-P and CV GMAW was 0.27 and 0.25 mm-$A^{-1}s^{-1}$, according to Richardson and Lesnewich, respectively. The α_- data were more than three times greater than α_+ measurements made by the prior researchers, which demonstrates the melting potency of an EN arc.

The β_+ determined from Fig. 6 varied from 0.7 to 1.2 x 10^{-4}, $A^{-2}s^{-1}$ over the test conditions. As shown in Table 2, Lesnewich determined β_+ to equal approximately 0.7 x 10^{-4}, $A^{-2}s^{-1}$ at this wire diameter for steel CV GMAW. Independent CV GMAW spray measurements performed in this investigation found β_+ equaled to 0.9 to 1.0 $A^{-2}s^{-1}$. Therefore, the β_+ determinations for the EP pulse period were within the range and agreed with CV spray measurements. β_+ did increase slightly with decreasing prepulse droplet volume.

The α_+ coefficients were both positive and negative and varied from –0.35 to 0.35 mm-$A^{-1}s^{-1}$ for the different VP-GMAW conditions. As shown in Table 2, the α_+ coefficients for GMAW-P and CV GMAW spray were 0.27 and 0.25 mm-$A^{-1}s^{-1}$ for 1.2- to 1.14-mm electrodes per Richardson and Lesnewich, respectively. The large α_+ differences determined for the VP-GMAW process were attributed to the large range of prepulse droplet volume produced with different EN period waveforms.

The droplet volumes plotted in Fig. 7 were calculated from the high-speed video data just before entering the peak pulse period (Table 3). These measurements were scaled to include the droplet remainder immediately after detachment from the previous pulse. As mentioned earlier, the arc rapidly climbed the electrode tip as the current was pulsed when the droplet was small. This provided concentrated melting of the electrode extension where the arc covered it. However, large droplets inhibited further melting of the electrode tip, and this effect was shown by the negative α_+ data. Large droplets significantly reduced arc melting because the arc was rooted on the droplet bottom. A negative coefficient indicated that the electrode extension was increasing in length and the arc length was decreasing.

Concentrated Melting Theory

A theory was developed to describe the dependency of electrode melting rate in VP-GMAW on 1) EN time at constant EN current, and 2) the prepulse droplet volume for EP pulsing. The theory was named the "concentrated melting theory" and is defined as follows:

"The melting potency of GMAW current waveforms is strongly dependent on arc concentration at the electrode tip above the droplet interface, and the droplet size and growth process. Virgin electrode metal is consumed rapidly when the arc is permitted to climb over and concentrate on the electrode extension. Droplet growth is rapid in current transients when the arc climbs the electrode tip causing extension burnoff. During a waveform constant current period, the electrode melting rate decreases once the burnoff is complete and the droplet size inhibits further arc concentration and climb on the electrode. Once the arc is rooted on the droplet bottom, the electrode melting rate will continue to decrease as the droplet grows until drop detachment."

The concentrated melting theory applies to open-arc GMAW processes that employ current waveform that pulse the current and/or polarity to regulate metal transfer. Droplet transfer in VP-GMAW occurred during the EP pulse. Observations made during high-speed video analysis found that the EN arc climbed over the electrode tip (Fig. 3), which had a small droplet remainder, as soon as the current switched polarity and the EN arc was ignited. The arc cathode was distributed over a large electrode tip area. This was quite different from the CV processes like spray transfer where the arc is stable and continuously covers a portion of the electrode tip. This EN arc behavior was also observed by Norrish (Ref. 34). In steady-state EN GMAW, Norrish observed that the arc formed a multispot cathode that climbed the electrode after drop detachment. Once a droplet formed, the arc switched to a single spot cathode mode and rooted on the droplet bottom. The observations by Norrish reinforce the concentrated melting theory for EN waveforms.

Higher EN currents promoted larger arc plasmas that covered more of the solid electrode extension tip. The electrode extension area that was enveloped by the EN arc melted early in the EN period. Once a large droplet formed, the electrode melting rate decreased because the arc concentrated the heat on the droplet. Therefore, high current waveforms that used low EN time had much larger droplet volume growth rates, V_D, compared to long EN times as shown in Fig. 4. Droplet growth rate was dependent on the concentrated melting based on the size of the arc plasma and time. Once the electrode extension burnoff saturated, the melting rate decreased since the arc was concentrated on the droplet instead of solid electrode. Analysis of the high-speed image data showed that the electrode extension meltback was the greatest at the beginning of the EN period (Table 1). At EN times up to 20 ms, the change in electrode extension, Δx, saturated at 9 to 11 ms into the period for EN currents that were 60 A or higher.

The concentrated melting theory also applied to EP pulse waveforms. The prepulse droplet volume had a significant effect on the α_+ coefficient. High-speed video images were taken to show how the prepulse droplet affected the electrode extension burnoff. When the prepulse droplet volume was small, the arc was observed to rapidly climb as the current increased over the electrode tip behind the droplet as shown in Fig. 8. A column of electrode would collapse and mix with the droplet. The arc eventually became rooted on the droplet that grew from electrode melting and extension burnoff. Further electrode melting was limited when the detachment process started with the formation of a neck. The arc followed the droplet through the detachment process. A decrease in melting rate was observed during the necking process where the electrode tip was observed to solidify after the droplet bridge ruptured, and at the same time the arc length shortened. The arc would then jump to the electrode tip after drop detachment to maintain the circuit where a new droplet was initiated. Large prepulse droplets completely blocked the EP pulse arc from climbing on the electrode extension — Fig. 9. Here, the electrode melting rate was significantly reduced during the EPP pulse providing no additional electrode extension burnoff. As the neck formed, the arc followed the detaching drop. The tip of the electrode partially solidified during the rupture of the neck since the arc was removed. These visual observations together with the DBR data show that the melting rate of VP-GMAW waveforms was strongly dependent on the transient behavior between the arc in each period and the droplet formation process. The prediction of VP-GMAW melting rate (Ref. 12) required detailed understanding of these mechanisms.

A source of error was fume generation from droplet heating once the arc rooted on it. Since droplet volume calculations per Equation 3 were proportional to the sum of the WFS_{DAQ} and $\Delta x/t$, there was no term added to subtract fume losses. This is an area for future work and further development of the DBR method. The true droplet volume also could not be measured from the high-speed video since the droplet profile oscillates during welding and does not provide a perfect sphere for video analysis. With respect to fume, Ushio showed that VP-GMAW produced significantly less fume compared to GMAW-P and CV GMAW on aluminum alloys (Refs. 35, 36). Based on the data developed here for steel, it is believed that fume losses are probably minimized with VP-GMAW for steel, too, since the melting rates are so much higher than CV GMAW and GMAW-P. On future welding applications, optimized waveforms that minimize droplet heating by controlling the duration of the waveform periods relative to the droplet growth and detachment process will provide a lower fume process.

Conclusions

1. Melting rate was very dependent on current waveform, polarity, and droplet size, and metal transfer events if they occurred, during each waveform period. The transient conditions of current waveform and metal transfer produced rapid changes in arc behavior, which strongly influenced the melting rate for each period of various VP-GMAW waveforms.

2. The concentrated melting theory was developed to explain the significant increase in electrode extension burnoff and droplet growth rate that occurred at short EN time as a function of current, and during EP peak pulse when the prepulse droplet volume was small. The highest electrode extension burnoff and droplet growth rate occurred when the arc was permitted to climb over the solid electrode tip producing rapid concentrated melting. Likewise, large molten droplets were found to promote a negative electrode extension burnoff and a decreased droplet growth rate. The arc rooted on large droplets providing additional heating but limited additional electrode melting.

3. The DBR method was found to yield good experimental measurements for α and β coefficients used in melting rate equations for complex waveforms like those used in VP-GMAW. The coefficients were not as physically linked to α and β, like the prior research, but provided characterization of second-order behavior for electrode melting rate in each period of the waveform.

4. EN time affected the melting rate as a function of EN current. The melting rate contribution from electrode extension burnoff increased as the EN time decreased in a range from 23 to 3 ms. This was measured by the change in the β_- coefficient. This change was related to the slope of the burnoff diagram, which increased when burnoff rate increased as a result of electrode extension burnoff.

5. The melting rate of the EP periods, both background and peak, were related to the prepulse droplet volume. Large prepulse droplets, which formed in the EN period, decreased the EP melting rate since the arc concentrated more on the droplet than above it on the unmelted electrode extension. The arc was observed to follow the droplet during detachment and some solidification of the molten tip occurred before the arc reattached to the tip at drop transfer. This reduced the electrode melting rate of EPP periods.

6. For EP pulse waveforms, the prepulse droplet volume effect on melting rate was measured by a change in the α_+ coefficient, which was negative for some DBR measurements that had large prepulse droplet volumes. The negative influence was not a result of reduced heating, but a result of preferential heating of the droplet instead of melting the electrode tip. The electrode extension increased under these conditions resulting in a shorter arc length.

Acknowledgments

Edison Welding Institute (EWI) sponsored this collaborative dissertation project at Cranfield University's Centre for Welding Research. OTC Daihen Robots is acknowledged for provided the welding equipment.

References

1. Ogasawara, T., Maruyama, T., Saito, T., Sato, M., and Hida, Y. 1987. A power source for gas shielded arc welding with new current waveforms. *Welding Journal* 66(3): 57–63.

2. Maruyama, T., Okada, M., Hida, Y., Honma, M., and Minato, T. 1995. Current waveform control in gas shielded arc welding for robotic systems. Kobelco Technology Review, No. 18, April, pp. 10–14.

3. Nacey, T. 1995. The effect of dynamic variables on GMAW arc characteristics — Controlling the power supply response. *The Fabri-*

cator 25(2): 18–20.
4. Nacey, T., and Pagano, K. 1995. Advancements in DC and AC low current pulse GMAW. *Proceedings from ICAWT 11th Annual Conference*, Columbus, Ohio, Paper No. 2-3(C).
5. Maruo, H., and Hirata, Y. 1988. MIG welding with rectangular wave AC. Technology Reports of the Osaka University. Vol. 38(1935): 237–245.
6. Maruyama, T., et al. 1988. Polarity ratio control GMA welding power source, data for the JWS 118th Welding Method Research Committee.
7. Tanimoto, J., Minooka, M., and Nishida, Y. 1988. Development of the AC pulsed MAG welding process. IIW Asian Pacific Regional Welding Congress, 36th Annual AWI Conference.
8. Okada, M. 1989. Sensarc PC350 EP/EN ratio-controllable GMA welding power source. Masashi OKADA, Welding Equipment Robot Department, Welding Division, Kobelco Technology Review, No. 6.
9. Okada, M. 1992. Sensarc AL350 penetration-controllable MIG welding power source for aluminum alloy. Kobe Steel, Factory Automation and Robotics Group, New Business Division, Kobelco Technology Review, No. 6.
10. Harada, S., Ueyama, T., Mita, T., Innami, T., and Ushio, M. 1999. The state-of-the-art of AC-GMAW process in Japan. *IIW Doc. XIII-1589-99*, pp. 1–10.
11. Ueyama, T., Tong, H., Harada, S., and Ushio, M. 2000. Improve sheet metal welding quality and productivity with AC pulsed MIG welding system. *IIW Doc. XII-1629-00*, pp. 86–102.
12. Harwig, D. D. 2003. Arc behavior and metal transfer in the VP-GMAW process. PhD dissertation, Cranfield University.
13. Lesnewich, A. 1958. Control of melting rate and metal transfer in gas-shielded metal arc welding — Part I — Control of electrode melting rate. *Welding Journal* 37(8): 343-s to 353-s.
14. Allum, C. J. 1983. MIG welding- time for a reassessment. *Metal Construction*, pp. 347–353.
15. Richardson, I. M., Bucknall, P. W., and Stares, I. 1994. The influence of power source dynamics on wire melting rate in pulsed GMA welding. *Welding Journal* 73(2): 32-s to 37-s.
16. Amin, M. 1981. Synergic pulse MIG welding. *Metal Construction*, June, pp. 349–353.
17. Amin, M. 1983. Pulse current parameters for arc stability and controlled metal transfer in arc welding. *Metal Construction*, May, pp. 272–278.
18. Nixon, J. H., and Norrish, J. Determination of pulsed MIG process parameters. *Synergic MIG Supplement*, pp. 4–7, Pulse Parameters for XMT 300 CC/CV.
19. Kim, Y. S., and Eagar, T. W. 1993. Metal transfer in pulsed current gas metal arc welding. *Welding Journal* 72(7): 279-s to 287-s.
20. Joseph, A. 2001. Assessing the effects of GMAW pulse parameters on arc power and weld heat input. Masters thesis, The Ohio State University, Columbus, Ohio.
21. Lucas, W., and Needham, J. C. 1975. Why not AC MIG-welding? *The Welding Institute Research Bulletin*, March, pp. 63–67.
22. Lucas, W. 1978. Solid wire AC MIG welding. *Welding Research International* 8(2): 102–127.
23. Dymenko, V. V., and Zaruba, I. I. 1979. Stabilizing the arc discharge during welding with AC. *Automatic Welding* 31(3): 25–29.
24. Nakanishi, M., Katsumoto, N., Komizo, Y., Hasunuma, S., and Seta, I. 1983. Development of AC MIG arc welding. *The Sumitomo Search*, No. 28, October, pp. 73–86.
25. Tsushima, S., and Fujita, H. 1992. Pulse generator for high-current AC-MIG welding process — Development of AC-MIG welding process (Report 2).
26. Tsushima, S., Ohkita, S., and Horii, Y. 1992. Effects of oxygen on the toughness of Ti B containing AC MIG weld metal — Development of AC MIG welding process (Report 3). pp. 56–63.
27. Tsushima, S., and Kitamura, M. 1994. Tandem electrode AC-MIG welding — Development of AC-MIG welding process (Report 4). *Welding International* 8(8): 599–605.
28. Tsushima, S., Horii, Y., and Yurioka, N. 1994. Application of AC-MIG narrow-gap welding to butt joints in 980 MPa high-strength steels (5th Report) —Development of AC-MIG welding. *Welding International* 8(7): 525–531.
29. Talkington, J. E. 1998. Variable polarity gas metal arc welding. The Ohio State University, Columbus, Ohio, thesis.
30. Ushio, M., Nakata, K., and Tanaka, M. 2000. AC pulsed GMA welding of Al-Mg alloy — Fume and welding arc phenomena. Productivity Beyond 2000, IIW Asian Pacific Welding Congress, The WTIA 43rd National Welding Congress, pp. 859–873.
31. Ushio, M., Nakata, K., Tanaka, Tong, H., and Mita, T. 1994. Fume generation in Al-Mg alloy welding with AC-pulsed GMAW welding method. *Trans. of JWRI* 23(1).
32. Harwig, D. D., Joseph, A., and Dierksheide, J. E. 2002. Capability of variable polarity GMAW for automotive applications. AWS Sheet Metal Welding Conference X, Detroit, Mich., May 15–17.
33. Harwig, D. D., Joseph, A., Anderson, C., and Moore, J. 2000. Characteristics of variable polarity (AC) GMAW power supplies. *Proceedings from ICAWT 2000*, AWS, Orlando, Fla., Dec. 6–8.
34. Norrish, J. 1974. High deposition MIG welding with electrode negative polarity. *Proceedings from 3rd Intl. Conf. on Advances in Welding Processes*, The Welding Institute, May 7–9, pp. 121–128.
35. Ushio, M., Nakata, K., and Tanaka, M. 2000. AC pulsed GMA welding of Al-Mg alloy — Fume and welding arc phenomena. Productivity Beyond 2000, IIW Asian Pacific Welding Congress, The WTIA 43rd National Welding Congress, pp. 859–873.
36. Ushio, M., Nakata, K., Tanaka, Tong, H., and Mita, T. 1994. Fume generation in Al-Mg alloy welding with AC-pulsed GMAW welding method. *Trans. of JWRI* 23(1).

Finite Element Modeling Predicts the Effects of Voids on Thermal Shock Reliability and Thermal Resistance of Power Device

The thermal-mechanical effects of void size and location in lead-free solder heat-sink attachment of power devices is investigated

BY J. CHANG, L. WANG, J. DIRK, AND X. XIE

ABSTRACT. Three-dimensional finite element modeling (FEM) analysis was conducted to investigate the effects of the void size and location on the reliability of Sn-Ag-Cu heat-sink attachment. The results showed that void size does not have a significant effect on the strain/stress distribution, unless it is near the corner of the solder attachment, a location originally with higher stress. This is generally in agreement with the experimental results that a heat-sink attachment with an average of 37.5% void can survive more than 3000 cycles of thermal shock at –40° to 125°C. The void size had a significant effect on thermal dissipation. A 20% voids would cause the chip temperature to rise more than 5.1°C, which would obviously degrade the reliability of the device. Compared to void size, the location of voids is less significant. Void size of 10% at a different location causes chip temperature variation around 1°C.

Introduction

The reliability of the semiconductor devices is critical for designers and manufacturers. Electronic power devices are developed with increasing power capability, high voltage, and high current (Ref. 1). The typical loads for electronic power devices are high temperatures and temperature changes. As reported, in a typical power device, 4% of controlled power is dissipated as heat in the device. So thermal and thermal-mechanical management is important for power devices (Ref. 1).

In a power device assembly, materials with different thermal and mechanical properties are bonded together to constitute a complicated system. The cyclic stress/strain will be produced in the assembly due to the coefficient of thermal expansion (CTE) mismatch of different layers during operation (Ref. 2). Soft solder is often used for the heat-sink attachment because it has very good mechanical and heat dissipation performance; also, it allows plastic deformation, so that stresses due to temperature excursions and CTE mismatches during device service can be relaxed (Ref. 3). But accumulations of the plastic deformation may produce solder fatigue cracks and eventually cause the failure of the solder attachment.

Reliability of the most commonly used Sn-Pb eutectic solder has been extensively investigated and has been well understood. However, due to environmental and health concerns, Sn-Pb eutectic solder is being replaced by lead-free solders, among which Sn-Ag-Cu is the dominant candidate for use in reflow soldering technology (Ref. 4). Although quite a large number of studies have concentrated on this new alloy system from laboratory research to small-scale production, more data are needed before a solid understanding can be established.

Voids are easily formed in the solder joint. It became a more critical problem when lead-free solder was used in recent years because of its comparatively poor solderability. Voids are formed due to the outgassing of flux entrapped in the solder joint during reflow (Ref. 5). The solder paste contains 35~65 vol-% volatile materials. The outgassing is generally produced by the evaporation of solvent and additives in the solder paste. Some gases may be entrapped between the printed circuit board (PCB) and components causing voids to be formed during cooling. Previous studies have indicated that the reflow process and solder materials are the most significant factors that affect void formation (Refs. 6, 7).

There are no universal criteria regarding void size and location (Ref. 8). The factors that affect void formation are complex, and it is difficult to study the effect of void on reliability because many variables in the assembly process are not controllable regarding void formation. Most studies about the effect of voids on reliability are focused on Sn-Pb eutectic solder in BGA/CSP joints (Refs. 8, 9). The results show that big voids, especially when the voids are greater than 50% of the solder joint area, had been considered one of the critical issues in joint strength and reliability. Small voids also have effects on reliability, but it is dependent on the number and location.

From the thermal point of view, voids in solder layers become one of the main defects affecting the heat dissipation (Ref. 10). The overall effect of voids is to decrease the solder cross-section area available for heat dissipation. The heat dissipation is especially important for power devices. Industrial practices often set 10% voids as the highest limit for general heat-sink attachment and 5% for higher requirements.

This paper investigates the effect of void size and location in Sn-Ag-Cu heat-sink attachment on the thermal shock reliability and thermal resistance of power devices using 3-D finite element modeling (FEM). The degradation of heat-sink attachment by SnAgCu lead-free solder during thermal shock has been verified by experiment. Samples with high voiding percentages were selected for the investi-

J. CHANG (changjunling@yahoo.com.cn), *L. WANG, J. DIRK, and X. XIE are with DaimlerChrysler SIM Technology Co., Ltd., Shanghai, P. R. China. CHANG and XIE are also with Shanghai Institute of Microsystem and Information Technology, Chinese Academy of Science, Shanghai, P. R. China.*

KEYWORDS

Voids
Sn-Ag-Cu
Thermal Shock
Equivalent Plastic Strain
Equivalent Stress
Thermal Resistance

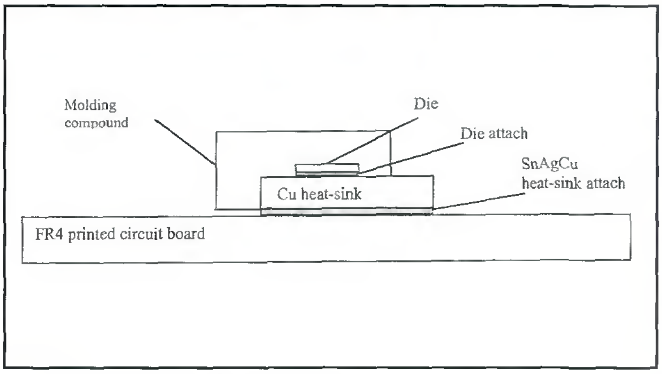

Fig. 1 — Schematic layout of structure.

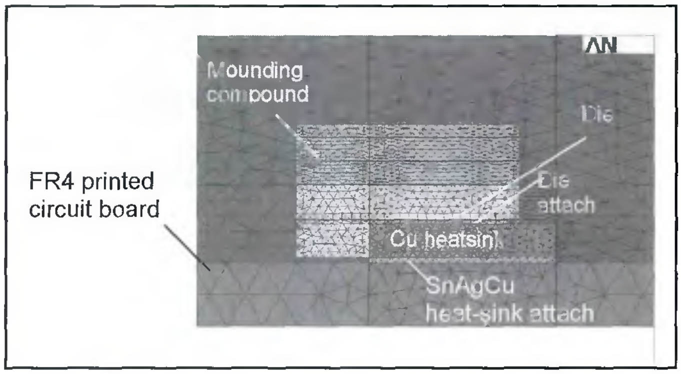

Fig. 2 — Simulation mesh model.

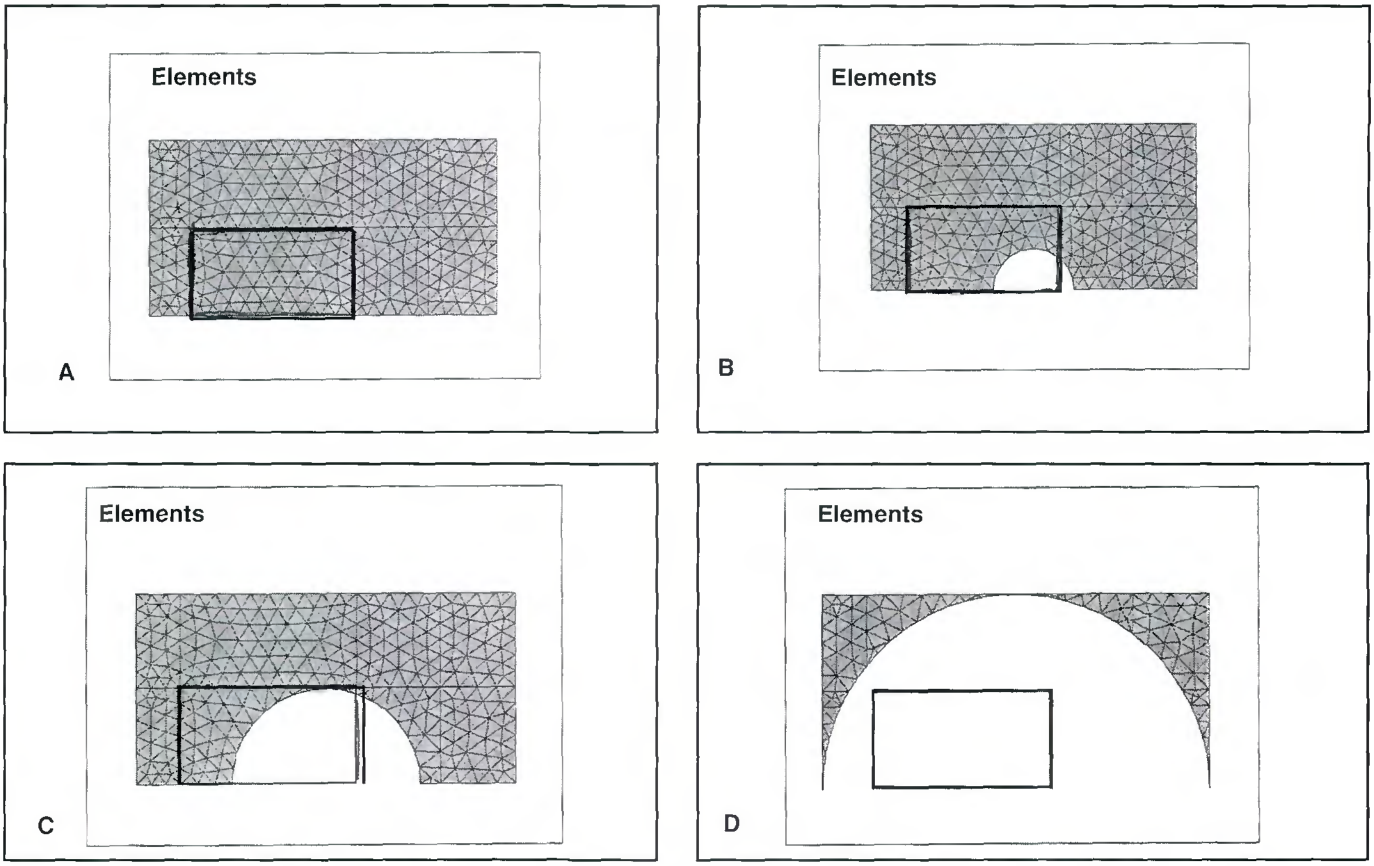

Fig. 3 — Heat-sink attachment model of different voiding percentages. (Black rectangle is the location of die.) A — 0%; B — 5%; C — 20%; and D — 79%.

Table 1 — Material Properties Used in the Simulation

	Young's modulus (GPa)	CTE (ppm/°C)	Density, ρ ($x10^{-6}$kg/mm^3)	Specific heat, C_p (J/kg·°C)	Conductivity, K (W/mm·°C)	Poisson's ratio
Silicon	131	2.7	2.32	750	0.084	0.3
FR4	16	16	1.80	1260	2.0E-4	0.28
Copper	120	17	8.96	385	0.386	0.35
Sn3.0Ag0.5Cu	38.70-0.176 x T	25	8.41	192	0.050	0.35
Pb97.5Sn	24.1-0.028 x T	28	10.90	136	0.036	0.3
Molding	15	18	1.80	126	1.6E-3	0.3

gation in order to get information on the significance of void formation on the reliability of SnAgCu heat-sink attachment. All FEM simulations were performed using *ANSYS* software.

FEM Simulation on Thermal Mechanical Strain/Stress

Geometry Model and Material Properties

A DPAK device soldered on the PCB was selected for the simulation. The cross section of the geometry model is illustrated in Fig. 1. The device and substrate were bonded together with Sn3.0Ag0.5Cu

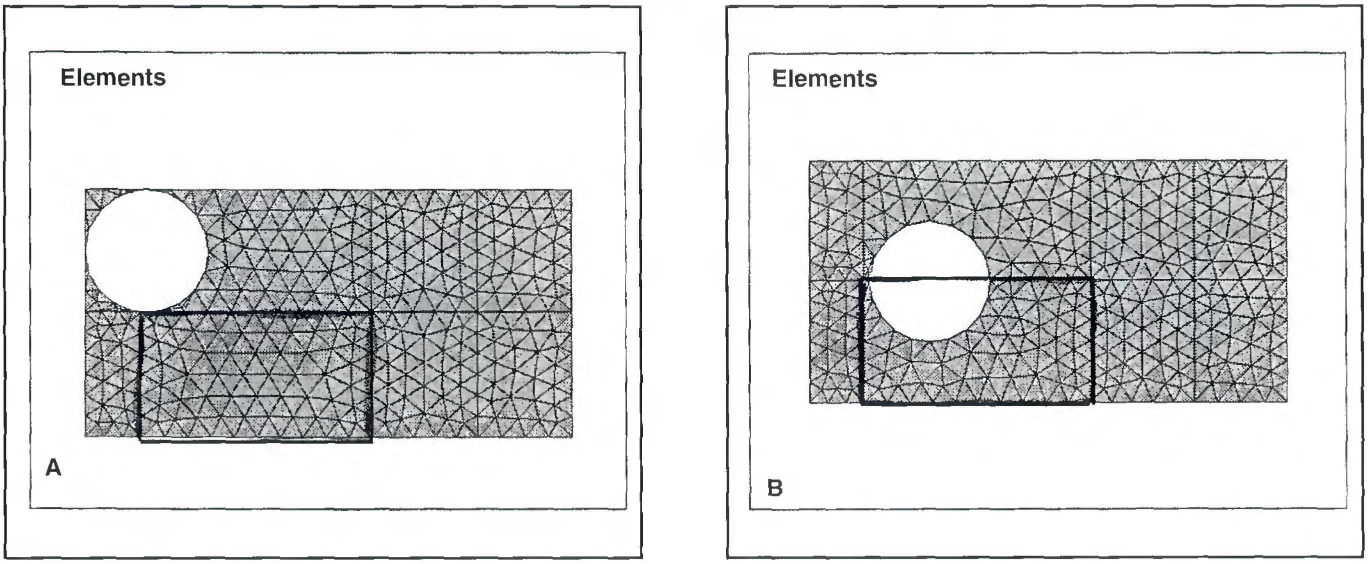

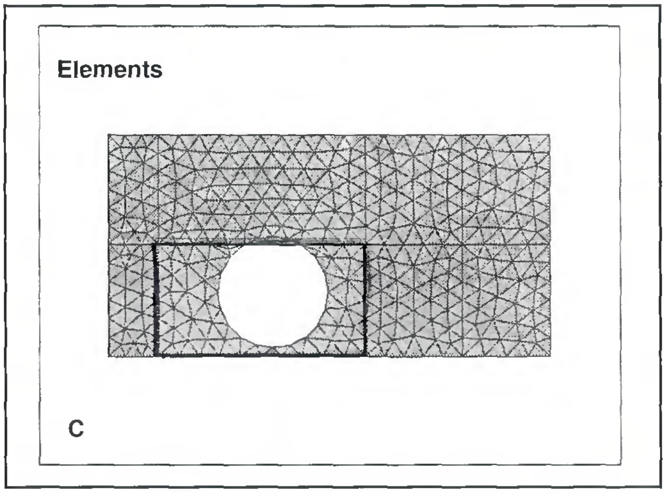

Fig. 4 — Heat-sink attachment model with voiding percentage of 10% at different locations. (Black rectangle is the location of die.) A — 10%-II; B — 10%-II; and C — 10%-III.

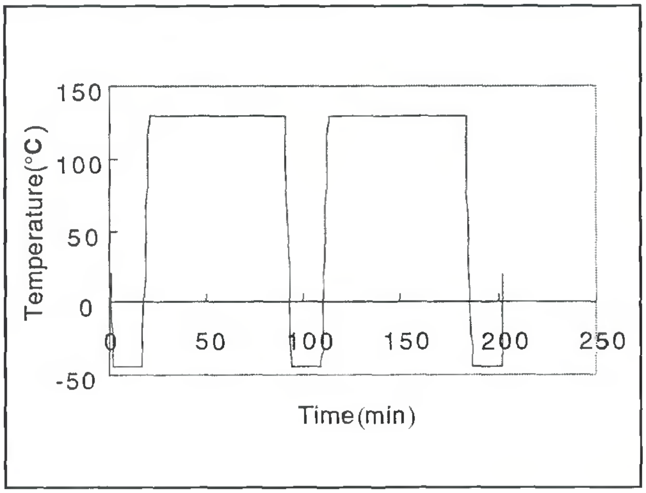

Fig. 5 — Cycles of temperature loading of simulation.

heat-sink attachment. Inside the package, a high lead solder Pb97Sn3 was used for die attachment. Since Sn3.0Ag0.5Cu solder and die attach Pb97Sn3 solder are viscoplastic in nature, the viscoplastic Anand model was used to present the Sn3.0Ag0.5Cu solder and die attach Pb97.5Sn solder behavior. All the other materials are considered to be elastic. Material properties used in this simulation are shown in Table 1 (Ref. 11). For Sn3.0Ag0.5Cu and Pb97Sn3 solder, material properties used in the Anand model are shown in Table 2 (Ref. 11).

Meshing Model and Loading Condition

Meshing Model

In this study, 3D-1/2th symmetric models were used. All voids in the heat-sink attachment were assumed to be circular and leads in the package were ignored for simplification. The mesh model is shown in Fig. 2. The geometry data were directly taken from a cross section of real specimen measurements.

The heat-sink attachment model with different void sizes and locations is shown in Figs. 3 and 4, respectively. The voiding percentages 5, 10, and 20% were selected as levels of interests, and a 79% void selected as a worst case reference. For 10% voids, three typical locations were chosen for the modeling and simulation.

Loading Conditions

Room temperature was taken as the zero stress point. It is assumed that viscoplastic deformations take place at all nonzero stress values. Figure 5 shows the cycles of temperature loading of the simulation. The start of thermal loading was at the stress-free state of 25°C. The dwell time at –40° and 125°C was 15 and 75 min, respectively. The ramp rate was 50°C/min.

Table 2 — Parameters Used in Anand Model

Material parameters	Sn3.0Ag0.5Cu	Pb97Sn3
A (sec^{-1})	5.87 x 10^6	3.25 x 10^4
Q/R (°K)	7460	15600
ξ	2.00	7.00
m	0.0942	0.0143
s (MPa)	58.3	72.7
n	0.015	0.00437
h_0 (MPa)	9350	1790
a	1.50	3.73
s_0 (MPa)	45.9	15.1

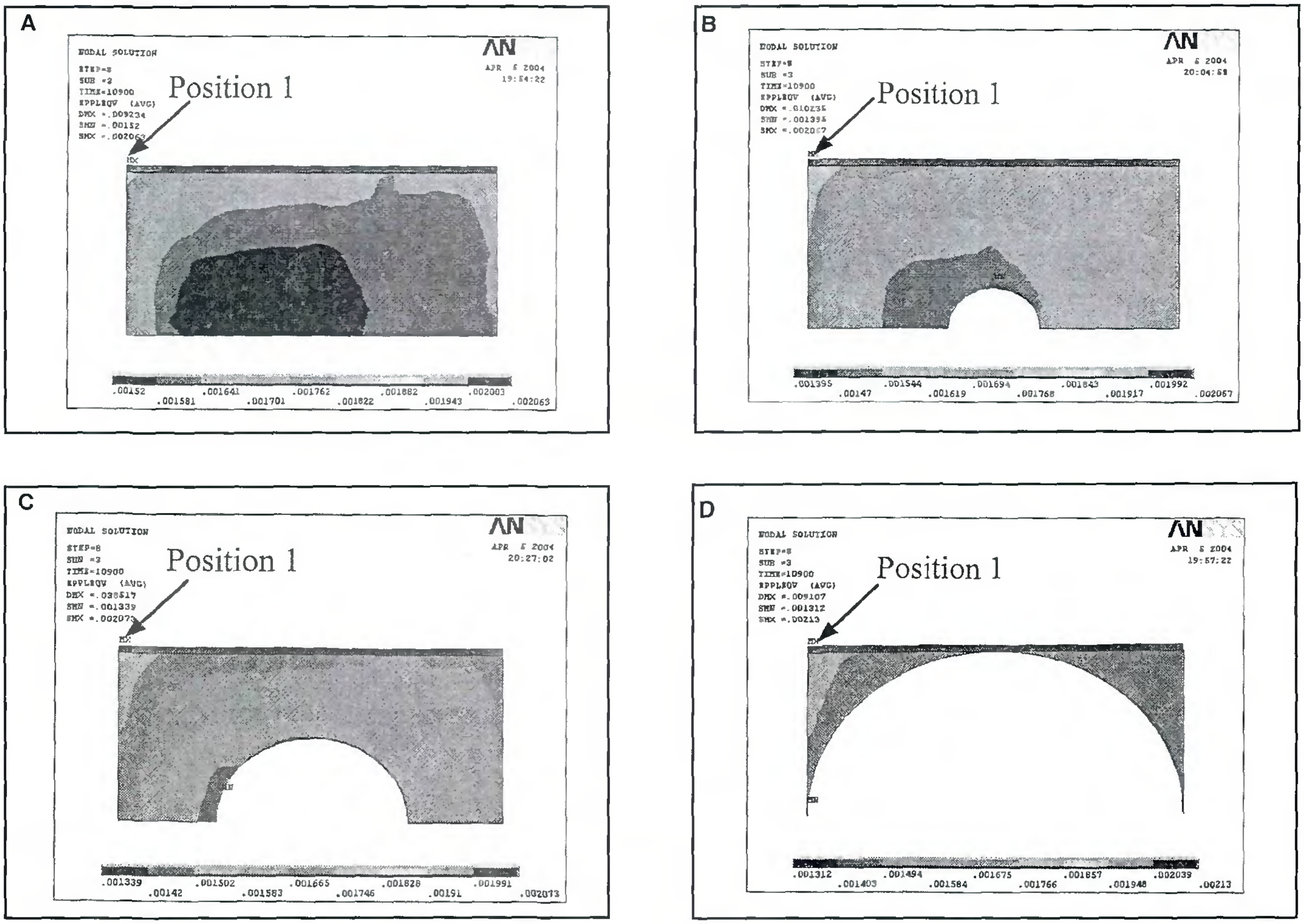

Fig. 6 — Equivalent plastic strain distribution in SnAgCu heat-sink attachment with different voiding percentages after 125°C dwell. A — 0%; B — 5%; C — 20%; and D — 79%.

Table 3 — Thermal Mechanical Simulation Results

Void percentages (%)	Maximum equivalent plastic strain (%)	Maximum equivalent stress	Increase in maximum equivalent plastic strain compared to no void (%)	Increase in maximum equivalent stress compared to no void (%)
0	0.2063	32.041	0	0
5	0.2067	32.055	0.194	0.044
20	0.2073	32.014	0.482	–0.084
79	0.2130	31.760	3.146	–0.885
10–I	0.2283	32.124	9.636	0.258
10–II	0.2054	31.904	–0.438	–0.429
10–III	0.2072	32.016	0.434	–0.078

The time/temperature profile was obtained from real measurement data. The simulations were performed for several cycles (typically 2 or 3 cycles) until the stress/strain hysteresis loop stabilized.

Thermal-Mechanical Strain/Stress Simulation Results

Equivalent plastic strain distribution of heat-sink attachment with different voiding percentages and different void locations after 125°C dwell are shown in Figs. 6 and 7, respectively. The maximum equivalent plastic strain occurred at the corner of the heat-sink attachment (position 1 in Figs. 6 and 7). Equivalent plastic strain distribution was circular. The outer heat-sink attachment had relatively larger equivalent plastic strain. The distribution of equivalent plastic strain distribution was almost the same for different voiding percentages and different void locations.

Maximum equivalent plastic strain and maximum equivalent stress of different void sizes and locations compared with the no void case is listed in Table 3. Void size had almost no effect on the maximum equivalent plastic strain. The increase in maximum equivalent plastic strain was less than 3.5%, even when the voiding percentages reached 79%, compared to the maximum equivalent plastic strain of no voids.

While void location affected the maximum equivalent plastic strain to some extent, the increase in maximum equivalent plastic strain reached 9.636% when the voids were at the corner of the heat-sink attachment (10%-I). The maximum equivalent plastic strain even decreased when the voids were at location 10%-I.

Maximum equivalent stress decreased in most cases except when the voiding percentages were 5 and 10%-I. But the changes in maximum equivalent stress were small (<±1%) whether for different void sizes or different void locations.

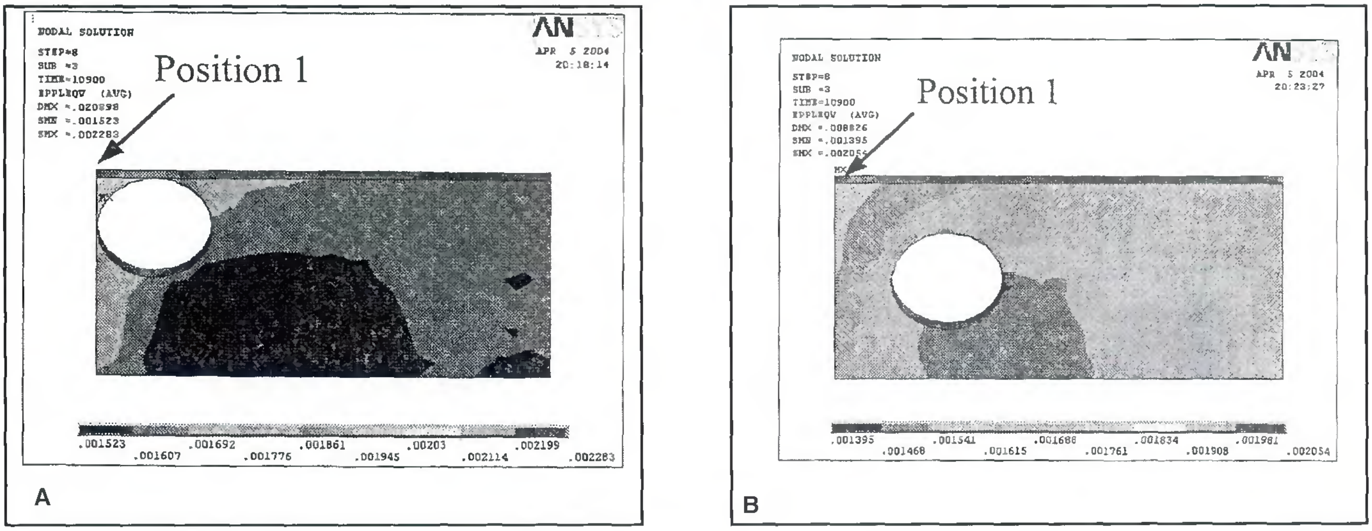

Thermal Analysis

Thermal Analysis Loading Condition

For the thermal analysis, the simulation was based on a heat conduction equation. Chip was the only heat source in assembly. All the materials were assumed to be isotropic and uniform in thermal conductivity. The heat transfer coefficient at the topside of device was obtained through free convection just as vertical plate.

The exterior surface of the PCB board, except the region under the device, was set at 50°C. Chip power was 1 W and its volume was 2.4 x 2.58 x 0.22 mm^3, so its heat generation rate (heat flow per unit volume) was 0.73 W/mm^3.

Heat dissipation ability is characterized by thermal resistance with the following formula (Ref. 12):

$$R = \frac{\Delta T}{q} \qquad (1)$$

where ØT is temperature difference in °C, q is dissipated power in W, and R is thermal resistance in °C/W.

Thermal Resistance of Solder Attachment

The temperature distribution on the chip of different voiding percentages and different void locations is shown in Figs. 8 and 9. The trend of temperature distribution was almost the same for different voiding percentages and different void locations. The distribution was circular. The outer chip surface has relatively lower temperature. And the left side had a higher temperature compared to the right side.

But the maximum chip temperature of different voiding percentages and void locations was significantly different, as shown in Table 4. With the increase in void sizes, the chip temperature increased. The maximum chip temperature increased 0.8°C compared to no voids when the voiding percentages was 5%. And it increased to 5.1° and 27.2°C when the voiding percentages were 20 and 79%, respectively. The changes in the maximum chip temperature were relatively small (<1°C) for different void locations.

Thermal resistance compared with the case no voids is also listed in Table 4. With increasing void size, the thermal resistance increased. The thermal resistance increased 1.06% compared to no voids when the voiding percentage was 5%, and it increased to 6.53 and 27.18% when the voiding percentages were 20 and 79%, respectively.

For void locations, the closer the voids were to the chip side, the larger the thermal resistance when the voiding percentage was 10%. The thermal resistance increased 1.11% when the voids were at the corner, and it increased to 2.03% when the voids were close to the center of the heat-sink attachment compared with no voids. However, the effect of void location is less significant than voiding percentages.

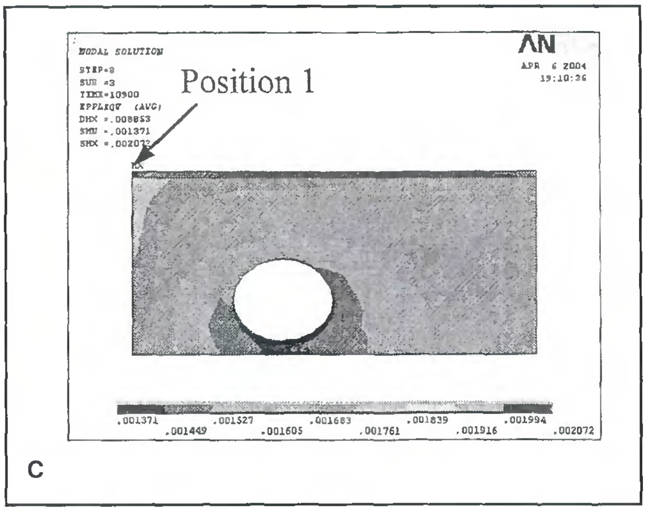

Fig. 7 — Equivalent plastic strain distribution of heat-sink attachment with different void location after 125°C dwell. A — 10%-I; B — 10%-II; and C — 10%-III.

Experimental Validation

Experimental Procedure

Figure 10A shows the photo of the sample for experimental validation, and Fig. 10B shows the four Dpak devices with higher magnification.

The thermal shock tests were performed in the range –40° to 125°C, with 15 min dwell at –40°C and 75 min dwell at 125°C. Eleven boards were subjected to thermal shock until 3000 cycles. The detailed analysis methods have been introduced in a previous paper (Ref. 13).

Experimental Results

Voiding Percentages

The typical heat-sink attachment of the specimen had big voids from one to three and many small voids. The range of voiding percentages was from 33 to 48%, and the average voiding percentage was 37.5%. An X-ray image of a typical specimen is shown in Fig. 11.

Solder Fatigue and Delamination between Cu/Cu_3Sn

Figure 12 shows SEM images of a cross section after 3000 thermal shock cycles.

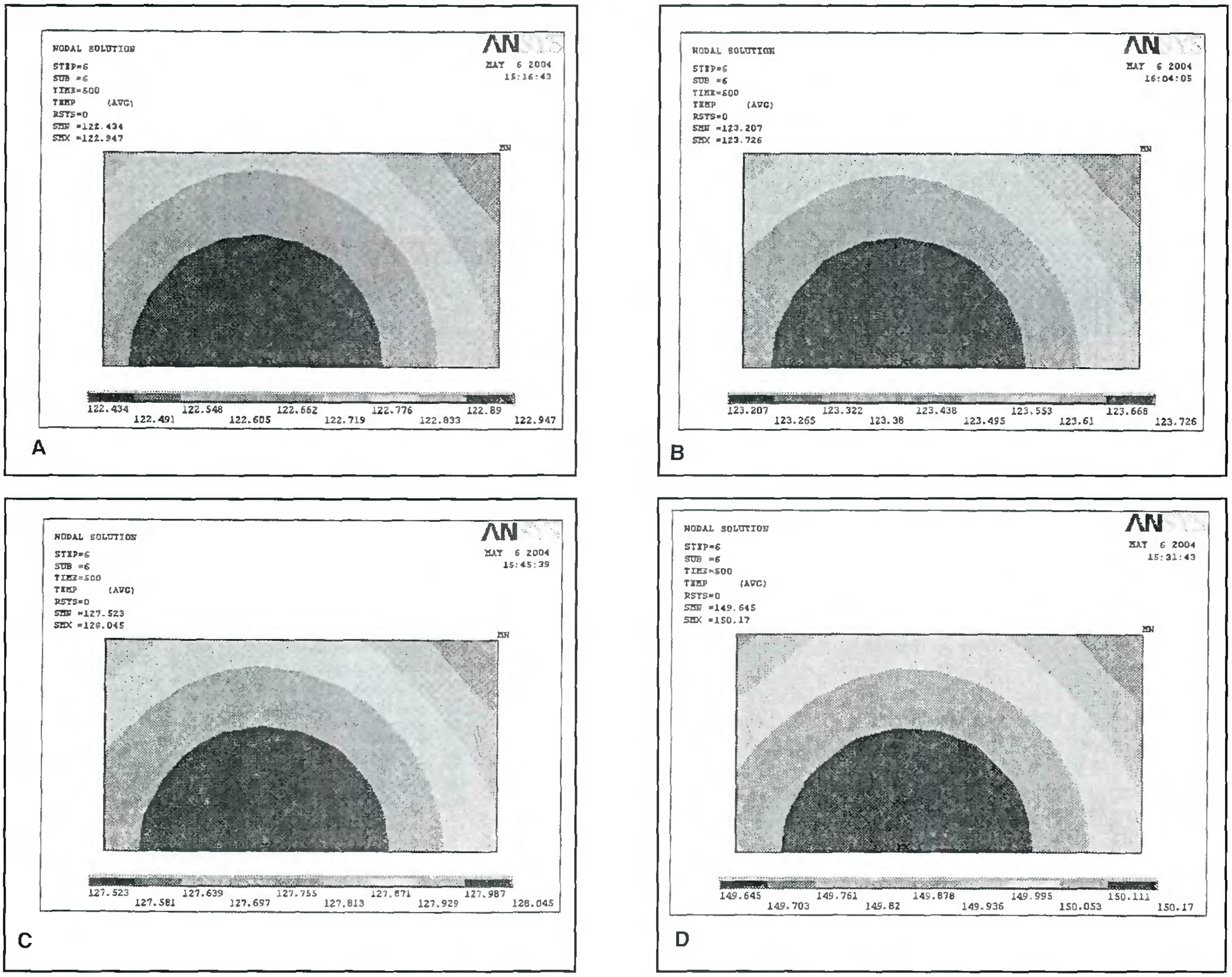

Fig. 8 — The temperature distribution on the chip from topside of different heat-sink attachment voiding percentages. A — 0%; B — 5%; C — 20%; and D — 79%.

Table 4 — Thermal Analysis Resnlt of Simnlation

Void percentages (%)	Max chip temp (°C)	ΔT (°C)	Thermal resistance (°C/W)	Increase in thermal resistance as compared to heat-sink attachment with no void (%)
0	122.947	72.947	72.947	0
5	123.726	73.726	73.726	1.06
20	128.045	78.045	78.045	6.53
79	150.170	100.170	100.170	27.18
10–I	123.762	73.762	73.762	1.11
10–II	124.421	74.421	74.421	1.98
10–III	124.456	74.456	74.456	2.03

Besides voids, only small solder joint fatigue cracks were found. These fatigue cracks were found either at the two ends of the cross section where the distance to neutral point (DNP) was largest or initiated at a large void location and propagated into the solder. Unexpectedly, the dominant degradation was found to be Kirkendall voids at along almost the whole Cu/Cu_3Sn interface, but not solder fatigue. More detailed experiment results can can be found in a previous paper (Ref. 13).

Discussion

The FEM results showed that the increase in maximum equivalent plastic strain was less than 3.5%, even when the voiding percentage reached 79%. The thermal shock experimental test also confirmed that the heat-sink attachment with large voiding percentages (voiding percentages ranged from 33 to 48%) had a thermal shock cycle lifetime above 3000 cycles, and the dominant degradation mechanism was not solder fatigue but interface delamination due to Kirkendall effects.

The specimens subjected to the present investigation typically contain 1–3 big voids and many small voids. In all cases, experimental validation confirmed that the major failure mode is interfacial degradation due to Kirkendall voids, not solder fatigue. So although several large voids and one large void with equal size may perform differently in thermal-mechanical performances, the present single-void approach is enough to provide an insight to the effects of void percentage and to give rough reference values to their significance. More studies are needed to

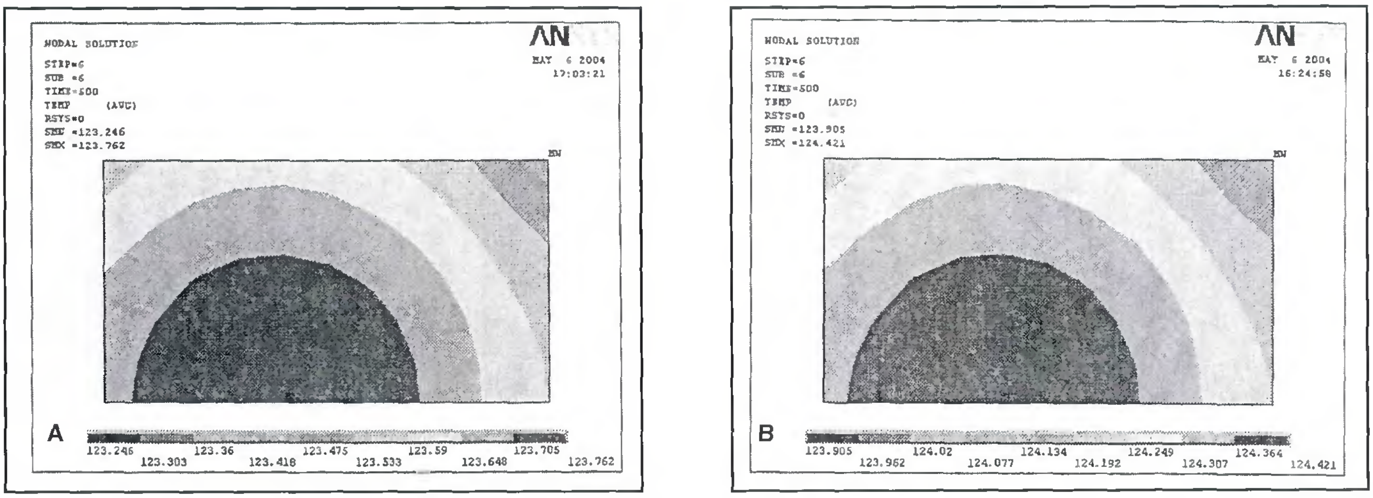

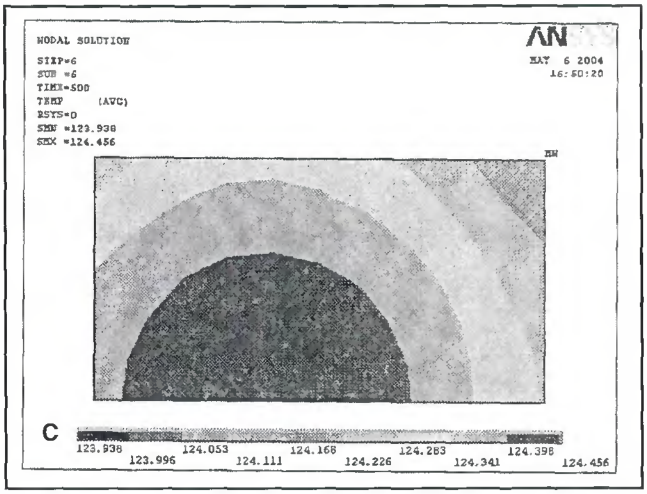

Fig. 9 — The temperature distribution on chip from topside of different heat-sink attachment voids locations. A — 10%-I; B — 10%-II; and C — 10%-III.

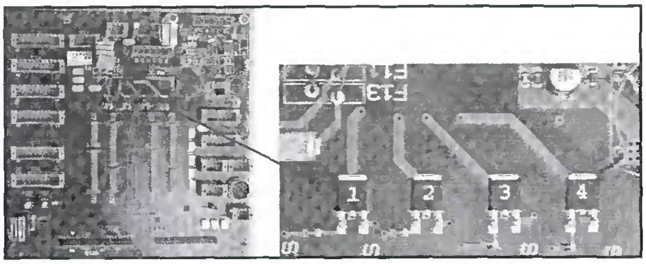

Fig. 10 — A — The surface mount assemblies; B — enlarged Dpak power device on PCB.

get a deeper understanding of multiple large voids. Exact experimental validation of such studies will be impractical, if not possible, as it is very difficult to control the exact void size and location.

Although generally speaking, void size seems to be insignificant to solder attachment lifetime from both FEM and experiment results, some attention needs to be paid to the effect of void locations. When a 10% void exists near the corner of the solder attachment, a location with largest DNP and thus highest stress/strain, the maximum equivalent plastic strain increased by 9.6%.

Different from the effects on thermal-mechanical properties, the voids on heat dissipation show significant effects on voiding percentages, but not too much on void location.

When the void percentage was 5%, the maximum chip temperature increased 0.8-°C and thermal resistance increased 1.06% compared to when there were no voids. This was acceptable in general. When the void percentage reached 20%, the maximum chip temperature increased 5.1°C and thermal resistance increased 6.53% compared to when there were no voids. This value may indicate an obvious degraded reliability. The maximum chip temperature increase reached 27.2°C and thermal resistance increased 27.18% compared to when there were no voids when the void percentage further increased to 79%. This is clearly not acceptable from the thermal dissipation point of view.

For void locations, the closer the voids were to the chip side, the larger the thermal resistance when the void percentage was 10%. Because the chip was the only heat source, the further the voids were from the chip, the lower the temperature, and the less effect the voids had on thermal resistance. But the changes in the maximum chip temperature were relatively small (<1°C) for different void locations. The void locations did not have a great effect on the thermal resistance in this case.

The simulation results agree well with common industrial practices. For general heat-sink attachments, the high limit of void percentages is often set to 10%, while for high-performance requirements, 5% is often required. Due to equipment limitation, experimental validation was not performed on heat dissipation.

Conclusions

Based on the investigations, the following conclusions can be made.

1. Generally speaking, void percentages did not affect the thermal-mechanical performance of the heat-sink attachment very much.

2. Void location has a much bigger effect on the maximum equivalent plastic strain compared to void percentages. For voids at the relative center of the heat-sink attachment (10%-III), the increase in maximum equivalent plastic strain was 0.434% compared to when there were no voids. For voids at the corner of the heat-sink attachment (10%-I), the increase in maximum equivalent plastic strain reached 9.636%, and the maximum equivalent plastic strain even decreased 0.438% when the voids were at location 10%-II.

3. The void percentages had a significant effect on thermal dissipation. With the increase in void percentages, chip temperature and thermal resistance increased. The thermal resistance increased 1.06% compared to no voids, and it increased to 6.53 and 27.18% when the void percentages were 20 and 79%, respectively. But the effect of void location on thermal dissipation was relatively small, and the changes in the maximum chip temperature were less than 1°C for different void locations.

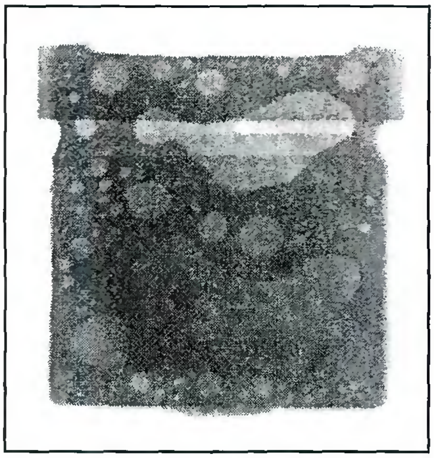

Fig. 11 — X-ray image of typical specimen in this investigation (voiding percentages, 37.6%).

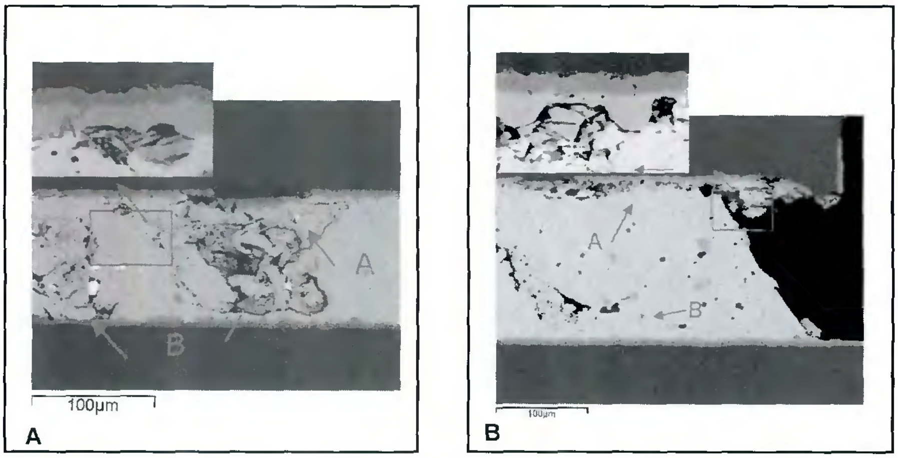

Fig. 12 — Typical SEM images of a cross section after 3000 thermal shock cycles. A — Delamination between Cu/Cu_3Sn; B — solder fatigue.

References

1. Ye, H., Lin, M., and Basaran, C. 2002. Failure modes and FEM analysis of power electronic packaging. *Finite Element in Analysis and Design* 38: 601–612.
2. Wu, CC.M.L., Lai, J.K.L., and Wu, Y. 1998. Thermal-mechanical interface crack behavior of a surface mount solder joint. *Finite Element in Analysis and Design* 30: 19–30.
3. Evans, J., and Evans, J. Y. 1998. Packaging factors affecting the fatigue life of power transistor die bonds. IEEE Trans. *Components Packaging Manuf. Technol. Part A* 21(3): 459–468.
4. Zeng, K., and Tu, K. N. 2002. Six cases of reliability study of Pb-free solder joints in electronic packaging technology. *Materials Science and Engineering R* 38: 55–105.
5. Chan, Y. C., Xie, D. J., and Lai, J. K. 1996. Experimental studies of pore formation in surface mount solder joints. *Material Science and Engineering* B38: 53–61.
6. Lee, N.-C., and O'Hara, W. B. 1995. Voiding in BGA. *Proceeding of Surface Mount International.* California, pp. 462–471.
7. O'Hara, W. B., and Lee, N.-C. 1996. Voiding mechanism in BGA assembly. *The International Journal of Microcircuits and Electronic Packaging* 19(3): 190–198.
8. Yanus, M., Srihari, K., Pitarresi, J. M., and Primavera, A. 2003. Effect of voids on the reliability of BGA/CSP solder joints. *Microelectronics Reliability* 43: 2077–2086.
9. O'Hara, W. B., and Lee, N.-C. 1998. Controlling solder joint voiding in BGA assembly. *Surface Mount Technology Magazine* 12(4): 68–72.
10. Ciampolimi, L., Ciappa, M., Mallberti, P., Regli, P., and Fichtner, W. 1999. Modeling thermal effects of large contiguous voids in solder joints. *Microelectronics Journal* 30: 1115–1123.
11. Janz, D. T. 2004. Reliability of discrete power devices with lead free solder joints. M.S. dissertation. Institute for Microsystem Technology, Albert Ludwigs University, Freiburg.
12. Tummala, R. R., Rymaszewski, E. J., and Klopfenstein, A. G. 2001. *Microelectronics Packaging Handbook*, Publishing House of Electronics Industry, Beijing, pp. 214.
13. Chang, J., Janz, D., Kempe, W., and Xie, X. 2004. Degradation of Sn-Ag-Cu heat-sink attachment during thermal shock cycling. *Soldering and SMT.* accepted.

Preparation of Manuscripts for Submission to the *Welding Journal* Research Supplement

All authors should address themselves to the following questions when writing papers for submission to the Welding Research Supplement:

◆ Why was the work done?
◆ What was done?
◆ What was found?
◆ What is the significance of your results?
◆ What are your most important conclusions?

With those questions in mind, most authors can logically organize their material along the following lines, using suitable headings and subheadings to divide the paper.

1) **Abstract.** A concise summary of the major elements of the presentation, not exceeding 200 words, to help the reader decide if the information is for him or her.

2) **Introduction.** A short statement giving relevant background, purpose, and scope to help orient the reader. Do not duplicate the abstract.

3) **Experimental Procedure, Materials, Equipment.**

4) **Results, Discussion.** The facts or data obtained and their evaluation.

5) **Conclusion.** An evaluation and interpretation of your results. Most often, this is what the readers remember.

6) **Acknowledgment, References and Appendix.**

Keep in mind that proper use of terms, abbreviations, and symbols are important considerations in processing a manuscript for publication. For welding terminology, the *Welding Journal* adheres to AWS A3.0:2001, *Standard Welding Terms and Definitions.*

Papers submitted for consideration in the Welding Research Supplement are required to undergo Peer Review before acceptance for publication. Submit an original and one copy (double-spaced, with 1-in. margins on 8 ½ x 11-in. or A4 paper) of the manuscript. A manuscript submission form should accompany the manuscript.

Tables and figures should be separate from the manuscript copy and only high-quality figures will be published. Figures should be original line art or glossy photos. Special instructions are required if figures are submitted by electronic means. To receive complete instructions and the manuscript submission form, please contact the Peer Review Coordinator, Doreen Kubish, at (305) 443-9353, ext. 275; FAX 305-443-7404; or write to the American Welding Society, 550 NW LeJeune Rd., Miami, FL 33126.

TECHNICAL PROGRAM ABSTRACT SUBMITTAL
Annual FABTECH International & AWS Welding Show
Atlanta, Georgia, October 30 – November 2, 2006
(Complete a separate submittal for each paper to be presented.)

Primary Author:
Affiliation:
Mailing Address:

City: **State/Province** **Zip/Mail Code** **Country:**
Email:

Co-Author(s):

Name: Affiliation Address: City: State/Province Zip/Mail Code Country: E-Mail:	Name: Affiliation: Address: City: State/Province: Zip/Mail Code: Country: E-Mail:
Name: Affiliation: Address: City: State/Province: Zip/Mail Code: Country: E-Mail:	Name: Affiliation: Address: City: State/Province: Zip/Mail Code: Country: E-Mail:

Answer the following about this paper
Original submittal? Yes ☐ No☐ Progress report? Yes ☐ No☐ Review paper? Yes ☐ No☐ Tutorial? Yes ☐ No☐
What welding processes are used?
What materials are used?
What is the main emphasis of this paper? Process Oriented ☐ Materials Oriented ☐ Modeling ☐
To what industry segments is this paper most applicable?
Has material in this paper ever been published or presented previously? Yes ☐ No☐
If "Yes", when and where?
Is this a graduate study related research? Yes ☐ No☐
If accepted, will the author(s) present this paper in person? Yes ☐ Maybe ☐ No☐

Keywords: Please indicate the top four keywords associated with your research below

____________________ ____________________

____________________ ____________________

Guidelines for abstract submittal and selection criteria:
- Only those abstracts submitted on this form will be considered. Follow the guidelines and word limits indicated. Complete this form using MSWord. Submit electronically via email to techpapers@aws.org.
-

Technical/Research Oriented
- New science or research.
- Selection based on technical merit.
- Emphasis is on previously unpublished work in science or engineering relevant to welding, joining and allied processes.
- Preference will be given to submittals with clearly communicated benefit to the welding industry.

Applied Technology
- New or unique applications.
- Selection based on technical merit.
- Emphasis is on previously unpublished work that applies known principles of joining science or engineering in unique ways.
- Preference will be given to submittals with clearly communicated benefit to the welding industry.

Education
- Welding education at all levels.
- Emphasis is on education/training methods and their successes.
- Papers should address overall relevance to the welding industry.

☑ Check the category that best applies:

☐ Technical/Research Oriented ☐ Applied Technology ☐ Education

Proposed Title (max. 50 characters):
Proposed Subtitle (max. 50 characters):

Abstract:

Introduction (100 words max.) – Describe the subject of the presentation, problem/issue being addressed and its practical implications for the welding industry. Describe the basic value to the welding community with reference to specific communities or industry sectors.

Technical Approach, for technical papers only (100 words max.) – Explain the technical approach, experimental methods and the reasons why this approach was taken.

Results/Discussion (300 words max.) – For technical papers, summarize the results with emphasis on why the results are new or original, why the results are of value. For other papers, elaborate on why this paper is of value to the community, describe key work in the field and provide an integration of these separate activities into a "continuum."

Conclusions (100 words max.) – Summarize the conclusions and how they could be put to use – how and by whom.

NOTE: Abstract must not exceed one page and must not exceed the recommended word limit given above

Note: Presentations should avoid the use of product trade names.

Return this form, completed on both sides, to

AWS Education Services
Technical Papers 2006
550 NW LeJeune Road
Miami FL 33126
FAX 305-442-7451

MUST BE RECEIVED NO LATER THAN 7 April 2006.

Abstracts may also be submitted electronically on the AWS website:
http://www.aws.org/w/s/conferences_call/

Use these convenient, postage-paid inquiry cards to request free information about the products or services advertised in this issue of *Welding Journal.*

For information about specific advertisements: Circle the key number on the card that matches the number on the bottom of the ad.

FREE INFORMATION • FREE INFORMATION

For faster processing, please FAX this card to (630) 739-9700.
Type or print the information and copy before faxing.
This fax number is for the service bureau only, not AWS.

Please send literature on items circled at right:

March 2006 Card void after September 1, 2006

Name ________ Title ________

Company ________

Address ________

City ________ State ________ Zip ________

Phone: ________ Fax: ________

E-mail ________

Please circle an entry for each category:

I. TYPE OF BUSINESS
1. Construction
2. Primary Metal Products
3. Fabricated Metal Products
4. Transportation
5. Petrochemical
6. Misc. Repair Services
7. Educational Services
8. Utilities
9. Other

II. JOB FUNCTION/TITLE
1. Corp. Management
2. Plant Mgmt.
3. Engineer
4. Welding or Cutting Oper.
5. Quality Control
6. Sales
7. Purchasing
8. Education
9. Other

III. PURCHASING AUTHORITY
1. Recommend
2. Specify
3. Approve

IV. NUMBER OF EMPLOYEES
1. Under
2. 50 to 99
3. 100 to 499
4. 500 to 999
5. 1000 to 2499
6. 2500 to more

V. ANNUAL DOLLAR VOLUME
1. Under $1 Million
2. $1 Million to 5 Million
3. Over $5 Million

VI. THIS INQUIRY IS FOR
1. Immediate Purchase
2. Future Project
3. General Information

1	35	69	103	137	171	205	239	273
2	36	70	104	138	172	206	240	274
3	37	71	105	139	173	207	241	275
4	38	72	106	140	174	208	242	276
5	39	73	107	141	175	209	243	277
6	40	74	108	142	176	210	244	278
7	41	75	109	143	177	211	245	279
8	42	76	110	144	178	212	246	280
9	43	77	111	145	179	213	247	281
10	44	78	112	146	180	214	248	282
11	45	79	113	147	181	215	249	283
12	46	80	114	148	182	216	250	284
13	47	81	115	149	183	217	251	285
14	48	82	116	150	184	218	252	286
15	49	83	117	151	185	219	253	287
16	50	84	118	152	186	220	254	288
17	51	85	119	153	187	221	255	289
18	52	86	120	154	188	222	256	290
19	53	87	121	155	189	223	257	291
20	54	88	122	156	190	224	258	292
21	55	89	123	157	191	225	259	293
22	56	90	124	158	192	226	260	294
23	57	91	125	159	193	227	261	295
24	58	92	126	160	194	228	262	296
25	59	93	127	161	195	229	263	297
26	60	94	128	162	196	230	264	298
27	61	95	129	163	197	231	265	299
28	62	96	130	164	198	232	266	300
29	63	97	131	165	199	233	267	301
30	64	98	132	166	200	234	268	302
31	65	99	133	167	201	235	269	303
32	66	100	134	168	202	236	270	304
33	67	101	135	169	203	237	271	
34	68	102	136	170	204	238	272	

Please mail:
❑ 305- List of AWS publications
❑ 306- Information on AWS Membership

NO POSTAGE NECESSARY IF MAILED IN THE UNITED STATES

BUSINESS REPLY MAIL
FIRST CLASS PERMIT NO. 11992 MIAMI, FL

POSTAGE WILL BE PAID BY ADDRESSEE

WELDING *Journal*

C/O CREATIVE DATA
519 E BRIARCLIFF RD
BOLINGBROOK IL 60440-9882

NO POSTAGE NECESSARY IF MAILED IN THE UNITED STATES

BUSINESS REPLY MAIL
FIRST CLASS PERMIT NO. 11992 MIAMI, FL
POSTAGE WILL BE PAID BY ADDRESSEE

WELDING *Journal*
C/O CREATIVE DATA
519 E BRIARCLIFF RD
BOLINGBROOK IL 60440-9882

Use these convenient, postage-paid inquiry cards to request free information about the products or services advertised in this issue of *Welding Journal.*

For information about specific advertisements: Circle the key number on the card that matches the number on the bottom of the ad.

FREE INFORMATION • FREE INFORMATION

Please send literature on items circled at right:

March 2006 Card void after September 1, 2006

Name__________ Title__________

Company__________

Address__________

City__________ State______ Zip______

Phone:__________ Fax:__________

E-mail__________

Please circle an entry for each category:

I. TYPE OF BUSINESS
1. Construction
2. Primary Metal Products
3. Fabricated Metal Products
4. Transportation
5. Petrochemical
6. Misc. Repair Services
7. Educational Services
8. Utilities
9. Other

II. JOB FUNCTION/TITLE
1. Corp. Management
2. Plant Mgmt.
3. Engineer
4. Welding or Cutting Oper.
5. Quality Control
6. Sales
7. Purchasing
8. Education
9. Other

III. PURCHASING AUTHORITY
1. Recommend
2. Specify
3. Approve

IV. NUMBER OF EMPLOYEES
1. Under
2. 50 to 99
3. 100 to 499
4. 500 to 999
5. 1000 to 2499
6. 2500 to more

V. ANNUAL DOLLAR VOLUME
1. Under $1 Million
2. $1 Million to 5 Million
3. Over $5 Million

VI. THIS INQUIRY IS FOR
1. Immediate Purchase
2. Future Project
3. General Information

1	35	69	103	137	171	205	239	273
2	36	70	104	138	172	206	240	274
3	37	71	105	139	173	207	241	275
4	38	72	106	140	174	208	242	276
5	39	73	107	141	175	209	243	277
6	40	74	108	142	176	210	244	278
7	41	75	109	143	177	211	245	279
8	42	76	110	144	178	212	246	280
9	43	77	111	145	179	213	247	281
10	44	78	112	146	180	214	248	282
11	45	79	113	147	181	215	249	283
12	46	80	114	148	182	216	250	284
13	47	81	115	149	183	217	251	285
14	48	82	116	150	184	218	252	286
15	49	83	117	151	185	219	253	287
16	50	84	118	152	186	220	254	288
17	51	85	119	153	187	221	255	289
18	52	86	120	154	188	222	256	290
19	53	87	121	155	189	223	257	291
20	54	88	122	156	190	224	258	292
21	55	89	123	157	191	225	259	293
22	56	90	124	158	192	226	260	294
23	57	91	125	159	193	227	261	295
24	58	92	126	160	194	228	262	296
25	59	93	127	161	195	229	263	297
26	60	94	128	162	196	230	264	298
27	61	95	129	163	197	231	265	299
28	62	96	130	164	198	232	266	300
29	63	97	131	165	199	233	267	301
30	64	98	132	166	200	234	268	302
31	65	99	133	167	201	235	269	303
32	66	100	134	168	202	236	270	304
33	67	101	135	169	203	237	271	
34	68	102	136	170	204	238	272	

Please mail:
❑ 305- List of AWS publications
❑ 306- Information on AWS Membership

NOTE:
To speed the processing of your inquiry, please provide ALL the information requested on the card. This will make it easier for the companies to follow up on your request as soon as possible.

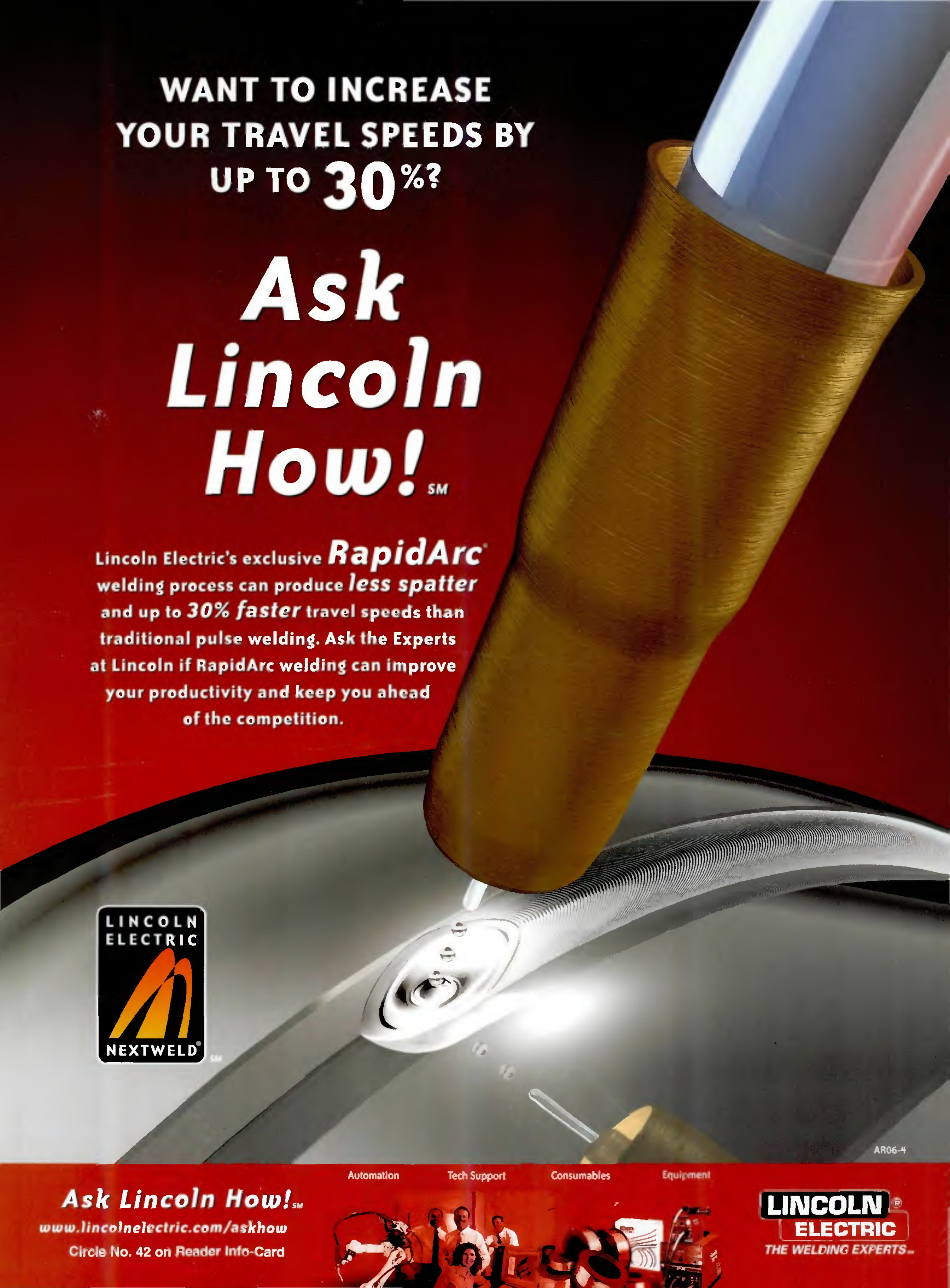
WANT TO INCREASE
YOUR TRAVEL SPEEDS BY
UP TO 30%?
Ask
Lincoln
How!SM
Lincoln Electric's exclusive RapidArc welding process can produce less spatter and up to 30% faster travel speeds than traditional pulse welding. Ask the Experts at Lincoln if RapidArc welding can improve your productivity and keep you ahead of the competition.
LINCOLN ELECTRIC
NEXTWELD SM
AR06-4
Automation
Tech Support
Consumables
Equipment
Ask Lincoln How!SM
www.lincolnelectric.com/askhow
Circle No. 42 on Reader Info-Card
LINCOLN ELECTRIC
THE WELDING EXPERTS